Serotonergic neurons of the nucleus raphe Magnus in the control of nociceptive transmission in the dorsal horn of the spinal cord : an optogenetic study in different pathophysiological contexts

Franck Aby

université de BORDEAUX

THÈSE PRÉSENTÉE

POUR OBTENIR LE GRADE DE

DOCTEUR DE

L'UNIVERSITÉ DE BORDEAUX

Ecole Doctorale des sciences de la vie et de la santé

Spécialité Neurosciences

Par Franck Aby

Les neurones sérotoninergiques du noyau raphé Magnus dans le contrôle de la transmission nociceptive dans la corne dorsale de la moelle épinière : une étude optogénétique dans différents contextes pathophysiologiques

Sous la direction de : Pr Pascal Fossat

Soutenue le 13 Décembre 2019

Membres du Jury

Mme. Nadjar, Agnès	Professeur	NutriNeuro Bordeaux	Présidente
Mme. Pezet, Sophie	Maître de conférences	ESPCI Paris	Rapportrice
Mr. Poisbeau, Pierrick	Professeur	INCI Strasbourg	Rapporteur
Mme, Antri, Myriam	Maître de conférences	Neuro-Dol Clermont-Ferrand	Examinatrice
Mr. Herry, Cyril	Directeur de recherche	Neurocentre Magendie Bordeaux	Membre invité

université de BORDEAUX

THÈSE PRÉSENTÉE

POUR OBTENIR LE GRADE DE

DOCTEUR DE

L'UNIVERSITÉ DE BORDEAUX

Ecole Doctorale des sciences de la vie et de la santé

Spécialité Neurosciences

Par Franck Aby

Serotonergic neurons of the nucleus raphe Magnus in the control of nociceptive transmission in the dorsal horn of the spinal cord: an optogenetic study in different pathophysiological contexts

Under the supervision of: Pr Pascal Fossat

Defended on december, 13th, 2019

Jury members

Mme. Nadjar, Agnès	Professeur	NutriNeuro Bordeaux	Chair
Mme. Pezet, Sophie	Maître de conférences	ESPCI Paris	Rapporteur
Mr. Poisbeau, Pierrick	Professeur	INCI Strasbourg	Rapporteur
Mme, Antri, Myriam	Maître de conférences	Neuro-Dol Clermont-Ferrand	Reviewer
Mr. Herry, Cyril	Directeur de recherche	Neurocentre Magendie Bordeaux	Invited member

Titre : Les neurones sérotoninergiques du noyau raphé Magnus dans le contrôle de la transmission nociceptive dans la corne dorsale de la moelle épinière : une étude optogénétique dans différents contextes pathophysiologiques.

Résumé :

La douleur est une sensation et une expérience émotionnelle désagréable résultant de stimulations potentiellement nuisibles pour protéger l'intégrité du corps. Un mécanisme endogène impliquant le système PAG-RVM, module la sensation de douleur en filtrant les entrées nociceptives. Un équilibre entre des influences excitatrices et inhibitrices contrôle la transmission nociceptive et une perturbation de cet équilibre conduit à l'installation de douleurs pathologiques. Dans ce travail, nous avons utilisé une approche optogénétique pour cibler spécifiquement les neurones sérotoninergiques (5-HT) du noyau du raphé Magnus (RMg) projetant sur la corne dorsale de la moelle épinière. Nous avons montré que ces neurones exerçaient une action analgésique tonique par une diminution de l'excitabilité des neurones de projection de la corne dorsale de la moelle épinière. Cet effet étant indépendant du sexe. Nous avons également observé que les neurones sérotoninergiques (5-HT) sont indirectement liés aux neurones de projection par l'intermédiaire d'interneurones inhibiteurs locaux. Puis, nous avons montré que les neurones sérotoninergiques (5-HT) du RMg recevaient des projections des neurones à somatostatine du ventro-latérale de la substance grise périaqueducale (vlPAG) exerçant une facilitation descendante de la transmission nociceptive. Fait intéressant, nous montrons que dans un modèle de neuropathie périphérique, l'action inhibitrice des neurones à sérotonine (5-HT) du RMg est transformée en influence excitatrice, aussi bien chez les mâles que les femelles, en raison d'un déplacement de l'équilibre du chlore au sein de la moelle épinière. Ces résultats suggèrent que la même voie descendante peut être à la fois excitatrice et inhibitrice dans des conditions pathologiques, révélant des informations cruciales sur les changements à long terme associés à la douleur chronique.

Mots clés : Douleur, moelle épinière, réseaux neuronaux, 5-HT, SST, KCC2, WDR, excitabilité, douleur neuropathique, genre, électrophysiologie *in vivo*, optogénétique, pharmacologie.

Unité de recherche

Institut Interdisciplinaire de Neurosciences CNRS UMR5297

Centre Broca Nouvelle-Aquitaine, 146 rue Léo Saignat 33076 BORDEAUX

Title: Serotonergic neurons of the nucleus raphe Magnus in the control of nociceptive transmission in the dorsal horn of the spinal cord: an optogenetic study in different pathophysiological contexts

Abstract:

Pain is an unpleasant sensation and emotional experience elicited by potentially harmful stimulations to protect the integrity of the body. An endogenous mechanism involving the PAG-RVM modulatory system control pain sensation by filtering nociceptive inputs. A balance between both excitatory and inhibitory influences control nociceptive transmission and impairment in this balance leads to the development of pathological pain. In the present study, we used an optogenetic approach to specifically target serotoninergic neurons (5-HT) that projected to the dorsal horn of the spinal cord. We showed that these neurons exerted a tonic analgesic action through a decreased excitability of projection neurons of the dorsal horn of the spinal cord. This effect is gender independent. We also observed that 5-HT neurons are indirectly connected to projection neurons through local inhibitory interneurons. Then, we showed that 5-HT neurons of the RMg received descending inputs from the SST neurons of the ventro-lateral part of the periaqueductal gray (vlPAG) that exerted downward facilitation on pain transmission. Interestingly, we show that 5-HT inhibitory action is switched to an excitatory influence in a model of peripheral neuropathy due to a spinal chloride equilibrium shift. These results suggest that the same descending pathway can be both excitatory and inhibitory upon pathological conditions, providing crucial insights about long-term changes associated with chronic pain.

Keywords: Pain, spinal cord, neural networks, 5-HT, SST, KCC2, WDR, excitability, neuropathic pain, gender, *in vivo* electrophysiology, optogenetics, pharmacology.

Unité de recherche

Institut Interdisciplinaire de Neurosciences CNRS UMR5297

Centre Broca Nouvelle-Aquitaine, 146 rue Léo Saignat 33076 BORDEAUX

RESUME DE LA THESE

La douleur est un système d'alerte essentiel qui protège l'organisme contre les lésions tissulaires réelles ou potentielles. La sensation de douleur est généralement désagréable mais s'atténue une fois le corps averti du danger et la zone endommagée sûre. Ce contrôle de la douleur est dû à l'existence d'un système endogène capable de moduler la transmission douloureuse. Ce système endogène est mobilisé aussi bien dans un contexte de stress aigu, dans lequel la sensation de douleur peut être efficacement diminuée ou supprimée, que par un contrôle inhibiteur nociceptif diffus (DNIC). Le système de contrôle endogène de la douleur est principalement constitué par une voie descendante contrôlant la transmission nociceptive directement au niveau de la corne dorsale de la moelle épinière, premier relais par lequel passent les informations nociceptives. Il est considéré dans la littérature que les voies descendantes excitatrices et inhibitrices contrôlent toutes deux la transmission nociceptive. Cependant, l'équilibre entre les deux influences est altéré dans le cas de douleur pathologique, ce qui favorise les facilitations plutôt que les inhibitions. La voie descendante de la douleur implique différents noyaux du tronc cérébral qui projettent directement ou indirectement sur la moelle épinière. Les projections indirectes, notamment ceux provenant de la partie ventro-latéral de la substance grise périaqueducale (vlPAG), ont généralement un relais sur le bulbe rostral ventromedial (RVM) d'où projettent des influences inhibitrices et excitatrices sur la corne dorsale de la moelle épinière. Au sein de la RVM, les cellules sérotoninergiques (5-HT) constituent une importante population neuronale se limitant à des noyaux précis (noyau obscurus, paragigantocellularis et raphé Magnus). Les neurones 5-HT du noyau raphé Magnus (RMg) projettent vers la partie dorsale de la moelle épinière et sont impliqués dans le contrôle de la douleur. Ce contrôle de la transmission nociceptive est fortement dépendant du contexte physiopathologique. De plus, il existe une grande diversité de récepteurs 5-HT affectant différemment les neurones de la corne dorsale. **Cependant, à ce jour, le rôle exact des neurones 5-HT du RMg dans la transmission nociceptive n'est toujours pas éclairci**.

Afin de déterminer le rôle exact des neurones 5-HT du RMg dans la transmission nociceptive, nous avons utilisé une approche à la fois virale, pharmacologique et électrophysiologique chez les souris ePet-cre qui exprime la cre-recombinase spécifiquement dans les neurones à 5-HT.

Tout d'abord, nous avons confirmé la bonne expression de la cre-recombinase limitée aux neurones 5-HT dans le raphé Magnus (RMg) ainsi que dans le raphé dorsal (DR) et le raphé médian (MR) en croisant des souris ePet-cre à des souris rapportrices Ai9. Par un marquage

immunohistochimique de la tryptophane hydroxylase 2 (TPH2) nous avons observé une co-localisation avec des neurones cre positif s'élevant à 83,8%. Nous avons également observé une population dense de fibres 5-HT dans la corne dorsale de la moelle épinière confirmant ainsi les projections 5-HT sur la moelle épinière. Puis, en utilisant une souris Gad67-GFP, nous avons confirmé que les neurones 5-HT du RMg ne sont pas des neurones GABAergiques mais présentaient un degré élevé d'interaction avec eux.
Ainsi nous nous sommes rendus compte que les souris ePet-cre nous donnaient un outil crucial pour étudier le rôle précis de ces neurones dans la transmission nociceptive.

Dans un second temps, afin de valider notre approche virale, nous avons réalisé une injection stéréotaxique d'un virus inductible permettant ainsi l'expression d'opsine ChR2 dans les neurones 5-HT du RMg. Puis trois semaines après, nous avons réalisé des enregistrements de neurones 5-HT exprimant les opsines en patch-clamp en courant imposé sur tranches de RMg. Nous avons observé que la stimulation optogénétique à 475nm induisait d'une part une dépolarisation neuronale rapide et reproductible et qu'un mode de stimulation à 5Hz/5ms induisait d'autre part un train de potentiels d'action suivant fidèlement la stimulation optogénétique. En revanche, la stimulation optogénétique à 525nm induisait une forte hyperpolarisation qui s'estompait avec l'arrêt de la stimulation **confirmant ainsi que notre approche optogénétique nous permettait de moduler l'activité des neurones à 5-HT du RMg**. De plus, en accord avec la littérature, nous avons observé des projections 5-HT du RMg visibles dans les couches profondes de la corne dorsale de la moelle épinière.

Afin d'étudier les conséquences d'une manipulation des neurones 5-HT du RMg, nous avons effectué une stimulation optogénétique de ces neurones à l'aide de fibres optiques placées aussi bien au-dessus du RMg que de la partie lombaire de la moelle épinière. En comportement, chez des souris 5-HT cre en absence de lésion nerveuse, nous avons observé que l'inhibition optogénétique sélective des neurones 5-HT que ce soit au-dessus de la RMg ou de la corne dorsale spinale induisait une importante hypersensibilité mécanique et thermique confirmant ainsi que les neurones RMg 5-HT étaient toniquement actifs et jouaient un rôle crucial dans le contrôle de la transmission nociceptive. En revanche, l'activation optogénétique des neurones 5-HT ou de leurs projections, au-dessus de la RMg ou de la corne dorsale de la moelle épinière, engendrait une importante analgésie mécanique et thermique. **Par conséquent, nous avons pu en conclure que les neurones RMg 5-HT exerçaient une inhibition tonique descendante de la transmission nociceptive constituant ainsi un des contrôle inhibiteur descendant endogène de la douleur**.

En raison des différences entre les sexes dans l'intégration de la douleur, nous avons comparé la manipulation des neurones 5-HT chez les sujets mâles et femelles et n'avons observé aucune différence entre les deux.

Pour confirmer les cibles spinales de la manipulation des neurones 5-HT, nous avons effectué des enregistrements électrophysiologiques *in vivo* des neurones de la corne dorsale en ciblant spécifiquement les neurones à convergence (WDR) qui sont des neurones de projection recevant entre autres des entrées nociceptives des fibres C. Nous avons d'abord évalué la conséquence d'une inhibition des neurones RMg 5-HT sur l'activité des WDR, et nous avons observé que l'inhibition optogénétique des projections 5-HT entraînait une augmentation de l'activité spontanée des WDR et de leur réponse aux entrées nociceptives de fibres C ainsi qu'une augmentation de leur capacité à être sensibilisé. D'autre part, l'activation optogénétique des fibres descendantes RMg 5-HT directement au-dessus de la moelle épinière induisait une diminution significative des réponses évoquées des neurones WDR aux entrées nociceptives et une diminution significative de leur capacité à être sensibilisés. **Par conséquent, nous montrons que les neurones 5-HT du RMg projetant sur la corne dorsale de la moelle épinière, inhibent constitutivement la transmission nociceptive en diminuant l'excitabilité des WDR.**

Dans le but de déterminer les cibles des neurones 5-HT du RMg sur les microcircuits de la corne dorsale, à l'aide de marquages immunohistochimiques de la tryptophane hydroxylase 2 (TPH2), chez des souris Gad67-GFP, nous avons observé des potentiels boutons synaptiques de terminaison de neurones 5-HT sur des neurones GABA dans les couches profondes de la corne dorsale de la moelle épinière. Pour confirmer ces connexions au réseau inhibiteur local, nous avons dans un premier temps comparé, chez des souris 5-HT cre injectées avec un AAV inductible marqué à la GFP, les appositions entre les neurones GFP positifs et les neurones excitateurs (TLX3) ou inhibiteurs (PAX2) et nous avons constaté que les projections 5-HT sont nettement plus en contact avec les interneurones inhibiteurs. Puis, nous avons confirmé la présence de contacts réels entre les neurones RMg 5-HT et les neurones inhibiteurs, en utilisant des souris Gad 67-GFP*5-HT cre dans lesquelles SynMYC-revWPRE (marqueur de terminaison synaptique) a été exprimé dans les neurones RMg 5-HT. À l'aide d'un immunomarquage sur une fine coupe transversale de la partie lombaire de la moelle épinière, nous avons trouvé des boutons synaptiques des projections 5-HT sur les neurones à GABA et à parlvalbumine. Dans un second temps, afin de déterminer le rôle fonctionnel de ces contacts, nous avons éliminé les inhibitions induites par les neurones GABAergique/glycinergiques dans

la corne dorsale spinale via l'injection de picrotoxine. Nous avons observé que la stimulation optogénétique des projections RMg 5-HT n'induisait plus une inhibition de la transmission nociceptive. En effet, en réalisant un enregistrement électrophysiologique associé à une stimulation optogénétique des projections 5-HT au-dessus de la moelle épinière, nous avons observé qu'un blocage de la neurotransmission GABAA/GlyR suite à une injection intrathécale de picrotoxine, n'induisait plus de diminution de la réponse évoquée des WDR aux stimuli nocifs. **Par conséquent, nous avons montré que l'inhibition tonique descendante de 5-HT du RMg sur la transmission nociceptive passe par une excitation directe des interneurones inhibiteurs GABAergic/glycinergic dans les couches profondes de la moelle épinière qui à leur tour inhibent les neurones WDR de la corne dorsale de la moelle épinière.**

Dans un deuxième temps, en collaboration avec l'équipe de Cyril Herry, nous avons essayé de déterminer comment l'activité des neurones RMg 5-HT était modulée. Pour ce faire, à l'aide d'immunomarquages nous avons observé des potentiels boutons synaptiques de terminaison de neurones GABAergiques, glutamatergiques et exprimant de la somatostatine (SST) sur des neurones 5-HT. **Nous avons d'abord établi le rôle fonctionnel des neurones SST du vlPAG sur la transmission nociceptive spinale en utilisant des souris SOM-IRES-cre**. Dans une approche comportementale, nous avons effectué des manipulations optogénétiques de ces neurones en utilisant des fibres optiques implantées bilatéralement au-dessus du vlPAG. L'inhibition optogénétique des neurones SST a provoqué une importante analgésie mécanique et thermique, ce qui démontre que les neurones SST du vlPAG exercent une facilitation tonique descendante de la transmission nociceptive. Cet effet facilitateur est confirmé par l'activation optogénétique des neurones SST qui provoque une hypersensibilité mécanique et thermique significative. **Par conséquent, nous déterminons que les neurones SST du vlPAG exercent une facilitation tonique descendante sur la transmission nociceptive qui est opposé à l'action des neurones 5-HT sur la transmission nociceptive.**

Ensuite, nous avons réalisé des enregistrements électrophysiologiques des neurones de la corne dorsale, centré également sur les neurones à convergence. Nous avons observé que l'inhibition optogénétique bilatérale des neurones SST du vlPAG induisaient à la fois une diminution significative de la réponse des neurones WDR en réponse aux entrées nociceptives ainsi qu'une diminution significative de leur capacité de sensibilisation. En revanche, l'activation optogénétique bilatérale des neurones SST du vlPAG a induit une augmentation significative de la réponse WDR aux entrées de fibres C nociceptives ainsi qu'une augmentation de leur capacité à être sensibilisés. **Par conséquent, nous avons montré que les neurones SST**

du vlPAG facilitent la transmission nociceptive en augmentant l'excitabilité des neurones de la corne dorsale.

Puis, afin de déterminer les circuits neuronaux impliqués dans cet effet, nous avons évalué, dans un premier temps, les cibles des neurones SST vlPAG dans la RVM et en particulier dans le RMg. En développant une stratégie virale et un marquage immunohistochimique, nous avons observé une apposition entre les projections SST du vlPAG et les neurones 5-HT de RMg projettant sur la moelle épinière. Nous avons également observé l'existence de projection de neurones SST du vlPAG en faible quantité dans la corne dorsale de la moelle épinière, en particulier dans la couche superficielle. On peut donc conclure que parmi les projections du vlPAG sur le RMg, **il existe un circuit de neurones SST du vlPAG qui projettent vers des neurones 5-HT du Raphé Magnus projetant sur la moelle épinière (voie indirecte). De plus, certains neurones SST établissent aussi des connections directes de longue portée sur la moelle épinière (voie directe).**

Afin de déterminer le rôle fonctionnel des différentes projections (directe et indirecte) des neurones SST du vlPAG sur la transmission nociceptive, nous avons tout d'abord évaluer le rôle fonctionnel du circuit SST du vlPAG - 5-HT du RMg sur la transmission nociceptive (voie indirecte), chez des souris SOM-IRES-CRE en comportement, nous avons réalisé une activation optogénétique des projections SST du vlPAG au-dessus du RMg et observé une hypersensibilité mécanique et thermique significative. Puis, nous avons observé que l'activation optogénétique des projections SST du vlPAG au-dessus de la RMg entraînait également une hyperexcitabilité des neurones WDR. Cependant, en évaluant le rôle fonctionnel des projections directes des neurones SST du vlPAG sur la moelle épinière par des enregistrements électrophysiologiques unitaires ciblant les WDR associés à une stimulation optogénétique au-dessus de la moelle épinière, nous n'avons observé aucun changement dans l'excitabilité des WDR. **Par conséquent, nous pouvons en conclure que les neurones SST du vlPAG exercent une facilitation tonique descendante sur la transmission nociceptive via une action probable sur des neurones 5-HT du RMg**.

Dans un troisième temps, nous avons étudié les conséquences de la modulation des neurones 5-HT du RMg sur la transmission nociceptive en condition neuropathique.

La 5-HT est connue pour faciliter la transmission de la douleur dans un contexte pathologique. Nous avons utilisé le modèle de neuropathie périphérique de lésions nerveuses partielles (SNI) pour étudier les conséquences de la manipulation optogénétique des neurones 5-HT du RMg sur la transmission nociceptive. Nous avons d'abord confirmé que la procédure SNI provoque une hypersensibilité mécanique et thermique à la douleur. Il est intéressant de noter que suivant

la même approche que celle que nous avons adoptée dans le cas d'une douleur aiguë, l'inhibition optogénétique des neurones 5-HT ou de leurs projections au-dessus de la RMg ou de la corne dorsale de la moelle épinière respectivement ne produisent plus aucun changement dans la sensibilité mécanique et thermique, ce qui suggère que dans un contexte pathologique, les neurones 5-HT du RMg perdent leur effet analgésique tonique. En revanche, l'activation optogénétique au-dessus de ces mêmes neurones ou de leurs projections, curieusement, a induit une diminution significative du seuil de douleur mécanique et de la latence thermique de la douleur. **Cet effet était également indépendant du sexe puisque aucune différence n'a été observée chez les mâles et les femelles testés**. **Ainsi, dans la douleur neuropathique, les neurones 5-HT du RMg perdent leur effet analgésique et exercent une facilitation descendante sur la transmission de la douleur.** En effectuant des enregistrements electrophysiologiques, nous avons montré que l'inhibition optogénétique des projections 5-HT du RMg n'engendrait aucun changement dans l'excitabilité des WDR, tandis que l'activation optogénétique des projections 5-HT du RMg induisait une hyperexcitabilité des WDR. **Par conséquent, en cas de douleur neuropathique, nous avons montré que les neurones 5-HT se projetant sur la corne dorsale facilitent la transmission nociceptive en augmentant la réponse des WDR aux entrées de fibres C, ce qui entraîne une hyperexcitabilité des WDR**. Ensuite, nous avons étudié si la mise en place de la neuropathie pouvait induire des modifications des cibles des neurones 5-HT sur la corne dorsale de la moelle épinière pouvant ainsi expliqué l'effet opposé de ces neurones à 5-HT sur la transmission nociceptive. Nous avons constaté que les fibres 5-HT se projettent toujours principalement sur les interneurones inhibiteurs. Ayant précédemment montré que l'effet analgésique des neurones à 5-HT en condition de douleur aiguë dépend des interneurones inhibiteurs et des courants chlorure médiés par les récepteurs canaux GABA/glycine, **l'homéostasie des ions chlorures des interneurones inhibiteurs de la corne dorsale pourrait être impliquée dans la facilitation médiée par les neurones 5-HT du RMg en condition de douleur neuropathique**.

Dans un modèle de douleur neuropathique incluant le SNI, il a été démontré que les mécanismes de désinhibition médiés par une déficience dans l'activité des co-transporteurs (Na^+-K^+-Cl^-) KCC2 (Doyon, 2011 ; Kaila et al., 2014) sont responsables d'une partie de l'hyperexcitabilité neuronale et de l'hypersensibilité de la douleur (Coull et al., 2005 ; Beggs et al., 2012). **Nous avons donc évalué la conséquence du changement de l'équilibre en chlorure des fibres afférentes ou des neurones WDR sur l'entraînement sérotoninergique opposé observé chez les souris témoins et les souris SNI, en utilisant une approche pharmacologique pour stimuler le co-transporteur KCC2 chez la souris SNI**. En effet,

1h30 après un traitement par voie orale avec de la CLP290 chez des souris 5-HT cre présentant une hypersensibilité mécanique et thermique, la même stimulation optogénétique des projections 5-HT du RMg chez les mêmes animaux provoque une analgésie mécanique et thermique significative, absente lors de l'utilisation du véhicule seul. Cet effet inhibiteur n'est pas lié au sexe puisqu'il est équivalent chez les mâles et les femelles. Ainsi, dans les conditions neuropathiques, nous avons montré que la facilitation induite par la RMg 5-HT est due au déséquilibre du gradient de chlore résultant de la diminution de l'activité du co-transporteur KCC2 et qu'une augmentation de l'activité du co-transporteur KCC2 peut inverser les conséquences du SNI. Puis, nous avons observé que la superfusion de CLP290 au-dessus de la moelle épinière supprime l'augmentation de l'excitabilité des WDR induite par l'activation optogénétique des projections 5-HT au-dessus de la moelle. **Par conséquent, dans des conditions de douleur neuropathiques, nous avons montré que l'hyperexcitabilité WDR induite par la 5-HT du RMg est une conséquence de la diminution de l'activité du cotransporteur KCC2.**

Enfin, nous avons évalué les conséquences d'un blocage de KCC2 chez des souris naïves par injection ip de furosémide. Nous avons observé que l'activation optogénétique des projections 5-HT du RMg provoquait une hypersensibilité mécanique et thermique. Cet effet était équivalent chez les mâles et les femelles.

En conclusion, la manipulation de KCC2 a orienté le signe de l'influence descendante de 5-HT sur la transmission nociceptive, qui passe de l'inhibition de la douleur à la facilitation dans un contexte pathologique. L'ensemble de ces résultats suggère fortement que les changements dans l'équilibre en chlorure de la corne dorsale de la moelle épinière des souris neuropathiques influencent le contrôle de la douleur endogène.

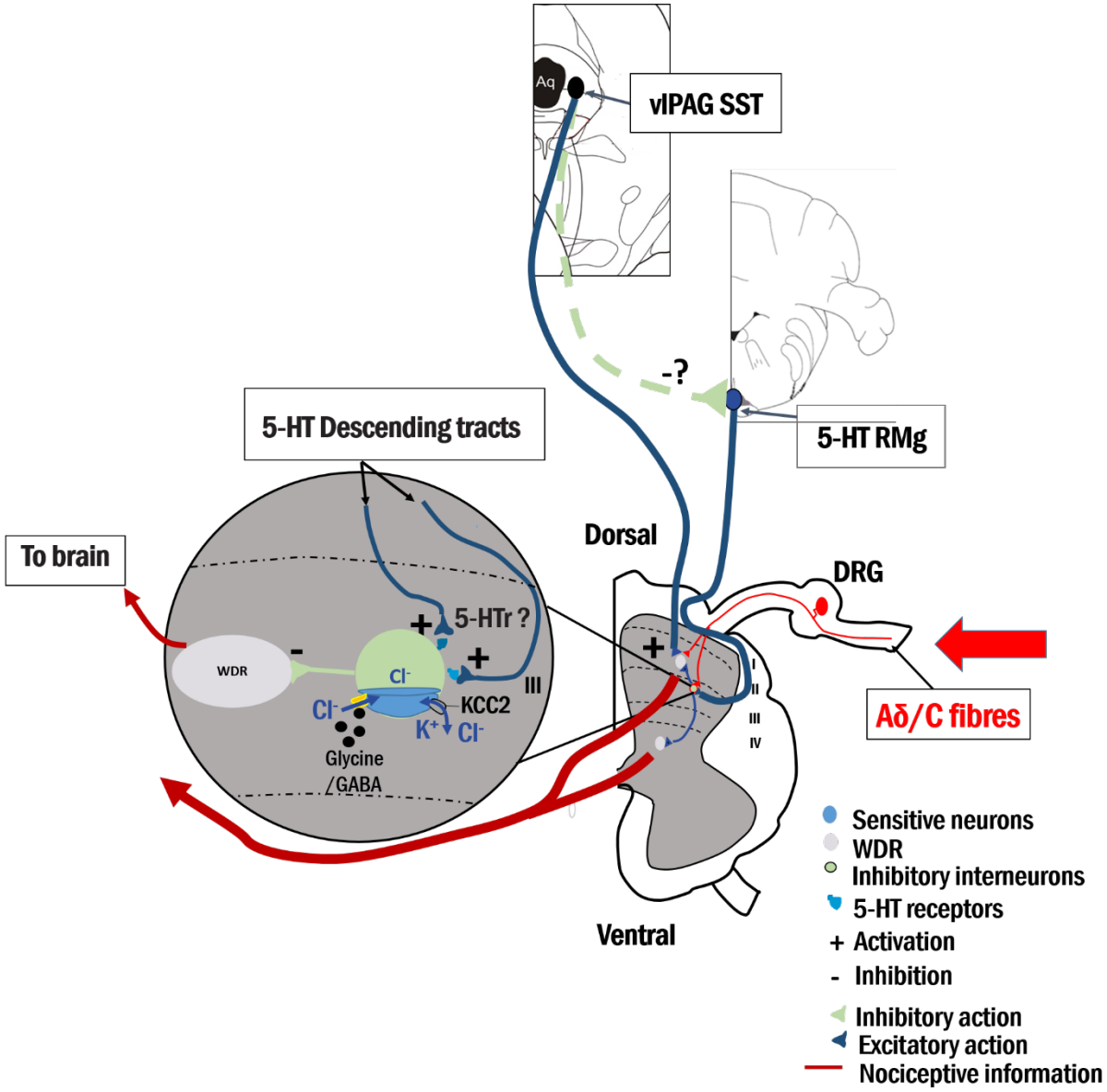

Figure 1 : Schéma récapitulatif du contrôle de la transmission nociceptive dans la corne dorsale de la moelle épinière par les voies descendante supra-spinale, le rôle des interneurones à somatostatine du vlPAG et des neurones sérotoninergique du RMg.

Remerciements

Je tiens tout d'abord à remercier sincèrement les membres du jury de thèse : le Dr. Pierrick Poisbeau et le Dr. Sophie Pezet pour avoir accepté de juger ce travail et d'en être les rapporteurs, Dr. Antri Myriam pour avoir bien voulu examiner ce travail, Dr. Herry Cyril pour cette collaboration ainsi que toute l'assistance et conseils apportés au cours de ces années et le Dr. Nadjar Agnès pour avoir accepté de présider cette soutenance. Au détour d'un congrès, d'un symposium ou d'une conversation privée, comme ce fut déjà le cas par le passé, j'aurai toujours plaisir à vous saluer et discuter de nos travaux.

Je tiens à exprimer ma profonde gratitude et mon estime au Dr Marc LANDRY, directeur du laboratoire, qui m'a chaleureusement accueilli au sein de son équipe et qui s'est toujours rendu disponible pour échanger et partager que ce soit sur des sujets de recherche que sur des sujets relatifs à l'expérience de la vie.

Je remercie bien évidemment tous les membres de la Team LANDRY, en commençant par notre aîné le Pr. André CALAS, pour toute l'expérience partagée, les conseils prodigués ainsi que pour toutes ses anecdotes. Merci au Dr. Yves LE FEUVRE, pour ses conseils et son aide, au Dr. Alexandre FAVERAUX, pour tous les moments de partage autour d'une table ou d'un ballon de basket, au Dr Christel BAUDET pour tous ses conseils, les moments de rigolade et de partage.

Je tiens à adresser des remerciements bien particuliers au Dr Rabia BENAZZOUZ ; je n'aurai que trop peu de mots pour définir tout ce qu'elle a su m'apporter, je me contenterai juste de lui dire merci, merci d'être qui elle est et merci pour tous ces moments passés et j'espère à venir. Merci Rabia, merci pour tout.

Je porte une attention toute particulière à mon cher et tendre Directeur de thèse Pascal FOSSAT pour « **TOUTE** » la « **PATIENCE** » dont il a fait preuve durant ces 5 années. Merci de t'être autant investi durant toutes ces années. Outre le fait de m'avoir enseigné l'art délicat de l'électrophysiologie unitaire *in vivo*, je te remercie pour toute la rigueur scientifique inculquée, pour ton soutien en toutes circonstances et ce malgré les très nombreux « **IL VA FINIR PAR ME TUER UN JOUR** ». Merci d'avoir répondu présent à toutes ces idées les plus farfelues les unes que les autres que j'ai pu te présenter.

Sur un plan plus personnel, merci pour ton amitié, tes conseils, ton aide et encore une fois tout ton soutien. Merci d'être mon Pascal (pour le reste on se verra en aparté).

Merci aux étudiants qui ont partagé notre quotidien et animé le bureau des étudiants : Yazid, Amanie, Mariam, Nino, Constantin, Laura, Anthony, et j'en oublie certainement. Et merci à ceux qui le partagent encore et qui prendront la relève : Zoé, Yadali, Cynthia et Thibault, merci pour ces moments de joie et de folie.

Un merci tout particulier à Sara et à Walid qui ont fait leur stage de master1 et 2 sur le projet 5-HT, merci pour votre aide et merci d'avoir été des amours.

Je n'oublie pas ceux qui nous ont précédés ; Houda et ses petites questions, Otmane mon frère pour tous ces moments de partage, de souffrance, de rigolade et j'en passe, Joao, qui a commencé sa thèse en même temps que moi et à qui je souhaite le meilleur pour la suite, Olivier pour son amitié et son aide, Maria, Charline et Anaïs pour tous nos moments d'échange et de partage, Sébastien pour nos discussions, nos matchs de basket et pour son aide.

Petite pensée pour tous les thésards de 3ème ou 4ème année qui ont soutenu ainsi que ceux qui vont le faire dans les années à venir (Thiago, Thomas et j'en oublie) avec une attention toute particulière pour mon Vladimir, merci à toi d'être qui tu es.

Un grand merci aux autres équipes IINS pour leur aide, avec une mention spéciale pour la TEAM MULLE (remerciements particuliers à Séverine, Gael, Dario, Noel, Sandrine), la TEAM GAMBINO (Frédéric, Elisabetha, Nicolas), la TEAM GROC (Julien, François, Joana), la TEAM ROUX (Camille, Edith, Pascal, Tiphaine et Lisa) et la TEAM HUMEAU (Urielle, Yann et anciennement Hajer).

Un grand merci à la plateforme *in vivo* et plus particulièrement à Audrey, Mélissa Amandine, Guillaume, Laetitia et Elisabeth qui ont pris soin de nos lignées de petites souris et pour le super travail qu'ils font au quotidien.

Je remercie également Christel (merci pour tout), Fabrice, Sébastien, Magali, Monica du BIC pour m'avoir formé et apporté leur aide sur l'utilisation des différents plateformes et logiciels, Mélina et Sabrina pour toute leur expérience partagée en microscopie électronique. Merci pour ces moments de fous rires.

Je tiens à remercier chaleureusement Rémi, pour nos moments d'échange et d'entraide. Merci également à Jessica et sa relève pour l'énorme travail qu'ils effectuent et ont effectué au sein de l'institut et pour leur aide précieuse. Merci de nous mettre dans d'aussi bonnes conditions de travail !

Merci à toute l'équipe administrative; Cédric, Mélanie, Marie-France, Marie-Noelle, Arlette, Martine, Pauline, Philippe, Laurent et jean François qui font un travail remarquable et sont toujours disponibles pour nos nombreuses questions et autres angoisses au quotidien.

Un grand merci aux autres équipes du Campus notamment celles de Magendi avec une attention toute particulière pour l'équipe FRICK (Mélanie et Andréas), l'équipe HERRY (attention spéciale à Cyril, Nanci, Ha Rang, Suzana, Marianne, Valentine), l'équipe OLIET (attention spéciale à Aurélie, Philippe, Aude, Nadège, et Stéphane, l'équipe de l'IMN avec une mention spéciale pour la Team BENAZZOUZ (Abdelhamid BENAZZOUZ, Lamiaa, Frédéric et Kéri-Ann), l'équipe de l'école des neurosciences (Sandrine, Antonella, Mariella…). Merci à vous pour tous ces moments partagés au cours de cette thèse.

Un grand merci à vous mes intimes ; ceux qui m'accompagnent depuis ma toute petite enfance mais aussi ceux qui ont croisé mon chemin un peu plus tard et qui ne l'ont plus quitté depuis. Merci pour votre présence, vos encouragements, votre soutien, vos appels et votre amour. On est ensemble !

Elsa, merci pour ton soutien, ton amour, ta folie et ta joie de vivre qui rendent mon quotidien tellement plus agréable. Je te remercie de bien vouloir me suivre dans ma folie, merci de savoir me canaliser et lire en moi. Merci d'avoir voulu m'accompagner dans cette expérience aussi bien professionnelle que personnelle.

Spéciale dédicace à ma famille, merci à vous tous pour tout ce que vous avez fait et continuez de faire pour moi. Merci pour vos conseils, votre soutien, votre amour, votre force et votre présence au quotidien à mes côtés. Que dire de plus que vous ne savez déjà, sachez juste que je vous aime toujours un peu plus que la vieille et un peu moins que le lendemain et que cette thèse est aussi la vôtre.

Pour terminer, je tiens à partager une pensée toute particulière pour ceux qui m'ont quitté (Mes amours M. et Mme ALEXANDRE, Tonton Johnson, Tonton et Tantie Cole, Tantie Marina et vous mes ami(e)s parti(e)s si tôt…). Merci à vous pour tout ce que vous avez fait pour moi ; merci pour votre amour, votre soutien, votre présence… Sachez que je vous aime et que les promesses faites seront tenues.

Merci à toi mon Dieu pour tout ce que Tu fais pour moi.

Avant- propos

L'ensemble des travaux de thèse présenté dans ce manuscrit a été réalisé au sein de l'Institut Interdisciplinaire de Neurosciences CNRS UMR5792 dirigé par Dr. Daniel Choquet dans l'équipe « Mécanisme central de la sensibilisation à la douleur » dirigée par le Pr. Marc Landry sous la direction du Pr. Pascal Fossat et les résultats obtenus au cours de ce projet sont en cours de publication. Cependant au cours de ma thèse, j'ai contribué à la réalisation d'autres projets qui ont donné lieu aux publications suivantes :

Publications

Causal link between developmental n-3 PUFA deficiency and motivation deficits.
Ducrocq, F and Walle, R and Contini, A and Oummadi, A and Caraballo, B and Van der Veldt, S and Boyer, M and **Aby, F** and Tolentino-Cortez, T and Helbling, JC and Martine, L and Grégoire, S and Cabaret, S and Vancassel, S and Layé, S and Kang, JX and Fioramonti, X and Berdeaux, O and Barreda-Gómez, G and Masson, E and Ferreira, G and Ma, D W. L. and Bosch-Bouju, C and De Smedt-Peyrusse, V and Trifilieff, P.
En revision pour Cell Metabolism, DOI: 10.2139/ssrn.3382436

Windup of Nociceptive Flexion Reflex Depends on Synaptic and Intrinsic Properties of Dorsal Horn Neurons in Adult Rat.
Aby, F; Bouali-Benazzouz, R; Landry, M; Fossat, P.
Preprints 2019, 2019100006 (doi: 10.20944/preprints201910.0006.v1).

Inflammatory-induced spinal dorsal horn neurons hyperexcitability is mediated by P2X4 receptors.
Aby F, Whitestone S, Landry M, Ulmann L, Fossat P.
Pain Rep. 2018 May 23;3(3):e660. doi: 10.1097/PR9.0000000000000660.

Calcium signalling through L-type calcium channels: role in pathophysiology of spinal nociceptive transmission.
Roca-Lapirot O, Radwani H, **Aby F**, Nagy F, Landry M, Fossat P.
Br J Pharmacol. 2018 Jun;175(12):2362-2374. doi: 10.1111/bph.13747. Epub 2017 Mar 24. Review.

Group I metabotropic glutamate receptor plasticity after peripheral inflammation alters nociceptive transmission in the dorsal of the spinal cord in adult rats.
Radwani H, Roca-Lapirot O, **Aby F**, Lopez-Gonzalez MJ, Benazzouz R, Errami M, Favereaux A, Landry M, Fossat P.
Mol Pain. 2017 Jan-Dec;13:1744806917737934. doi: 10.1177/1744806917737934.

LIST OF ABBREVIATIONS

5-HT: 5-hydroxytryptamine (serotonin)

AAV: Adeno-Associated Virus

ACC: Anterior Cingulate Cortex

ACd: dorsal Anterior cingulate Cortex

ACH: Acetylcholine

ACSF: Artificial Cerebro Spinal Fluid

ArchT: Archaerhodopsin

BSA: Bovine Serum Albumin

CAG: Chicken β Actin promoter

CEA: Central Amygdala

ChR2: Channelrhodopsin 2

DA: Dopamine

DRG: Dorsal Root Ganglia

FG: Fluorogold

GABA: Gamma-Aminobutyric Acid

GAD 65-67: Gamma-Aminobutyric Acid gene promoter 65 and 67

GAD67: Gamma-Aminobutyric Acid gene promoter 67

GFP: Green Fluorescent Protein

Glu: Glutamate

Gly: Glycine

IASP: International Association for the Study of Pain

IP: Intraperitoneal

IT: Intrathecal

KCC2 Potassium-chloride transporter member 5

P2X: Purinergic Receptor Ionotropic

PAG: Periaqueductal grey

PBS: Phosphate-buffered saline

PFA: Paraformaldehyde

PWT: paw withdrawal threshold

rACC: rostral Anterior Cingulate Cortex

SERT: Serotonin transporter

SNI: Spared nerve injury

SOM or SST: somatostatin

SUDO: simplified up and down

Syn: Synaptaphysin

TPH2: Tryptophan hydroxylase 2

DIO: Double-floxed Inverse Open reading frame

DMSO: Dimethyl sulfoxide

DR: Dorsal Raphe

eGFP: Enhanced Green Fluorescent Protein

MR: Median Raphe

RMg: Raphe Magnus

RMg 5-HT: Serotonin neurons of the raphe Magnus

RVM: medulla rostral ventral

VGLUT1-3: Vesicular transporter of glutamate 1 and 3

vlPAG SST: somatostatin neuron of the Periaqueductal grey ventrolateral

WDR: Wide dynamic range

YFP: yellow-fluorescent protein

I. INTRODUCTION

A. PAIN

1. Concept and Definition

From ancient times, pain has always been a major issue of mankind, and therefore became the centre of attention and the object of ongoing struggle to understand and control it. Time after time, pain has been conceptualized in different ways, reflecting the contemporary spirit of the age and, therefore, has changed over recorded history with changing world views. It appeared that for primitive humans, there is a causal relationship between painful disease or pain caused by injury and magic fluids intrusion, evil spirits, or demons into the body (Tainter, 1948). By contrast, for the ancient Egyptians *(Figure 2)*, painful adversity was most related to Lord's will or dead spirits (Leipzig, 1875), especially according to our good deeds we felt more or less evil. Idea behind the concept that the heart symbolizing our good deeds, was the centre of sensation.

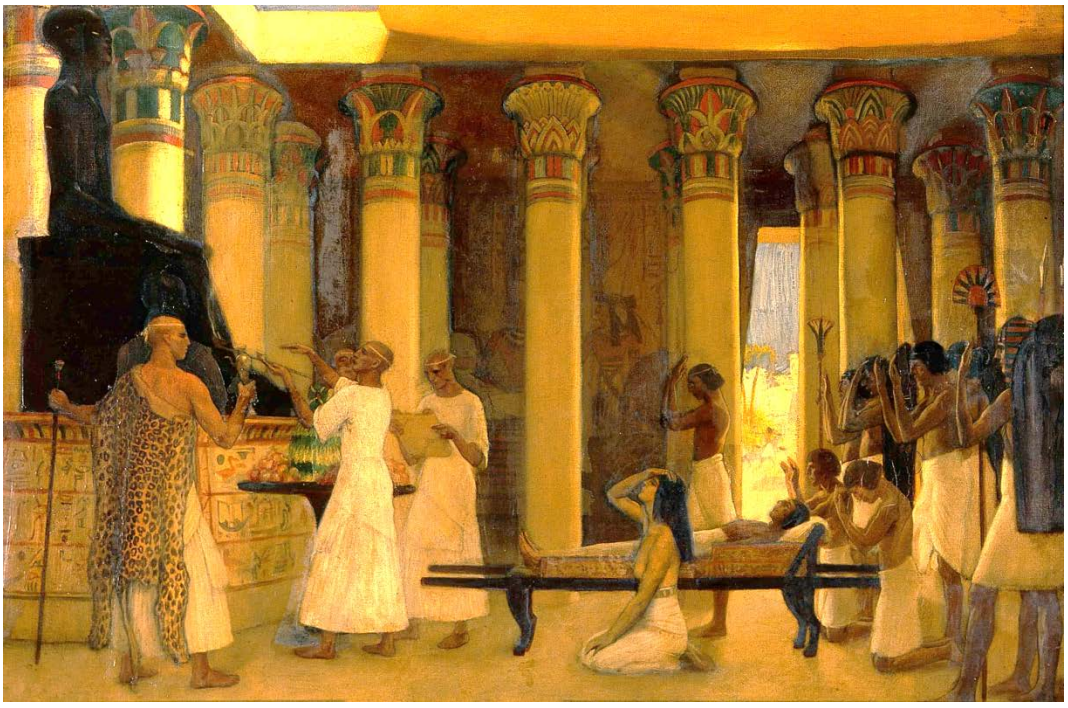

Figure 2 : Illustration of the doctors reciting an incantation and praying the gods to assist the patient's healing before initiating any treatment (from School History, 2018).

For ancient Chinese *(Figure 3)*, pain has been considered to be due to an imbalance of two opposing unifying forces the *Yin* (passive force) and the *Yang* (active force), which result to a major disruption of flow of *the chi*, the vital energy associated with these two forces which

diffuse along the body through a 14 meridians network each linked to an internal organ or function and then affecting the organ or function associated (Saunders, 1967).

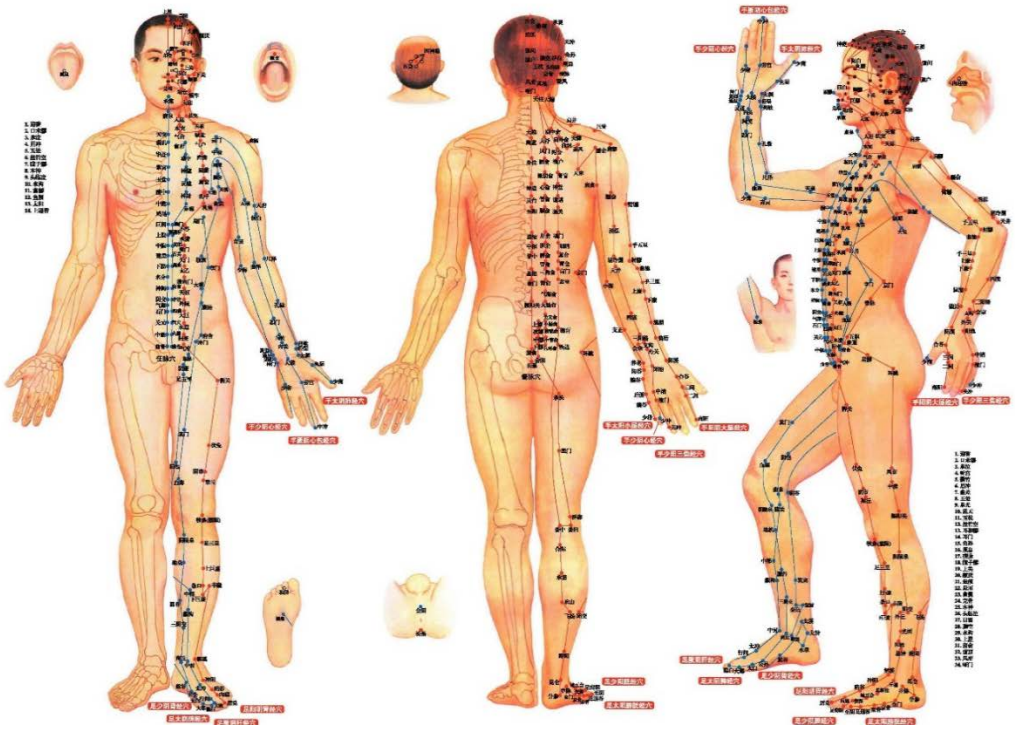

Figure 3 : Illustration of meridians in Traditional Chinese Medicine (from TCM, Woodbridge, 2019). Meridians in traditional Chinese medicine (TCM) are interconnected channels of the human body through which Chi, the body's vital energy flows. There are several types of them related to the theories the anma, the Ying and the Yang and the five elements. TCM aims first and foremost to maintain the harmony of energy within the body as well as between the body and external elements base on balance within the meridians. Health is related to the body's ability to maintain the dynamics necessary to cope with aggression. On the other hand, the disease occurs when the body has lost its ability to adapt.

Concept close to the theory of the "*Corpus Hippocratium*" with the idea of a balance of the four moods, blood, phlegm, yellow bile and black bile in which pain occurred when there is an imbalance in one of these humours (Keirsey, 1998), theory-based on ancient Greece belief where the nature of sensory inputs and sensory organs of the body was put at the centre of their concerns (Keele, 1957). Starting in the Middle Age, in Europe, the concept that the centre of the sensory perception is more the brain than the heart appeared notably with the work of Albertus Magnus (Fulop-Miller, 1938) on the localisation of "*the sensorium commune"* in the anterior cerebral ventricle and suggest that more than being the centre of the sensation, the brain had the ability to temper the heart. This concept evolved notably through the contribution of great scientists such as Leonardo da Vinci, Vesalius (Vesalius et al., 1543) and Varolius (Keele, 1957) with the idea that pain sensation was related to touch sensibility and nerves were considered as tubular structures. It is only centuries later (nineteenth century) with the

development of the pain research that emerged "*The doctrine of Specific Nerve Energies*" a theory in which external sensation or information from different part of the body are only provided by sensory nerves from each of the five senses (sight, hearing, smell, taste and touch) to the brain (Müller, 1838). From the seventeenth and during the remainder of the nineteenth century, the concept of pain evolved approaching the current concepts with different theories as the intensive theory (summation) where pain is considered, not as a unique sensory experience but rather as an outcome of any type of strong sensory stimulation, which suggested that intense activation of any sensory modality (stronger than usual) is unpleasant (Erb, 1874) or the specificity theory where the information is sent out from the periphery to the higher brain centre and come back in motor command without any alteration (*Figure 4)*, but also with the Von Frey's theory which suggests that pain is conveyed by specific fibres from the receptors at the periphery to spinal cord and following specific pain pathways in the neuraxis and even insinuates the existence of a pain centre.

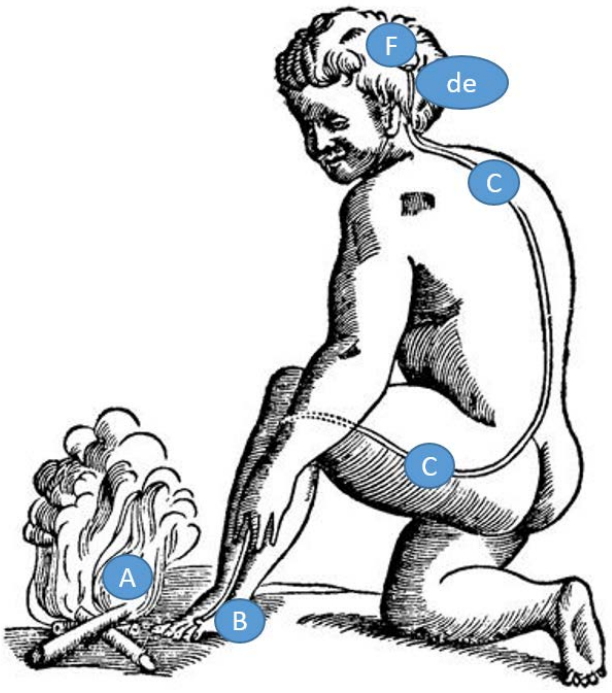

Figure 4 : Illustration of Descartes 'pain pathway: "Particles of heat" (A) activate pain nerves in a spot of skin (B) and these signals are transmitted (C) to the brain (de) where they are reflected into motor nerves that draw the foot away from the heat stimulus. (Descartes, 1648)

Thereafter, the pattern theory integrated the idea of a modulation of the afferents transmission in the substantia gelatinosa of the spinal cord dorsal horn before prior to full integration by the higher brain centre and a comeback in motor command which is more commonly known as the spinothalamic tract (Goldscheider, 1884). It is only recently that pain has been considered as

the outcome of complex interactions between central and peripheral nervous system notably thanks to the work of the physiologists Ronald Melzack and Patrick Wall in 1965 and their "Gate control theory" (*Figure 5*, Melzack and Wall, 1965) where a painful, nociceptive stimulus carried by nociceptive fibre is modulated in the substantia gelatinosa of the spinal cord through presynaptic inhibition from incoming beta-fibres. This mechanism suggests the existence of a balance between painful inputs form small diameter afferent fibres (nociceptor) and non-painful inputs coming from large diameter afferent fibres (non-nociceptor), and all this is under the control of supraspinal sites that could further modulate pain. Then, a couple of year later, in 1992, the neuromatrix theory, evolving from the gate control theory of pain, described pain as "a multidimensional experience produced by characteristic *neurosignature* patterns of nerve impulses generated by a widely distributed neural network—the *body-self neuromatrix*—in the brain" (*Figure 6*, Melzack, 2001). Theory in which the pain felt is not only due to the integration of the painful information coming in over the nociceptive fibre to the pain center in the brain but through the balance between the painful information and the generation of subjective experiences involving a complex network of systems that interact to modify and influence the perception and response to noxious stimuli, and explain how pain could persist in the absence of noxious stimuli.

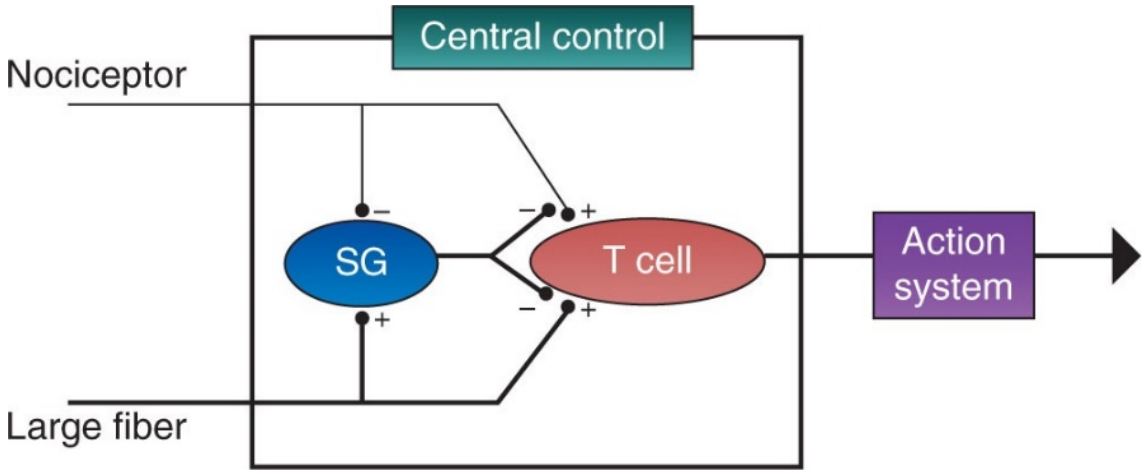

Figure 5 : Schematic diagram of the Melzack-Wall gate control theory of pain mechanisms (1965). Aβ (Large-diameter) and C-fibre (small-diameter) afferent fibres project to the substantia gelatinosa (SG) and first central transmission (T) cells. The inhibitory effect (-) of SG on the afferent terminals is increased (+) by activity in Aβ fibres and decreased by activity in C-fibres. A specialized system of Aβ fibres (the central control trigger) activates certain cognitive processes that influence the modulating properties of the spinal gating mechanism via descending fibres (Melzack and Wall, 1965).

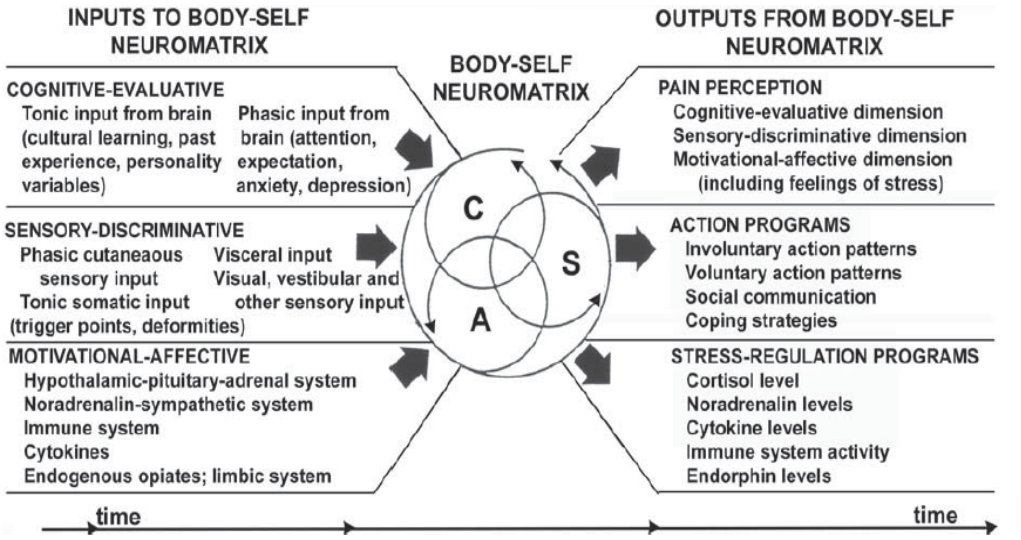

Figure 6 : Factors that contribute to the patterns of activity generated by the body-self neuromatrix, which comprises sensory (S), affective (A), and cognitive (C) neuromodules (Melzack, 2001).

Thus, as history as proven, behind pain sensation, different concepts have evolved, substantially shaped by the advances in research resulting in a definition accepted by the majority and proposed by the International Association for the Study of Pain (Merskey and Bogduk, 1994), Pain is now defined as "an unpleasant sensory and emotional experience associated with actual or potential tissue damage, or described in terms of such damage" *(Figure 7*). Therefore, pain is considered as a personal experience which involves neural mechanisms that arbitrate both sensory and hedonic functions. That's the reason why pain is subjective and its study is delicate and complex.

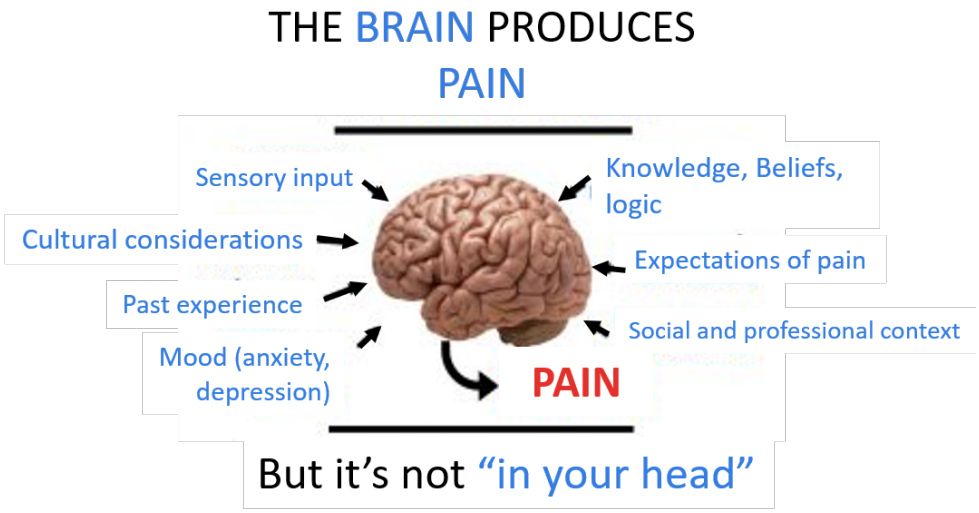

Figure 7 : Description of non-exhaustive factors which participate in pain perception. Modified from Dr Caleb Burgess (Burgess, 2019)

2. Pain physiology

a) *Physiological pain*

Pain, notably its physiological aspect, can be described as a warning mechanism with a protective role, with the aim to keep tissue damage to a minimum following a noxious and potentially damaging stimulus. It corresponds to a cascade of modifications increasing with the intensity of the noxious stimulus, occurring in the peripheral and central nervous system, and responsible for the perception of pain. However, neuronal excitation in nociception is not only a static process of proportionality between intensity of the stimulus and the behavioural responses, but some dynamic changes can also occur as the result of a leftward shift of the stimulus-response curve, which takes place both at the peripheral or at the central nervous system (as known as the sensitization). To get a real grasp of this complex phenomenon, Melzack and Casey put forward the idea of seeing pain as a three dimensions: The sensory discriminative component which refers to the perception of pain including the location, intensity, characteristic and duration; the motivational affective component referring to the unpleasantness of pain; and the cognitive component which refers to all the factors in terms of past experiences and probability of outcome based on individual's beliefs (e.g., culture, past experiences etc…) related to pain which can influence both the sensory discriminative and the motivational affective dimensions negatively or positively (*Figure 8*, Melzack and Casey, 1968). In contrast, it is important to remember that a greater distinction should be made between pain and nociception. Nociception, unlike the pain, is the neural process of encoding and processing noxious stimuli (IASP, 2019a) resulting from a thermal, mechanical, or chemical energy acting on specialized nerve ending (nociceptors) to the central nervous system and it is only when sensory information reaches the cerebral cortex that the perception of pain takes place.

Unfortunately, a dysregulation of pain mechanism may occur and become pathological, notably when it loses its safety aspect and becomes no longer helpful for the protection of the integrity of the organism as an acute warning mechanism but on contrary, becomes chronic and debilitating.

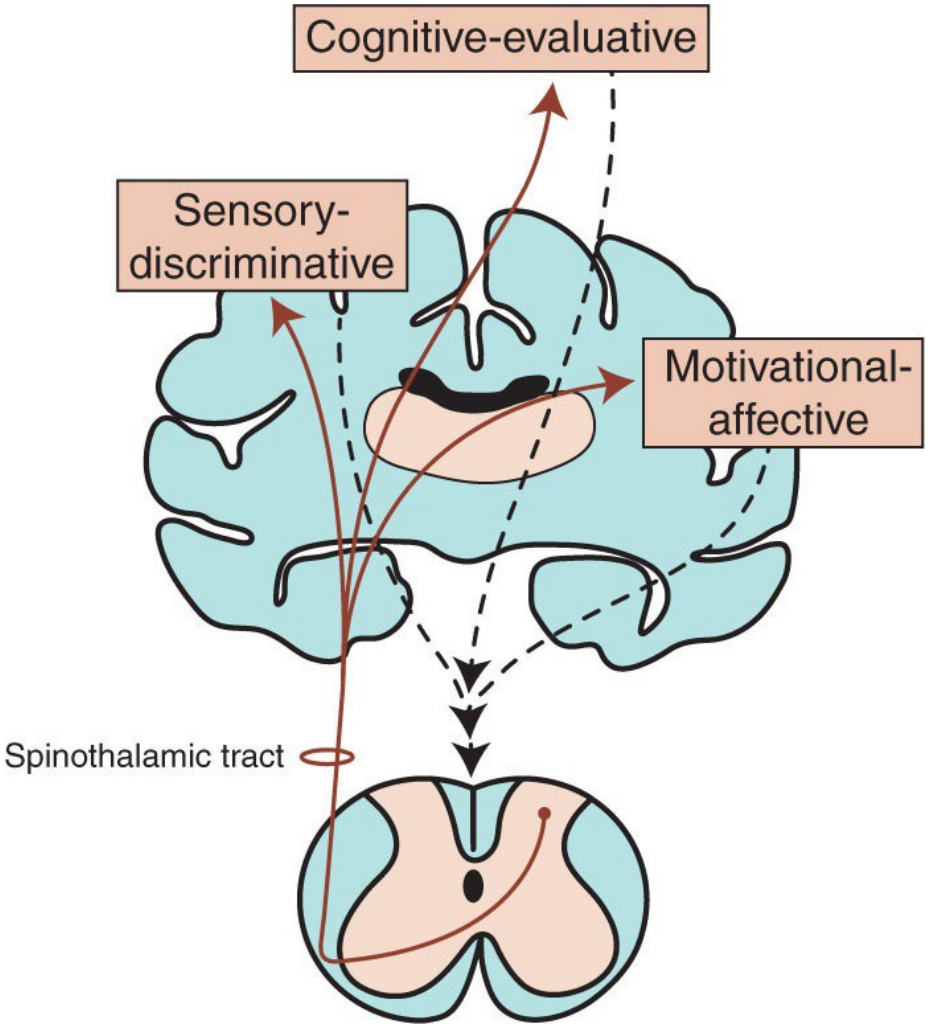

Figure 8 : The dimensions of pain as outlined by (Melzack and Casey, 1968) described in the text above.

b) *Sensitization*

Neuronal excitation in nociception is not only a static process of proportionality between intensity of the stimulus and the behavioural responses but it may be subjected to dynamic changes, known as the sensitization, which is described as "a phenomenon which *i*ncreased responsiveness of nociceptive neurons to their normal input, and/or recruitment of a response to normally subthreshold inputs."(IASP, 2019a), including a modification (decrease) of the threshold and an increase in suprathreshold response. Phenomenon, which can occur both at peripheral and at the central nervous system (defined respectively as the peripheral and central sensitization), considered to be a key element of the physiological pain, but at some point can participate in emphasising the dysregulation of physiological pain, in chronic pain.

c) *Pathological Pain*

Nevertheless, other manifestations of pain related to tissue injury can occur, notably when its perception is no more proportional to the intensity of the noxious stimulus and becomes chronic and incapacitating (Cervero and Laird, 1996). Alterations of the pain pathway, which lead to hypersensitivity characterised by an exaggerated response to noxious stimuli associated with a lowered threshold to noxious stimuli which is defined as a hyperalgesia, both at the site of the tissue damage (primary hyperalgesia), and surrounding the area of primary tissue or nerve injury bordering uninjured tissue (secondary hyperalgesia) (Treede et al., 1992) and the appearance of pain response to innocuous stimuli (allodynia); *(Figure 9)*. Hyperalgesia and allodynia highlight changes in either the peripheral or central nervous systems, referred as **peripheral or central sensitization**, respectively. This phenomenon implies several factors such as genetic and environmental factors, which contribute to sensitization resulting in persistent (chronic) pain in some individuals (even after healing has normally taken place) characterized also by the abnormal state and function of the spinal cord neurons, which become hyperactive. Under normal condition, the nociceptive sensory system returns to a baseline functional state as soon as healing takes place. Unfortunately, many components of sensitization can persist and manifest themselves as chronic pain and hyperalgesia, especially when the nervous system itself is injured leading to chronic neuropathic pain.

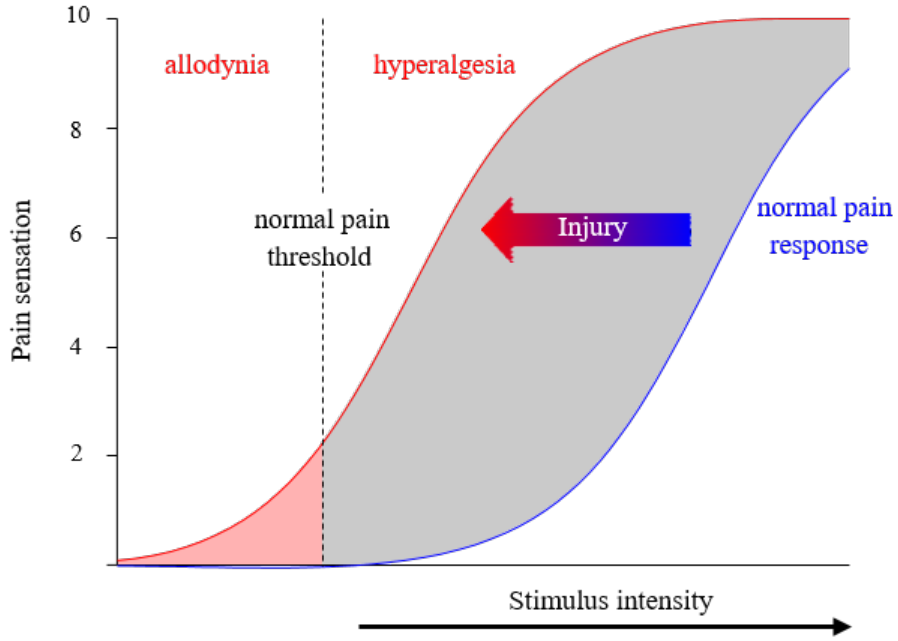

Figure 9 : Schematic representation of sensitization of nociceptors response to a peripheral stimulus induces by a tissue injury. In blue, weak or innocuous stimuli do not evoke pain sensation in normal condition. In red, sensitization in response to a stimulus after tissue damage, shifting the response function to the left. A moderate painful stimulus is now perceived as intense (i.e., pain hyperalgesia) and a previous innocuous stimulus can be perceived as painful (i.e., allodynia). Adapted from (Cervero and Laird, 1996).

d) *Pain State Classification*

Pain is the most commonly symptom observes in medicine, which may be expressed in different ways, can occur in any part of the body and affect any system, be acute or chronic, sporadic or constant. That is why, in the aim of a better understanding of pain disorders and to guide assessment or treatment, it is important to classify the different pain state.

i. According to the Mechanistic/Etiology

Six different types of pain can be distinguished based on the physiopathological mechanism.

- Nociceptive pain

  Nociceptive pain, defined as “pain that arises from actual or threatened damage to non-neural tissue and is due to the activation of nociceptors”(IASP, 2019a), represents the normal response to noxious stimuli or injury of tissues (skin, muscles, visceral organs, joints, tendons, or bones). It is caused by ongoing activation of nociceptive afferent fibres (Aδ and C nociceptor) through mechanical, thermal, or chemical stimulation (Costigan et al., 2009). Depending on the location of the nociceptors involved,

nociceptive pain may also be subdivided into visceral pain, deep somatic pain, and superficial somatic pain.

- Neuropathic Pain

  Neuropathic pain, defined by the IASP as "pain caused by a lesion or disease of the somatosensory nervous system" and in such of terms as "burning, stabling, electrical, shooting pain…" by the patient, is caused by a primary lesion or dysfunction affecting the somatosensory nervous system (Merskey and Bogduk, 1994) both from peripheral nerves (peripheral neuropathic pain) to the central nervous system which is a regional pain associated with aberrant sensibility to temperature and to noxious stimulation (Bouhassira et al., 2005).

- Nociplastic Pain

  Recently adopted, nociplastic pain is defined by the IAPS as "a pain that arises from altered nociception despite no clear evidence of actual or threatened tissue damage causing the activation of peripheral nociceptors or evidence for disease or lesion of the somatosensory system causing the pain"(IASP, 2019a).

- Psychogenic Pain

  Pain disorder associated with psychological, emotional or psychosocial factors such as depression, anxiety and bipolar disorder, obsessive-compulsive behaviour, which describes both short- and long-term episodes of pain that occur usually in the absence of any objective inflammatory or physical pathology that could explain the pain sensation (Toda, 2007), People experiencing psychogenic pain even if brief episodes, as well as persistent symptoms, described it as very real and painful.

- Mixed Pain

  Pain defines as a "complex overlap of the different known pain types (nociceptive, neuropathic, nociplastic) in any combination, acting simultaneously and/or concurrently to cause pain in the same body area (*Figure 10)*. Either mechanism may be more clinically predominant at any point in time. Mixed pain can be acute or chronic (Freynhagen et al., 2019).

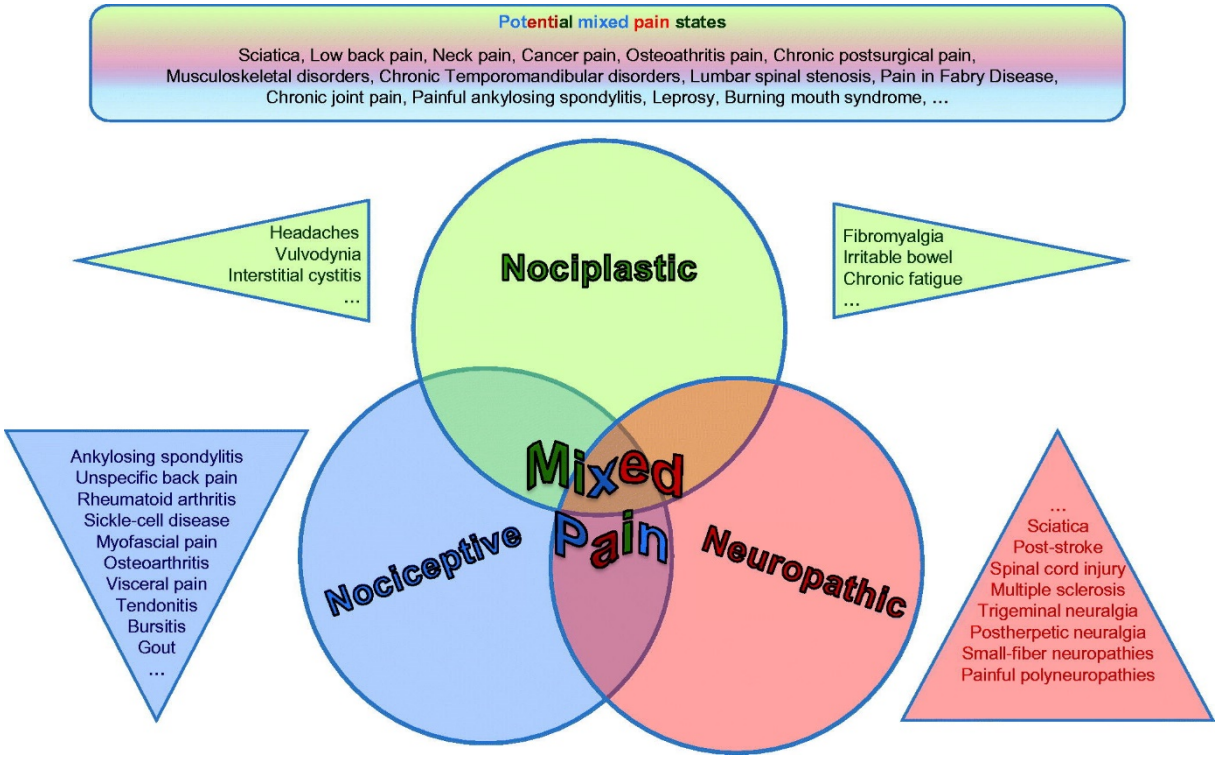

Figure 10 : Representation of "mixed pain" defined as the overlapping of the nociplastic, nociceptive and neuropathic pain (Freynhagen et al., 2019)

- Idiopathic Pain

  Idiopathic pain is defined as a pain that occurs when there is no known physical or physiological cause or that persists after the trauma or pathology has healed (Bouhassira and Attal, 2012; Cheng, 2018). It arises generally from neurological dysfunction, not damage (such as fibromyalgia, temporomandibular disorders…).

ii. According to the Anatomic perception

It is a conventional classification of pain based on the anatomical location from which pain is perceived, allowing in some cases to determine the possible cause (e. g. low back pain, headaches, joint pain, cardiac pain... each referring to the specific location of the symptoms). Nevertheless, some criticism can be raised on the importance of such a classification on setting up a therapy notably due to the lack of anatomically defined specificity in the neurophysiology of pain. Indeed, pain is not always associated with a precise anatomical location but rather as a relaying pain. For example, pain from internal organs, which do not have nociceptors, is not well localized and may masks the origin of this pain, particularly in the case of cardiac pain,

which can be felt in the left shoulder of the body without necessarily being associated with chest pain.

iii. According to the Duration

Traditionally, one common way to classify pain is to differentiate it according to a temporal criterion. It is a measurable characteristic allowing differentiation between acute (including pain associated with tissue damage, inflammation, or a disease process that is of relatively brief duration regardless of how intense) and chronic pain (for pain that persists for extended periods of time). Conventionally, considering the duration of the symptoms, it has been well admitted that pain can be divided into groups (Backonja et al., 2010; Swieboda et al., 2013):

- Acute pain, which is defined as a pain that lasts less than 3 to 6 months.
- Chronic pain, which is defined as a pain lasting for more than 3 to 6 months, or persisting after a complete tissue healing or beyond the course of an acute disease.
- Survived pain, which describes a persisting pain despite the healing of the tissue damage, which resulted in acute pain

However, this criterion may lead to a lack of understanding of pathology because a single dimension of duration is not necessarily link to pathological factors.

iv. According to the Intensity

It is a conventional pain classification based on the intensity of perceived patient pain. Although the fact that the sensation of pain is subjective, making it the most difficult feature to assess, a common point of the intensity of pain is its tolerance. That is why, in the aim to evaluate intensity visual, categorical or analogue scales are used to compare pain with the worst pain than the patient ever suffered (*Figure 11)*.

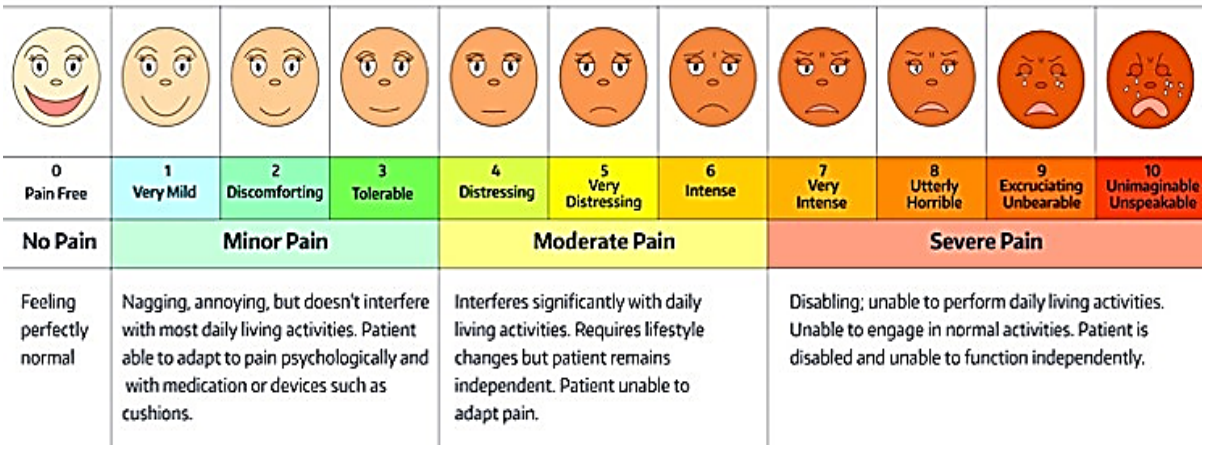

Figure 11 : Comparative pain scale chart used to assess pain by an increasing factor. Scales consisting of a horizontal line, more or less 10 cm in length, one hand of which is "0", meaning literally no pain and at the opposite end "10", meaning the strongest pain endured in life. (Moyle, 2015)

e) *Multidimensional Classification of Pain*

Pain experience, as described above, covers different components such as physical, psychological or social component often resulting in suffering. Suffering which can be described as a threat to the intactness of individual's self-concept and integrity such as our desire of happiness and health (Schmidt and Willis, 2007) resulting from aggression to the physical or emotional components of pain including loss of physical function, social isolation, family distress, and a sense of inadequacy or spiritual loss (Benzon et al., 2018).

Therefore, pain approach should be multidimensional to encompass all these different modalities. As an alternative to the unidimensional approaches, a comprehensive taxonomy of pain should consider multifactorial assessment *(Table 1)* rather than a single dimension such as (Serlin et al., 1995; Cleeland et al., 1996; Sela et al., 2002) :

- Physical effects and symptoms
- Functional effects (such as social consequence)
- Psychological factors (anxiety, fear …)
- Spiritual aspect

Table 1 : Proposal of a comprehensive taxonomy of pain based upon multifactorial assessment (Turk and Okifuji)

Pain Parameters:
Anatomy/System
Duration/Intensity/Quality
Associated Abnormality (physical/psychological)
Underlying Diseases:
Signs/Symptoms
Pain Mechanisms:
NEUROPHYSIOLOGICAL
Primary afferent involvement
CNS involvement
Psychological
Cognitive–Affective–Behavioral Involvement
Cognitive appraisal of pain
Coping
Affect/mood
Environment

3. Anatomy and physiology of the pain

a) *From nociception to pain sensation*

Pain, as described above, is considered a physiological protective system essential to the survival, well-being, learning and adaptation of human being. However, it can become pathological, notably when, in absence of tissue damage or following appropriate healing of injured tissue, it occurs or persists and then become no longer useful as a protective system and become chronic and debilitating. Thus, an understanding of the physiological mechanism underlying pain perception will provide key elements to apprehend the mechanisms of acute and chronic pain.

One approach to understanding the pain sensation is to follow the nociceptive signal pathways also called nociception (a physiological process of activation of neural pathways by stimuli that are potentially or currently damaging to tissue) from the periphery (detected by specialized peripheral sensory neurons as known as the nociceptor) to the brain through the spinal cord.

Four distinct processes are necessary for a nociceptor to convey noxious information to the CNS, with the starting point being signal transduction, which occurs in the peripheral terminals of primary afferent neurons.

i.Sensory afferent fibres from the periphery to spinal cord

Sensory afferent fibres originating in the peripheral terminal group together to form spinal nerves, each supplying a distinct area of skin (dermatome), and overlapping more or less the dermatomes of neighbouring spinal nerves and later splitting to form a ventral and dorsal roots. Dorsal roots exclusively relate to sensory information. These sensory afferent fibres can be classified physiologically according to their physical characteristics such as axon diameters, conduction velocity and function into different groups: A fibre group with subtype Aα (or group I; thickly myelinated fibres, muscle proprioceptors), Aβ (or group II; less myelinated fibres, low-threshold mechanoreceptors), Aδ (or group III; thinly myelinated fibre, mechanoreceptor-thermoreceptor), and C fibre group (or group IV; unmyelinated fibres, polymodal receptor). It is generally admitted that transduction of noxious signals from most spinal cord innervated tissues is mediated by the thinly myelinated Aδ fibres and unmyelinated C fibres with free nerve ending (nonspecialized); nevertheless, to a lesser extent, thickly myelinated fibres may also play a role in pain sensation (especially from the skin). To get more in detail we will mainly focus our attention on one type of nociceptor (mechano-heat-sensitive nociceptor), the cutaneous fibres which are able to respond to stimuli that are potentially or actually tissue-damaging (noxious stimuli), such as intense mechanical stimuli (pinch, pressure, indentation), algesic chemical, or elevated thermal (> 45 ° C) stimuli.

The Aα/β fibres, as described above, are large-diameter myelinated fibres with the fastest peripheral conduction velocity. They are mainly involved in the transmission of non-nociceptive input, such as hair movement, pressure or small touch and also seem to play a tonic inhibitory role on the nociceptive input through the recruitment of inhibitory interneurons in the substantia gelatinosa of the spinal cord thus modulating nociceptive input from the same spinal segment (main mechanism of the gate control theory (Melzack and Wall, 1965).

The Aδ fibres are, to a lesser extent compare to Aα/β fibres, thinly myelinated fibres with intermediate velocity. Depending on the specificity of their response to stimulation, Aδ fibres can be divided into two types (Treede et al., 1998): On one hand, the mechano-heat nociceptors which mainly respond to intense and potentially harmful mechanical and heat stimulation, and on the other hand the polymodal Aδ fibres which respond both to mechanical, thermal, and chemical stimulation. However, it has been shown that the mechanonociceptor Aδ fibres neuronal activity may lead to hyperalgesia through the increase of their discharge resulted from thermal stimulation. In addition, the Aδ fibres are considered to be responsible for the first pain sensation, pricking pain, sharpness, and transient sensation (Basbaum et al., 2009).

Furthermore, Aδ fibres can also be subdivided into two main classes depending on their neuronal activity: Type I (HTM: high threshold mechanical nociceptors) responds to both mechanical and chemical stimuli with a relative high heat thresholds (>50°C, (mediated by vanilloid receptor-like protein 1 (TRPV1) receptors and more recently TRPM3 (Vriens et al., 2011) and the calcium-activated chloride channel ANOI (Cho et al., 2012)) (Basbaum et al., 2009). Nevertheless, if the heat stimulus is maintained, these afferents will respond at lower temperatures and then will sensitize (i.e., the heat or mechanical threshold will drop) in the setting of tissue injury, whereas type II Aδ nociceptors have a much lower heat threshold with a very high mechanical threshold.

The C fibres, which consist of the smallest, unmyelinated, and most slowly conducting fibres, are also heterogeneous and mostly polymodal (including population both heat and mechanically sensitive CMHS (Perl, 2007) and represent the major part of the sensory afferent input and are mostly mobilized by nociceptive stimulation including the ability to be activate by action potential activity in another fibre termed coupling (Meyer et al., 1985). Most of them respond also to chemical stimuli in addition to noxious mechanical and cold/heat ("hot burning sensation") stimuli (Davis et al., 1993). Moreover, data from C fibres in humans suggest that C-fibre activity is associated with a prolonged burning sensation. However, they are also involved in non-nociceptive somatosensory information such as in the sensation of pleasant touch mediates (Liljencrantz and Olausson, 2014; Kambrun et al., 2018) by C-tactile fibre (C-LTMR) which are low-threshold mechanoreceptors with small receptive fields (Wessberg et al., 2003) found in hairy skin and responding to slow and light stroking (Vallbo et al., 1999); and itchy skin called pruritus (Ständer et al., 2003), "paradoxical heat" (Campero et al., 2009).

ii. Biphasic sensation of pain: first and second pain sensation

The combined activation of these two groups of afferents, such as by an intense brief heat stimulus, results in a dual-pain sensation as Aδ fibres convey the rapid-onset *first pain* sensation, a pricking pain, leading to a nociceptive withdrawal reflex. Whereas C fibres mediate the slower-onset, burning *second pain* sensation following intense heat stimulation to the skin and leading to a diffuse deep pain sensation (Meyer and Campbell, 1981). Combined, Aδ- and C-fibre nociceptors transduce and transmit sensitive information to the central nervous system (CNS) concerning the intensity, location, and duration of noxious stimuli (*Figure 12)*.

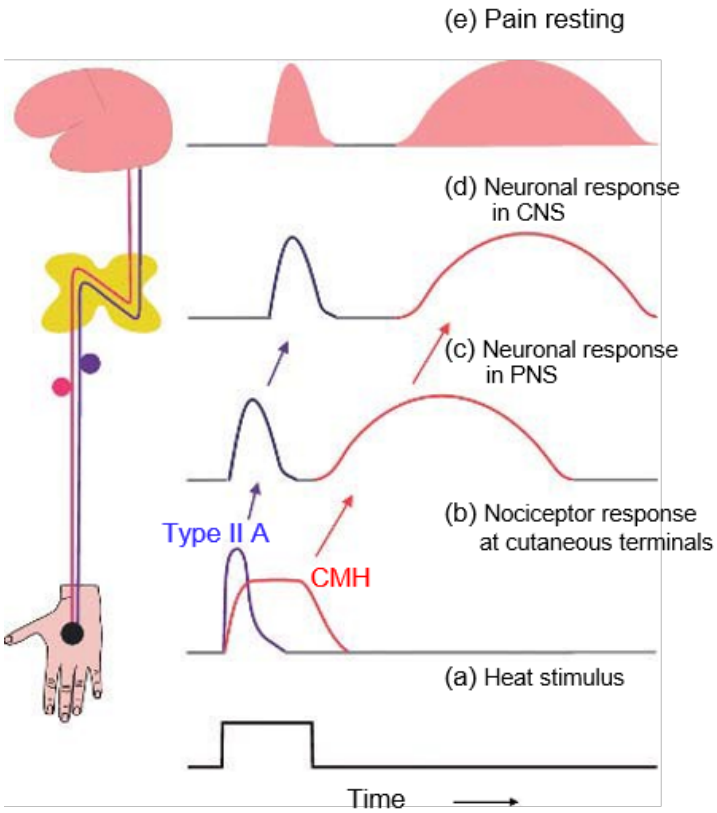

Figure 12 : First and second pain following an intense heat stimulus on hairy skin. A stepped heat stimulus (a), on hairy skin, is firstly signalled by Aδ fibres (A fibre type II), It leads to a dual pain sensation, an intense pain followed after a pause by a burning pain (e). Heat stimuli nearby pain threshold trigger two classes of nociceptors on hairy skin, Aδ fibres and C fibres (mechano-heat-sensitive afferents, CMHs) (b). The signal reaching the central nervous system (CNS) is both delayed and broader than the signal at the receptor terminals. The Aδ fibres which have a faster conduction velocity reach the CNS faster than the C-fibres, resulting in the broadening of the nociceptive signal (Ringkamp and Meyer, 2009),

iii. detection of nociceptive stimuli:

Based on the description of Sherrington about a century ago, nociceptor is a sensory receptor defined by the IASP (IASP, 2019a) as “a high-threshold sensory receptor of the peripheral somatosensory nervous system that is capable of transducing and encoding noxious stimuli”. They are free nerve endings present more or less everywhere in the body notably in the skin (both in the epidermis and the dermis), muscle, blood vessel (inner layers of the blood vessel wall), bones (marrow and the periosteum), joints (capsule, synovium, the ligaments and the tendons) and internal organs (loosely and unevenly distribution), except the brain (Willis and Coggeshall, 2012) with a variation in terms of density of innervation between as well as within tissue. Most of these free ending fibres are polymodal and respond to different modalities, including mechanical (pinching, piercing or biting), thermal (warmth or cold), and

chemical stimulation (*Figure 13)* (Meyer, 2013; Wang et al., 2018). Different types of receptors are sensitive to these specific stimuli: mechanical (involving MDEG, DRASIC, TREK-1 receptor), chemical (TRPV-1, ASIC, DRASIC receptor), thermal (involving TRPV1-2-3-4 receptors for the heat and TRPM8 and TRAP1 receptors for the cold) (Scholz and Woolf, 2002)

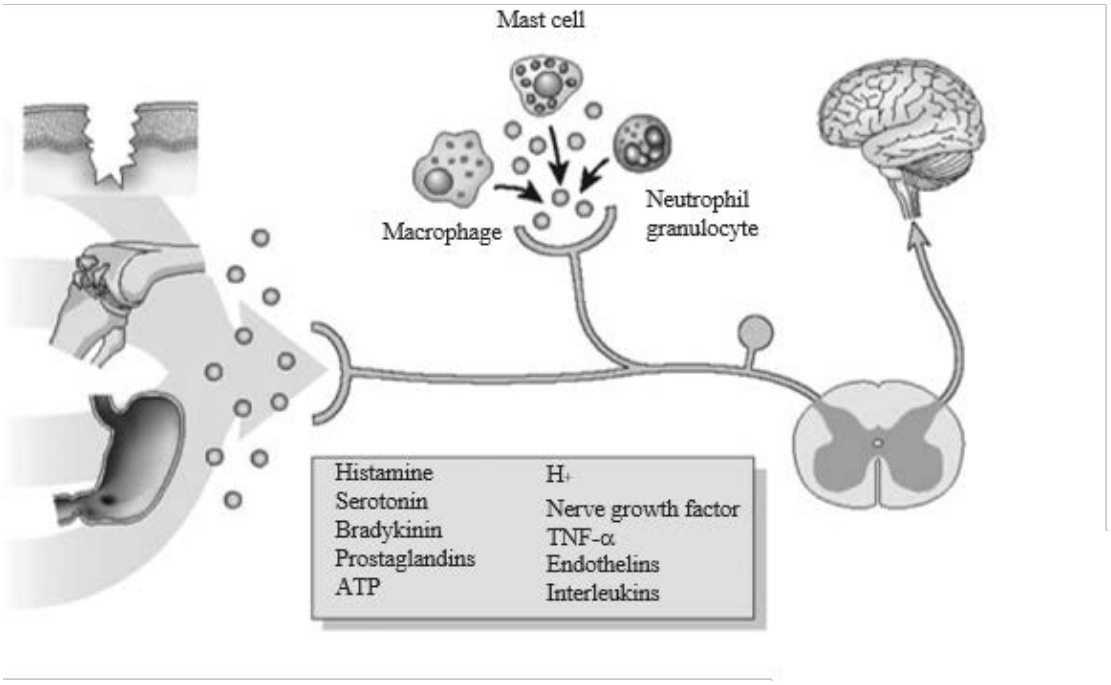

Figure 13 : Illustration of the activation of nociceptor resulting from tissue inflammation. Tissue inflammation leads to the release of a number of proinflammatory mediators that can excite and sensitize nociceptors. (Scholz and Woolf, 2002).

Second, receptor activation usually results in the depolarization of the peripheral terminal. Depending on the intensity of the depolarization, the fourth element is an action potential that transmits information all along the peripheral nervous system to the central nervous system (*Figure 14 & 15).* Peripheral sensory neurons (first-order neurons), with their cell bodies remaining in the dorsal root ganglia, transmit impulses from the site of transduction at their peripheral terminal to the spinal cord where the central terminals contact second-order neurons. Second-order neurons located in the spinal cord constitute the second component in the transmission network. These cells send ascending projections to diverse supraspinal structures such as thalamus and various brainstem and diencephalic structures. Finally, brainstem and diencephalon neurons project to various cortical sites including somatosensory cortices (SI, SII) and limbic structures such as the anterior cingulate cortex (ACC). At this level, final stage of the nociceptive process, noxious neural activity in the somatosensory transmission pathway results in a subjective sensation of pain (due to the convergence of nociceptive and normal somatic sensory information in the same area). Phenomenon described as perception.

However, all along pain transmission, alterations may occur on the neural activity, phenomenon known as pain modulation. Pain modulation is particularly important at the level of the dorsal horn of the spinal cord where second-order neuron activity is modulated by either excitatory or inhibitory influences. I will present modulatory aspects in afferent fibres and second-order neurons.

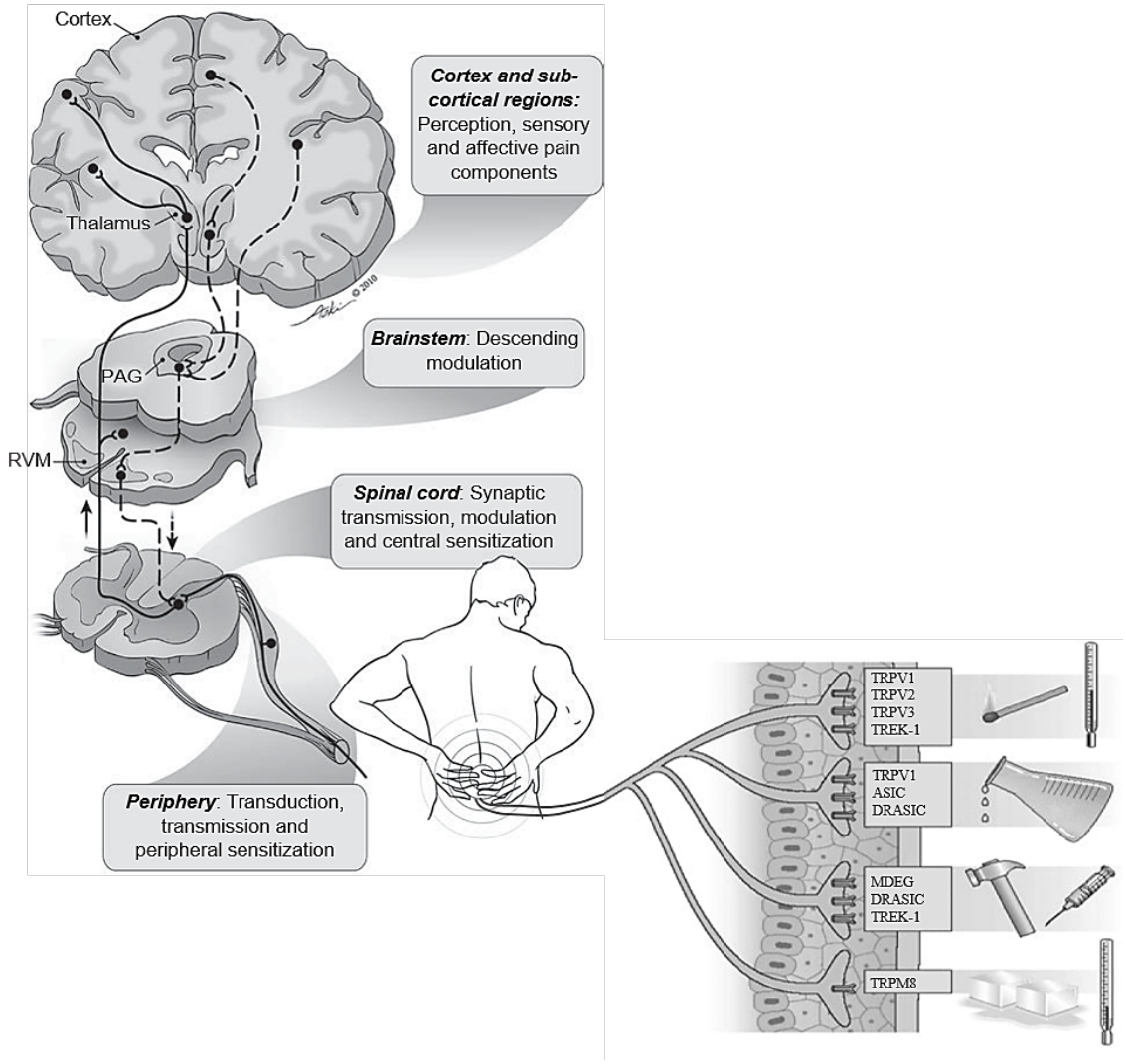

Figure 14 : Representation of nociceptive pathways from the peripheral nociceptor activator to the brain through four different processes, transduction, transmission, modulation, and perception of pain. Pain results from nociceptive (but also inflammatory, or neuropathic not described here) mechanisms that occur in the periphery. Activation of specific receptors located on the nociceptor results to the transduction of noxious thermal (cold and heat), chemical, and mechanical stimuli (Scholz and Woolf, 2002) Ascending afferent and descending modulatory pathways are shown. PAG, Periaqueductal gray; RVM, rostral ventromedial medulla; SI somatosensory cortex I. (adapt from Benzon et al., 2018)

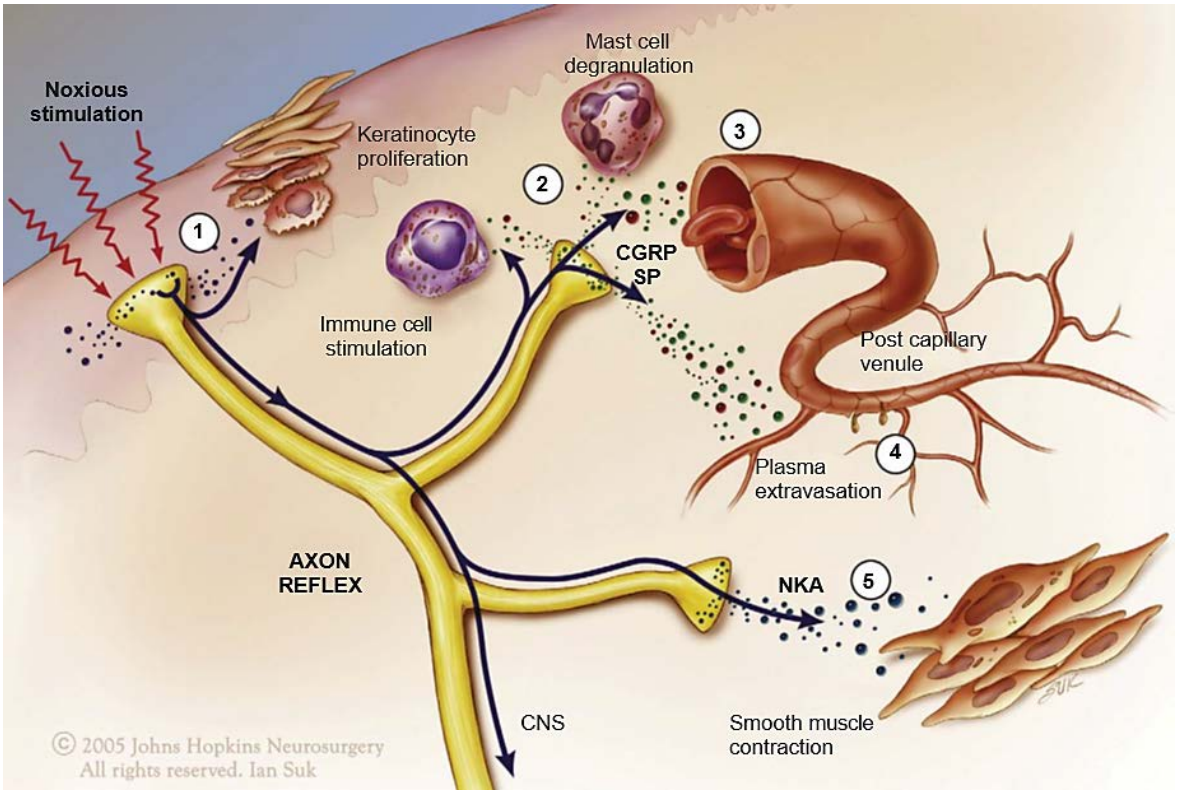

Figure 15 : Efferent actions of nociceptors. A noxious stimulus at the nociceptor terminals leads to action potentials propagation from the nociceptive fibres not only to the central nervous system but also antidromically into peripheral branches resulting in the release of neuropeptides such as neurokinin A (NKA), substance P and calcitonin gene-related peptide (CGRP). These neuropeptides released can then stimulate epidermal cells (with proliferation of keratinocytes) (1) and immune cells (or degranulation of mast cell) (2) or lead to vasodilatation (3), plasma extravasation (4), and smooth muscle contraction (5). (Artwork by Ian Suk, Johns Hopkins University(McMahon and Meyer, 2013))

iv. Peripheral sensitization: primary hyperalgesia

When tissue damage occurs, it results in an increase in the responsiveness of nociceptor called sensitization. Various substances such as potassium, prostaglandins, histamine, or bradykinins (pronociceptive compound) are released, inducing an immune response (*Figure 16)*. Together, inflammatory and immune factors will lead to the sensitization of the nociceptor (peripheral sensitization) directly within the lesion and in the surrounding neurons (Fischman et al., 2010; Chiu et al., 2012). Sensitization following the release of these factors results in a pain enhancement at the site of injury termed primary hyperalgesia (Lewis, 1935), which is manifested as a leftward shift of the stimulus-response function that relates the magnitude of pain to stimulus intensity (*Figure 17)*.

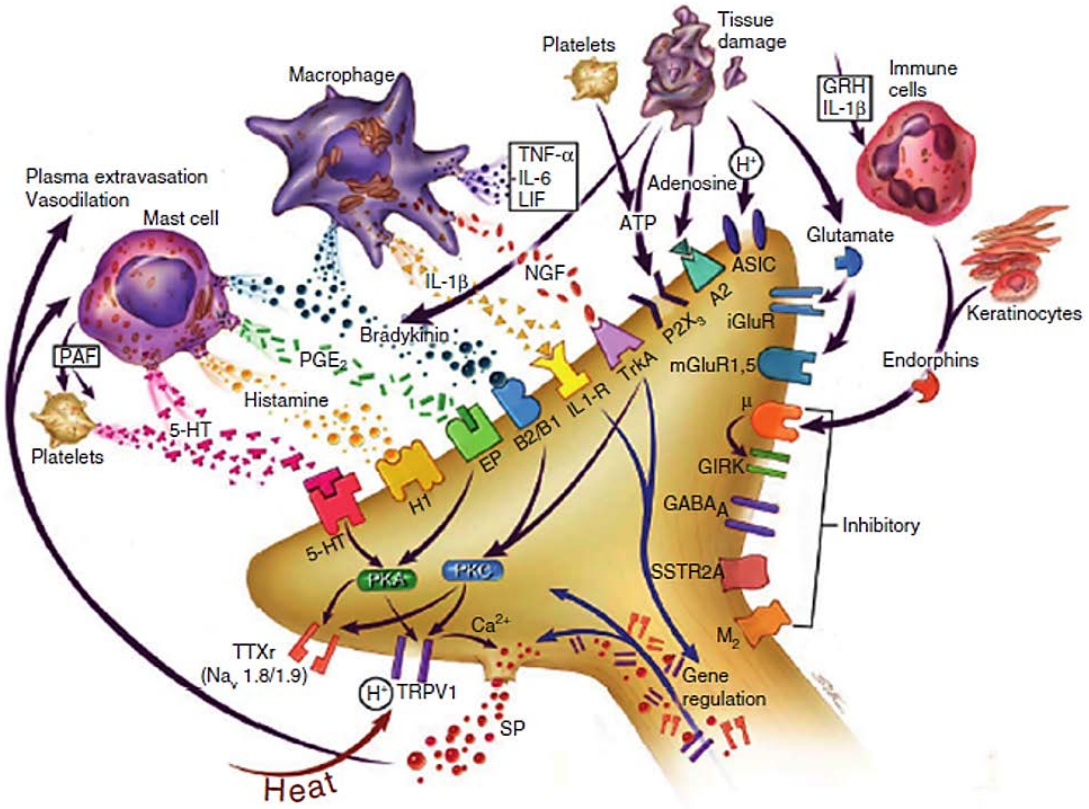

Figure 16 : Potential peripheral sensitization mechanism after inflammation (Meyer, 2013). At the peripheral terminal, activation of nociceptor by inflammation and/or tissue injury lead to the release of numerous chemicals mediators (such as H+, purines (adenosine, ATP), NGF, cytokines (TNF-α) and interleukins (IL-1β, IL-6), LIF, PGE2, bradykinin, histamine, 5-HT, PAF, and endothelin) from non-neuronal and neuronal cells that may alter the sensitivity of peripheral nerve terminals directly or indirectly (via coupling to one or more peripheral membrane-bound receptors, respectively including ASICs, K2P, and TRP channels, GPCRs , P2X and RTK receptors). Ligand binding to these receptors may induce a cascade of events that includes activation of second-messenger systems (PKA and PKC) and alters gene regulation. (Artwork by Ian Suk, Johns Hopkins University; adapted from (Woolf and Costigan, 1999).5-HT, serotonin; ASICs, acid-sensitive ion channels; ATP, adenosine triphosphate; CRH, corticotropin-releasing hormone; GIRK, G - protein-coupled inward rectifying potassium channel; IL-1β, IL-6, interleukins ; H+, proton; K2P, two-pore potassium channels IL - 1 β, interleukin - 1 - beta; IL - 6, interleukin - 6; LIF, leukemia inhibitory factor; μ, mu-opioid receptor; M 2, muscarinic receptor; mGluR, metabotropic glutamate receptor; NGF, nerve growth factor; PAF, platelet-activating factor; PGE 2 , prostaglandin E 2 ; PKA, protein kinase A; PKC, protein kinase C; SSTR2A, somatostatin receptor 2A; TNF - α , tumor necrosis factor-alpha; TrkA, tyrosine kinase receptor A; TRPV1, transient receptor potential vanilloid 1; TTXr, tetrodotoxin-resistant sodium channel

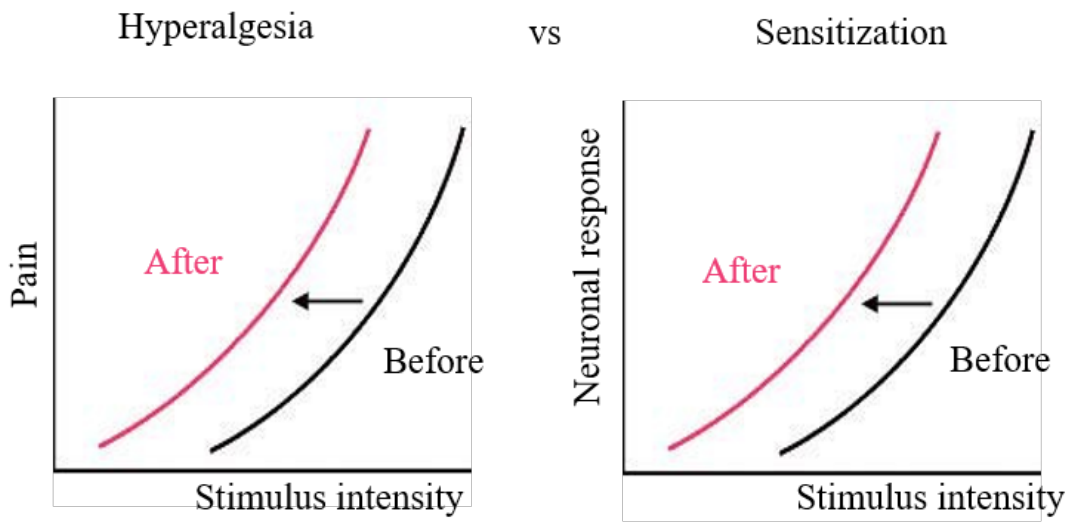

Figure 17 : Concept of hyperalgesia and sensitization. The concept of hyperalgesia is characterized by a leftward shift of the stimulus-response function that relates the magnitude of pain to stimulus intensity including a decrease in pain threshold, an increase in pain in response to suprathreshold stimuli and spontaneous pain. Whereas sensitization is characterized by a leftward shift in the stimulus function that relates the neural response to stimulus intensity including a decrease in threshold for response, an increase in response to suprathreshold stimuli and spontaneous activity (illustration from (Ringkamp and Meyer, 2009).

v. Target of primary afferent: the dorsal horn second-order neurons

- Gross description of the dorsal horn

Considered as the first relay of incoming sensory information including integration and processing, the dorsal horn of the spinal cord has been divided into three broad regions: the marginal zone, the substantia gelatinosa and the nucleus proprius. Based on cytoarchitectural criteria (Rexed, 1952, 1954), the grey matter of the dorsal horn (which is mostly made up of multimodal neurons varying in size) is divided into six laminae (I to VI), including functional differences in dorsal horn neurons (DHNs) both in different and within laminae as well as in different projection patterns (*Figure 18)*. Moreover, in each lamina of the spinal dorsal horn, cells, axons and terminals ending have a distinctive chemical profile, which has been shown to change following a lesion (Willis and Coggeshall, 1991). Besides this description, the dorsal horn of the spinal cord encompasses the final arborisation and endings of primary afferent fibre; local circuit neurons (excitatory and inhibitory interneurons); projection neurons to the brain (nociceptive and non-nociceptive second-order neuron); propriospinal neurons, which interconnect different levels of the spinal cord; and descending axons from several supraspinal sources.

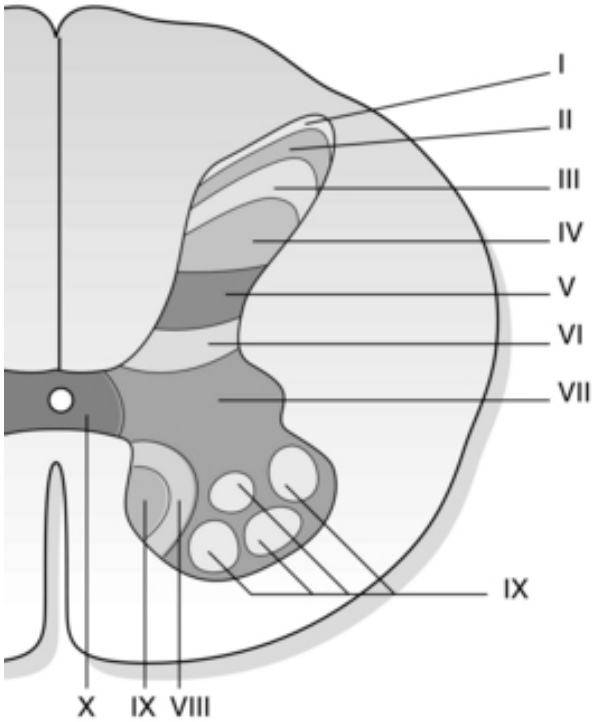

Figure 18 : Rexed's description of the spinal cord laminae. Within Dorsal horn gray matter encompasses laminae I to VI (or posterior grey column;(Carpenter, 1985; Cramer et al., 2014)) whereas laminae VIII to IX is associated with the ventral horn (or anterior grey column). Laminae VII and X constitute the lateral grey column with laminae X surrounding the central canal and laminae VII more lateral including intermediomedial nucleus, intermediolateral nucleus, posterior thoracic nucleus in the thoracic and upper lumbar region. Lamina I *termed the marginal zone contains a high density of projection neurons processing nociceptive information including* nociceptive-specific *neurons (excited solely by nociceptors) and* wide dynamic range *neurons (also in lamina V–VI) (responded to both nociceptive and mechano-heat-receptive input).* Lamina II *called the substantia gelatinosa which can be distinct between lamina II-outer (IIo) and lamina II-inner (Iii) also receive major input from both nociceptive and nonnociceptive neurons. As regard with lamina III, it is neuropil present similarity with lamina II but has slightly larger cells and myelinated axons with low-threshold (including proprioceptors). Deeper* Laminae IV *and* V *are characterized by neurons of various sizes (prominent large cells for one and longitudinally oriented myelinated axons for the other).* Lamina VI, *presented only in cervical and lumbosacral enlargements, constitute a transition zone between the primary afferent-dominated dorsal horn and the ventral horn, with descending input predominating the mainly receive* ***Low-threshold muscle afferents and both low- and high-threshold cutaneous****. Nevertheless, a population of neurons (nociceptive and WDR) responding to noxious mechanical and thermal stimuli has been reported in the vicinity of the spinal cord central canal in* lamina X *(Honda, 1985; Honda and Perl, 1985)*

- Primary afferent targets

Incoming afferent fibres of all types (*Table 2)*, establish a complex web of connections with DHNs, triggering a plastic pattern of excitatory and inhibitory inputs that determines the firing of DHNs mediate spinal reflex responses and projections to higher brain areas. With regard to Aδ and C fibres that convey the nociceptive signal to the spinal cord, they have first synaptic contacts with second-order neurons, in the superficial zones of the dorsal horn (I, II)

and deep lamina V (Fields, 1987). Also these afferents also make synaptic contact with an important network of inhibitory and excitatory interneurons that modulate the nociceptive signal before DHNs that project to superior brain centres. Regarding Aδ nociceptors, they project to lamina I as well as to deeper dorsal horn (lamina V) whereas low threshold, rapidly conducting Aβ afferents, which respond to light touch, project to deep laminae (III, IV, V and to a lesser extent lamina II, notably the distal part of the arbours of hair follicle afferents (Brown and Fyffe, 1981)). By contrast, C nociceptors project more superficially to laminae I and II with some extension to laminae III (Gobel et al., 1981; LaMotte, 1977) (*Figure 19)*. In addition, electrophysiological approaches demonstrate that DHNs within lamina I are generally responsive to noxious stimuli (through Aδ and C fibres), DHNs in laminae III and IV are primarily responsive to innocuous stimulation (via Aβ), and DHNs in lamina V receive a convergent innocuous and noxious input via direct (monosynaptic) Aδ and Aβ inputs and indirect (polysynaptic) C fibres inputs *(Table 3)*. These second-order neurons can be divided into two distinct population: the nociceptive specific neurons and the wide dynamic range (WDR) neurons (Guilbaud, 1997; Meyer, 2006; Terman, 2001).

Table 2 : Classification of nerve fibres depending on morphological characteristic, conduction velocity and type of nerve transmission (adapt from (Gasser, 1941; Lloyd, 1962))

Muscle nerve	**Cutaneous nerve**	**Myelination**	**Avg. fibre diameter (µm)**	**Avg. Velocity (m/s)**	**Receptive field quality/ Receptor type**
I	Aα	Thick	12-20	72-120	Proprioceptive function / Proprioceptors (Muscle spindle, Golgi tendon organ)

II	Aβ	Medium	6-12	30-75	Small touch/ mechanoreceptor (Merkel nerve ending, Tactile corpuscle, Lamellar corpuscle, Bulbous corpuscle)
III	Aδ	Thin	1-5	4,36	Small, sharp, first pain/ Mechano-nociceptor (Free nerve ending)
IV	C	None	0,4-2	0,5-2	Large, dull/ nociceptor (Free nerve ending)

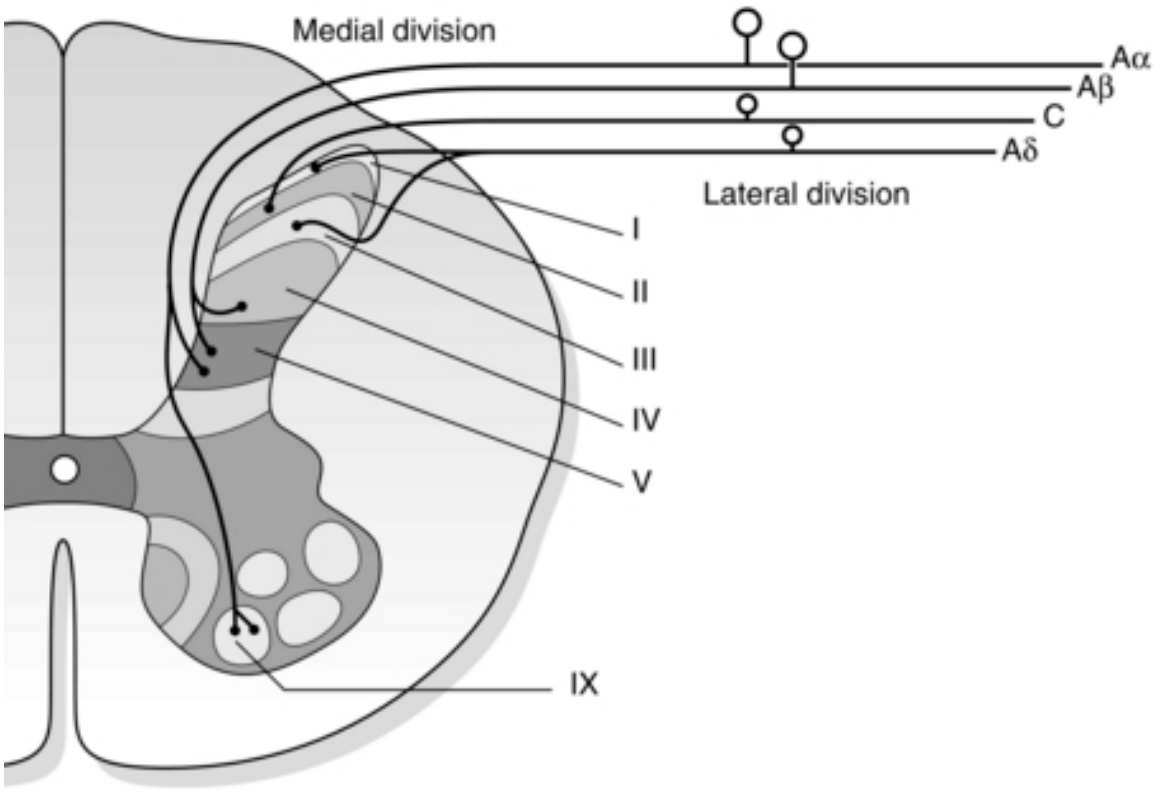

Figure 19 : Afferent fibres terminations in the spinal cord. Large fibres (Aα and Aβ) enter in the medial division and small fibres (Aδ and C) enter in the lateral division of the dorsal root *(Waxman, 2017)*.

Table 3 : Afferent fibres ending in the dorsal horn based on (Woolf et al., 1992)

Afferents	Terminal zones in dorsal horn
Large diameter myelinated Aα/β-fibres	III, IV and V
Small diameter myelinated Aδ-fibre	I and V
Unmyelinated C-fibres	II and III

- Nociceptive second-order neurons

Second-order neurons are classified according to electrophysiological criteria such as responsiveness to cutaneous and deep tissue stimuli and the pattern of response elicited: Class1 neurons or low threshold neuron if excited only by innocuous stimuli, class 2 or wide dynamic range neuron / convergent neurons (WDR) if excited by both innocuous and noxious stimuli and class 3 or high threshold/ nociceptive-specific neuron (NS) if excited only by noxious stimuli (*Figure 20)*. In terms of nociception, we will mainly focus our attention on two types of spinal second-order nociceptive neuron (which are also projecting neurons): the nociceptive-specific neuron (NS) and the wide dynamic range neuron (WDR).

Nociceptive-specific neurons respond only to noxious stimulation under physiological conditions. They are mostly found in the superficial laminae of the dorsal horn (I and II) and are mainly recruited by Aδ or C primary afferent fibres. Depending on their recruitment by Aδ or the combination of Aδ and C fibres they can be divided into subclasses: NS responsive only to noxious heat and pinch; polymodal nociceptive neurons, responsive not only to noxious heat and pinch but also to innocuous and noxious cold (HPC) (Craig, 1994; Dostrovsky and Craig, 1996; Han et al., 1998).

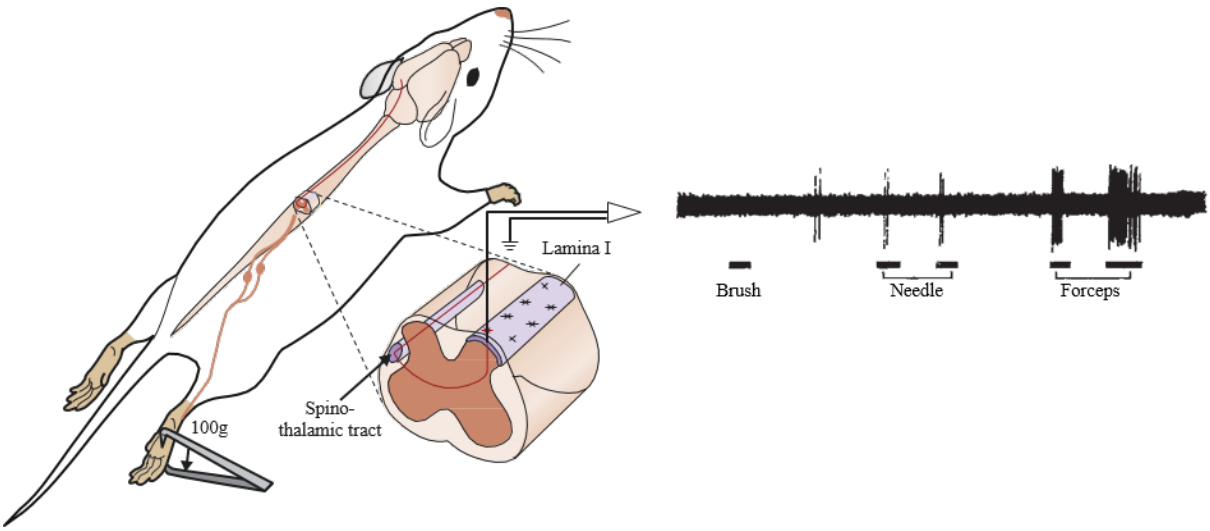

Figure 20 : Single unit recording from NS neuron in the rat lumbar cord showing responses to stimuli applied to the centre of the hind paw. Mainly high noxious pressure induces a high level of firing while applications of needle or brush evoked weak or no response (data from Light et al., 1979)

Wide dynamic range or convergent neurons are mostly found in deeper laminae of the dorsal horn (III to V) and to a lesser extent in the superficial laminae. WDR receive input from both nociceptive Aδ or C fibres as well as low-threshold Aβ fibres and hence are activated by both innocuous and noxious stimuli and include interneurons involved in polysynaptic reflexes (*Figure 21)*. They constitute a volume of information, determined by the intensity, duration and area stimulated. Interestingly, these neurons are believed to play a key role in pain, indeed, in animal models, it has been shown that inflammatory pain leads to multiple modifications of WDR properties such as change in the receptive field, the neuronal discharge frequency and neuronal membrane permeability to ion exchange, all suggesting to play a role in the chronicity of pain (Le Bars, 2002). Finally, they are the main output of the dorsal horn network and they represent a good image of dorsal horn network activity. In the present manuscript, we will focus on WDR neurons regarding our electrophysiological approaches.

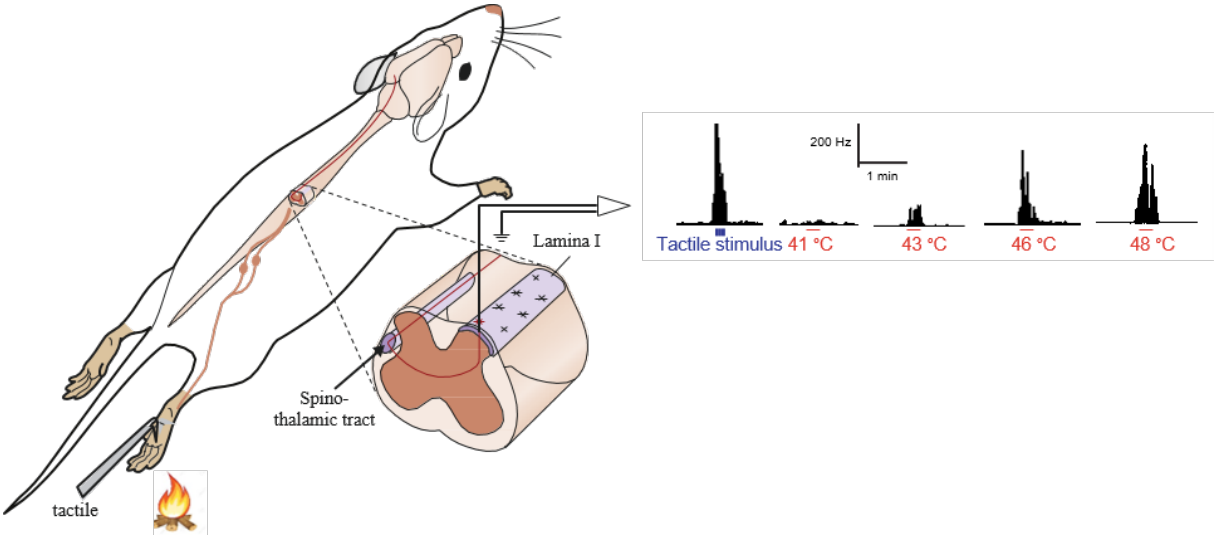

Figure 21 : A Ratemeter recording from a WDR neuron in the rat lumbar cord WDR neuron showing responses to stimuli applied to the centre of the hind paw. Light pressure induce a high level of firing while applications of radiant heat (indicated by a fire illustration) evoked increasing responses depending on the temperature within the noxious range data from (Le Bars and Chitour, 1983).

- Spinal sensitization: secondary hyperalgesia

At the level of the dorsal horn, an increased volley of nociceptive information from primary afferent fibres to the second-order neuron (NS and WDR mainly) triggers a prolonged but reversible increase in the excitability and synaptic efficacy of these neurons termed central sensitization (Woolf, 2011). Phenomenon describes by the IASP as "Increased responsiveness of nociceptive neurons in the central nervous system to their normal or subthreshold afferent input" (IASP, 2019a), and may be characterised by distinct mechanisms including those triggered by shorter-lasting activity such as wind-up and heterosynaptic potentiation and those triggered by both alterations in microglia, membrane excitability, gene transcription which can contribute to long-lasting effects such as long term potentiation (Sandkühler, 2007; Vardeh et al., 2016).

Regarding the homosynaptic potentiation, wind-up is described as a progressive increase in neuronal discharge in response to repetitive and low-frequency nociceptive stimulations (Mendell, 1966; Fossat et al., 2007) (*Figure 22)*. Different mechanisms lead to the expression of windup. It can be presynaptic due to an increase calcium level in afferent terminals, or postsynaptic due to activation of SP (NK1) receptors or NDMA receptors, but also due to intrinsic properties of WDR neurons (Reali et al., 2011; Edmondson, 2017).

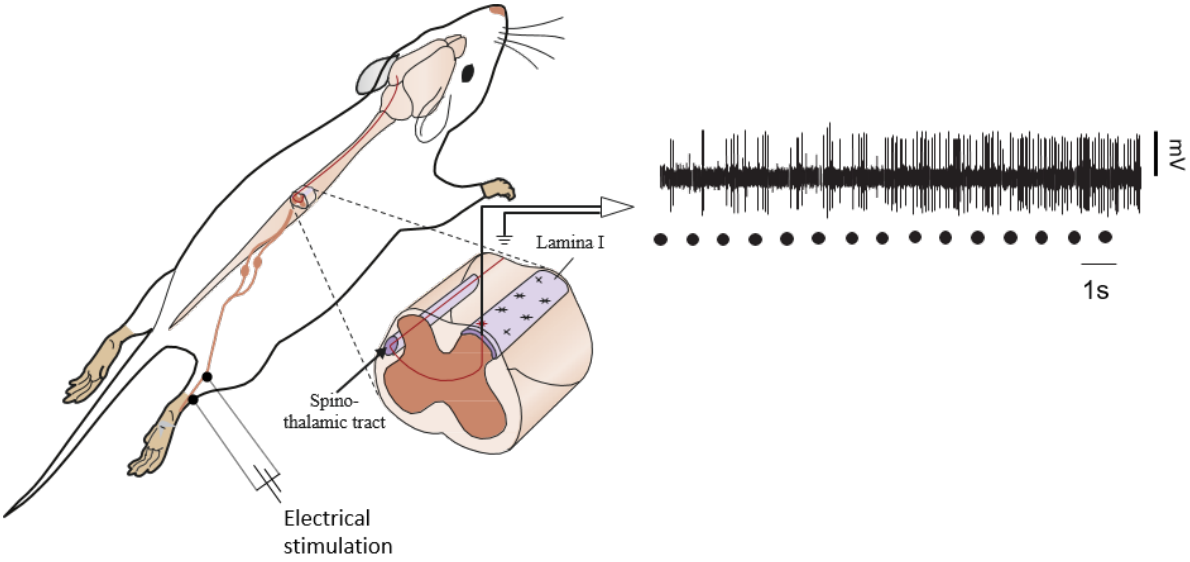

Figure 22 : Windup of a DHN in response in the rat lumbar cord to repetitive stimulation of the sural nerve region (dots) (data from Fossat et al., 2007).

Spinal cord heterosynaptic sensitization is a phenomenon by which two different connections can elicit long term plasticity of the DHNs. Heterosynaptic potentiation lasts much longer than windup. Moreover, heterosynaptic potentiation induces a decrease in the threshold of the incoming stimuli shifting subthreshold inputs from nociceptors (Aδ and C fibres) and Aβ fibres into suprathreshold. These changes may lead to hyperalgesia (stimuli originating from Aδ and C fibres), allodynia (stimuli originating from Aβ fibres) but also secondary hyperalgesia induced by the recruitment of fibres outside the primarily injured area.

One example of spinal cord heterosynaptic sensitization is long-term potentiation (LTP). Indeed, in the dorsal horn of the spinal cord, a persistent increase in synaptic strength following high frequency stimulation (HFS, reflecting the discharge of a subtype of C-fibres at the beginning of noxious mechanical stimuli, (Handwerker et al., 1987)) or low frequency stimulation (LFS reflecting to discharge rates of C-fibres during peripheral inflammation (Puig and Sorkin, 1996)) at synapses of nociceptive nerve fibres (C-fibres) is consider to be a synaptic amplifier of nociception (Liu and Sandkühler, 1997; Sandkühler, 2007).

In addition, other mechanisms may also explain central sensitizations, for instance, alterations in post-translational processing (such as ion channels phosphorylation) and gene transcription, immune cell/glia activation, and disinhibition in spinal cord and/or brain may lead to a longer-lasting change in the dorsal horn neurons thus contributing to the persistence of hyperalgesia, allodynia and secondary hyperalgesia.

Neuron-immune cell interactions are increasingly recognised as being a key for physiological and pathological processes in the central nervous system notably in the context of inflammation and neuropathic pain. Microglia in the spinal cord is activated in case of peripheral nerves injury leading to up-regulation of purinergic receptor P2X4. Activation of P2X4 receptors is responsible for release of brain-derived neurotrophic factor (BDNF). BDNF induces downregulation of KCC2 transporter in projection neurons and a chloride imbalance. This change in chloride equilibrium induces a phenomenon of disinhibition where GABA inputs are not inhibitory and this bring about hyperexcitability in the dorsal horn of the spinal cord. (Coull et al., 2005; Price et al., 2005; Doyon, 2011; Gagnon et al., 2013; Kaila et al., 2014), *Figure 23*. The role of P2X4 in DHNs hyper-excitability has also been observed in a model of persistent inflammation (*Figure 24*; Aby et al 2018).

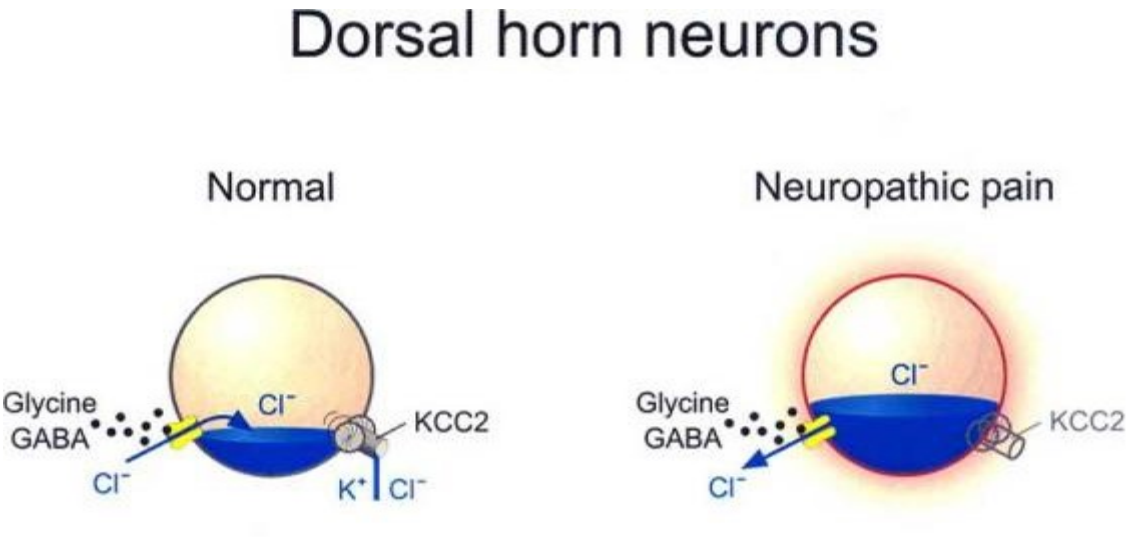

Figure 23 : Role of Cation Chloride Cotransporters KCC2 in the regulation of Cl^- reversal potential. In adult dorsal horn neurons in physiological condition, the extrusion of Cl^- through KCC2 maintains the anion reversal potential hyperpolarizing. However, disruption KCC2 expression/activity following peripheral nerve injury causes an outflux of Cl^- in the cytosol which inverts the anion flux upon GABA-A or glycine receptor activation, and thus reverses their action (Price et al., 2005)

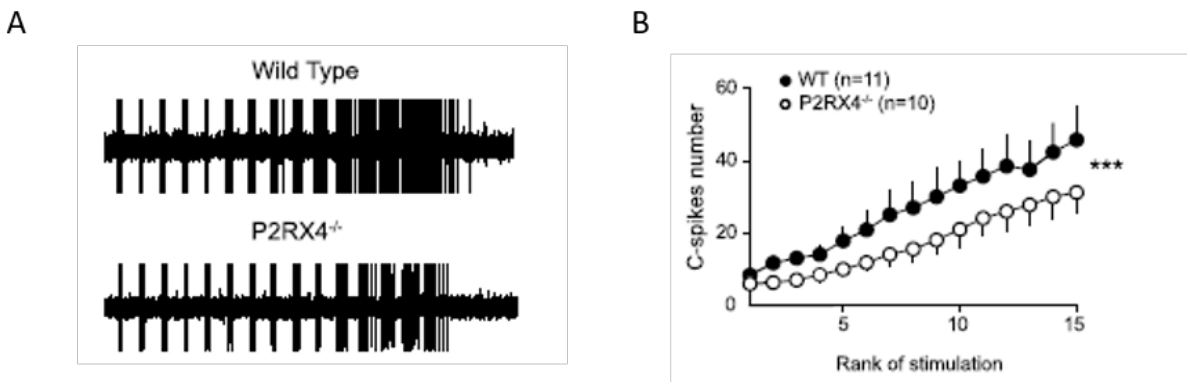

Figure 24 : Electrophysiological consequence of a P2x4 receptor depletion in mouse model of persistent pain, In vivo data shows that in persistent pain condition both (A) the amplitude of wind-up which is a form of sensitization to pain that is not expressed by peripheral fibres and thus restricted to the dorsal horn, and (B) the intensity response curve (IR) are decreased in P2RX4 -/- mice as compared to WT mice. 001). P2RX4-/-, mutant mice deleted from P2X4 receptor; WT, wild-type (data from (Aby et al., 2018).

b) *Endogenous pain modulation mechanism*

At the level of the dorsal horn of the spinal cord, fibres coming from different brain areas modulate pain transmission. The concept of modulation refers to the mechanism by which pain is suppressed or increased within the dorsal horn of the spinal cord The existence of an endogenous control of pain has been first observed earlier, during the World War II by Dr Beecher (Beecher, 1946) that noticed that there was no correlation between the amplitude of the wound and the pain sensation of injured soldiers. Three different mechanisms have been enlightened to control pain, the segmental inhibition, the endogenous opioid system, and the descending control.

i. Segmental inhibition

In 1965, Melzack and Wall proposed the "gate theory of pain control," which describes the ability of pain transmission from the Aδ and C nerve fibres to the dorsal horn to be blocked or diminished *(Figure 25)*. To go further on the spinal gating mechanism, sensory information to spinal transmission neurons are carried via two classes of fibres, non-nociceptive information is transmitted via large diameter *A-fibres* while nociceptive information is transmitted via small-diameter *C-fibres (including* Aδ fibres). The gating component is played out by interneurons of the substantia gelatinosa and they modulate input to the spinal transmission neurons through either presynaptic inhibition or facilitation of afferent fibres. Activity in large diameter A-fibres triggers substancia gelatinosa interneuron that, in turn, inhibits synaptic transmission in C-fibre

resulting in hypoalgesia. Moreover, activity in small-diameter C-fibres inhibits substancia gelatinosa interneuron and this disinhibition increases synaptic transmission resulting in hyperalgesia. In other words, one can "close the gate" by enhancing the output of the large-diameter A-fibres. This led to the development of the TENS unit (transcutaneous electrical nerve stimulation). With such protocol, the activation of large myelinated Aβ fibres (touch/proprioception) inhibits nociceptive transmission.

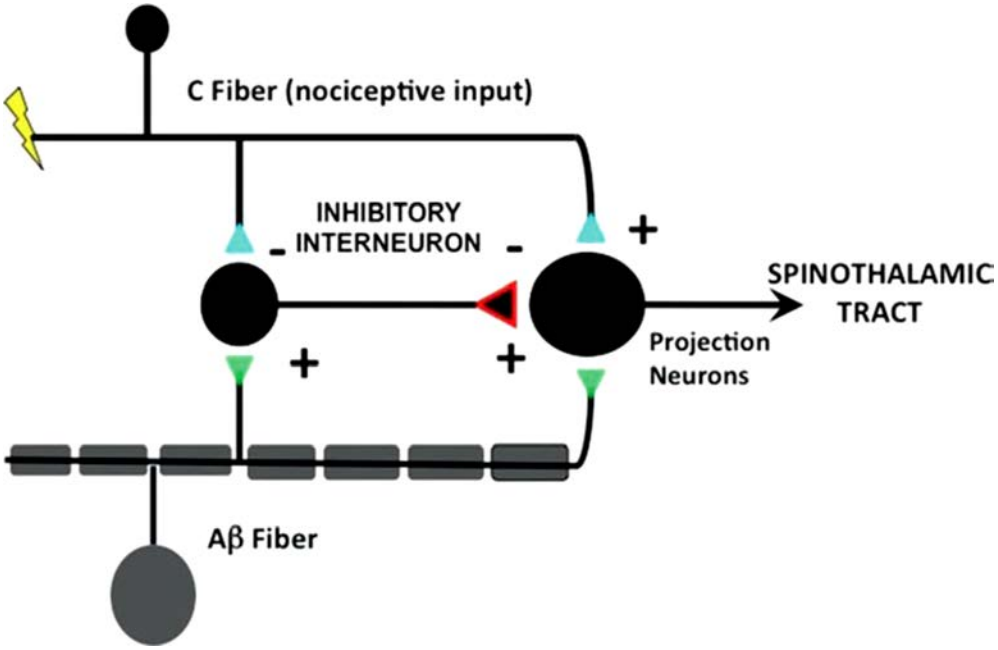

Figure 25 : The gate control theory of pain (Melzack and Casey, 1968). Nociceptive signals conveyed by the peripheral C fibre inhibit the inhibitory interneuron in the substantia gelatinosa while propagating excitatory information to the spinothalamic tract. When mechanoreceptors are activated, the inhibition from the C fibre at the inhibitory interneuron is lowered, and the nociceptive signal to the spinothalamic tract is in competition with proprioceptive signals from the mechanoreceptors. + Excitatory synapse, – inhibitory synapse (Sufka and Price, 2002).

ii. Endogenous opioid system

Observations in mammals of both opioid receptors concentrated in the brainstem (periaqueductal gray and ventral medulla) as well as in the spinal cord (lamina II of the dorsal horn) and production of endogenous compounds (enkephalins, endorphins, and dynorphin) that bind to these opioid receptors lead to the concept of Diffuse Noxious Inhibitory Controls (DNIC) where a localized nociceptive stimulation can produce a diffuse analgesic effect over the rest of the body, an analgesic approach known as counter-irritation (Marinelli et al., 2002; Fields, 2004; Lima et al., 2017), notably after inflammation (de Resende et al., 2011). Indeed, it has been shown that opioids receptors modulate the pain transmission by reducing the dorsal

horn neuron activity following nociceptive stimuli resulting in DNIC analgesia (de Resende et al., 2011).

iii. Descending system

This system involving periaqueductal gray matter in the upper brain stem, the locus coeruleus, the nucleus raphe Magnus, and the nucleus reticularis gigantocellularis in the rostroventral medulla contributes to the descending pain suppression pathway and then inhibits ascending nociceptive information from the nociceptive pain pathway (*Figure 26)*. The axons involved in this pathway descend down the bilateral dorsolateral funiculus and synapses in laminae I, II, and V of the spinal cord. Some of the common inhibitory neurotransmitters are serotonin as well as norepinephrine. Drugs that serve to block the reuptake of these neurotransmitters prolong their inhibitory action on the spinal cord neurons involved in pain transmission, leading to pain relief (Patetsos and Horjales-Araujo, 2016). This explains the use of serotonin-norepinephrine reuptake inhibitors and tricyclic antidepressants for their analgesic properties. Nevertheless, these drugs can cause due to improper drug tolerance or an acute drug intoxication from the patient, a pathologic state such as serotonin syndrome which is the product of the overactivation of both the central and peripheral serotonin receptors as a result of high levels of serotonin following inhibition of serotonin uptake, decreased serotonin metabolism, increased serotonin synthesis, increased serotonin release, and then activation of serotonergic receptors (Volpi-Abadie et al., 2013; Tschirdewahn and Eyer, 2019).

From here, to get more in detail in the comprehension of pain modulation, we will mainly focus our attention on the descending pain control notably those mediated by the brainstem with a focus on the raphe Magnus mainly and the periaqueductal gray.

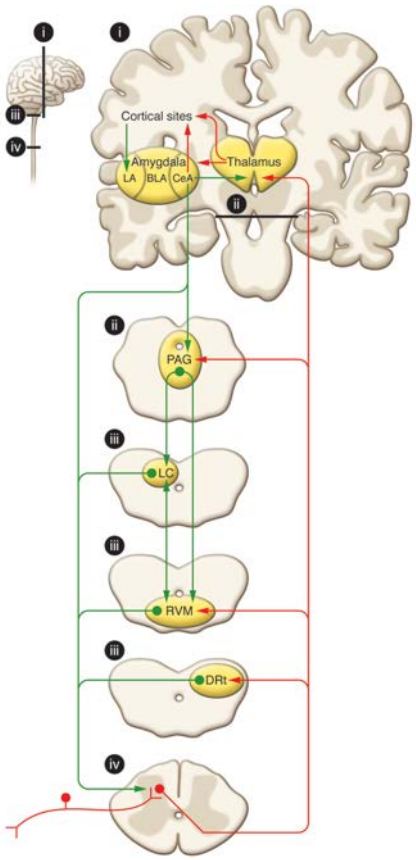

Figure 26 : Schematic representation of pain modularity circuitry. Following a noxious stimulus, nociceptive information conveys by the noxious primary afferent will reach the dorsal horn of the spinal cord and then trigger the projection neuron. The projection fibres ascend contralaterally through the spinothalamic tract and then target the thalamus, and collateral projections also target mesencephalic nuclei, including dorsal reticular nuclei (DRt), the rostro ventral medulla RVM, and the midbrain periaqueductal gray PAG. Descending projections from the DRt are a critical component of the diffuse noxious inhibitory control (DNIC) pathway. Descending pain modulation is mediated through projections to the PAG, which also receives inputs from other sites, and communicates with the RVM as well as other medullary nuclei that send descending projections to the spinal dorsal horn through the dorsolateral funiculus (DLF). The noradrenergic locus coeruleus (LC) receives inputs from the PAG, communicates with the RVM, and sends descending noradrenergic inhibitory projections to the spinal cord. Antinociceptive and pronociceptive spinal projections from the RVM positively and negatively modulate nociceptive inputs and provide for an endogenous pain regulatory system. Ascending (red) and descending (green) tracts are shown schematically. Areas labelled "i–iv" in the small diagram correspond with labelled details of the larger diagram. (Ossipov et al., 2010)

B. RAPHE MAGNUS DESCENDING CONTROL

Pain is closely controlled or modulated by the central nervous system (CNS). However, the intensity of the perceived pain is not necessarily proportional to the amount of stimulus under different conditions. Despite the fact that psychological factors contribute to the variability of pain, the most important underlying mechanisms responsible for the modulation of pain sensation are the existence of endogenous pain modulatory systems, in which brainstem descending pathways play a fundamental role (Millan, 2002a). The evidence of descending pain control came with the study Reynolds (Reynolds, D. V., 1969) who highlighted that focal brain stimulation of the midbrain periaqueductal gray (PAG) produced sufficient analgesia to allow surgery in rats without the use of chemical anaesthetics and later confirmed by Liebeskind and colleagues that quickly confirmed this finding and concluded that stimulation of the PAG activated a normal function of the brain: pain inhibition (Mayer, D. J. *et al*., 1971; Mayer, D. J. and Liebeskind, J. C., 1974). However, later evidence indicates that pain modulation is not limited to inhibition. Descending pathways also facilitate pain transmission at the spinal level (Ren, K. *et al*.,2000; Millan, M. J., 2002; Gebhart, G. F., 2004). Indeed, new lines of evidence suggest that the descending pathways exhibit dramatic plasticity and are actively involved in the development of persistent pain after tissue or nerve injury (Porreca, F. *et al*., 2002; Ren, K. and Dubner, R., 2002; Gebhart, G. F., 2004; Vanegas, H. and Schaible, H.-G., 2004).
To date, the most well-characterized endogenous pain modulatory pathway involves a circuitry linking the midbrain PAG, rostral ventromedial medulla (RVM), and the spinal cord in which the first two is often viewed as the “back-bone” (Mason, 2005)

1. The Periaqueductal Gray

The PAG comprises heterogeneous cell populations surrounding the Sylvius aqueduct with function to integrate sensory and motor responses (Bandler, R. and Shipley, M. T., 1994; Cameron, A. A. *et al*., 1995a; 1995b). It extends rostrally from the pericoerulear area of the pons to the opening of the third ventricle. Both the dorsal raphe nucleus ventromedial to the Sylvius aqueduct and the cuneiform nucleus lateral to the ventrolateral PAG are also considered a functional entity of the PAG for descending pain control (Jensen, T. S. and Gabhart, G. F., 1988; Fields, H. L. and Basbaum, A. I., 1999). The anatomical studies highlight the importance of the midbrain PAG in descending pain modulation (Menetrey, D. *et al*., 1982; Hylden, J. L.

K. *et al*., 1986; Azkue, J. J. *et al*., 1998), PAG provides major input to most areas that are involved in endogenous pain control, including RVM (RMg), and to a lesser extent the spinal cord (Jensen, T. S. and Gabhart, G. F., 1988; Fields, H. L. and Basbaum, A. I., 1999). Moreover, the stimulation-produced analgesia induced by the PAG stimulation was limited to nociceptive processing and could not be explained by more gross stimulation produced deficits in sensory or motor function. Additionally, it eliminates behavioral and spinal dorsal horn neuronal responses to noxious stimuli including electric shock applied to the tooth pulp or limbs, noxious heating of the tail and hind paws, noxious pinching of the limbs, and injection of irritants into the viscera (Sessle, B. J. *et al*., 1981; Dostrovsky, J. O. *et al*., 1983; Gebhart, G. F., 1988). Stimulation mediating analgesia inducing antinociception from the PAG also involve a spinal release of 5-HT and NE, and both spinal 5-HT receptors and α_2 adrenoreceptors (Camarata and Yaksh, 1985). However, in particular conditions, the PAG can also mediate descending facilitation of the nociception (Vanegas and Schaible, 2004; Zambreanu et al., 2005). Moreover, inactivation of the RVM prevents the antinociceptive effects of stimulation of the PAG, indicating that the connection from the PAG (dorsomedial, lateral and ventromedial column) to the RVM is the neuroanatomical basis for descending modulation of nociception by the PAG. In addition, depending on the site of stimulation, the antinociception evoked will be associated with different behaviour. Indeed, antinociception produced by stimulation of the ventrolateral PAG is often accompanied by immobility (related to a defensive fear response such as freezing) both mediated by glutamatergic neurons (Lau and Vaughan, 2014; Tovote et al., 2016a). Indeed, it has been shown that the vlPAG contains diverse subpopulations of neurons (inhibitory and excitatory interneurons) including somatostatin (which we have proposed to study in my thesis) with distinct neurochemical properties that regulate excitatory and inhibitory neurotransmission and then plays critical and complex roles in processing nociception (Brenner et al., 2012; Samineni et al., 2017)

PAG–RVM projection neurons express neuropeptides, excitatory amino acids, and serotonin. Functional studies involve excitatory amino acids, endogenous opioids, and serotonin in the recruitment of the RVM by the PAG to produce antinociception.

2. Nucleus Raphe Magnus (RMg) of the RVM

The RMg can be considered as the brainstem output from the PAG-RVM system, receiving a dense innervation from the PAG and projecting to the dorsal horn through the dorsolateral funiculus. It is the primary relay in mediating the antinociceptive effects of

activation of PAG neuron. RVM neurons are likely to receive spinothalamic inputs, either through direct connections to their widespread dendritic arbours or relayed via other brainstem regions such as nucleus reticularis gigantocellularis or the PAG (Fields and Basbaum, 2005). The primary outputs from the RVM are thus descending projections to the dorsal horn, both directly and via the mesopontine tegmentum. Earlier it has been shown that electrical stimulation of the RMg produces strong antinociception that can be reversed by intrathecal 5-HT receptor antagonists but also NE antagonists and GABA antagonists (Pertovaara, 2006; Dogrul et al., 2009; Ossipov et al., 2010). However, low-intensity electrical stimulation of the RVM and infusions of neuropeptides and *N*-methyl-D-aspartic acid (NMDA) in this region have been shown by various groups to facilitate nociceptive processing (Neubert et al., 2004; François et al., 2017). Moreover, inactivation studies highlight lesions implicating the RVM in a variety of models of hyperalgesia and persistent pain following noxious stimulation of a remote body part, and in neuropathic pain models (Porreca et al., 2001; Vanderah et al., 2001) and consequently demonstrate a facilitating role of the RVM in a variety of enhanced pain state including neuropathies. One evidence to support the RVM bidirectional control is the neural composition of the RVM. Some of which can be identified as, based on the responses of RVM neurons to noxious stimulation, the OFF-cell (that are inhibited by noxious stimulation and excited by opioids) and ON-cell (that are excited by noxious stimulation and inhibited by opioids), both associated with the suppression (OFF-cell) and facilitation (ON-cell) of the nociception (Fields, 2004; Benarroch, 2014). In addition, there are other types of cells, identified as neutral cell including those containing 5-HT which is implicated in descending facilitation as well as descending inhibition of nociception (Suzuki et al., 2004). Then, RVM mediate both descending facilitation and inhibition, an important question is to determine when these different pathways are activated and if changes happened in different pathological contexts.

A plethora of transmitters have been shown to play a major role in descending pain control (Millan, 2002a; François et al., 2017; Yam et al., 2018). The most studied and established candidates include endogenous opioid peptides, noradrenaline, and serotonin (5-HT). All these transmitters participate in inhibition and facilitation of pain transmission through their respective receptor subtypes. Our attention will be mainly focused on the 5-HT which is one of the first neurotransmitters identified as being involved in descending pain control, which exact role is still mattered of debate.

a) *The Serotonin 5-HT*

i. General introduction

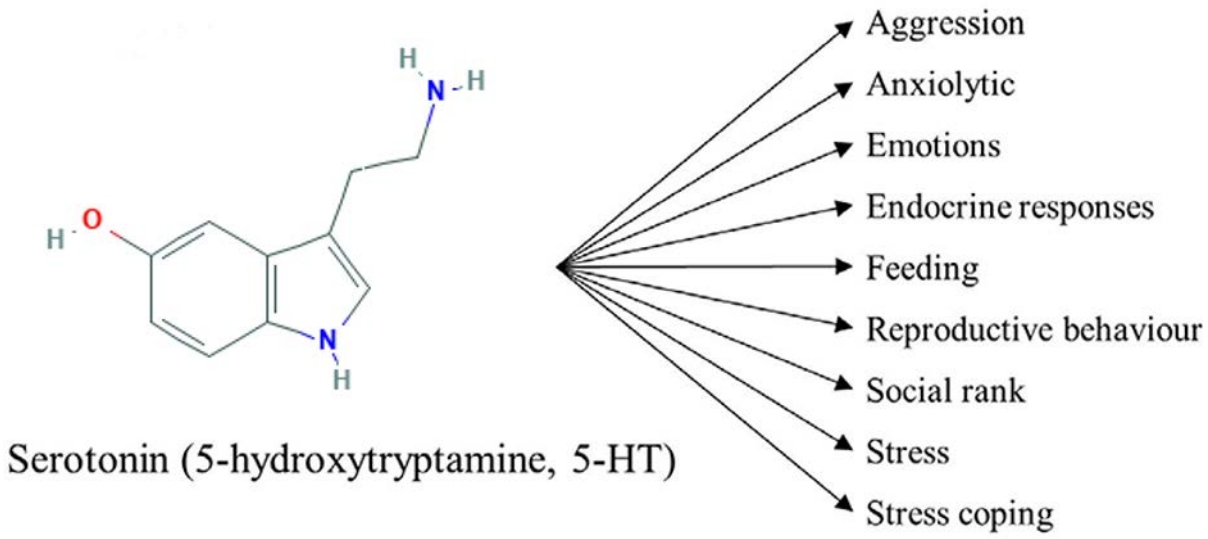

Figure 27 : 5-HT chemical structure and its diverse involvement in the CNS (Backström and Winberg, 2017)

Considered as the hormone of happiness, the 5-hydroxytryptamine; (5-HT) better known as serotonin *(Figure 27),* is one of the major neurotransmitters of the central nervous system (CNS). It is a monoamine widely distributed within the organism, synthesized both in the periphery nervous system (PNS) as a hormone (enterochromaffin cells in the gastrointestinal tract and to a lesser extent platelets (Mohammad-Zadeh et al., 2008) as well as Mast cell during inflammatory response (Meyer, 2013) and the CNS as a neurotransmitter (in serotonergic neurons) where it represents not more than 3 to 5% of the total of 5-HT (Mengod et al., 2006). Nevertheless, in the CNS, it is implicated in multiple modulating actions such as the regulation of mood and emotion, sleep/wake cycle, emesis, food intake, sexual behaviour, neurovegetative homeostasis and other cognitive functions as well as migraine and nociception (Müller and Jacobs, 2010) whose current implication is well-established but with a role still unclear because of contradictory conclusions on antinociceptive or pronociceptive role.

ii. Peripheral vs central 5-HT

Although present in both the PNS and the CNS, it is important to note that for the general belief, there is a compartmentalization of the 5-HT to the large benefit of the periphery carried

out by the brain-blood barrier (BBB) thereby preventing any transport from one compartment to another and ensuring the quantitative and qualitative stability of these two separate compartments.

At the peripheral level, 5-HT covering approximately 90 to 95% of 5-HT of the body, is mainly synthetized in the gut by enterochromaffin cells of the mucosa via mainly the tryptophan hydroxylase 1 (TPH1) and released into the bloodstream, where it is carried by circulating platelets (Rudnick, 1977; Hranilović et al., 1996; Walther et al., 2003) through the action of the membrane serotonin transporter SERT, which is also expressed on lymphoblast (Faraj et al., 1997), monocytes (Yang et al., 2007), enterochromaffin cells, endothelial cell (Wheatcroft et al., 2005) and placental syncitiotrophoblasts (Balkovetz et al., 1989). It (5-HT) is transported all over the entire vascularized tissues (and later metabolised by the liver) to act as a hormone with main function in haemostasis and other non-neuronal process such as cardiovascular, pulmonary and genitourinary system without forgetting an immunomodulatory role (modulation of cytokine secretion in monocytes/macrophages cell) (Arreola et al., 2015; Herr et al., 2017). Indeed, along with other pro-inflammatory mediators such as histamine, prostaglandins, bradykinin, leukotrienes, amines, purines, cytokines and chemokines, it is one of the constituents of the "inflammatory soup", which appears to play a major role in the cellular processes that lead to pain in case of inflammation or tissue damage (Hamon and Bourgoin, 1999) by an excitatory effect on peripheral nerve fibre. Notably, it has been shown that systemic administration of monoamine (subcutaneously or intravenously) reproducing the endogenous peripheral hyperalgesic action of the 5-HT leads to sensitization of the nociceptive primary afferents (Aδ and C fibres) and the nociceptive neurons located in the dorsal roots ganglia, from which these fibres are derived, thus contributing to a peripheral hyperexcitability which in turn leads to a hyperalgesia. (Sommer, 2004; Sasaki et al., 2006). Phenomenon, which is related to a rapid increase of the resting plasma 5-HT concentrations in the case of platelet activation at the site of thrombus formation or inflammation (Duerschmied et al., 2009; Mössner and Lesch, 1998). Pronociceptive effect which may be 5-HT receptors dependent. (Hamon and Bourgoin, 1999; Sommer, 2004; Sasaki et al., 2006; Godínez-Chaparro et al., 2011).

At the central level, in spite of its small representation with regards to the periphery (only 3 to 5% of the 5-HT of the body), 5-HT as a neurotransmitter, innervates all the neuroaxis and thus modulates the activity of a wide variety of human brain processes, behavioural and neuropsychological processes such as mood, perception, reward, sleep cycles, aggression, appetite, learning (Veenstra-VanderWeele et al., 2000). However, 5-HT has also been

recognized to have a role in endogenous supraspinal pain-modulating systems (Basbaum and Fields, 1978) where its action remains the subject of much debate (Millan, 2002a). Indeed, through many experimental studies, it has been shown that brainstem stimulation, depending upon the stimulus parameters, can cause both analgesia (Yaksh and Wilson, 1979; Le Bars and Villanueva, 1988) and hyperalgesia (Zhuo and Gebhart, 1991) effects on the pain behaviour in animals, action both mediated by descending serotonergic pathway. One reason underlying this two-fold action of 5-HT may lie in the fact that there is a multiplicity of 5-HT receptors present both at the periphery and the central nervous system with opposite effect in terms of pain. For instance, it has been shown that changes in term of behavioural response as reply to thermal, mechanical or inflammatory noxious stimuli in mutant mice deficient in either type of 5-HT receptors can be sometimes weaker, sometimes stronger than those observed in wild type mice associated (i.e., of same genetic background) depending on the type of 5-HT receptors target of the genetic mutation (Kayser et al., 2007; Brenchat et al., 2012) *(Figure 28).*

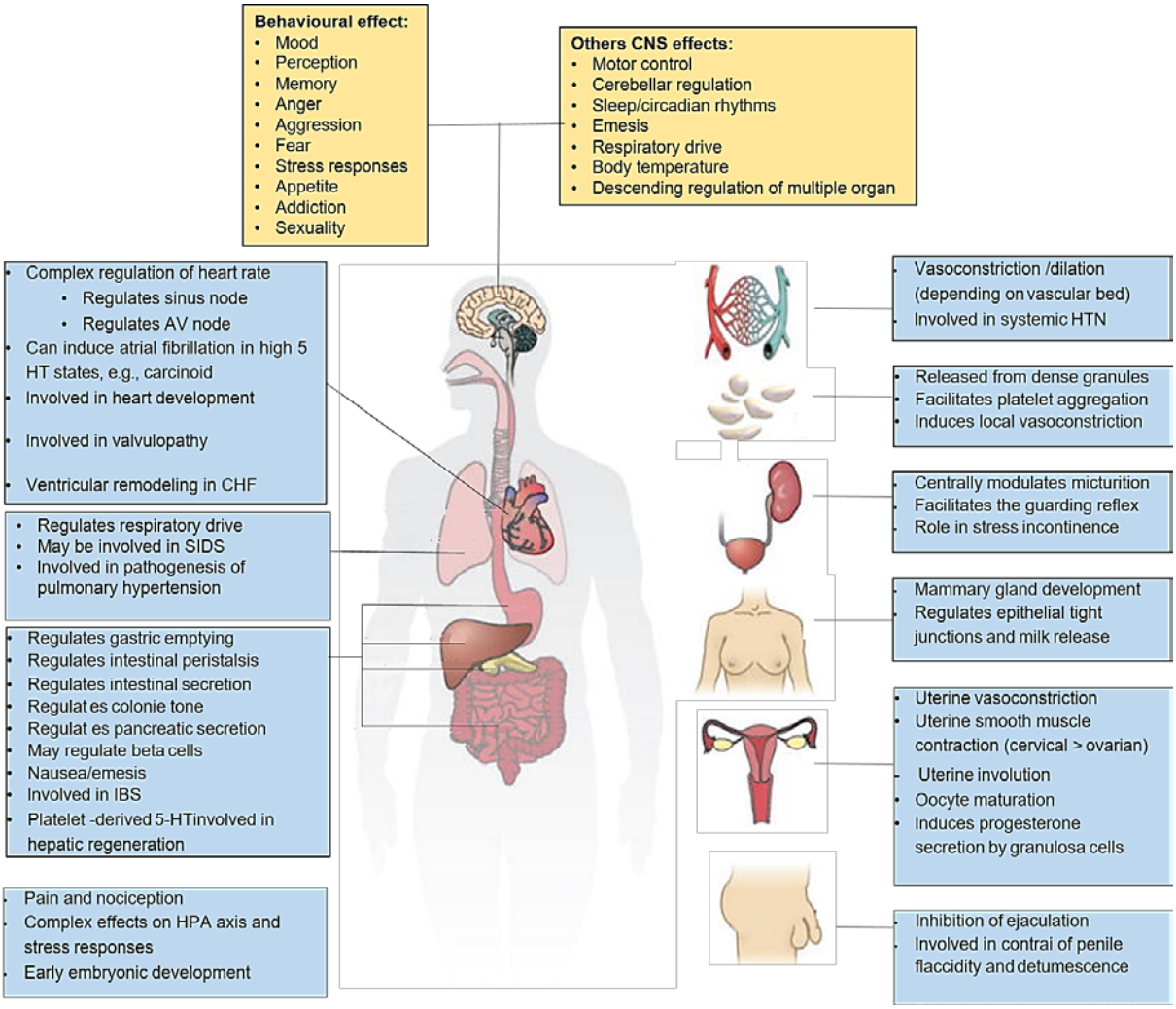

Figure 28 : Various effect of 5-HT on the peripheral (blue frame) and central nervous systems (yellow frame) adapt from *(Berger et al., 2009)*. 5-HT, serotonin; AV, atrioventricular; CHF, congestive heart failure; CNS, central nervous system; HPA, hypothalamic-pituitary-adrenal; HTN, hypertension; IBS, irritable bowel syndrome; SIDS, sudden infant death syndrome.

iii. Neuroanatomy of central 5-HT

Early formed during the embryogenesis (days 11-12 on gestational stage), the 5-HT system is proposed to play a role in the organisation of the developing nervous system (cytoarchitectonic organisation of the raphe for instance) notably by acting on neurite outgrowth and other neural differentiation function including the synaptogenesis (Lauder, 1990). In addition, a correlation has been highlighted between the lineage of the 5-HT-synthesizing neurons and the joint action of a cascade of transcription factors located caudally to the midbrain-hindbrain structured in two cellular clusters in rhombomeres 1 – 3 (giving rise to rostral raphe cluster) and 5 – 7 (giving rise to caudal raphe cluster) compartments (Alenina et

al., 2006; Kiyasova and Gaspar, 2011). Among them, Pet-1, which is a 5-HT specific transcription factor expressed in embryonic and adult serotonergic neurons (Hendricks et al., 1999; Kiyasova and Gaspar, 2011) and thus, *Pet1* represents the privileged candidate gene to be used in Cre recombinase/loxP-based strategies to specifically target serotonergic neurons (Scott et al., 2005a) *Figure 29*.

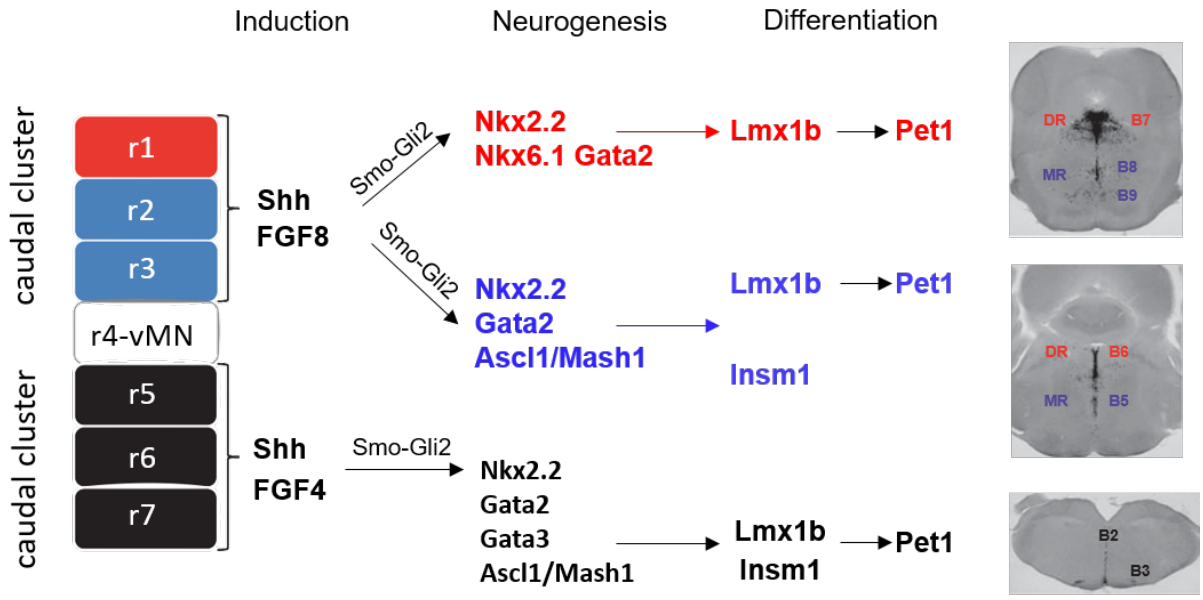

Figure 29 : Development of raphe 5-HT neurons. Summarization of the transcription factors known to control region-specific differentiation in the hindbrain. In the rostral cluster of 5-HT neurons, Shh and Fgf8 control induction and activate via Gli2 transcription factors: Nkx2.2+ Nkx6.1+ Gata2+Ascl1 / Mash1 in rhombomere 1 (in red) and Nkx2.2+ Gata2+Ascl1 / Mash1 in rhombomeres 2 and 3 (in blue). Lmx1b and Pet1 (in red) control the terminal differentiation for the dorsal raphe (DR) 5-HT neurons, whereas that in the median raphe (MR) is controlled by Lmx1b, Pet1 and Insm1 activated by Ascl1 / Mash1 (in blue). Transcriptional regulation of the 5-HT neuron development in the caudal cluster is regulated by Shh and Fgf4 during induction, Nkx2.2+ Gata3+Ascl1 / Mash1 during neurogenesis and Lmx1b, Pet1 and Insm1 for the terminal differentiation. Tph2 expression (in situ hybridization) on coronal sections shows the rostral level containing the B7 DR and B8 MR, and a caudal level containing the B2 nuclei that arise from the caudal hindbrain cluster. r1–r7, rhombomere 1–7; vMN: ventral motor neuron (illustration from Kiyasova and Gaspar, 2011)

Organizationally, the cell bodies of serotonergic neurons are exclusively located in the brainstem (medulla and midbrain) and particularly in cluster of cells named B1 to B9, according to their caudorostral distribution (Dahlstroem and Fuxe, 1964) and were centred on the midline raphe nuclei, extending into the subnuclei of the lateral reticular formation, from which the axonal projections give rise to a dense axonal innervation to nearly all over the CNS *(Figure 30)*.

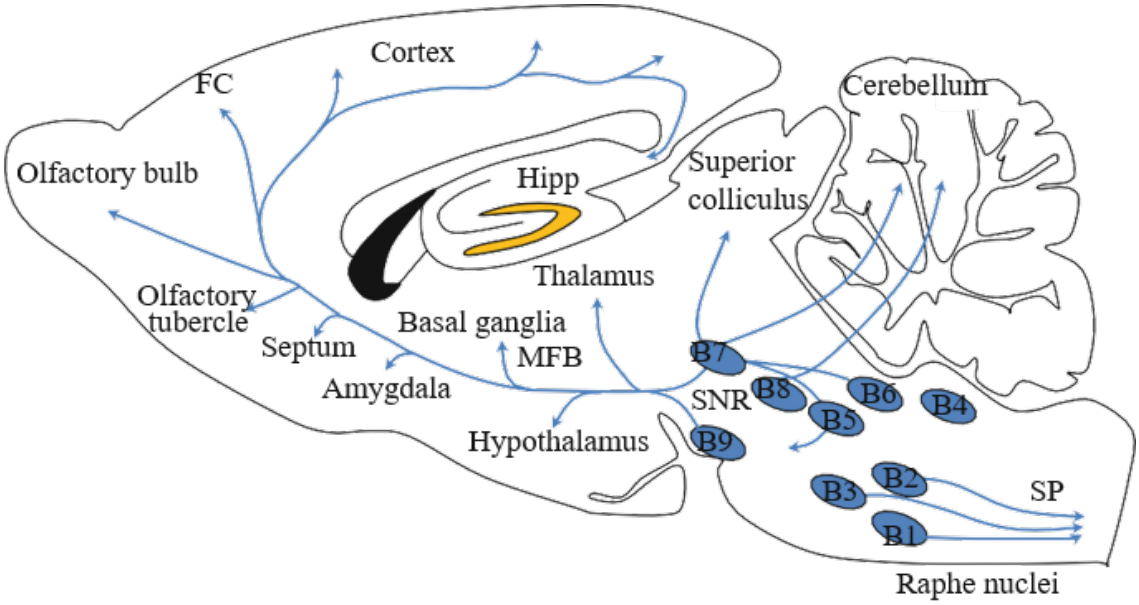

Figure 30: Serotonergic pathway in the CNS of rodents, serotonergic cell body location (B1 to B9) and their major projections. FC, frontal cortex; MFB, Medial Frontal Bundle; SNR, Substantia nigra reticularis; SP, Spinal cord (Lesch and Waider 2012)

Indeed, these neurons are divided into two populations. On one hand, a rostral group which includes 5-HT neuron of B5 to B9 nuclei, locates in the midbrain and rostral pons (caudal linear ⇔ B8 group; dorsal raphe nuclei ⇔ B6 and B7 groups; median raphe nuclei ⇔ B8 and B5 groups and dorsal limit of the medial lemniscus ⇔ B9 group), with a major projection targeted to the forebrain (cerebral cortex, olfactory bulb, hypothalamus, thalamus etc.) and to a lesser extent to the brainstem and with various afferent projection from lateral habenula, the medial septum and the diagonal band of Broca and the ventral pallidum as well as several hypothalamic projections (medial and lateral pre-optic areas, lateral, dorsal, ventral and posterior divisions of the hypothalamus), the ventral tegmental areas, the laterodorsal tegmentum nuclei, and the cingulate cortex using both GABA or glutamate as a neurotransmitter (Behzadi et al., 1990; Peyron et al., 1998; Lee et al., 2003, 2005a, 2005b). Also, there are ascending projections from RMg and RPA nuclei and glycinergic projection (ventral and ventrolateral periaqueductal gray neurons, medullary rostral paragigantocellularis and rostral ventromedial reticular nuclei neurons) (Behzadi et al., 1990; Wang et al., 1992; Rampon et al., 1999). And on the other hand, a caudal group, which includes 5-HT neuron of B1 to B4 bulbar nuclei located in the caudal pons and the medulla (raphe Magnus, obscurus and pallidus nuclei, lateral medullary reticular formation), with a major projection targeted to

the spinal cord (Segu and Calas, 1978; Björklund and Skagerberg, 1982; Bowker et al., 1983; Kwiat and Basbaum, 1992; Mason, 1999) *Table 4*. It is important to note on one hand that both groups have projections to the brainstem and on the other hand the subnuclei of the serotonergic group have distinctive afferent and efferent connections, with some entities more related to the sensory, motor or limbic systems. Indeed, serotonergic neuron from B1 (raphe pallidus) and B2 (raphe obscurus) nuclei are targeting particularly the ventral horn of the spinal cord (somatic motor nuclei, cranial phrenic, trunk and limb motor neurons (Arita et al., 1993, 1995; Li et al., 1993; Ribeiro-do-Valle, 1997)), with projections featuring large varicosities and making direct synaptic contacts with the motoneurons (Ridet et al., 1993; Perrin et al., 2011), while the dorsal horn receives mainly afferents of B3 nuclei (nucleus Raphe Magnus RMg, lateral paragigantocellular nucleus, LPGi) with mainly small varicose fibres projections(Felten and Sladek, 1983; Azmitia and Gannon, 1986). In particular, the RMg serotonergic projections mainly reach the III-IV and V layers of the dorsal horn, while those from the LPGi remained confined to the I and II superficial layers (Ridet et al., 1993; Millan, 2002b; Gautier et al., 2017) with the particularity of being unmyelinated for some and partially myelinated for the others. Also regarding to 5-HT varicosities, most of them were shown to set up symmetrical synaptic contacts with the shaft of either nearby or distant dendrites in both cats and monkeys (Ruda and Gobel, 1980; Ruda et al., 1982) but also, it is suggested that the majority of serotonin transmission occurs through non-synaptic contacts between serotonin terminal varicosities and their targets, involving control of a paracrine mode neurons of the dorsal horn (Ruda et al., 1982; LaMotte and de Lanerolle, 1983). (see the illustration of type of contact *Figure 31* and *Table 5*).

In addition, this caudal group receive afferent projections from several areas of the brain such as several hypothalamic nuclei, the dorsolateral periaqueductal gray, the central nucleus of the amygdala, the bed nucleus of the stria terminalis, and the medullary reticular formation (Zagon, 1993; Hermann et al., 1997). Indeed, RMg receives convergent input from the pneumotaxic area in the medial parabrachial area and the retrofacial nuclei (Gang et al., 1993). There are also converging inputs from visceral sensory afferents and ventrolateral periaqueductal gray matter neurons onto RMg, Rob and RPa midline raphe neurons (Snowball et al., 1997). And there is also a caudal projection from the DR on the RMg and Rob and LPGi (Vertes and Kocsis, 1994).

Table 4 : The different serotonergic cell group and their projection (Dahlstroem and Fuxe 1964)

	Designation	Structure
Descending projection targeting to the spinal cord	B1	Nucleus raphe pallidus Caudal part of the ventrolateral medulla
	B2	Nucleus raphe obscurus
	B3	Nucleus raphe magnus Rostral part of the ventrolateral medulla Lateral paragigantocellular reticular nuclei
	B4	Periventricular grey matter *area postrema*
Ascending projection targeting to the forebrain	B5	Median nucleus raphe pontis
	B6	Dorsal nucleus raphe pontis
	B7	Dorsal raphe nucleus
	B8	Median raphe nucleus Nuceli raphe linearis
	B9	Medial lemniscus

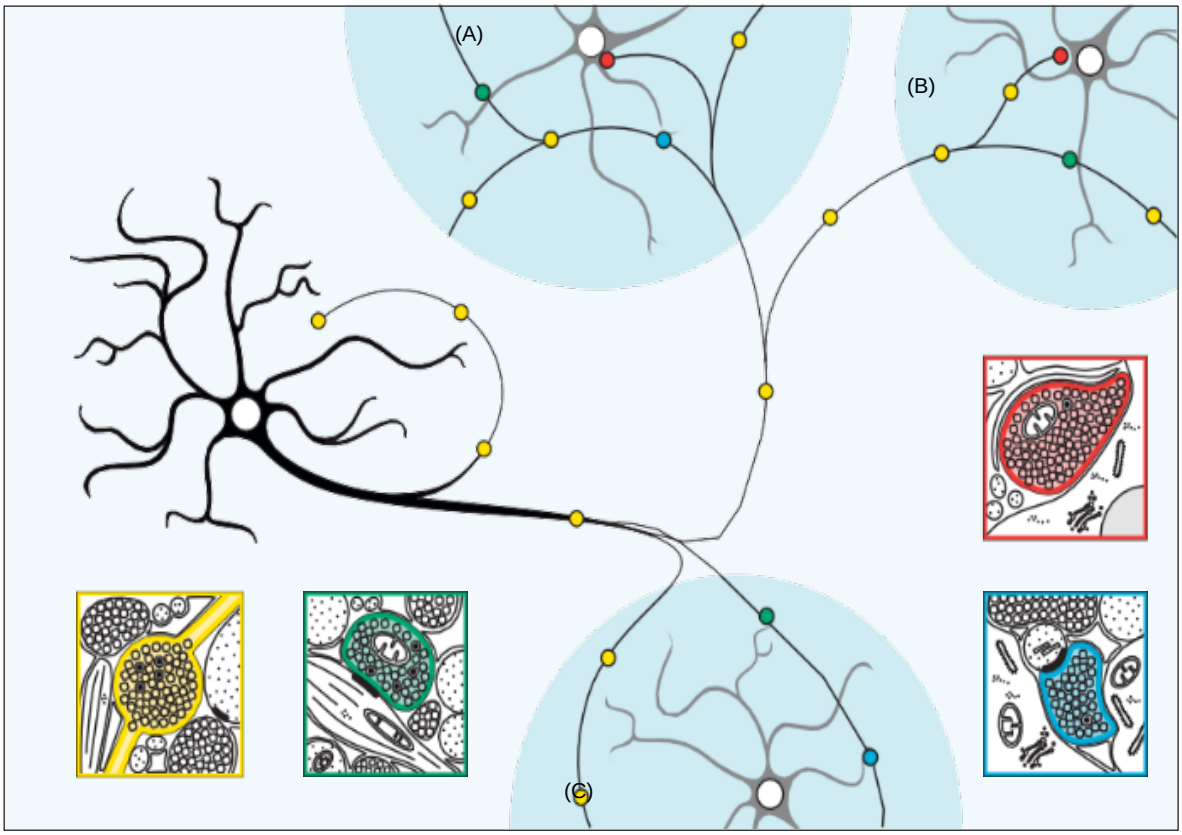

Figure 31 : Conventional 5-HT neuron schematic representation. As illustrated above, from one single 5-HT neuron, several different anatomical regions (A, B, C) may be innervated, as well as its nucleus of origin (through recurrent collaterals of its axon). Small coloured dots represent different types of 5-HT varicosities in the different territories of innervation, which are spread on the axon all along the distal branches, as for the yellow dot some of them do not make any synaptic contact, whereas others are provided with junctional complexes. Green dots correspond to the zone of membrane specialization, either symmetrical (inhibitory synapse) or asymmetrical (excitatory synapse), which make a contact with dendritic branches. Blue dots correspond to those who make contact with the dendritic spines (more rarely) and red dots to those with juxtapositions to cell bodies. All these various configurations are anatomical territory dependent and also axonal branches dependent, what is the same for the vesicular content of 5-HT varicosities which may also vary from one anatomical region to another, and in some regions (Descarries and Mechawar, 2000). For instance, at the level of the spinal cord, projections from the ROb and RPa to motoneurons have large varicosities and make direct synaptic contacts with the motoneurons while those from the RMg and LGPi which project via a dorsolateral pathway provide small varicose fibres to the dorsal horn in particulars predominantly laminae III and IV (for RMG) and laminae I and II (for LGPi) both participating in dual control of nociception

Table 5 : Estimation of 5-HT synaptic incidence (%) in spinal mammalian CNS (extract from Descarries et al., 2010)

Region	Species	Synaptic incidence
Spinal cord		
➢ *Dorsal horn*	Rat	37%
	Cat	
	Monkey	
➢ *Intermediolateral cell column*	Rat	100%
	Guinea pig	
	Rabbit	
➢ *Ventral horn*	Rat	95%
	Cat	
	Monkey	

iv.5-HT synthesis and metabolism

In the CNS as well as on the periphery, 5-HT is synthesized from L-tryptophan, an indispensable amino acid which comes exclusively from the diet in humans as well as in rodents *(Figure 32)*.

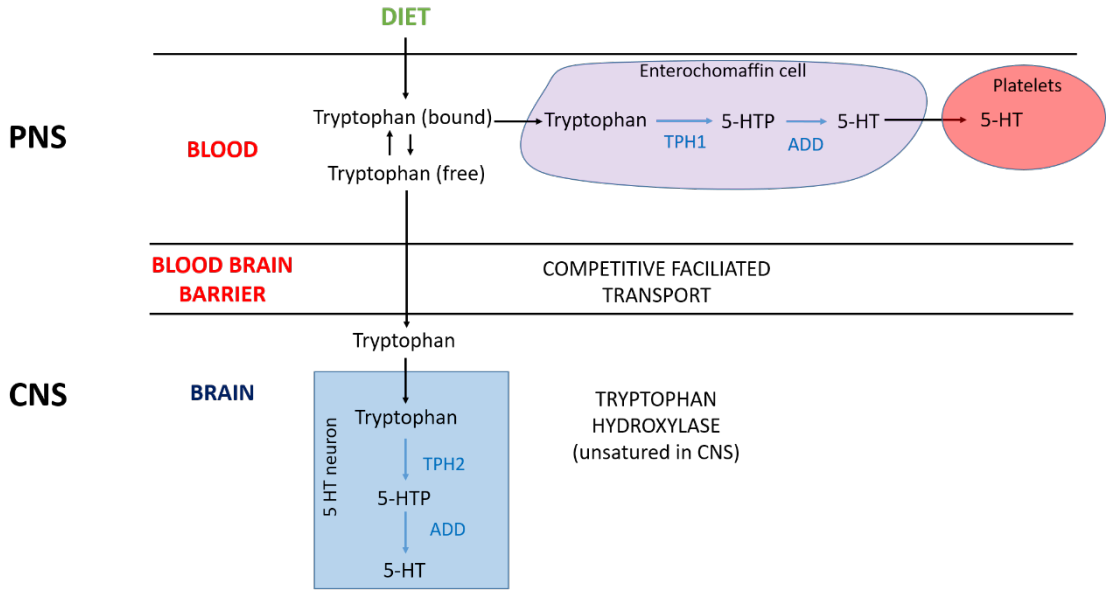

Figure 32 : Illustration of 5-HT synthesis from the diet to CNS and PNS. The circulating tryptophan is mainly bound to plasma protein so only free tryptophan is available to the large neutral amino acid transporter system (competitive facilitated transporter) which transports the essential amino acids across the blood brain barrier (BBB) adapt from (Marsden, 2010)

After its absorption, tryptophan is carried in the blood where it is mostly linked to the seralbumin. In its free form, tryptophan crosses the blood-brain barrier (BBB) by means of an active amino acid transport system which depends upon the presence of glucose and insulin, in competition with leucine, lysine and methionine. And tryptophan is easily uptake by all CNS cells, particularly 5-HT neurons (Hamon, 1995). The biosynthesis of 5-HT *(Figure 33)* in the brain is directly influenced by the extracellular level of tryptophan. In the presence of oxygen molecules and tetrahydropterine (proton donor), tryptophan is first hydroxylated to 5-hydroxytryptophane (5-HTP) by tryptophan-hydroxylase (limiting step of the 5-HT biosynthesis (Hamon, 1995)) which is available in two isoforms depending on their precise location, the tryptophan-hydroxylase 1 (TPH1) in the peripheral tissues, in particular entero-chromaffin cells in the gastrointestinal tract and the tryptophan-hydroxylase 2 which is limited to 5-HT neurons (Côté et al., 2003); then, 5-HTP is further processed by decarboxylation to 5-HT through an amino acid decarboxylase (an enzyme also involved in the decarboxylation of decarboxylating dihydroxyphenylalanine (DOPA; and expressed in all aminergic neurons (Hamon, 1995)).

Once synthesized, the cytoplasmic 5-HT is stored in synaptic vesicles at the presynaptic terminations of 5-HT neurons via the vesicular monoamine transporter 2 (VMAT2), an integral

presynaptic protein that regulates the packaging and subsequent release of monoamine such as dopamine and 5-HT from neuronal vesicles into the synapse (Harriott et al., 2018) and does so through an electrochemical proton gradient, produced by an ATPase located in the synaptic vesicle membrane (Narboux-Nême et al., 2011). In terms of 5-HT release into extracellular space, it can be done in different ways, the most common being a membrane depolarization following the arrival of an action potential at the level of the presynaptic serotonergic nerves terminals, starting factor of the Ca^{2+}-dependent vesicular serotonergic exocytosis (Reubi et al., 1978). There is also a non-conventional mechanism that takes place on 5-HT nuclei. It is a somatodendritic 5-HT release involving cytoplasmic 5-HT and only partly dependant on Ca^{2+} (Hery et al., 1982; Adell et al., 1993). It may correspond to a paracrine and/or autocrine mechanism exerted by 5-HT via a 5-HT_{1A} activation, an autoreceptor located at the level of somatodendritic compartment, on serotonergic neuron themselves (Lanfumey and Hamon, 2004).

Once released into extracellular space, 5-HT binds to its receptors, found on the pre- or postsynaptic neuron and induces a cascade signalling leading to excitation or inhibition of the postsynaptic neuron. Each receptor delivers a signal to the soma of the neuron, which can, by its cumulative effect, generate firing (insofar as it tends to bring the postsynaptic membrane potential closed to threshold for generating action potentials) or a transient hyperpolarization (since it tends to bring the membrane potential away from threshold for generating an action potential) of the postsynaptic neuron. It is important to note that 5-HT receptor activity can be controlled both in terms of duration and intensity thanks to different mechanism of inactivation, thus allowing to finely regulate extracellular concentration of 5-HT. At least two distinct mechanisms, on one hand, the reuptake, especially in serotonergic fibres, and its enzymatic degradation by monoamine oxidases and on the other hand the negative feedback control.

The reuptake mechanism involves essentially 5-HT neurons and allows 5-HT release from the extracellular space to be pulled back into the cytoplasm of the 5-HT neurons, 5-HT can either be stored again in synaptic vesicles or degraded (Hamon, 1995). This reuptake mechanism involves a 5-HT specific Na^+ /K^+ electrochemical gradient-dependent transporter, the 5-HT transmembrane transporter (5-HTT or SERT), which is argued to be one of the main regulating mechanism of the 5-HT effect on the postsynaptic 5-HT receptor. It is primarily expressed in 5-HT neurons (presynaptic 5-HT nerves terminals, axon and cell bodies in the raphe) and to a lesser extent in glial cells where it may play a second line of control (Bel et al., 1997; Hirst, 1998; Inazu et al., 2001). SERT contains 12 transmembrane domains, which is an important pharmacological target for antidepressives like the family of tricyclic antidepressives,

which blocks the recapture of 5-HT. Another mechanism for 5-HT inactivation is its enzymatic degradation by the monoamine oxidase A (MAO-A) and aldehyde dehydrogenase. The MAO-A transforms 5-HT into 5-hydroxy-indole acetaldehyde via oxidative deamination following by the oxidisation of the 5-hydroxy-indole acetaldehyde by aldehyde dehydrogenase into 5-hydroxyindolic acid (5-HIAA), the major metabolite of the 5-HT, which is eliminated via the urinary tract (Hamon, 1995).

The negative feedback control mechanism, for its part, involves 5-HT autoreceptors. Indeed, some lines of evidence suggests that both somatodendritic and nerve terminal autoreceptors take part in the control of 5-HT synthesis in 5-HT neuron. Notably the somatodendritic 5-HT_{1A} autoreceptor, a nerve impulse-regulating autoreceptor controlling 5-HT neuronal firing. Moreover, the axon terminal autoreceptor 5-HT_{1B}, which, independently of the existing level of the 5-HT neuronal firing, may mediate suppression of 5-HT biosynthesis by adjusting the availability of 5-HT storage and release in the CNS (Bel et al., 1997).

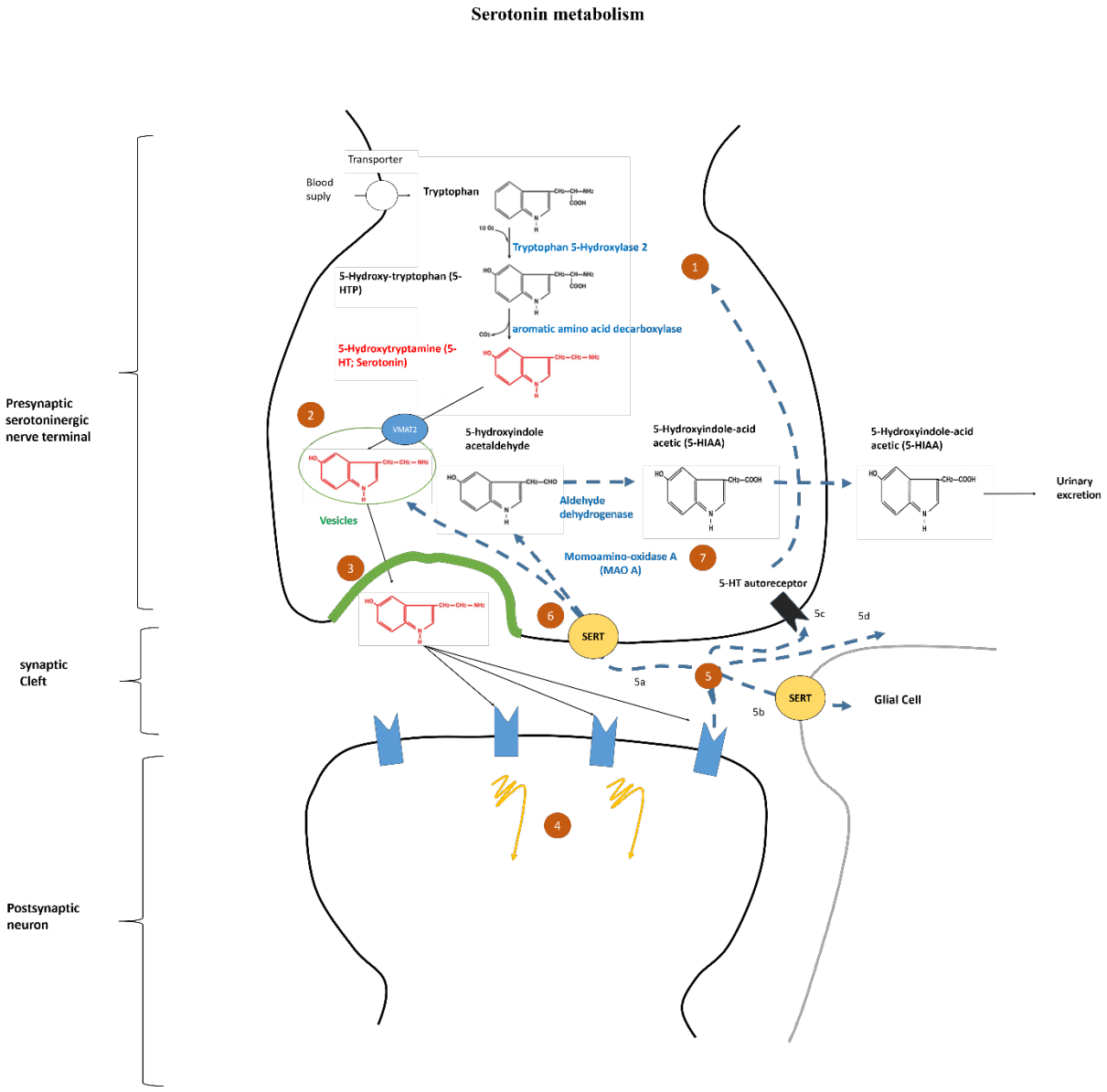

Figure 33 : CNS 5-HT synthesis and catabolism adpat from (Bourgoin, Gautier, and Hamon 2017). The serotonin is synthetized in the neuron (1), then by means of the VMAT2 is stored at the nerve terminal into vesicles (2) and released by exocytosis into the synaptic cleft (3). At this level, the serotonin binds to post synaptic neuron receptors and initiates a signalling cascade to the cell body of the postsynaptic neuron (4). After the activation of the receptor, the serotonin may get taken back up into the presynaptic neuron (5a), get taken up by a neighbouring glial cell (5b) or get bound to 5-HT autoreceptor (5-HT_{1B} at the level of 5-HT nerve terminal 5c or 5-HT_{1A}at the 5-HT somatodendritic level) (Adell et al., 1993; Hjorth et al., 1995) or may get diffused away from the synaptic cleft via extracellular fluid (5d). In the case of serotonin reuptaking, this is done through serotonin transporters (SERT, (Coleman, Green, and Gouaux 2016)), located along the presynaptic membrane, by a process of pulling back serotonin into the cell, where some of them gets reloaded into vesicles and will be reused (Bear, Connors, and Paradiso 2007) and the others get broken down by the monoamine oxydase A (MOA A) and eliminating from the cell as 5- Hydroxyindoleacetic (5-HIAA , a metabolite; 7)

v.Source and projection patterns of 5-HT to the DH

As mentioned above, the vast majority of the serotonergic innervation of the spinal cord in humans and other species is derived from the serotonin neuron of B1 to B4 bulbar nuclei and only a modest proportion is from the DR which predominantly projects to the thalamus, dorsal hippocampus, striatum, cerebral cortex which also send few collaterals to the spinal trigeminal nucleus (Beitz, 1982; Li et al., 1997; Wang and Nakai, 1994). Indeed, the RVM and more specifically the RMg, are the main source of serotonergic input to the spinal cord (and trigeminal nucleus) (Björklund and Skagerberg, 1982; Bowker et al., 1983; Kwiat and Basbaum, 1992; Mason, 1999). Widespread co-lateralisation is displayed throughout the spinal cord, trigeminal nucleus and medullary nuclei by the serotonergic fibres (Bowker and Abbott, 1990; Bowker et al., 1983), thus establishing an extensive network within the spinal cord with, especially, in laminae I/II (superficial laminae) which exhibit many varicosities whereas lamina IV/VI (deeper laminae) also present a dense network of serotonergic terminals (Basbaum and Fields, 1984; Maxwell et al., 1996; Stewart and Maxwell, 2000) *Figure 34.*

In addition, a plethora of axo-somatic and dendritic contacts of serotonergic terminals have been seen in the dorsal horn which for some of them have contacts between serotonergic terminals and projecting neurons (PN; *Figure 35-1*) projecting to different brain structure such as the thalamus and parabrachial nuclei (PBN) (Li et al., 1997; Millan, 1997).

Also, there is little evidence suggesting a juxtaposition between the serotonergic fibre and central primary afferent fibres (PAF, *Figure 35-2*) (Hamon and Bourgoin, 1999; Millan, 1997). However, some facts suggest a non-synaptically modulation of PAF activity by volume transmission (Ridet et al., 1993) or, via local inhibitory interneurons (ININs, *Figure* 35-3) as an alternative, including enkephalins (ENK) and GABA/glycine-containing populations receiving input from descending serotonergic pathways (Fields et al., 1991; Millan, 1997; Ruda, 1988; Tsuchiya et al., 1999). Moreover, considering the presence of individual classes of 5-HT receptors which either enhance or decrease neuronal activity and the different location of specific 5-HT receptor types on PAF terminals and PN (or excitatory interneuron) on one hand, and on ININs on the other hand respectively facilitating or relieving the passage of nociceptive information to the brain. All of these pieces of evidences provide information to better understand the complex pattern of pro-and antinociceptive actions of 5-HT in the DH.

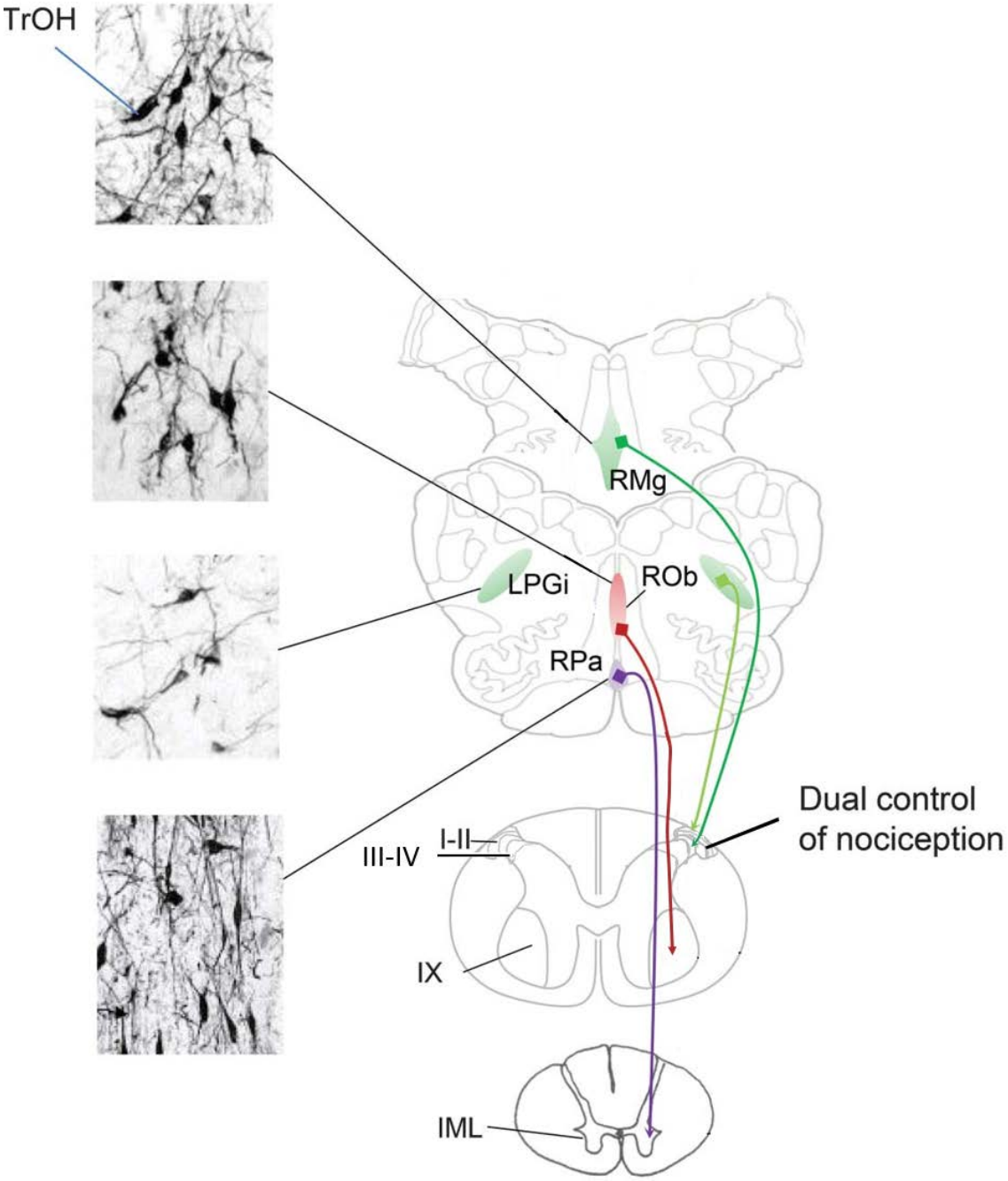

Figure 34 : Distribution of the medullary serotonergic neurons projecting to DH (nucleus raphe Magnus (RMg), raphe obscurus (ROb), and raphe pallidus (RPa), and in the ventrolateral reticular formation, including lateral paragigantocellular reticular nucleus (LPGi)). Medullary serotonergic neurons send bulbospinal axons to all laminae of the spinal cord, with for the ROb and RPa 5-HT neuron, projection to the somatic motor nuclei including motoneurons of lamina IX and also to the IML and for the RMg projection to the dorsal horn and trigeminal nucleus caudalis and innervates laminae I, II, III and IV essentially. At the level of the spinal cord, 5-HT increases the excitability of motoneurons but has dual effects on nociceptive processing in the dorsal horn (antinociceptive or pronociceptive effect according to the receptor subtype and the pathophysiological state). Intermedioteral cell column (IML); Nucleus raphe Magnus (RMg); Raphe obscurus (ROb); and Raphe pallidus (RPa). (adapt from Benarroch, 2014)

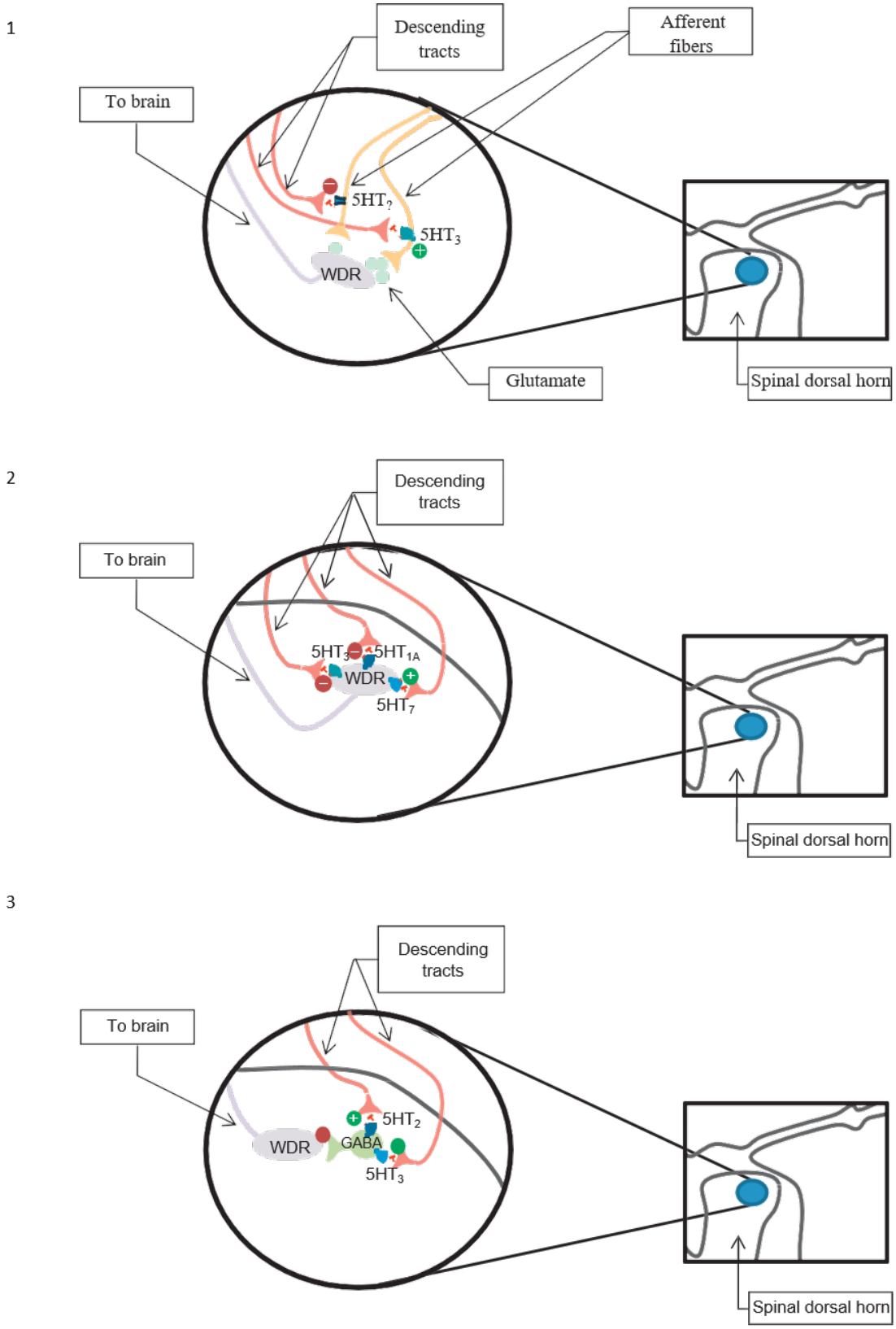

Figure 35 : Simplified schematic representation of the 5-HT descending fibres in the spinal cord (Müller and Jacobs, 2010). Illustration of apposition between 5-HT descending terminal and PAF (1), WDR (2) and ININ (3) which suggests a biphasic action of descending 5-HT on the spinal cord depending on the receptors involved. ININ, inhibitory interneuron; PAF, primary afferent fibres; WDR, wide dynamic range projecting neuron.

vi. Co-localisation of 5-HT with other transmitters

As it has been shown in the dorsal raphe nucleus (Kirifides et al., 2001), additionally to the 5-HT synthesis, the RMg is constituted by multiple other classes of neurone synthesising acetylcholine (Ach), gamma-aminobutyric acid (GABA), thyrotropin-releasing hormone (TRH), glycine, somatostatin, SP, ENK, dynorphin (DYN), galanin (GAL) and/or CCK (Bowker et al., 1983; Hökfelt et al., 2000; Kwiat and Basbaum, 1992; Maxwell et al., 1996; Millan, 1997; Wu et al., 1993). Also, from a sub-population of 5-HT neurons projecting to the DH, a colocalisation between the 5-HT and certain of the neurotransmitters mentioned above has been shown, such as SP, thyrotropin-releasing hormone, GABA, DYN and ENK, which probably interact with 5-HT in the modulation of nociceptive processing upon their concomitant release in the DH. In addition, it has been shown that approximately 25% of 5-HT neurons targeting superficial laminae contain GABA, despite the fact that they are largely lacking in neuropeptides (Antal et al., 1996; Maxwell et al., 1996; Stamp and Semba, 1995). On contrary, in deeper lamina V, little evidences suggest the presence of GABA in serotonergic fibres from which a sub-population contains SP, thyrotropin-releasing hormone and/or GAL (Bowker and Abbott, 1990; Maxwell et al., 1996). Clearly, whether they are co-localised with 5-HT or not, different transmitters contained in NRM-derived neurone projecting to the DH play an important role in the spinal modulation of nociceptive processing. Regardless of the amplitude of co-existence of 5-HT with other transmitters, considered that the antinociception effect elicited by stimulation of NRM as purely serotonergic would be erroneous.

vii. 5-HT receptors with regards to nociception

In the spinal nociceptive circuit, the role of 5-HT is complex and not yet defined (*Figure 36*). Experimental evidence tends to show that 5-HT may exert either antinociceptive or pronociceptive effects, depending on the physiological or pathophysiological state of the nociceptive system and the type of 5-HT receptors involved (Viguier et al., 2013). Indeed, 5-HT receptors can be found on terminals of primary afferent neurons as well as on projection neurons and excitatory and inhibitory interneurons.

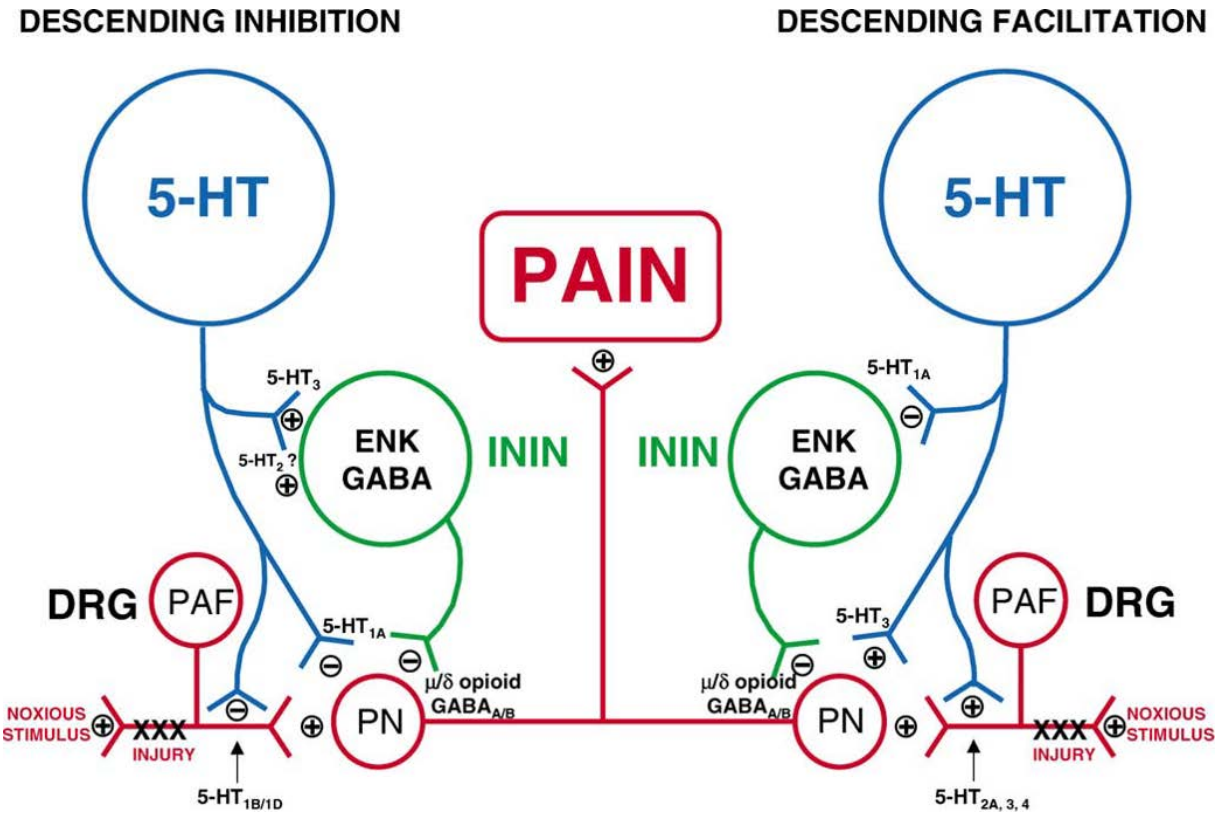

Figure 36 : Schematic representation of the role of the multiple classes of 5-HT receptor on the modulation of nociceptive processing in the DH. On the left-hand side, mechanisms mediating descending inhibition are indicated and, on the right-hand side, those expressing descending facilitation are shown. Actions are exerted at terminals of primary afferent fibres (PAFs), projection neurones (PNs) and inhibitory interneurons (ININs). (representation from Millan, 2002b)

To date, fifteen types of 5-HT receptors belonging to seven receptors classes (5-HT_1 to 5-HT_7) and exhibiting heterogeneity have been identified in human (Hannon and Hoyer, 2008). Except for the 5-HT_3, which is a ligand-gated cation channel belonging to the nicotine/γ-aminobutyrate (GABA) family (Faerber et al., 2007), all the others are G-protein-coupled receptors (Masson et al., 2012), *Table 6*. However, this classification has been defined on a pharmacological basis unrelated to the role of the downstream pathway.

5-HT1 receptor

They are coupled to Gi/o, within the adenylyl cyclase (AC) is inhibited, potassium (K^+) channels activated and voltage-gated Ca^{2+} channels inhibited. Generally, 5-HT_1 receptors are considered to have an inhibitory effect, they are divided into 6 class (from A to F (Barnes and Sharp, 1999)) and are present in the dorsal horn of the spinal cord (Zemlan and Schwab, 1991).

Located in the soma and dendrites of 5-HT neurons, 5-HT_{1A} receptors (the most studied in pain) act as inhibitory autoreceptors, reducing neuronal firing. They are found in the DH,

expressed postsynaptically mostly in lamina II, but also in deeper laminae (Hamon and Bourgoin, 1999), where 5-HT_{1A} receptors influence upon nociceptive processing is mediated by direct actions both pronociceptive (Millan, 1997) and antinociceptive (Millan, 1997, 2002a; Jeong et al., 2012) at intrinsic DH neurones such as ININs and PNs (EXINs).

5-HT_{1B} and its closely tied 5-HT_{1D} receptor, in terms of their primary structure, patterns of cellular coupling and ligand binding profiles (Barnes and Sharp, 1999)), are located presynaptically both in serotonergic terminals (autoreceptors) and in nonserotonergic terminals (heteroreceptors), where they inhibit neurotransmitter release. In the DH, 5-HT_{1B} receptors are mostly found postsynaptically to 5-HT fibres in laminae I and IV (Cortes-Altamirano et al., 2018) where they act as inhibitory autoreceptors on serotonergic terminals (Millan, 2002a; Cortes-Altamirano et al., 2018)

The 5-HT_1 family also includes the 5-HT_{1E} receptor (knowledge about its physiological role is scarce) and the 5-HT_{1F} receptors, which are expressed in presynaptic terminals (Castro et al., 1997; Hannon and Hoyer, 2008). Indeed, 5-HT_{1F} location, in the spinal cord itself, appears to be confined to PAF terminals, rather than generated by intrinsic DH neurones (Bruinvels et al., 1994; Adham et al., 1997; Castro e t al., 1997; (Hamon and Bourgoin, 1999); Ma, 2001; Wu et al., 2001d).

5-HT2 receptors

Composed of several subtypes, 5-HT_2 receptors are coupled to Gq/11 (Hannon and Hoyer, 2008), within the phospholipase C (respectively for 5-HT_{2A} or 5-HT_{2C}) and the phospholipase A_2 (for 5-HT_{2A}) is activated, with a production of inositol triphosphate (IP3), causing a Ca^{2+} release from the endoplasmic reticulum, and diacylglycerol (DAG), activating protein kinase C, which inhibits several K^+ channels (among other functions). 5-HT2 receptors, predominantly located postsynaptically, in PNs especially in laminae IIi (D'Amico et al., 2013; Peirs et al., 2014; Alba-Delgado et al., 2018).

5-HT_{2A} receptors, activated by selective agonists, are considered to facilitate the nociceptive transmission by increasing the dorsal horn neural activity (Thibault et al., 2008; Van Steenwinckel et al., 2008; Aira et al., 2012). Indeed, in inflammatory conditions, 5-HT_{2A} appeared to be involved in the induction of mechanical hypersensitivity (Alba-Delgado et al., 2018). However, due to its location on inhibitory interneurons, 5-HT_{2A} is also considered to be involved inhibition of the pain transmission (Xie et al., 2012).

Regarding 5-HT_{2B} receptors, their functional role in the modulation of nociceptive processing is not well-documented except that they are mainly expressed in the DH, with a little expression in rat DRG.

5-HT_{2C} receptors, the second major subunits of 5-HT_2 receptors, are expressed in the DH where it has been hypothesized that they may be produced by intrinsic DH neurons mainly in deep laminae (possibly on PNs). Their activation by specific agonists leads to an antinociceptive effect which involves GABAergic mechanisms. Moreover, 5-HT_{2C} receptor are mostly located on GABAergic ININs, which transforms the expected excitatory effect following their stimulation in an inhibitory effect throughout the CNS.

5-HT3 receptors

5-HT_3 receptors are belong to a Cys-loop family of ionotropic receptors, which includes the nicotinic cholinergic, $GABA_A$, and the glycine receptor. Also, they present two subunits (homomeric 5-HT_{3A} and heteromeric 5-HT_{3A}/5-HT_{3B}) and are described as nonselective cation channels which elicit fast depolarization. Their presynaptic location increases neurotransmitter release whereas their postsynaptic location increases activity of both projection neurons and inhibitory interneurons. 5-HT_3 receptors activation induces an entrance of Na^+ and CA^{2+} in the cell and, conversely, an exit of K^+. At the spinal level, they are located mainly in the superficial layer of the DH (Millan, 1997, 2002a), especially on C fibre sensitive to capsaicin as well as on GABAergic and ENK ININs (Xie et al., 2012) and on PNs (expressing NK1 receptor of substance P). These diverse locations both pre and postsynaptic at the spinal nociceptive pathway support the idea of the multiples effect led by the activation of 5-HT_3 receptor (Xie et al., 2012; Tan et al., 2019) sometimes antinociceptive (Xie et al., 2012), via the release of GABA from GABAergic ININs expressing 5-HT_3) sometimes pronociceptive (Tan et al., 2019). However, blocking the 5-HT_3 receptors elicited no significant modification of the dorsal horn neuron excitability in naïve mice (Green et al., 2000).

Gross description of 5-HT_4, 5-HT_6 and 5-HT_7 receptors

5-HT_4, 5-HT_6, and 5-HT_7 receptors are Gs protein positively coupled to adenylate cyclase (AC); cyclic adenosine monophosphate (cAMP, which modulates cAMP gated channels) produced by the stimulation of these receptors, leads to the phosphorylation of several proteins mediated by protein kinase A such as K^+ channels. These receptors are located both in the central and peripheral neurons and in other tissues such as the gut and the heart. In addition,

5-HT7 receptors are expressed postsynaptically, particularly in local interneurons of superficial laminae of the dorsal horn and presynaptically in peptidergic fibres, including nociceptive dorsal root ganglion afferents (Bardin, 2011; Bockaert et al., 2011).

5-HT_4 receptors are located in the superficial region of the dorsal horn (laminae I/II). Indeed, some early evidence shows that 5-HT_4 receptors synthesized in the DRG are transported to cutaneous and visceral terminals as well as on central terminals of nocisponsive PAFs in DH (Cardenas et al.,1997a; Doak and Sawynok, 1997; Espejo and Gil, 1998; Wu et al., 2001d), especially on the capsaicin sensible PAF terminals, suggesting their involvement in an antinociceptive presynaptic control via 5-HT from the periphery in inflammatory pain condition. A mechanism, which induces an inhibiting modulation of the spinal nociceptive transmission may involve the excitation of GABAergic ININs.

5-HT_6 receptors have been shown to have a facilitatory influence on neuronal activity (Barnes and Sharp, 1999). Their anatomical distribution in regions such as the amygdala, the thalamus and the PAG, as well as in the superficial layer of the DH leads to postulate its probable involvement in the descending serotonin modulation where it considered having a pronociceptive action.

5-HT_7 receptors, despite the lack of information regarding their role in nociception in the past, have recently been shown to have a role in the 5-HT modulation of the pain transmission. Early evidences suggest that 5-HT_7 has a pronociceptive excitatory role on nociception (Rocha-González et al., 2005) while an antinociceptive role has been shown on the nociception (Brenchat et al., 2012). A duality of effects of 5-HT_7 receptors sometimes pronociceptive sometimes antinociceptive, supports the idea of the existence of two populations of 5-HT_7 receptors.

5-HT_5 receptors

To date, two subunits of the 5-HT_5 receptors have been identified, 5-HT_{5A} and 5-HT_{5B} receptors which are still considered to be 'orphans' (Grailhe *et al*., 2001) with little information concerning 5-HT_{5B} (which may not be functional in human). Regarding descending control, early studies identified 5-HT_{5A} on neurons at a high concentration in the spinal trigeminal nucleus and in the spinal cord (Oliver et al., 2000), where they are found in the superficial DH and in the DRG which altogether rapidly led to postulate their involvement in the descending control of pain by the 5-HT (Cortes-Altamirano et al., 2018). Concerning their transduction mechanism, 5-HT_{5A} receptors have been identified to be coupled, via Gi proteins, to both K^+

channels (facilitatory) and AC (inhibitory), contributing to a hyperpolarization of the 5-HT_{5A} receptors expressing neurons (Francken et al., 2000; Thomas et al., 2000; Grailhe et al., 2001). Moreover, spinal 5-HT_5 receptors have been considered to have a controversial antinociceptive action mechanism, which may involve the hyperpolarization of PNs contacted by nocisponsive PAFs in the DH superficial layer.

Table 6 : Main pharmacological characteristics, cell signalling and 5-HT receptors locations involved in the serotonin modulation of the nociception (modified from Bourgoin, Gautier, and Hamon 2017)

Type of Receptor	Agonists	Antagonists	G protein-coupled receptor	Signal transduction de transduction		Spinal Cord (protein)	Dorsal Roots Ganglia (RNAm)	Location	Function
5-HT_{1A}	8-OH-DPAT	WAY-100,635	Gi/o	AMPc	↘	+++	–	Brainstem Raphe nuclei	Neuronal inhibition (involve in sleep, feeding, thermoregulation, anxiety
	Alnespirone	NAD 299		K^+	↗				
	F-13640	(S)-UH301		Ca^{2+}	↘				
5-HT_{1B}	CP 93129	GR 127,935	Gi/o	AMPc	↘	++	++	Substantia nigra & basal ganglia	Neuronal excitation (involve in contraction, cerebrospinal fluid)
	CP 94253	GR 555,622		K^+	↗				
	Triptans	SB 224,289		Ca^{2+}	↘				
		SB 236,057							
5-HT_{1D}	GR 46611	GR 127,935	Gi/o	AMPc	↘	+	+		
	L 694,247	BRL 15,572							
	Triptans	SB 714,786							
5-HT_{1E}				AMPc	↘				
5-HT_{1F}				AMPc	↘				
5-HT_{2A}	α-Me-5-HT	MDL-100,907	Gq/11	PLC	↗	+	+	Vascular & visceral smooth muscles, platelets, prefrontal cortex	Neuronal excitation, smooth muscle contraction, platelet aggregation, vasoconstriction
	DOI	MDL-11,939		PLA_2	↗				
	DOB	Kétansérine		K^+	↘				
	DOM	Sarpogrelate							
5-HT_{2B}	α-Me-5-HT	RS 127,445	Gq/11	PLC	↗	+	+	Gastric fundus	Contraction
	BW 723C86	SB 266,097							
5-HT_{2C}	CP 809,101	Ritansérine	Gq/11	PLC	↗	+	+	Choroid plexus, hypothalamus	Cerebrospinal fluid production, feeding behaviour & mood
	mCPP	RS-102,221							
	α-Me-5-HT	SB 206,553							
	MK-212	SB 221,284							
	Ro 60-0175	SB 242,084							

5-HT_4	BIMU-1, BIMU-8, BZTZ	DAU 6285	Gs	AMPc	↗	+	+	GIT (neurons of myenteric plexus & secretory cells…) & CNS (hippocampus, sup and inf colliculi)	Involved in intestinal secretion & peristatic reflex
	RS 67,506	GR 113,808		K^+	↘				
	Tégaserod	LY 297,582		Ca^{2+}	↗				
		SDZ-205,557							
5-HT_{5A}	5-CT	SB 699551	Gi/o	AMPc	↘	+	+	Closely related to 5-HT4 receptor/ mainly located in CNS	Unknown
5-HT_{5B}			Gi/o	Unknown					
5-HT_6	EMD 386,088	SB 271,046	Gs	AMPc	↗	+	+		
	WAY 181,187	SB 339,885							
	WAY 208,466	BGC 20-761							
5-HT_7	8-OH-DPAT	SB 258,719	Gs	AMPc	↗	+	+		
	AS-19	SB 269,970							
	E-55888	SB 656,104							
	E-57431								
	LP-44								
	MSD-5a								
5-HT_3	M-Cl-phényl-biguanide	Ondansétron	ligand-gated ion channel	Na^+, K^+, Ca^{2+}		++	++	Parasympathetic terminal in GI tract, including vagal & splanchic afferents/ CNS, solitary tract nucleus & in area postrema	Neuronal excitation, emesis (involve in anxiety)
	SR 57,277 A	Granisétron							
		Tropisétron							

↗ = activation ; ↘ = inhibition ; +, ++, +++ = graduel level of expression ; – : absence of expression ; AMPc = cyclic adénosine- monophosphate ; PLC : phospholipase C ; PLA_2 : phospholipase A_2

b) *Other neurotransmitters*

Besides the descending 5-HT fibres from the RMg, other descending monoaminergic fibres such as the dopaminergic fibres also mediate the descending modulation from the supraspinal sites (Millan, 1997, 2002b). Among them, the descending noradrenergic fibres involve a multiplicity of receptors including as α2 adrenoreceptors mediating antinociception in the DH. It is important to note that the two pathways can be coactivated and may act synergistically to participate in descending pain modulation. Furthermore, other types of neurotransmitters participate in descending pain modulation, including GABA and glycine

mostly present in the inhibitory interneuron. For instance, in the PAG, GABAergic terminal are abundant and relate to the fact that GABAergic neurons inhibit PAG output neurons involved in descending inhibition. Indeed GABAergic terminals from the PAG (including somatostatin) reach to the RVM, including the RMg (Morgan et al., 2008); as well as substance P (Commons and Valentino, 2002), acetylcholine (Cucchiaro et al., 2005), norepinephrine (François et al., 2017) etc…

3. Pain modulation as part of adaptative responses to physiological challenges

Stress-induced analgesia refers to the idea that any number of situations or experimental experiments that could be characterized as stressful induce behaviourally measurable, and sometimes quite potent, analgesia. For instance, stress-induced analgesia can be produced by electric shock, forced swim, and centrifugal rotation as well as biologically relevant threat stimuli such as odours from stressed animals of the same species or exposure to a predator. Analgesia is also elicited as a conditioned response to cues that have been paired previously with noxious or aversive events. This analgesia has been shown by a number of investigators to be mediated by the PAG–RVM system (Fanselow, 1986).

Two factors highlighted the idea that antinociception is recruited as part of defence behaviours: On one hand, antinociception is readily evoked by learned or innate danger signals and on the other hand, the observation that stress induces analgesia through activation of the PAG–RVM system. Pain behaviours must sometimes be inhibited in order to give higher precedence to more pressing needs such as escaping from an aggressor or avoiding detection by a predator. However, a more general view of pain modulation has now developed. Pain inhibition is currently viewed as one component of a number of organized responses that allow an organism to prioritize nociceptive behaviours relative to other internal and external demands. In addition to antinociception, such responses typically include autonomic, endocrine, and motor elements. One example of such an organized defence response would be antinociception as part of preparation for fight or flight when confronted by a predator. Although the circuitry through which the PAG–RVM system is brought into play in response to threat remains to be fully elucidated, inputs from the amygdala and hypothalamus are likely to be critical (Lumb, 2002)

C. AIM OF THE THESIS

Interestingly, according to the state of art, the PAG-RVM circuit involved in the descending modulation of the nociceptive signal in the spinal dorsal horn can be sometimes both facilitating and antinociceptive, notably depending on the physiological state. This can happen at the level of the RVM as well as of the PAG, and under the influence of different mechanisms such as those involved in stress or fear. Indeed, it has been shown that:

- In a physiological state, electrical stimulation of the RMg in the RVM induces a strong antinociceptive effect inhibiting the nociceptive signal at the spinal level associated with a 5-HT release. This effect can be reversed by the use of some antagonist of 5-HT, reflecting the antinociceptive role of the 5-HT in this modulation
- In agreement with this finding, in neuropathic pain, it has been shown a facilitating role of the 5-HT, mediated by the descending 5-HT fibres, has been shown.
- Also, it has been highlight that the PAG-RVM circuit involved in descending pain modulation is also involved in the mechanism leading to stress induce analgesia.

Taken together, those findings led us to ask:

- What is the exact role of the 5-HT RMg in the descending modulation on nociceptive transmission in acute pain as well as in pathological condition?
- What is the target of the RMg 5-HT descending fibres which mediate the 5-HT effect?
- How to explain the biphasic role of the 5-HT depending on the physiological condition?
- Is the PAG-RVM circuit implicated in the stress induce analgesia? Is it involved in the 5-HT RMg-spinal cord circuit regulation?

II. MATERIALS AND METHODS

In the aim to investigate *in vivo* both in freely moving and anaesthetised animal, the descending neuromodulatory pathways involving 5-HT and somatostatin in the vlPAG-RMg-DH circuitry, we developed an optogenetic approach that consists in both expressing light-activated microbial opsin proteins in specific neural populations and Cre-driver transgenic mice to target opsins to genetically specified neural subtypes.

A. EXPERIMENTAL APPROACHES

1. Ethical Statement

All experiments followed the European Union (Council directive 86/609EEC) and institutional guidelines for laboratory animal care and use. Institutional licence for hosting animals was approved by the French Ministry of Agriculture (APAFIS#3751-2016030711446220 v2). All efforts were made to minimize animal suffering respecting the 3R rules: reducing the number of animals used, replacing if possible and refining to limit signs of deterioration of the health status of mice.

2. Animals

a) *Epet-Cre (+/-) mice (5-HT-cre mice)*

Adult 5-HT cre mice (B6.Cg-Tg (FeV-cre) 1Esd/J, Jackson Laboratory (Scott et al., 2005b), males and females, expressing the CRE recombinase under the control of the FEV (ETS oncogene family) specific promoter of 5-HT neurons, were used and had between 6 and 10 weeks of age at the time of injection or implantation. They received cannula implantation 10 days prior to the onset of experiments and were maintained in a small social group (2-5 mice) under a standard 12:12 light/dark cycle, with food and water available *ad libitum* and enrichment devices, in constant temperature (21 ± 2 ° C) and humidity levels (60%).

b) *5-HT cre* Ai9 tdTomato mice*

Adult 5-HT cre mice were bred and crossed with Ai9 reporter mice homozygous for Rosa-GAG-LSL-tdTomato-WPRE-conditional allele under the control of a loxP-flanked STOP cassette (B6.Cg-*Gt(ROSA)26Sor*$^{tm9(CAG\text{-}tdTomato)Hze}$/J (Madisen et al., 2010) *Figure 37*. The offspring express robust tdTomato fluorescence following Cre-mediated recombination in neurons expressing cre recombinase. They are also maintained in a small social group setting (2-5 mice) under a standard 12:12 light/dark cycle, with food and water available *ad libitum* and enrichment devices, in constant temperature (21 ± 2 ° C) and humidity levels (60%).

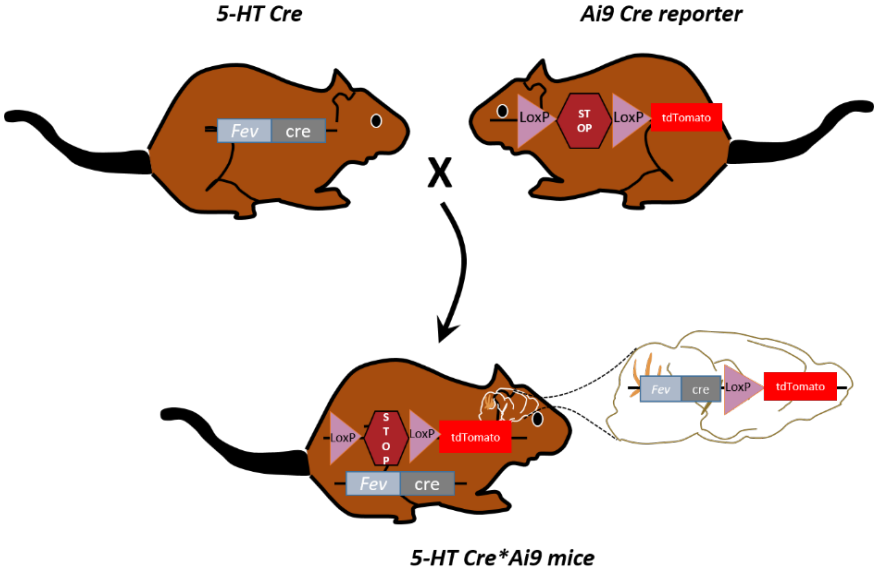

*Figure 37 : Development of 5-HT Cre*Ai9 tdTomato reporter mice designed to express tdTomato fluorescent protein only in 5-HT neuron. Cre recombinase expressing in 5-HT-neurons excises the loxP-flanked stop sequence and then allows robust tdTomato expression within 5-HT neurons.*

c) *GAD 67-GFP* 5-HT cre mice*

GAD 67-GFP knock-in adult mice, expressing enhanced Green Fluorescent Protein (EGFP) under the control of the mouse Gad1(GAD67) gene promoter (Gad1tm1.1Tama, thanks to the Friedrich Miescher Institute for Biomedical Research,Basel (Switzerland)(Tamamaki et al., 2003)), were bred and crossed with adult 5-HT cre mice (*Figure 38*). The resulting offspring express both Cre-recombinase in 5-HT neurons and robust EGFP fluorescence in GABAergic neurons. As for the other strains, they are maintained in a small social group setting (2-5 mice) under a standard 12:12 light/dark cycle, with food and water available *ad libitum* and enrichment devices, in constant temperature (21 ± 2 ° C) and humidity levels (60%).

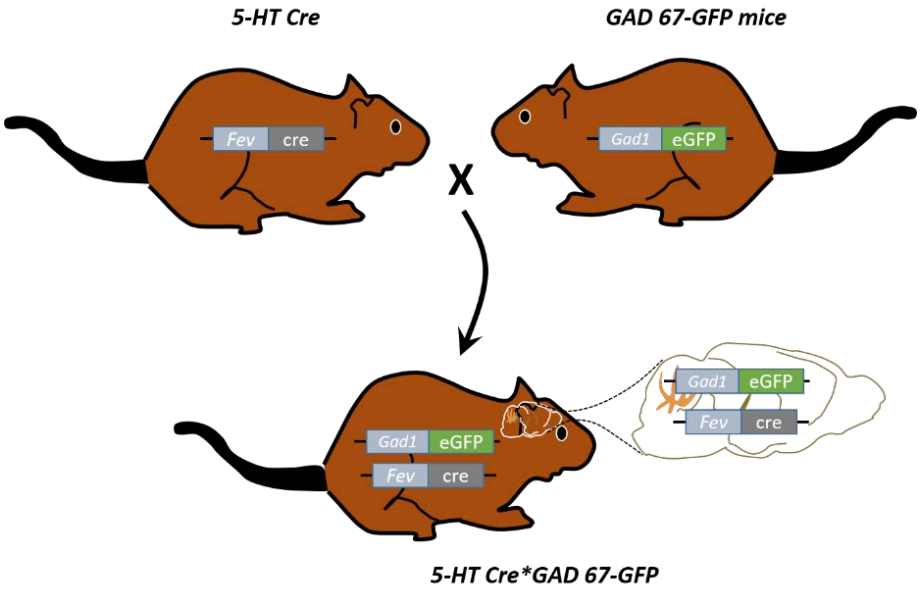

*Figure 38 : Development of 5-HT Cre*GAD 67-GFP mice designed to express both Cre-recombinase in 5-HT neuron and eGFP in GABAergic neuron.*

d) *SST-Cre (+/+) mice and SST-Cre (+/-) mice*

Adult SOM-IRES-cre mice ($Sst^{tm2.1(cre)Zjh}$/J mice, Jackson Laboratory (Taniguchi et al., 2011), male, expressing the CRE recombinase in the somatostatin-expressing neurons, were used and had between 6 and 9 weeks of age at the time of injection or implantation and received cannula implantation 10 days prior the onset of experiments. They were individually housed in a 12 h light/dark cycle with food and water available *ad libitum* and enrichment devices, in constant temperature (21 ± 2 ° C) and humidity levels (60%).

3. Surgical procedure

a) *Viral and tracer strategy*

For a functional specification of the role of descending 5-HT neurons of the RMg (RMg 5-HT) in the modulation of the nociceptive transmission in the dorsal horn of the spinal cord.

6- to 10-week-old B6.Cg-Tg (FeV-cre) 1Esd/J, male and female mice (Jackson Laboratory) were weighed then deeply anaesthetized under 4% isoflurane in an induction chamber then moved and maintained under 1.5% of isoflurane to be shaved and cleansed (area of interest) with alternating applications of Betadine red (soap) and yellow. Eyes were protected

with ocular gel (Ocry-gel, Lab TVM, France), 100µL (0.3µg/ml) of buprenorphine was intraperitoneally injected (and again 6 hours after the surgery), and 20 µL of lidocaine 1% was administered locally (scalp) to alleviate pain. In a second step, they were placed into a stereotaxic frame (RWD Desktop Digital Stereotaxic Instruments 68025, RWD) and the head was fixed with ear bars and maintained at 1.5-2% isoflurane, a feedback-controlled heating pad (FHC) ensured maintenance of core body temperature at 37 °C. Once a stable plane of anaesthesia was reached, the skin was opened to expose the skull and the surface was cleaned to expose the Bregma and Lambda. To specifically target the RMg of the RVM in the brainstem, three sites of injection were used, -5.6/ 0.0/ -5.6; -5.8/ 0.0/ -5.6 and -6.1/ 0.0/ -5.7 (antero-posterior/ medio-lateral/ dorso-ventral respectively (Hof and Young, 2000)) and a small hole (1mm of diameter) was drilled to expose the surface of the brain (Microdrill 78001, RWD ,). Pulled borosilicate glass capillaries (Ringcaps, disposable capillary pipettes with ring mark, DURAN, Hirschmann Laborgeräte, Germany) were used to microinject a total of 300nL (50nL/min) of selected viruses AAV-EF1a-DIOhChR2(H134R)-EYFPWPRE-pA or AAV-EF1a-DIOhChR2(H134R)-mCherryWPRE-pA, (ChR2 opsin, 4.5×10^12p/ml UNC Vector Core) for light-activation, or AAV-CAG-Flex-ArchT-GFP (ArchT opsin, 4.7×10^12p/ml, UNC Vector Core) for light-inhibition, or AAV-CAG-Flex-GFP or AAV-CAG-Flex-mCherry (GFP tag, 4.8×10^12p/ml, UNC Vector Core) as a control for both light and virus (Yizhar et al., 2011) at coordinates of interest (100nl each) to have a cell-type-specific expression of optical actuators (*Figure 39*). The micropipette was kept in the injection site 5 minutes after injection and then retracted slowly over 3 minutes. The surgical sites were sutured and cleaned with betadine and treated with 1% lidocaine. Animals were kept on a heating pad and monitored until full recovery (30 minutes) before being returned to their cage and continued to be group-housed after the procedure. In addition, post-operative observations were performed up to 3 days after surgery.

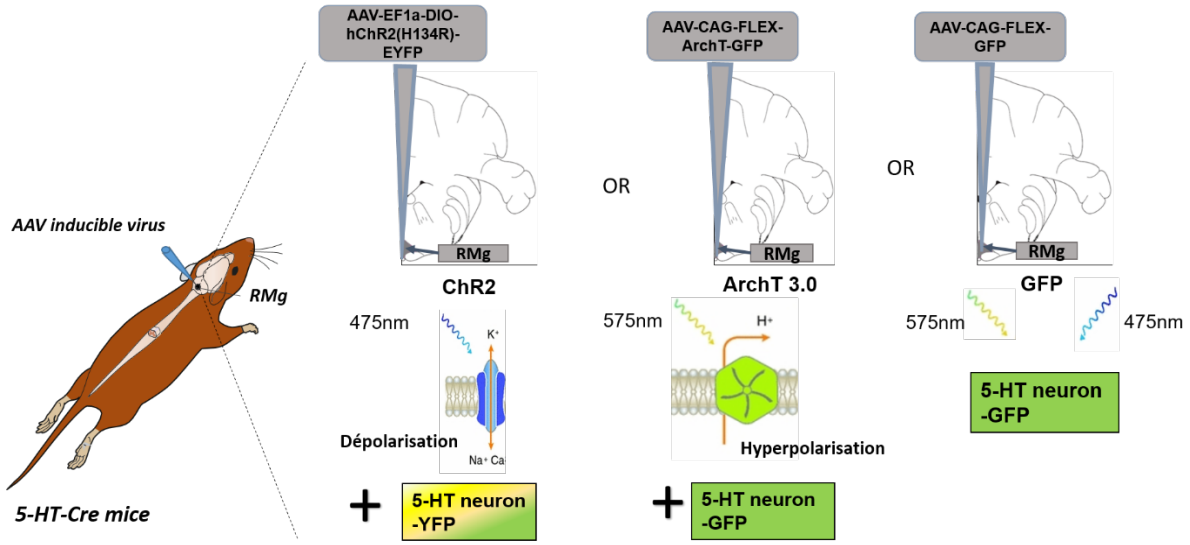

Figure 39 : Schematic representation of the viral strategy in 5-HT Cre mice.

For the functional specification of the role of vlPAG SOM neurons (vlPAG SST) in the descending modulation of the nociceptive transmission.

6- to 9-week-old Ssttm2.1(cre)Zjh/J mice were used, following the same protocol as described above, with the difference of the injection sites, 350nl of selected virus were microinjected into the bilateral vlPAG (-4.4/±1.5/ -2.45, 20° antero-posterior/ medio-lateral/ dorso-ventral, angle in degrees) to target precisely the somatostatin inhibitory interneurons (based on Tovote et al., 2016), *Figure* 40. Animals were kept on a heating pad and monitored until full recovery (30 minutes) and before being returned to their cage. As for the 5-HT-cre mice, post-operative observations were performed up to 3 days after surgery.

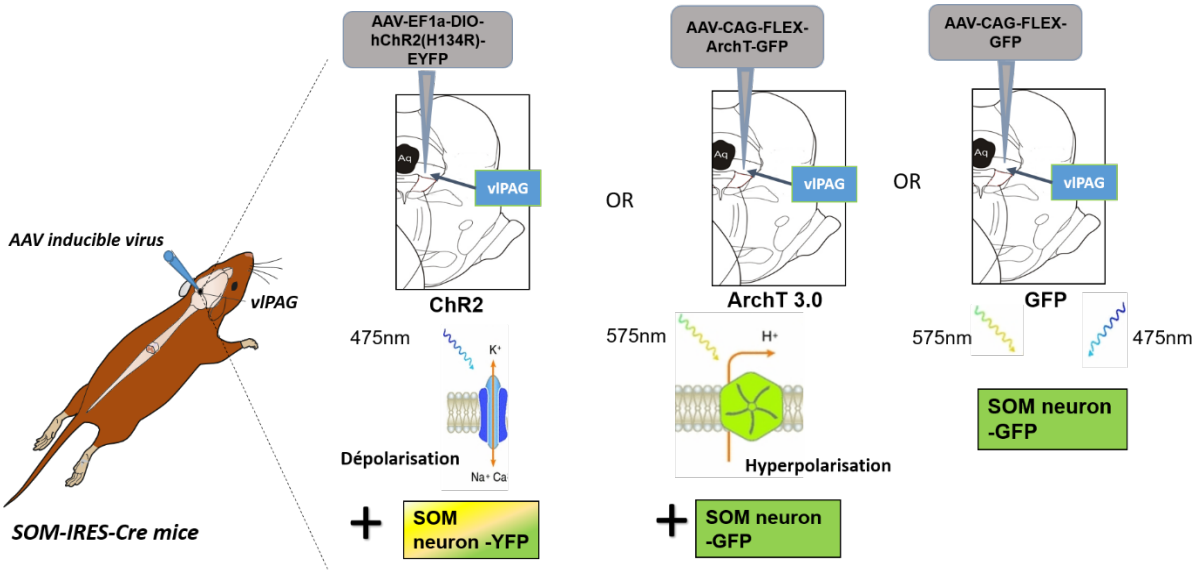

Figure 40 : Schematic representation of the viral strategy in SOM-IRES-Cre mice.

To characterise the anatomical distribution and a potential target of the somatostatin inhibitory interneuron of the vlPAG involved in the nociceptive transmission, in 6- to 9-week-old SOM-IRES-cre mice microinjected with AAV-CAG-FLEX-GFP bilaterally in the vlPAG used as an anterograde tracer (*Figure 41*), a total of 100nl of fluorogold (2%), used as a retrograde tracer was injected bilaterally at the level of the spinal dorsal horn (-100<x<-300µm dorso-ventrally).

In the aim to identify the potential target of RMg 5-HT projections to the spinal cord, 6- to 10-week-old 5-HT cre mice, followed the same protocol as described for the viral injection including the same viral quantity and the same coordinates with the difference of the use of AAV9-CAG-floxed-SynMYC rev-WPRE (Myc tag, 2.5×10^13p/ml, UNC Vector Core), which used as an anterograde tracer. Animals were kept on a heating pad and monitored until full recovery (30 minutes) before being returned to their cage and continued to be group-housed after the procedure. Also, post-operative observations were performed up to 3 days after surgery.

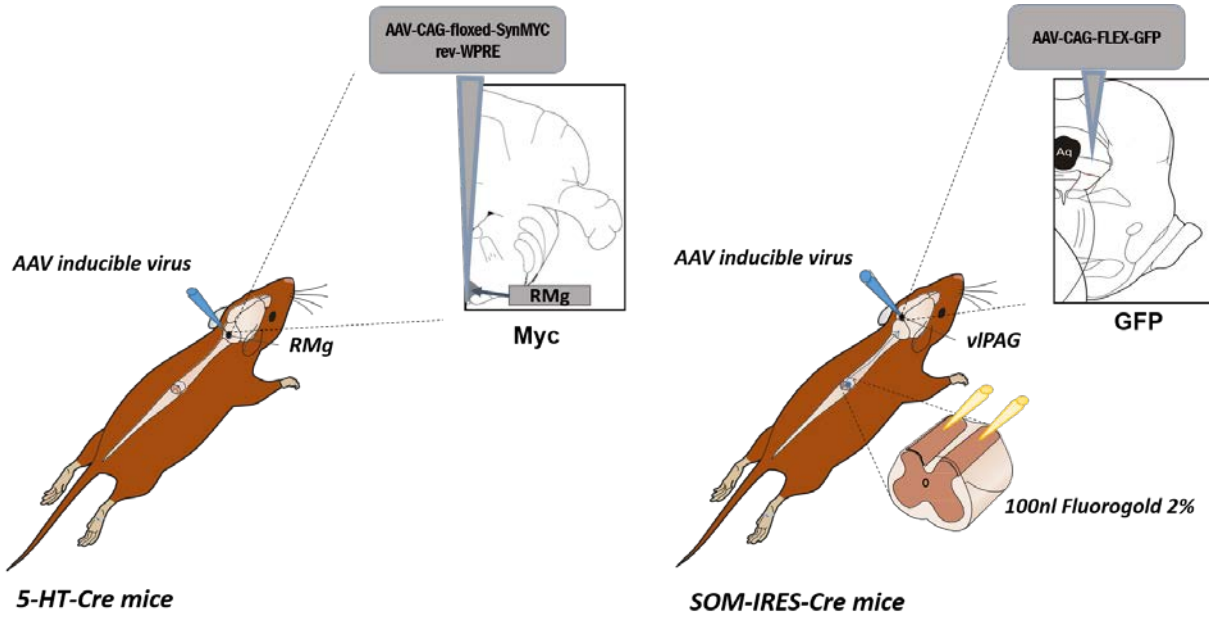

Figure 41 : Schematic representation of the tracer strategy in both SOM-IRES-Cre mice and 5-HT Cre mice.

b) *Fibre Optic Cannula Implantation*

For 5-HT cre mice

Optical cannulas including KFP2301LZXX LC ceramic ferrule no flange (OD, 25mm - ID 230 micron - conc < 20 micron) from AMS Technologies in combination with a multimode optical fibre (Ø200 µm Core TECS-Clad; 0.39 numerical aperture) from Thorlabs were implanted, in a group of animals, at 300µm above the RMg of the RVM (*Figure 42A*), in another group, above the spinal cord (*Figure 42B*) and in the latter group both at 300µm above the RMg and above the lumbar vertebrae of the spinal cord (*Figure 42C*), to deliver the activating light to both the 5-HT neurons expressing the selected opsins in the RMg and their projecting fibres. Before cannula implantation, optical fibres were prepared and cleaved to the appropriate length (5.5mm for the RMg and <0.5mm for the lumbar vertebrae) and light intensity emitted by the fibres was recorded using a Thorlabs power meter (PM-100D) and set to 10mW. The surgical protocols were similar for implantation in both the RMg and the spinal cord and identical in terms of asepsis and maintenance of core body temperature (at 37 °C) as described for the viral injections. Animals were kept on a heating pad and monitored until full recovery (30 minutes) before being returned to their cage and continued to be group-housed after the procedure. Post-operative observations were performed up to 3 days after surgery.

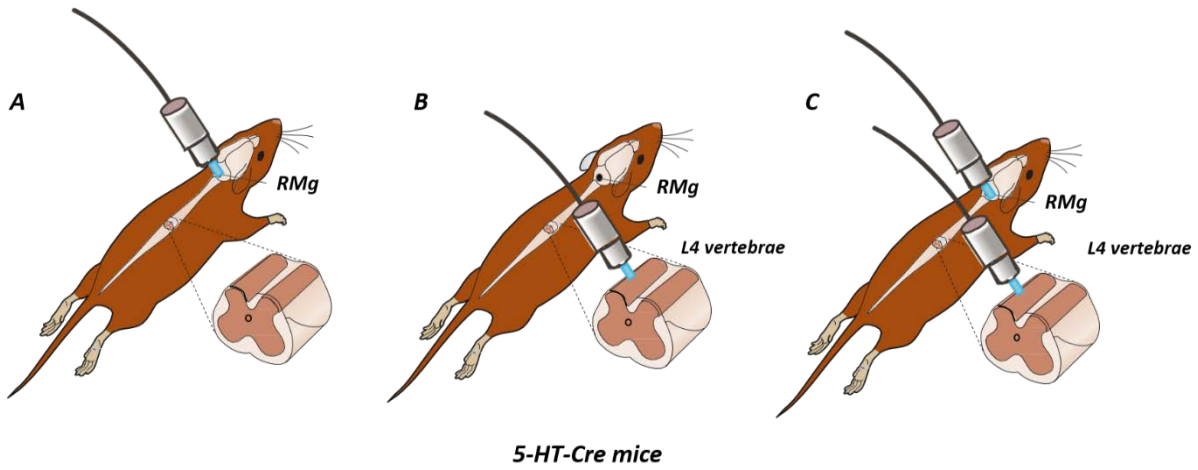

Figure 42 : Description of the fibre implantation strategy. A corresponds to the RMg implantation, B to the spinal implantation and C to both the RMg and the spinal implantation.

For RMg implantation, the skin was opened to expose the skull and the surface was cleaned to expose Bregma and Lambda. The coordinates to target the RMg were bregma -5.8, medio-lateral 0.0, dorso-ventral -5.2 (Al-Juboori et al., 2013), thus a small hole was drilled to expose the surface of the brain. Help by a stereotaxic cannula holder (Thorlabs), the optical cannula was lowered into the hole, and dental cement was used to secure in place. Once the cement was dry, it was covered with black nail varnish to reduce the risk of external illumination.

Spinal cord implantations (*Figure 43*) followed the protocol described in Christensen et al, 2016 (Christensen et al., 2016). A 1- to 2-cm incision was made slightly caudal to the peak of the dorsal hump to expose the lumbar spinal region. The L4 vertebra of interest was identified, and then a small incision was made between the tendons and the vertebral column on either side. L4 vertebra was then secured using spinal adaptor clamps, and all the tissue was removed from the surface of the bone. Using a micro drill, we removed the spinal processes and the surface of this vertebra. Next, a small hole was drilled approximately 2 mm from the midline, centrally on the rostral-caudal axis on either the left or right side. We positioned the optical fibre above the drilled hole and used a small amount of superglue around the drilled hole and over the surface of the bone to reduce the possibility of bone bleeds and to secure the cannula in place. After, we cemented the cannula in place using dental cement and, after the cement dried, we sutured and cleaned the skin surrounding the dental cement securing the cannula implantation. Mice were placed on a heating blanket to awake and recover before being

returned to their cage and continued to be group-housed after the procedure. Post-operative observations were performed up to 3 days after surgery.

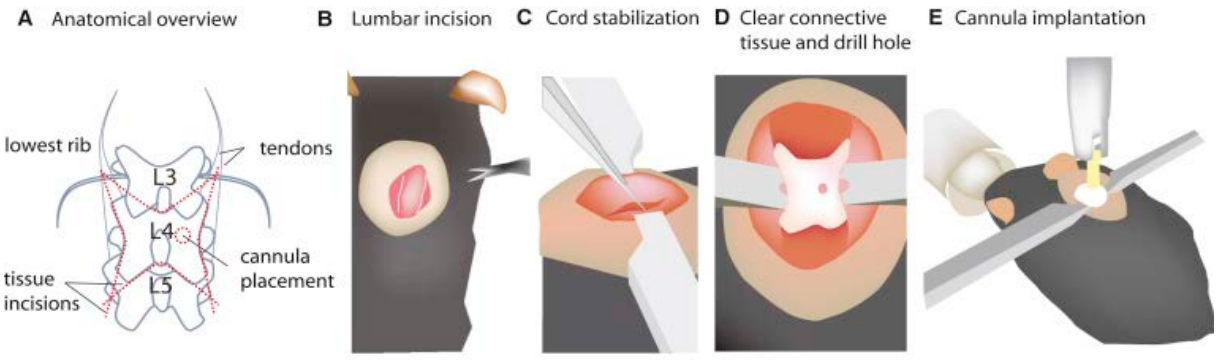

Figure 43 : Description of the cannula implantation above the spinal cord from (Christensen et al., 2016) A to E correspond to the steps to follow as described in the text above

The frequency and duration of light propagation were calibrated accordingly to the spontaneous frequency of 5-HT neurons, previously observed in the dorsal raphe nucleus at around 0.5-5hz (Sengupta et al., 2017). For ChR2 opsin activation, both *in freely moving and in anaesthetized animal*, blue light at 488nm was used with low-frequency stimulation and small duration pulses (2 minutes at 5hz5ms power set at 10mW/mm² with a laser from Changchun New Industries Optoelectronics TECH.CO.,Ltd, China) to depolarize both RMg 5-HT neurons and spinal 5-HT descending fibres. For ArchT opsin activation, both *in freely moving and in anaesthetized animal,* green light at 526.5 nm (power set at 10mW/m², laser light from ChangChun New Industries Optoelectronics TECH.CO.,Ltd, China) was used continuously during two minutes to hyperpolarize both RMg 5-HT neurons and spinal 5-HT descending fibres. Finally, for the adeno-associated virus tag with GFP, both blue light at 5hz5ms or green light continuously were used to control the potential harmfulness of the activating light both at the level of both RMg and spinal cord.

For SOM cre mice

Optical cannulas (KFP2301LZXX LC Ceramic Ferrule NO flange OD, 25mm - ID 230 micron - conc < 20 micron from AMS Technologies, associated with Ø200 µm Core TECS-Clad Multimode Optical Fibre, 0.39 numerical aperture from Thorlabs) were implanted into bilateral vlPAG or centrally in the RMg (Guo, 2006; Morgan et al., 2008; Tovote et al., 2016b) to deliver the activating light to the SST neurons expressing the selected opsins in the vlPAG or their projecting fibres respectively (*Figure 44*). Before implantation, the optical fibre was prepared and cleaved to the appropriate length (2.5mm for vlPAG and 5.5 mm for RMg) and

the light intensity emitted by the fibres was recorded using a Thorlabs power meter (PM-100D) and set to 10mW/mm². We used the stereotaxic protocol similar to RMg 5-HT cannulas implantation.

The skin was opened to expose the skull and the surface was cleaned to expose the Bregma and Lambda. The coordinates to target the vlPAG were bregma -4.4, medio-lateral ±1.0, dorso-ventral, -1.8 angles 10°, and the same coordinates as cited before to target the RVM (bregma -5.8, medio-lateral 0.0, dorso-ventral -5.2), thus a small hole was drilled to expose the surface of the brain. Help by a stereotaxic cannula holder (Thorlabs), the optical cannula was lowered into the hole, and dental cement was used to secure in place. Once the cement was dry, it was covered with black nail varnish to reduce the risk of external illumination.

The frequency and duration of the light propagation were calibrated according to the spontaneous frequency of STT neurons, previously observed in the vlPAG at around 0-5hz (Tovote et al., 2016b). For activating light of somatostatin interneurons both in freely moving and in anaesthetized animal, blue light at 488nm was used with low-frequency stimulation for small duration pulses (2 minutes at 2hz5ms) to depolarize both vlPAG STT neurons and STT descending fibres to the RMg. For ArchT opsin activation, green light at 526.5 nm was used continuously during two minutes to hyperpolarize both vlPAG STT neurons and STT descending fibres to the RMg. Finally, for adeno-associated virus tag with GFP, both blue light at 5hz5ms or green light continuously were used to control the potential harmfulness of the activating light both at the level of both vlPAG and RMg.

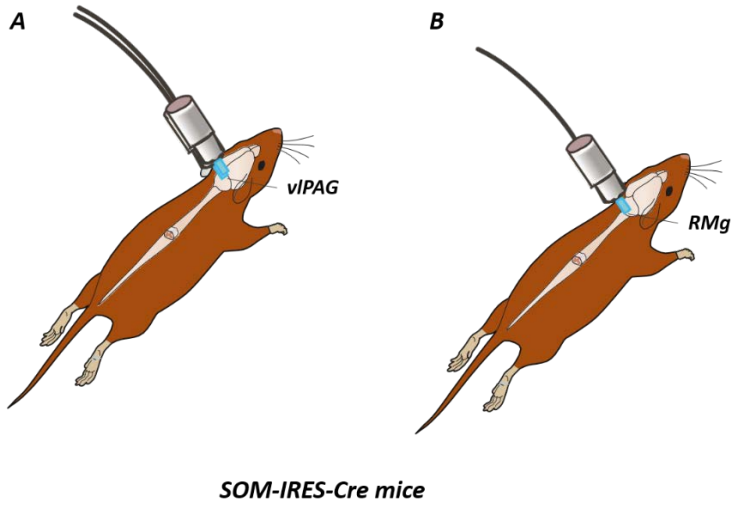

Figure 44 : Description of the fibre implantation strategy. A corresponds to the bilateral vlPAG implantation and B to the RMg implantation.

c) *Pathological pain model: Spared Nerve Injury*

As described in the introduction, pain is a consequence of activation of nociceptive afferents by an actually or potentially tissue-damaging stimuli, but in some cases, pain may arise by activity without suitable stimulation of its peripheral sensory endings. it happens after a lesion of the peripheral or central nervous system and it is termed neuropathic pain and define by the IASP as "pain initiated or caused by primary lesion or dysfunction in the nervous system". For our study, we used a model developed by Decorsted &Woolf (Decosterd and Woolf, 2000), the spared nerve injury (SNI) model (*Figure 45*), which resulted in a consistent and reproducible pain hypersensitivity for both mechanical and thermal stimuli in the territory of the spared sural nerve (Bourquin et al., 2006), maintained for several weeks; and with features which closely mimic the cardinal symptoms of clinically described neuropathic pain disorders. Briefly, the day prior to surgery, mice were tested for their mechanical threshold and thermal latency as described below. Then, the day of surgery, mice were anaesthetized under 2% of isoflurane and followed the same protocol as described on Cichon and al; 2018 (Cichon et al., 2018). A single skin incision was made into the mid-thigh level and the biceps femoris muscles were separated by blunt dissection to expose the sciatic nerve and its three main branches. The common peroneal and tibial nerves using 6-0 nylon suture were ligated and cut with small scissors, removing a 2-4 mm piece of each distal nerve stump, the sural nerve was kept intact. Avoid any stretching or contact with the spared sural nerve. The muscle and skin were then sutured using 6-0 silk. Aseptic techniques as described previously were used. Mice were allowed to recover on a warmed surgical pad until they were able to move freely. The first set of behavioural testing was carried out 4 days after the surgery.

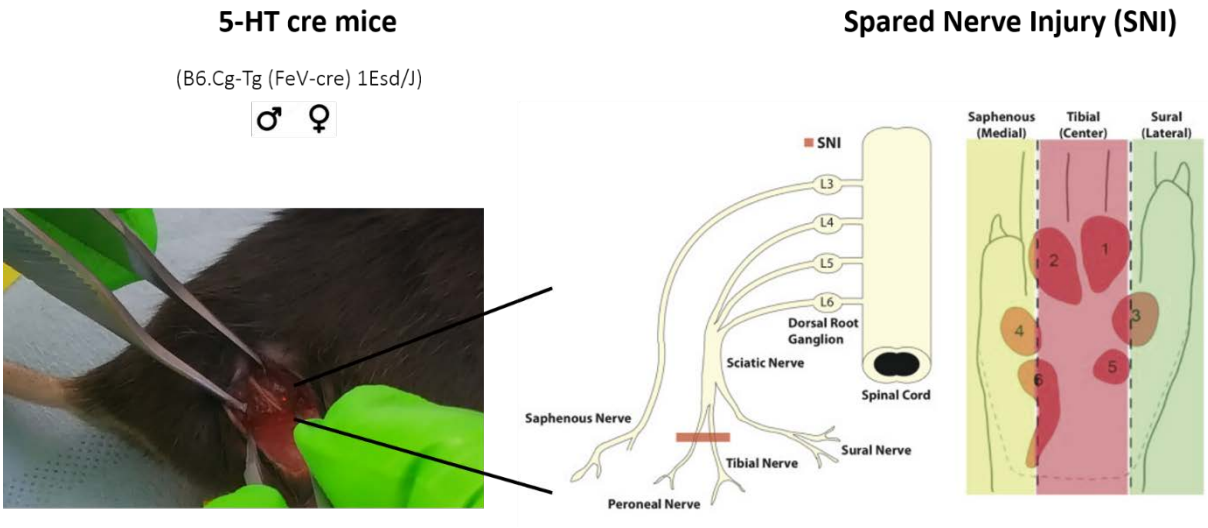

Figure 45 : Schematic representation of the Spared Nerve Injury (SNI). A transection and displacement of the common peroneal and tibial nerves, sparing the adjacent sural and saphenous nerves leading to complete denervation of the tibial innervated area (red) but leaves the medial (yellow) and lateral (green) sides of the hind paw glabrous skin intact (SNI illustration from (Duraku et al., 2012))

4. Pain Behaviour

a) *Mechanical Sensitivity*

Animals were placed in a square Plexiglas homemade frame (25*25*50cm) with a mesh grid on the floor (25cm in height). After 30 minutes of habituation, animals were tested for mechanical threshold using Von Frey Hairs (Bioseb, France). 5 successive tests were performed by applying a Von Frey Hair on the plantar surface of the hind paw in mice remaining on their four paws (*Figure 46*). We assessed the mechanical threshold using the simplified up and down (SUDO) techniques (Bonin et al., 2014). Starting from the 10th filament (2g), the response of the animal to the stimulation (withdrawal or not) will give the value of the next filament. The lower filament is tested if the animal withdraws the paw and the upper one in the other case. Five successive filaments are applied. Each set of test is separated by around 5 minutes. A series of SUDO was performed before, during and after optogenetic stimulation of both neurons and fibres of interest (RMg 5-HT neurons and vlPAG SOM neurons and their descending associated fibres). In the SNI model, we followed the same protocol as explained above with the difference of hairs which were applied to the lateral region of the hind-paws.

Mechanical threshold was evaluated using the last filament value +/-0.5 depending on the value of the fifth filaments. The equation $PWT_{force}=10^{(x*F+B)}$ where F is the PWT calculated

in terms of filament number using SUDO and x and B were determined from a linear regression of the logarithm of the empirically measured filament bending force plotted against the filament number using the equation: Log (bending force) = x * Filament number + B., for 7<F<14, x=0.182 and B=-1.47; 2<F<9, x=0.240 and B=-2) was used to transform the filament value into a value in g.

For mechanical allodynia, it was assessed by measuring the number of paws withdraw induced by a total of five repeated applications of Von Frey Hairs of same force on each paw (each application separated by 10 seconds for the same paw, 1 minute between the paw and 5 minutes between a set of experiment). These repeated measures were assessed before, during and after optogenetic stimulation and the value was converted in percentage of response to five repetitive mechanical stimuli.

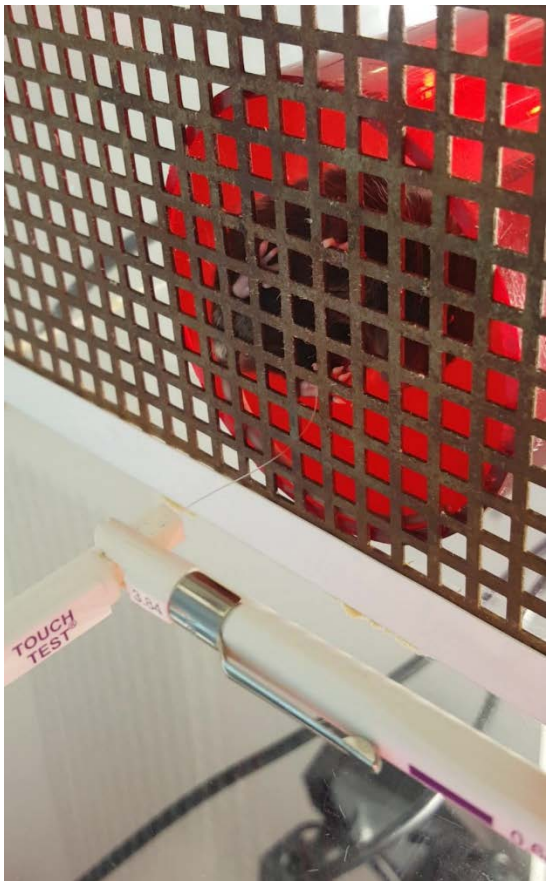

Figure 46 : Photography of a mechanical assessment with 0.6g Von Frey filament.

b) *Heat assessment*

Animals were placed in a Plexiglas cage with a transparent glass floor (Hargreaves method, IITC Inc. Life Science, Tem Sega, *Figure 47*). An infrared laser beam of calibrated value was applied on the plantar surface of the hind paw until the animal withdraws its paw and the value of the latency in seconds is measured. Three sets of test, separated by at least 5 minutes to avoid any sensitization, were performed before, during and after optogenetic stimulation of both neurons and their descending fibres. Within a set of test, each laser beam applied on the different hind paws (left and right) was separated from at least 2 minutes. The average value was then compared between conditions (Cheah et al., 2017).

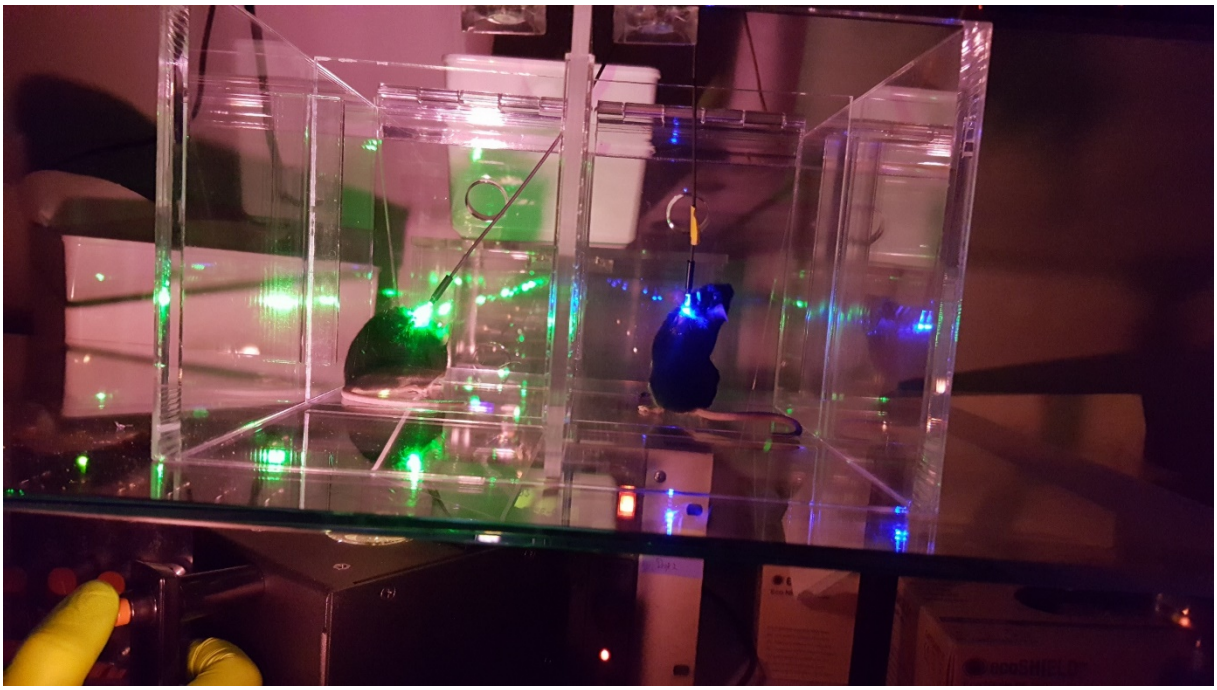

Figure 47 : Photography to illustrate a thermal assessment with a plantar test during optogenetic stimulation.

5. Pharmacological approach

a) *Intraperitoneal injection of furosemide or vehicle*

Intraperitoneal injection of furosemide (25mg/kg) dissolve in NaOH 1N with NaCl, or vehicle (NaOH+ NaCl) was done 30 minutes before the behavioural tests. Naïve SST-cre mice or 5-HT cre mice were maintained with one hand and a 26-gauge needle connected to a 1 µl syringe was inserted in the intraperitoneal right side of the mice.

b) *Intrathecal injection of Picrotoxin, Granisetron or vehicle*

Intrathecal injection of 10µl of picrotoxin (30 µM, (Zufall, 1992)) or vehicle (0.03% of DMSO in ddH_2O), Granisetron (2mM) or vehicle (NaCl 0.9%) (Tan et al., 2019) in naïve 5-HT cre mice was done 20 minutes before the behavioural tests. Naïve 5-HT cre mice were maintained with one hand by the pelvic girdle and a 27-gauge needle connected to a 10 µl Hamilton syringe was inserted in the subarachnoidal space between vertebrae L5 and L6.

c) *Per Os administration of CLP 290 or vehicle*

Oral administration of intrathecal injection of CLP 290 (100mg/kg) or vehicle (20% 2-hydroxypropyl-b-cyclodextrin) was done 1h30 before the behavioural tests. SNI 5-HT cre mice were maintained with one hand and a force-feeding needle connected to a 1 µl syringe was inserted into the throat to deliver the drug or the vehicle.

6. Electrophysiology recording

a) *In vivo extracellular recordings*

Mice were first anaesthetized with urethane 20% and placed on a stereotaxic frame (Unimécanique, Asnières, France). A laminectomy was performed on lumbar vertebrae L1–L3 and segments L4–L5 of the spinal cord was exposed. Extracellular recordings of WDR DHNs were made with borosilicate glass capillaries (2 MΩ, filled with NaCl 0.7M) (Harvard Apparatus, Cambridge, MA, USA). Electrodes were connected to an extracellular amplifier (DAM80; World Precision Instrument) connected to an analogic/numeric interface (Cambridge Electronic Device 1401, CED, UK). Data acquisition was performed using spike2 software (v7, Cambridge Electronic systems, UK). Glass micropipette was gently descended to the spinal cord. A repetitive brush was applied to identify local field potentials and the most responsive part of the peripheral receptive field was selected. Bipolar stimulation electrodes were inserted subcutaneously in the centre of the receptive field. Mild electric shocks above the threshold for C-fibre were generated until an extracellular unit can be unambiguously discriminated from the background noise. After 5 minutes' rest, the threshold for C response was determined and the criterion for the selection of a neuron was the presence of an A-fibre-evoked response (0-80ms) followed by a C-fibre-evoked response (80 to 300ms) to electrical stimulation of the ipsilateral

sciatic nerve. The threshold for C-fibre evoked response as well as and the mean number of C-evoked response were evaluated (*Figure 48)*.

Trains of electrical stimulations at 2-3 times the threshold for C-fibres were performed before, during and after optogenetic stimulations with an optic fibre place above the recording site, then a windup coefficient, which corresponds to the sum of the action potentials resulting from all the repeated stimulations subtracted by the number of action potentials induced by the response to the first stimulation multiplied by the number of stimulations is removed, was evaluated and compared between conditions.

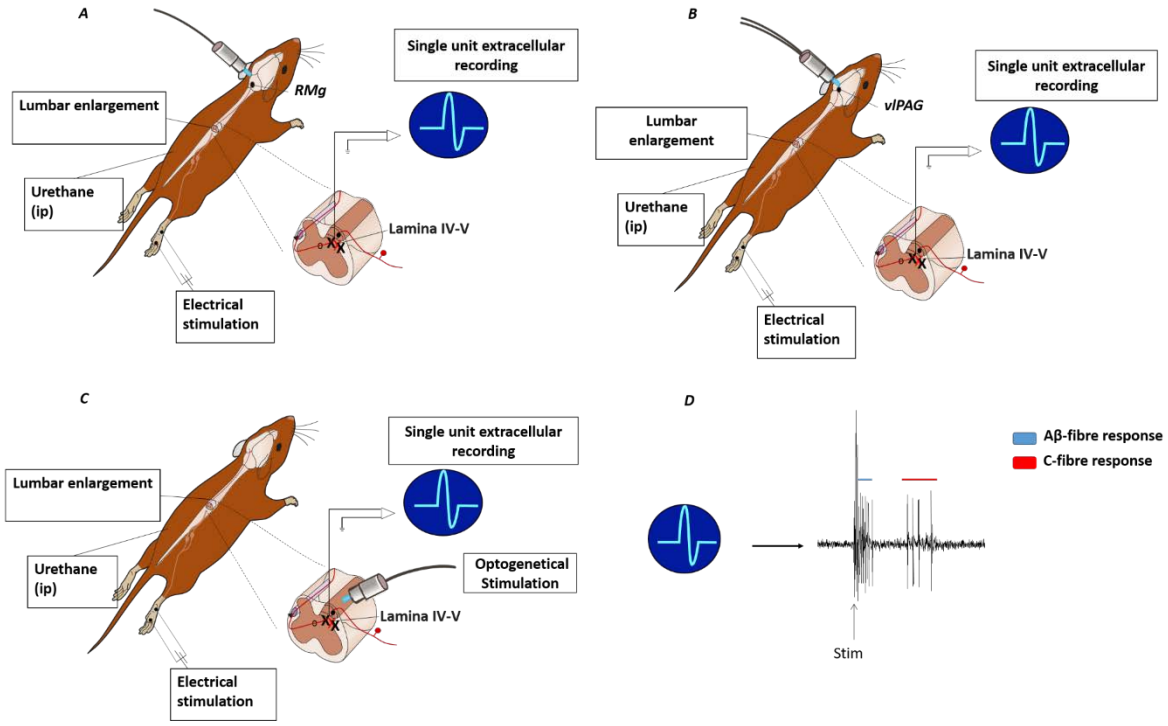

Figure 48 : Illustration of in vivo single-unit recording perform on both anesthetise 5-HT cre mice and SOM-IRES-cre mice in combination with both electrical (innocuous or noxious) and optogenetic stimulation (unilaterally in the RMg (A), or bilaterally in the vlPAG (B) or above the spinal cord (C)). (D) Wide dynamic range neuron (WDRs) response to peripheral stimulation consisting in a biphasic response with a fast response (blue) induced by activation of fast innocuous sensory fibres (Aδ fibres) followed by a late response induced by activation of noxious c-fibre (in red).

b) *In vitro Patch-clamp recordings*

Patch-clamp recordings were performed on brain slices from 4, 3 and 4 mice respectively for the GFP, ChR2 and ArchT group mice. Briefly, 6 to 12 weeks old mice were intracardially perfused during euthanasia (exagon/lidocaine: 300/30 mg/kg, IP) with ice-cold NMDG solution (containing in mM: 1,25 ascorbate, 3 Na-Pyruvate, 2 Thiourea, 93 NMDG, 93

HCL 37%; pH: 7,3-7,4; osmolarity: 305-310 mOsM). Brains were quickly removed and 250 µm slices containing the RMg were prepared with a VT1000S Leica vibratome in ice-cold oxygenated NMDG solution before recovery for 12-15 minutes into at 34°C in the oxygenated NMDG solution. Slices were then transferred at room temperature into aCSF solution (containing in mM: 124 NaCl, 2,5 KCl, 1,25 NaH2PO4, 2 MgCl2, 2,5 CaCl2, 227 2,5 D-glucose, 25 NaHCO3; pH: 7,3-7,4; osmolarity: 305-310 mOsM) for at least 1 hour. Slices were transferred in the recording chamber placed under a microscope (Nikon EF600) outfitted for fluorescence and IR-DIC video microscopy and perfused with oxygenated aCSF at 2-3 ml/min in the recording chamber. Viable RMg 5-HT neurons were visualized with a fluorescence video camera (Nikon, *Figure 49*). Borosilicate pipette (4-6 MΩ; 1.5 mm OD, Sutter Instrument) were filled with an intracellular solution (containing in mM: Kgluconate solution: 128 Kgluconate, 20 NaCl, 1 MgCl2, 1 EGTA, 0,3 CaCl2, 2 Na2-ATP, 0,3 Na-GTP, 0,2 cAMP, 10 HEPES; CsCl solution: 150 CsCl, 2 MgCl2, 1 EGTA, 3 Na2-ATP, 0,3 Na-GTP, 0,2 cAMP, 10 HEPES; 280-290 mOsM, pH 7.3-7.4). Recordings were made using a Multiclamp 700B amplifier, digitized using the Digidata 1440A interface and acquired at 2 kHz using pClamp 10.5 software (Axon Instruments, Molecular Devices, Sunnyvale, CA). Pipettes and cell capacitances were fully compensated but junction potential was not corrected. RMg 5-HT neurons were recorded in whole-cell current-clamp mode. Brain slices expressing ChR2 or control were opto-stimulated at 470nm (5Hz, 5ms pulse width) for 10 seconds every 30 seconds. Laser intensity was set as 5 $mW.mm^{-2}$. For brain slices expressing ArchT in RMg, 5-HT neurons were maintained in current-clamp at a firing frequency of 3 Hz while opto-stimulation at 532 nm was performed by applying constant light during 250 ms.

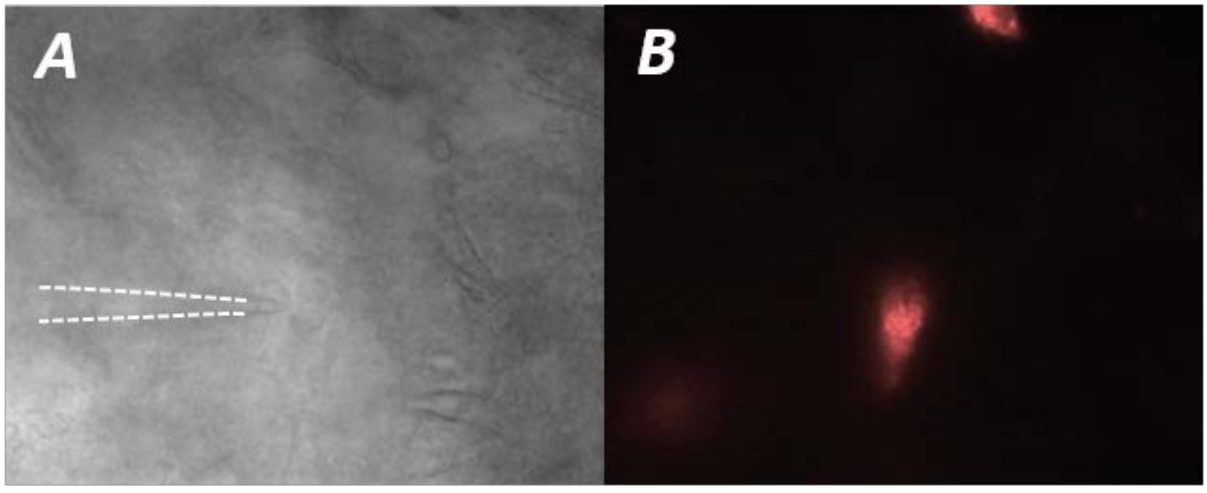

Figure 49 : Photography of the tissue of interest including borosilicate pipette in A and neurons expressing a mCherry tag induced by a viral infection observed via Nikon EF600 microscope.

7. Anatomical analysis

a) *Virus expression*

After completion of experiments, mice were euthanized with urethane and perfused through the left ventricle with 4% w/v paraformaldehyde (PFA) in 0.1 M PBS. Brain and spinal cords were extracted and dissected out and post-fixed for 3h at 4°C in the same solution then cryoprotected in a solution of 0.1 M PBS and 25% sucrose overnight and stored at -80°C. For verification of both the viral and tracer expression as well as the location of optic fibre in the vlPAG, the RMg and above the spinal cord (for the viral and tracer expression only), serial of 20µm thin slices containing the vlPAG, RMg and spinal cord of 5-HT cre or 5-HT cre*Ai9 or Gad67 GFP*5-HT cre or SOM-IRES-cre mice (depending on experimental study) were incubated free-floating in 0.1 M PBS containing Triton X-100 (0.3%), Bovine Serum Albumin (1%; Sigma-Aldrich) and chicken anti-GFP (1:1000; Averlabs) or chicken anti-mCherry (1:1000; Abcam) or rabbit anti-Myc tag (1:500; Euromedex) or mouse anti-Myc tag (1:500; Roche) antibodies overnight at 4°C. After washing in 0.1 M PBS, secondary antibodies, Alexa fluor 488 or 568–conjugated goat anti-chicken (1:500; Thermo Fischer Scientific) or Alexa fluor 568–conjugated goat anti-rabbit (1:500; Thermo Fischer Scientific) or Alexa fluor 488–conjugated goat anti-mouse (1:500; Thermo Fischer Scientific) were added in 0.1-M PBS for 2 hours at room temperature. Sections were finally viewed on a confocal microscope (*Figure* 50, Leica TCS SPE, Mannheim, Germany) fitted with a 20x dry objective and both 40x and 63x oil immersion 1.3 NA objective and confocal image stacks (0.75 µm steps) were acquired for each sample. Moreover, images of each section were also acquired with both nanozoomer slide scanner viewer (for an overview of the whole section) and an epifluorescence system (Leica DM 5000) fitted with a 20x dry objective.

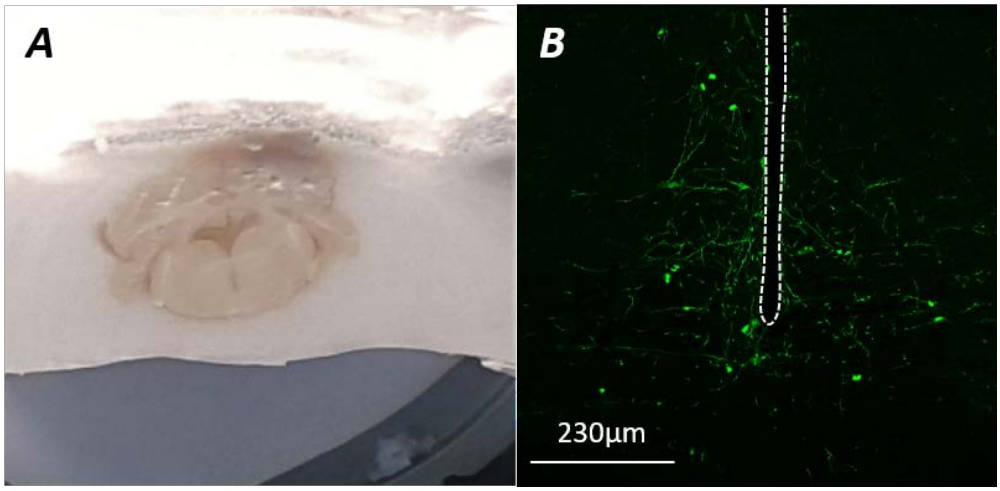

Figure 50 : Photography of mouse brain embedding in a tissue tek (Leica) and showing optical fibre trace (A) in a cryostat in the one hand and in the other confocal image of RMg 5-HT neuron expressing GFP tag with the injection site (B)

b) *Immunohistochemical study*

Spinal cord or RMg or vlPAG sections were incubated free-floating in 0.1 M PBS containing Triton X-100 (0.3%) and Bovine Serum Albumin (1%; Sigma-Aldrich). Depending on the experimental study (see results) and unless specified, the following antibodies were tested:

i. For 5-HT labelling

Sections of the RMg or the vlPAG or the lumbar part of the spinal cord of 5-HT cre*Ai9 or Gad67 GFP or SOM-ires-cre or wild type (WT) mice (depending on the experimental study) were incubated with rabbit anti-tryptophan hydroxylase 2 (TPH2) antibody (1:1000; Bio-techne), overnight at 4°C. After washing in 0.1 M PBS, a secondary antibody Alexa Fluor 488 (for 5-HT cre*Ai9 cre mice, 1:500; Thermo Fischer Scientific) or 568 (for Gad67 GFP or SOM-ires-cre or WT; 1:500; Thermo Fischer Scientific) conjugated donkey anti-rabbit 0.1M PBS was added for 2 hours at room temperature.

ii. For the assessment of excitatory, inhibitory and somatostatin neurons marker

- For glutamatergic (excitatory) labelling in combination with 5-HT labelling

Sections of the RMg of WT mice were incubated with guinea pig anti-VGLUT1 and anti-VGLUT2 antibodies (1:1000; Synaptic Systems) in combination with rabbit anti-TPH2 antibody (1:1000; Bio-techne), overnight at 4°C. After washing in 0.1 M PBS, secondary

antibodies Alexa Fluor 488 conjugated goat anti guinea pig (1:500; Thermo Fischer Scientific) with Alexa 568-conjugated goat anti-rabbit (1:500; Thermo Fischer Scientific) in 0.1M PBS was added for 2 hours at room temperature.

- For GABAergic (inhibitory) labelling in combination with 5-HT labelling

Sections of the RMg of Wild type mice were incubated with human anti-GAD GS.67-65 (1/1000, Sigma) in combination with rabbit anti-TPH2 (1:1000; Bio-techne) antibodies overnight at 4°C. After washing in 0.1 M PBS, secondary antibodies Alexa Fluor 488-conjugated goat anti-human (1:500; Thermo Fischer Scientific) associated with Alexa Fluor 568-conjugated goat anti-rabbit (1:500; Thermo Fischer Scientific) in 0.1M PBS were added for 2 hours at room temperature.

- For Somatostatin labelling in combination with 5-HT labelling

Sections of the RMg of Wild type mice were incubated with Guinea Pig anti-SOM (1/500, kindly gifted by Philippe Ciofi) in combination with rabbit anti-TPH2 (1:1000; Bio-techne) antibodies overnight at 4°C. After washing in 0.1 M PBS, secondary antibodies Alexa Fluor 488-conjugated goat anti-guinea pig (1:500; Thermo Fischer Scientific) associated with Alexa Fluor 568-conjugated goat anti-rabbit (1:500; Thermo Fischer Scientific) in 0.1M PBS were added for 2 hours at room temperature.

iii. For the assessment of excitatory and inhibitory interneurons in contact with raphe Magnus (RMg) 5-HT projections

- For Tlx3 (excitatory interneurons marker) in combination with 5-HT neurons viral expression labelling

Lumbar sections of the spinal cord of 5-HT cre mice expressing an AAV inducible virus tag with GFP in the 5-HT neurons of the RMg were incubated with guinea pig anti-Tlx3 antibody (1:1000, kindly gifted by Thomas Müller) in combination with chicken anti-GFP antibody (1:1000; Averlabs) overnight at 4°C. After washing in 0.1 M PBS, a first round of amplification was performed using a biotin-conjugated goat anti guinea pig (1:500; Jackson immune research) was added for 1hours at room temperature then after another wash in 0.1MPBS secondary antibodies Alexa 568–conjugated streptavidin (1:500; Molecular Probes) in combination with Alexa Fluor 488 conjugated donkey anti-Chicken (1:500; Thermo Fisher Scientific) in 0.1M PBS was added for 2 hours at room temperature.

- For Pax2 (inhibitory interneurons marker) in combination with 5-HT neurons viral expression labelling

Lumbar sections of the spinal cord of 5-HT cre mice expressing an AAV inducible virus tag with GFP in the 5-HT neurons of the RMg were incubated with Goat anti-Pax2 Human polyclonal antibody (1:300, Bio-techne) in combination with chicken anti-GFP antibody (1:1000; Averlabs) overnight at 4°C. After washing in 0.1 M PBS, secondary antibodies Alexa Fluor 568-conjugated donkey anti-goat (1:500; Thermo Fischer Scientific) associated with Alexa Fluor 488 conjugated goat anti-Chicken (1:500; Thermo Fisher Scientific) in 0.1M PBS was added for 2 hours at room temperature.

- For GABAergic inhibitory interneurons in combination with 5-HT neurons viral expression labelling

Lumbar sections of the spinal cord of Gad67-GFP*5-HT cre mice expressing an AAV inducible virus tag with Myc in the 5-HT neurons of the RMg were incubated with rabbit anti-Myc tag (1:500; Euromedex) antibody overnight at 4°C. After washing in 0.1 M PBS, a secondary antibody Alexa Fluor 568-conjugated goat anti-rabbit (1:500; Thermo Fischer Scientific) in 0.1M PBS was added for 2 hours at room temperature.

- For Parvalbumin inhibitory interneurons in combination with 5-HT neurons viral expression labelling

Lumbar sections of the spinal cord of 5-HT cre mice expressing an AAV inducible virus tag with Myc in the 5-HT neurons of the RMg were incubated with mouse anti-Myc tag (1:500; Roche) in combination with rabbit anti-parvalbumin antibody (1:5000; Bio-techne) antibodies overnight at 4°C. After washing in 0.1 M PBS, secondary antibodies Alexa Fluor 568-conjugated goat anti-rabbit (1:500; Thermo Fischer Scientific) associated with Alexa Fluor 488-conjugated goat anti-mouse (1:500; Thermo Fischer Scientific) in 0.1M PBS was added for 2 hours at room temperature.

After performing immunostaining, for each experiment, sections (vlPag, RMg or spinal cord) were then mounted on gelatine-coated slides with DakoCytomation Fluorescent Mounting Medium (Dako SA) and finally viewed on a confocal microscope (Leica TCS SPE, Mannheim, Germany) fitted with a 20x dry objective and both 40x and 63x oil immersion 1.3 NA objective and confocal image stacks (0.75 µm steps) were acquired for each sample and sequential acquisition was used to prevent cross-talk between Alexa 488 and Alexa 568. Then for a post-analysis by using imaris microscopy image analysis software (Bitplane):

- With regard to colocalisation between cell,

after estimating the diameter of each specifically labelled cell, we converted each cell as a sphere and then assessed the cells that were separated by 0nm from those with a difference of more than 0nm thus highlighting the cells colocating between them from those with a difference.

- With regard to appositions between cell and fibres,

after estimating the diameter of each specifically labelled cell and fibres, we converted each cell as a sphere and each fibre as a filament and then we assessed the filaments that are closed to (0nm apart) the edge of the cells of those that are far from them (more than 0 nm) thus highlighting the fibres that are in apposition with cells.

8. Statistical analysis

All statistical analyses were completed on GraphPad (Prism, version 8.0.2). Data set were collected and processed randomly and no statistical methods were used to predetermine sample sizes. Statistical comparisons were made using unpaired and paired t-test as well as one-way ANOVA (Unpaired and repeated measures).

For behavioural analysis, the mechanical threshold and thermal latency were compared before, during and after optogenetic stimulations. A one-way ANOVA was performed to compare between these three conditions.

For Electrophysiology: Spontaneous activity was evaluated by the mean frequency (in Hz) during 2 min before, during and after optogenetic stimulation of both 5-HT neurons of the RMg and SOM neuron of the vlPAG. A one-way ANOVA was then performed to compare each condition. Evoked responses to electrical stimulation of the peripheral receptive field. We measure the number of C-fibre induced spikes of WDR neurons after each electrical stimulation, for 4-5 stimulations before, during and after optogenetic stimulation. A one-way ANOVA was performed to compare the response during and after optogenetic stimulation to the response before. The windup response to trains of electrical stimulation at 2 times the threshold for C-fibres. From the windup response, a coefficient of windup was calculated before and during optogenetic stimulation. A Paired *t.test* was performed to compare the windup coefficient during optogenetic stimulation to the coefficient before.

All data were presented as the mean ± S.E.M. In all cases, $p<0.05$ was considered statistically significant. Individual *p* values are provided for each appropriate test in text.

9. Table of Resources

REAGENT or RESOURCE	SOURCE	IDENTIFIER
Experimental Models: Organisms/Strains		
Ai9 cre-reporter mice (Rosa-GAG-LSL-tdTomato-WPRE-conditional)	PIV Animal facility A1 Bordeaux University	B6.Cg-*Gt(ROSA)26Sor*$^{tm9(CAG-tdTomato)Hze}$/J
5-HT cre (Epet-Cre) heterozygous (+/-) knock-in-mice	The Jackson Laboratory	B6.Cg-Tg (FeV-cre) 1Esd/J, Jackson Laboratory N°012712
5-HT cre* Ai9 tomato	PIV Animal facility A1 Bordeaux University	N/A
GAD 67 – GFP mice	PIV Animal facility A1 Bordeaux University	Gad1tm1.1Tama
GAD 67-GFP*5-HT cre mice	PIV Animal facility A1 Bordeaux University	N/A
SST-Cre heterozygous (+/-) knock-in-mice	N/A	N/A
SST-Cre homozygous (+/+) knock-in-mice	The Jackson Laboratory	Ssttm2.1(cre)Zjh/J N°013044
Recombinant DNA and tracer		
AAV-CAG-FLEX-ArchT-GFP	Vector core (Boyden/MIT)	N/A
AAV-CAG-FLEX-GFP	Vector core (Boyden/MIT)	N/A
AAV-CAG-FLEX-mCherry	Vector core (Boyden/MIT)	N/A
AAV-EF1a-DIOhChR2(H134R)-EYFPWPRE-pA	Vector core (Deisseroth/Standford)	N/A
AAV-EF1a-DIOhChR2(H134R)-mCherryWPRE-pA	Vector core (Deisseroth/Standford)	N/A
AAV9-CAG-floxed-SynMYC-rev-WPRE	Vector core (Boyden/MIT)	N/A

Fluorogold	Sigma-Aldrich	Cat# 39286
Antibodies (Primary)		
Chicken polyclonal anti-GFP	Aves Labs	Cat# GFP-1010
Chicken polyclonal anti-mCherry	Kindly gifted	N/A
Goat anti- Pax2 Human polyclonal	Bio-techne	Cat# AF3364
Guinea Pig anti-SOM	Kindly gifted by Philippe Ciofi	N/A
Guinea Pig anti-TLX3	Kindly gifted by Thomas Müller	N/A
Guinea Pig anti-VGlut 1	Synaptic Systems	Cat# 135304
Guinea Pig anti-VGlut 2	Synaptic Systems	Cat# 135404
Human anti-GAD GS.67-65	Sigma	Cat# G5163
Rabbit anti-parvalbumin antibody	Bio-techne	Cat# AF5058
Mouse anti-Myc clone 9E10 (monoclonal)	Roche	N/A
Rabbit anti-myc tag (IgG polyclonal	Euromedex	Cat#06-549
Rabbit anti-Tryptophan hydroxylase 2	Bio-techne	NB 100-74555
Antibodies (Secondary)		
Biotin goat anti-guinea pig	Jackson immuno	Cat# 106-066-006
Donkey anti-goat Alexa 568	Thermo Fisher Scientific	Cat# A-11057
Donkey anti-rabbit Alexa 568	Thermo Fisher Scientific	Cat# A-10042
Donkey anti-mouse Alexa 568	Thermo Fisher Scientific	Cat# A-10037
Goat anti-chicken Alexa 488	Thermo Fisher Scientific	Cat# A-11039
Goat anti-chicken Alexa 568	Thermo Fisher Scientific	Cat# A-11041

Goat anti-human Alexa 488	Thermo Fisher Scientific	Cat# A-11013
Goat anti-guinea pig Alexa 488	Thermo Fisher Scientific	Cat# A-11073
Goat anti-mouse Alexa 488	Thermo Fisher Scientific	Cat# A-11008
Goat anti-rabbit Alexa 488	Thermo Fisher Scientific	Cat# A-32731
Goat anti-rabbit Alexa 568	Thermo Fisher Scientific	Cat# A-11011
Streptavidin Alexa 568 anti-biotin	Invitrogen	Cat# S-11226
Chemicals, Peptides, and Recombinant Proteins		
CLP 290	Kindly gifted by Yves De Koninck	NA
Furosemide	Sigma-Aldrich	Cat#F-4381
Granisetron hydrochloride	Tocris	Cat#2903
Hydroxypropyl-β-cyclodextrin	TCI AMERICA	Cat#H0979
Picrotoxin	Biotechne	Cat#1128
Urethane	Sigma-Aldrich	Cat#U2500
Software and Algorithms		
Adobe illustrator 2017	Adobe software	N/A
CED spike 2	Cambridge Electronic Design	N/A
Excel	Microsoft	N/A
Image J (Fiji)	NIH	www.imagej.nih.gov
Imaris Bitplane	Oxford instrument	N/A
GraphPad Prism 8	GraphPad Software	http://www.graphpad.com/scientificsoftware/prism/
NDP.view2	Hamamatsu	NDP.view2 Viewing software
PowerPoint	Microsoft	N/A
Word	Microsoft	N/A

B. RESULTS OF EXPERIMENTAL APPROACHES

1. Validation of animal model

B6.Cg-Tg (FeV-cre) 1Esd/J or 5-HT-cre (in this study) were firstly used to confirm the expression of the Cre-recombinase restrained to 5-HT neurons of the DR and the MR (Scott et al., 2005b) but no information for the RMg. In the case of SOM-IRES-cre mice, all validations have been performed mainly by our collaborators but data will not is.

a) *Characterisation of Cre-recombinase in the RMg*

First, to confirm that cre-recombinase is restrained to serotonin neurons in the dorsal raphe (DR), the median raphe (MR) and the raphe Magnus (RMg) we used adult 5-HT cre*Ai9 mice where we performed immunostaining against tryptophan hydroxylase 2 (TPH2), a specific enzyme of serotonin neurons *Figure* 51. Immunohistochemical analyses confirmed a good expression of Td tomato staining in the RMg and revealed that 82,06 % of TPH2 positive neurons are co-localised with Td tomato positive cells (*Figure* 51B, and 89.13% Td tomato/TPH2). In addition, we observed an abundant population of 5-HT fibres in the spinal dorsal horn confirming 5-HT projections to the spinal cord (*Figure* 51C).

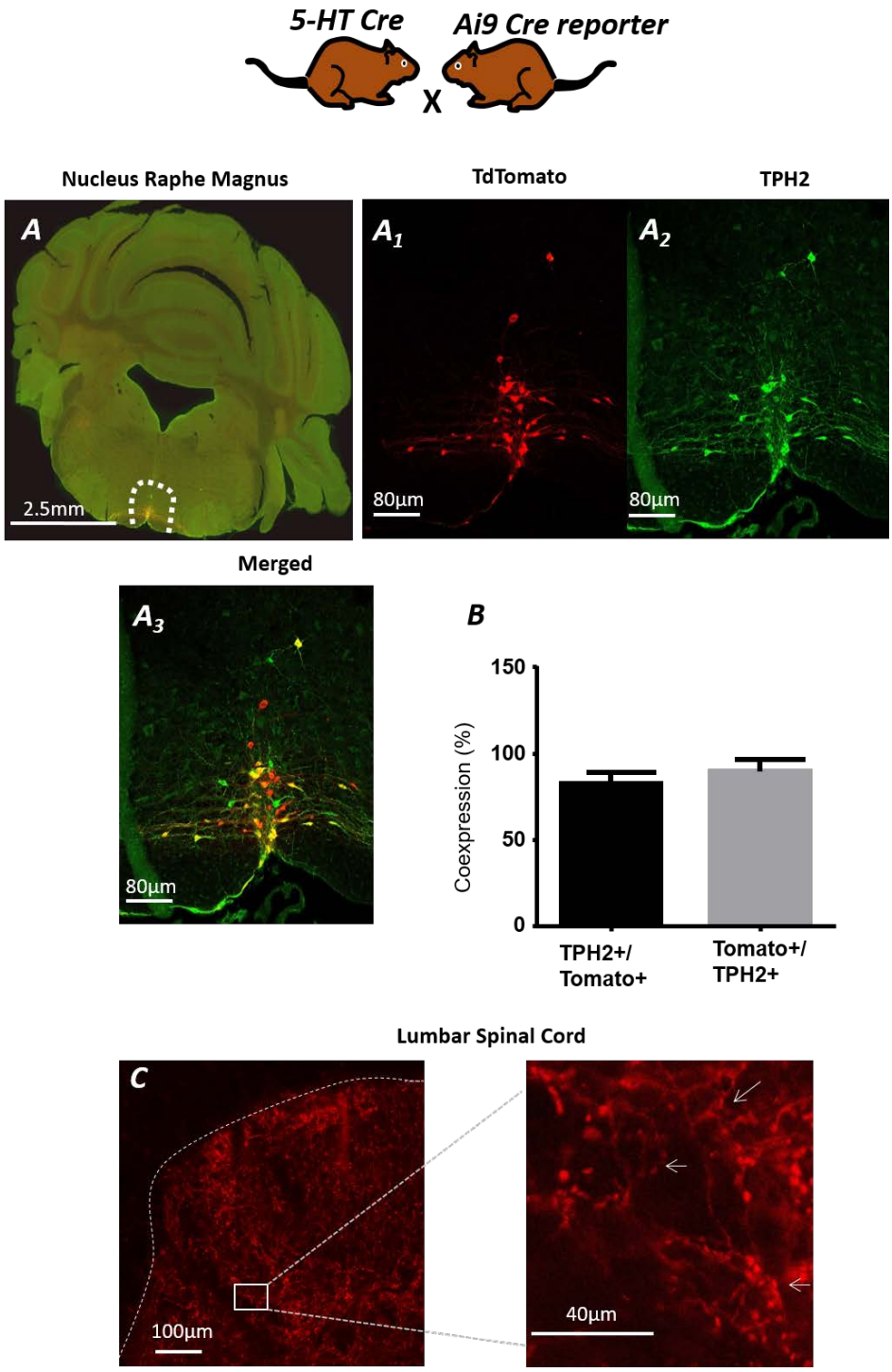

Figure 51 : Epifluorescence microscopy image (taken on Hamamatsu NANOZOOMER 2.0HT) of thin slice of 5-HT cre mouse brain including the RMg (surrounded by a white dashes; A) showing in red the td tomato cre-recombinase expressing cell (A1),in green the GFP TPH2 positive cell (A2) and in yellow colocalisation of both TPH2 and Ai9 cre positive cells (A3) showing up 82.06% of co-localisation (TPH2/Tomato using IMARIS microscopy image analysis software (Oxford instrument; B), data obtained from 4 slices of 3 different brains or spinal cord). We also observed a dense population of 5-HT fibres in the dorsal horn of the spinal cord (C). The zoom images A1-3 and C were taken with confocal microscope Leica DM6000 TCS SP5 MP FLIM.

Furthermore, as a control, we confirmed also a good expression of the cre-recombinase in 5-HT neurons of the DR and MR (*Figure* 52) as described by (Scott et al., 2005b). Thus, giving us a crucial tool to study precisely the role of RMg 5-HT in nociceptive transmission.

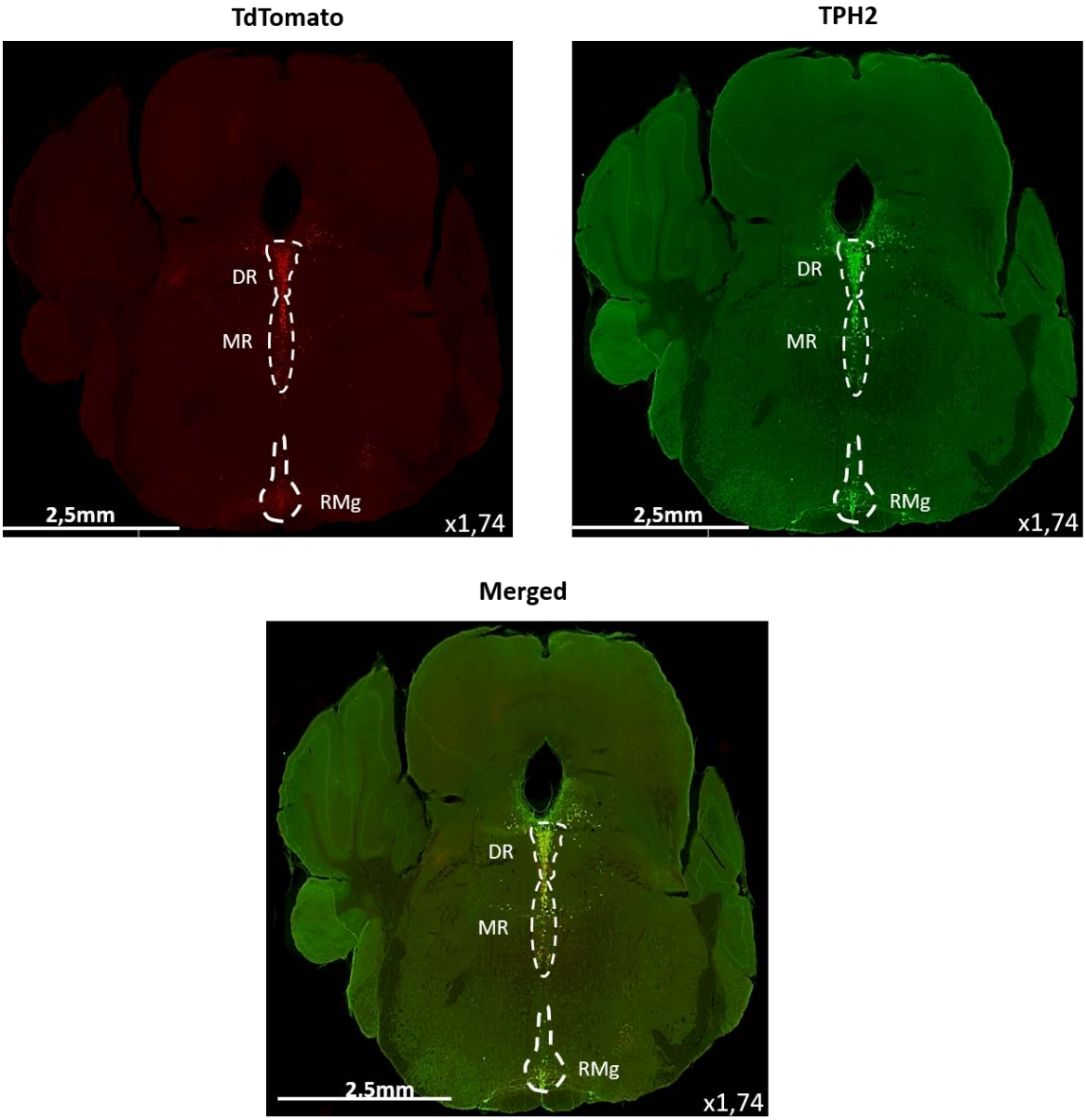

Figure 52 : Epifluorescence microscopy image (taken on Hamamatsu NANOZOOMER 2.0HT) of thin slice of 5-HT cre mouse brain including the DR, MR and RMg (surrounded by a white dashes respectively) showing in red the td tomato cre-recombinase expressing cell in each nucleus (DR, MR and RMg), as well as in green the GFP TPH2 positive cell and in yellow the co-localisation of both TPH2 and Ai9 cre positive cells showing up a dense co-localisation of both labelling in each nucleus (DR, MR and RMg respectively). Each time 4 slices from 3 different brains.

In the next step, we used adult Gad67-GFP mice expressing enhanced Green Fluorescent Protein (EGFP) under the control of the mouse Gad1(GAD67) gene promoter and as shown in *Figure 53*, TPH2 staining confirms that 5-HT is not GABAergic neurons. Indeed, by using imaris 3D reconstruction (*Figure* 53A4), we converted confocal stack images in 3D images thus enabling us to quantify contacts between TPH2 positive cells (represented in white spheres) and GAD-67 positive cells (represented in green spheres). Accordingly, as shown, we revealed no co-localisation between the Gad67-GFP representing spheres and TPH2 representing spheres but strong interaction between them (*Figure* 53B4).

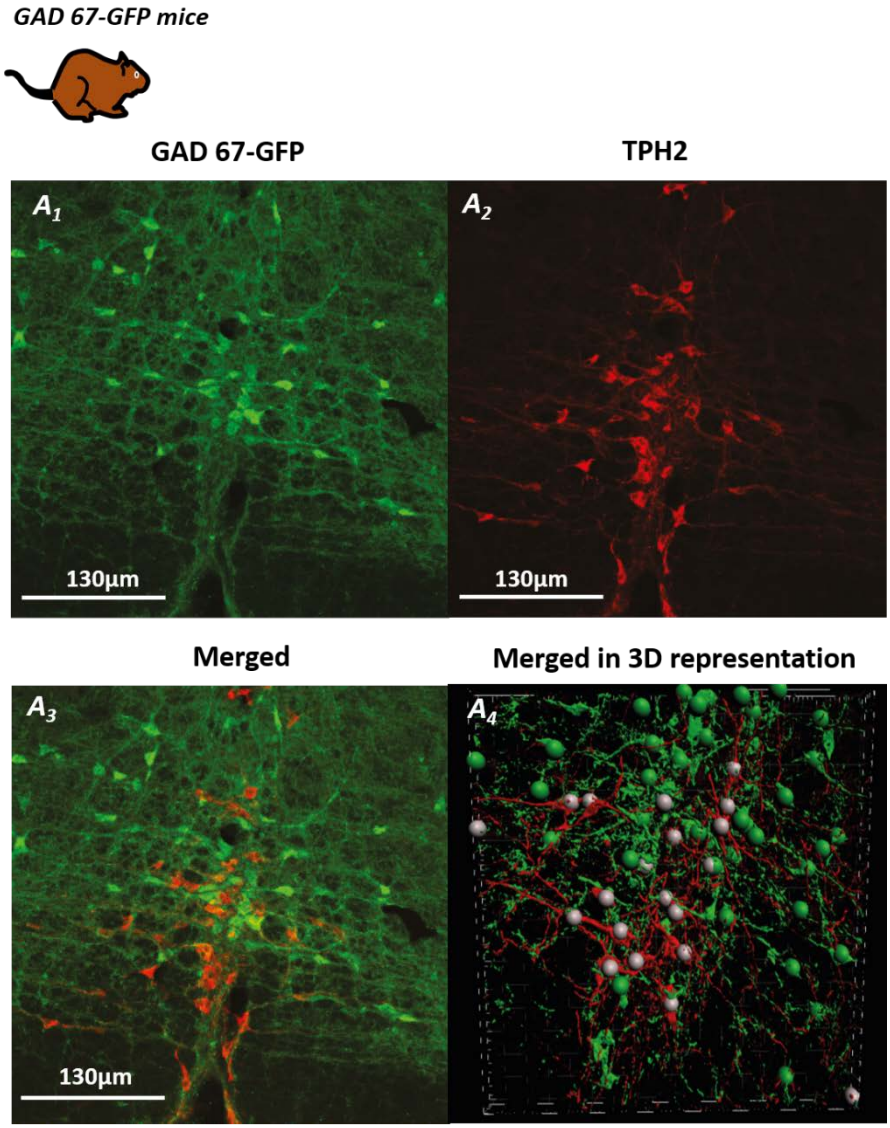

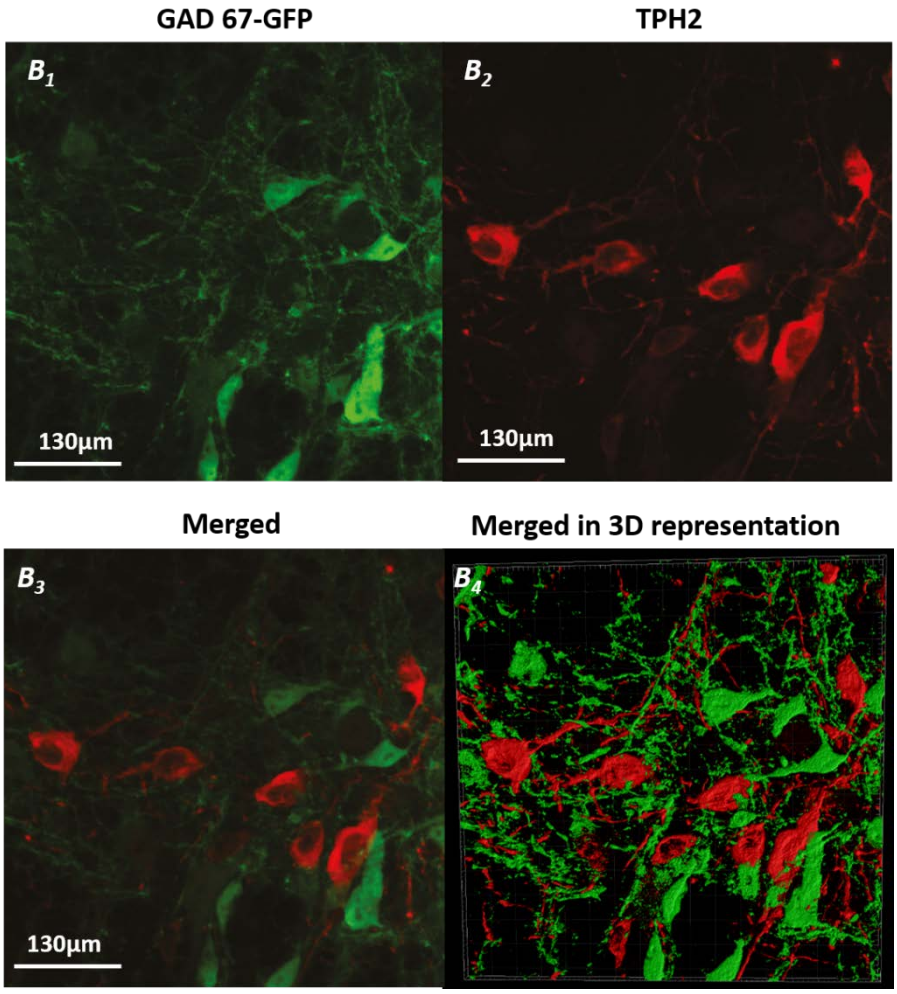

Figure 53 : Confocal and 3D images of TPH2 immunostaining in thin slice of RMg of Gad67-GFP mouse. TPH2 staining showed no co-localisation with GABAergic neurons expressing GFP. A1 and B1 show GAD 67-GFP GABAergic neurons, A2 and B2, TPH2 staining and A3 and B3 a merge of both TPH2 staining and GAD67-GFP GABAergic neurons. A4 and B4 represent 3D images of GAD 67-GFP/TPH2 merged confocal image (IMARIS microscopy image analysis software; Oxford instrument) showing no co-localisation between both cells but strong interaction between them.

2. Validation of our viral strategy

We assessed the efficiency of our viral approach by stereotaxic injection of a cre-dependent recombinant adeno-associated virus combined with a GFP tag (AAV-CAG-flex-GFP) in RMg of 5-HT cre*Ai9 mice and vlPAG of SOM-IRES-cre mice, then three weeks after RMg 5-HT and vlPAG SOM neurons expressed GFP tag (*Figure* 54). By using a immunohistochemical analysis of the labelled neurons related to the viral expression (*Figure* 54A1), in the 5-HT cre*Ai9 mice, we observed that 100% of cre-recombinase (*Figure* 54A2) has been infected by 250nl of virus (*Figure* 54A3) and also that the infected 5-HT fibres were mostly presented in deep layer of the dorsal horn of the spinal cord (*Figure* 54A4) according to

previous study in rat (Gautier et al., 2017). For SOM-IRES-cre mice, we observed an intense infection of somatostatin neurons following bilateral injection of 350nl virus (*Figure* 54B).

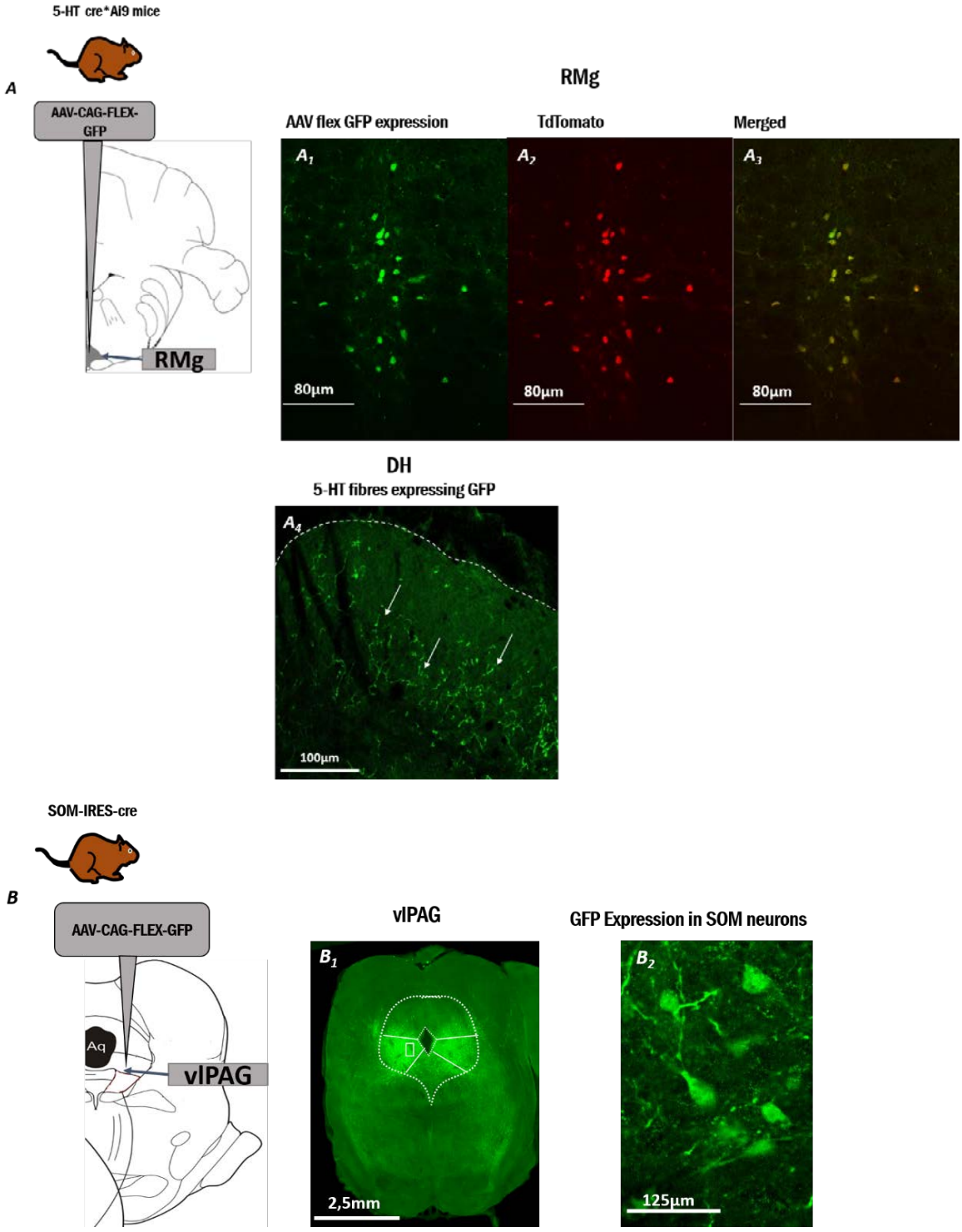

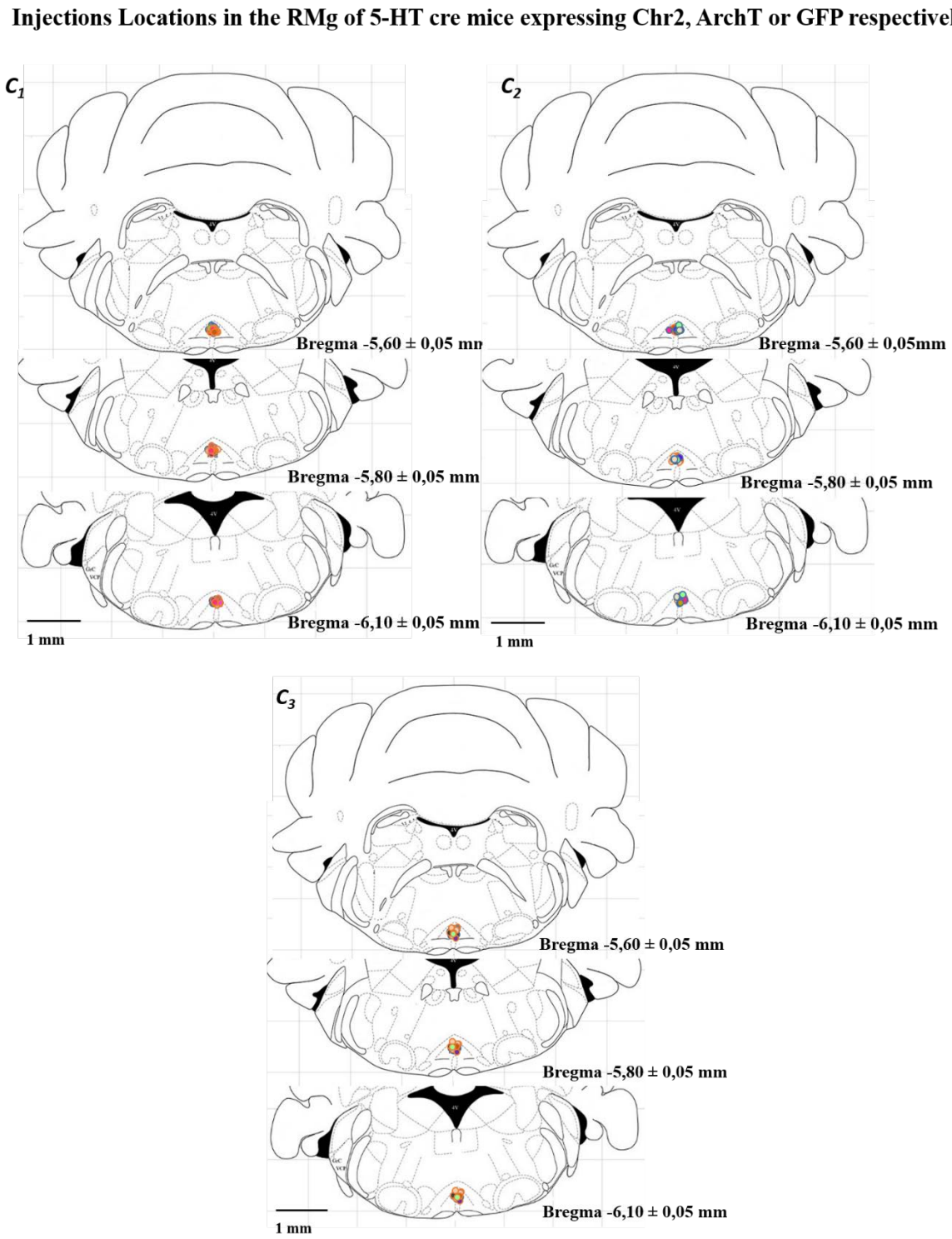

*Figure 54 : Confocal image of AAV infection in RMg of 5-HT cre*Ai9 mice or in vlPAG of SOM-IRES-cre mice (A1 and B1 respectively). As shown, for the RMg injection in 5-HT cre*Ai9 mice, 100% of cre-recombinase cell (A2) was infected with 250nl of AAV cre-inducible virus (A3). Also we observed tag expression extend to the projection of RMg 5-HT neurons mostly in deep layer of the dorsal horn of the spinal cord (A4). For the vlPAG injection in SOM-IRES-cre mice, a dense level of infection has been observed (B2) following an injection of 350nl of AAV cre-inducible virus. (C) Schematic representation after verification of the injection site location above the RMg of 5-HT cre mice expressing ChR2 (C1), ArchT (C2) and GFP (C3) respectively.*

Then, we ascertained the efficiency of manipulating neuronal activity by activating light, using slices of the RMg of 5-HT cre mice containing 5-HT infected neurons with the Channelrhodopsin 2 (ChR2 opsin for activating RMg 5-HT neurons) or the proton pump Archaerhodopsin (ArchT opsin for silencing RMg 5-HT neurons) or only a mCherry tag using cre-dependent adeno-associated vectors in combination with patch-clamp recording in current-clamp mode (*Figure 55*). In slices expressing ChR2-mCherry (*Figure* 55A1-3), optogenetic stimulation at 470 nm induced a fast and reproducible neuronal depolarisation, and a train of 5hz/5ms induced a train of action potentials that fairly followed light stimulation (Two-tailed paired *t.test* p=0.0156, n=7 ChR2-5-HT neurons) contrary to slices of 5-HT neurons expressing ArchT-GFP (*Figure* 55B), where a continuous optogenetic stimulation at 532 nm induced a strong hyperpolarisation. As a control, we also assessed the influence of the activating light, using mCherry-expressing slices (*Figure* 55C) where both 470 or 532 nm optogenetic stimulation at 5Hz/5ms or continuously (respectively) induced no modification in the neuronal activity.

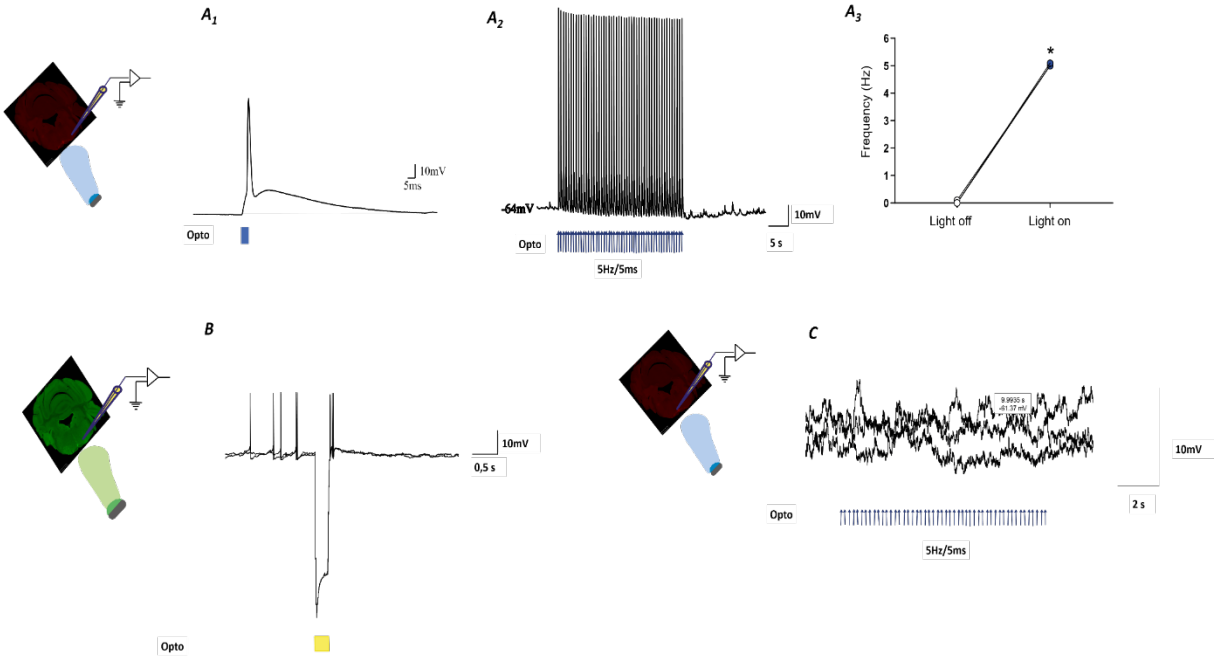

*Figure 55 : Ex vivo Patch-clamp whole-cell recording from RMg slices containing 5-HT infected neurons. Sample current-clamp traces (A1-2, B and C) showing light-evoked action potential firing of 5-HT neuron expressing ChR2 opsin or hyperpolarisation of 5-HT neuron expressing ArchT opsin or nothing in 5-HT neuron expressing GFP only (representative of 7, 1 and 9 cells respectively). (A3) 470nm optogenetic stimulation at 5Hz/5ms induced an increase of the discharge frequency of 5-HT neuron expressing ChR2 opsin (light off 0.014±0.015Hz compared to light on 5.014±0.014Hz). Measures are reported as mean ± SEM; *=p=0.0156 from Wilcoxon matched-pairs signed-rank test.*

3. Assessment of the optical fibre implantation on mechanical modality

First, after cannula implantation, mice remained housed in a group and displayed no visible signs of distress or pathology. Then, we assessed mouse mechanical threshold from mice implanted compare to those without any implantation and we observed no implantation related deficits (*Figure 56*). Furthermore, we verified cannula placement for the RMg implantation (as well as vlPAG implantation; *Figure 56D-E*) in the same time as we do viral expression verification (as described above) and for the spinal placement, we performed, in addition to mechanical threshold assessment, *in vivo* electrophysiological recording from the spinal cord segment in which we implanted our cannula (lumbar segment L4) and confirmed that dorsal horn neurons in that region had a receptive field on the plantar surface of the ipsilateral hind paw.

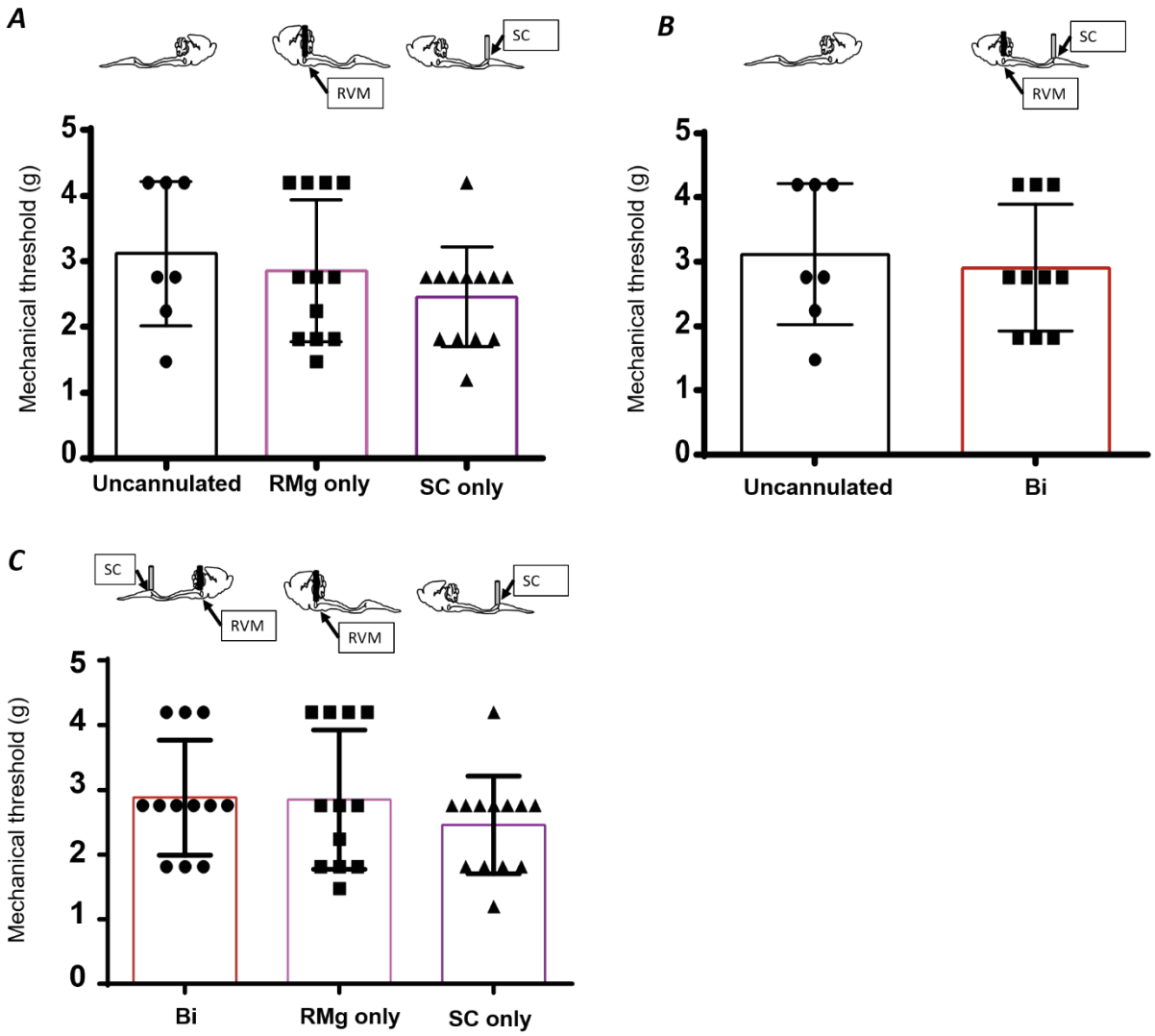

Fibres Locations above the RMg or the spinal cord of 5-HT cre mice

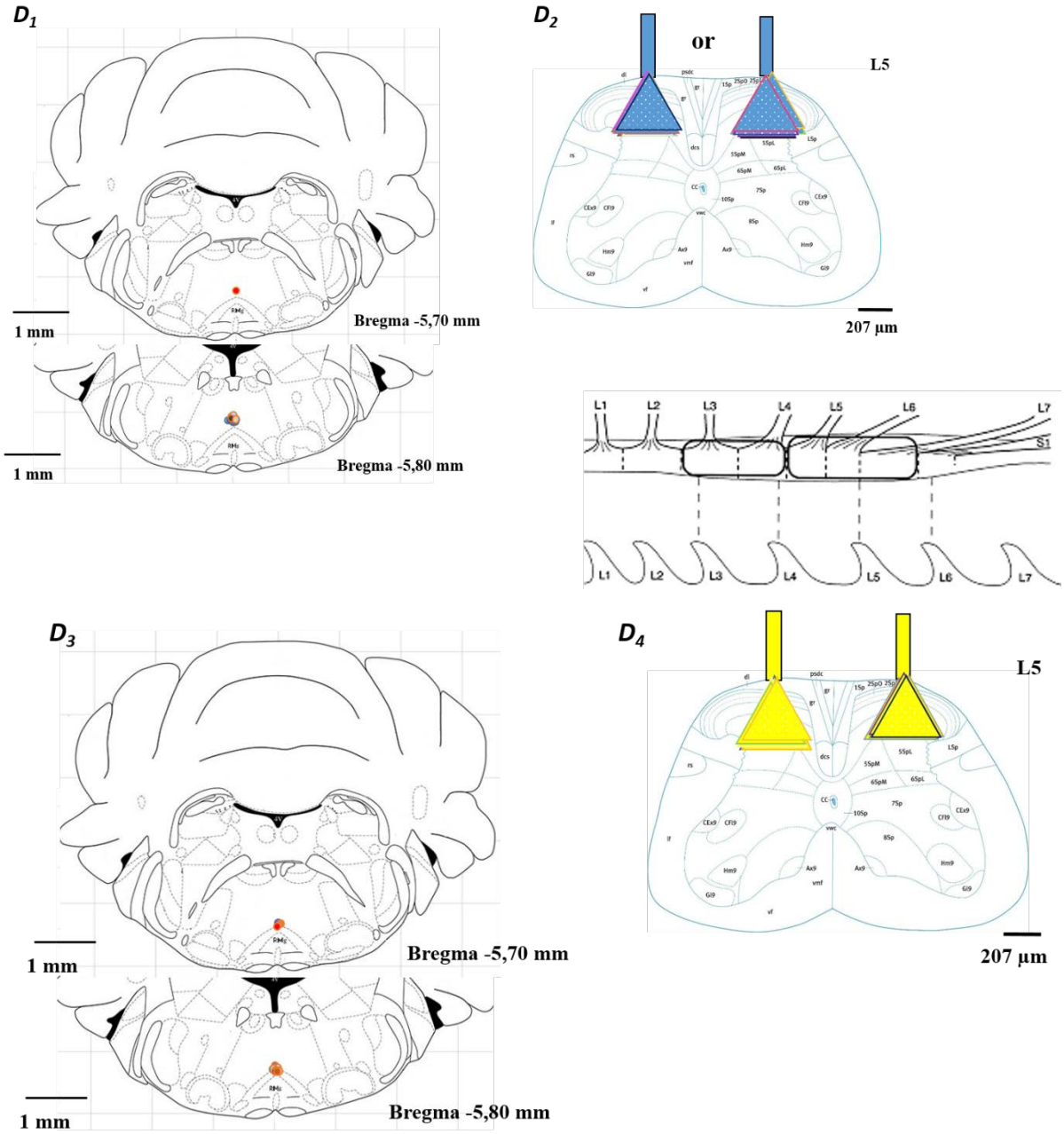

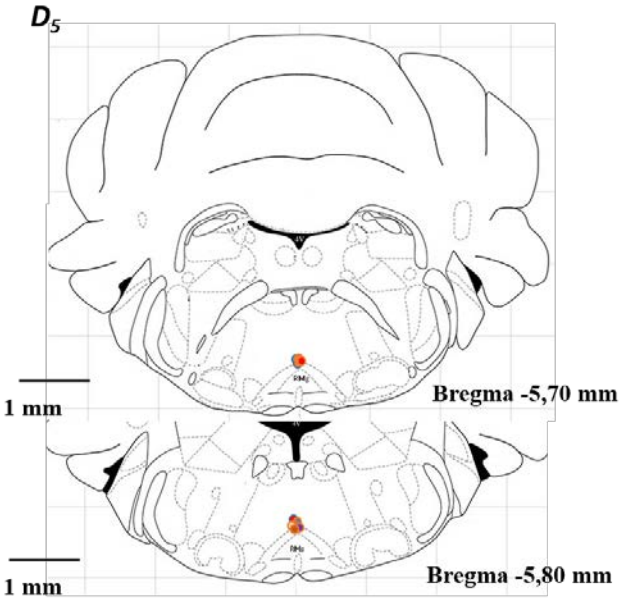
D5
1 mm
Bregma -5,70 mm
1 mm
Bregma -5,80 mm

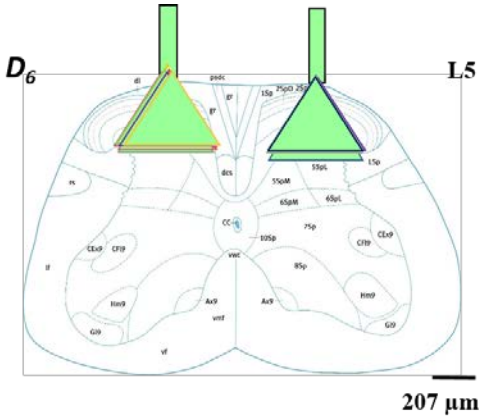
D6
L5
207 µm

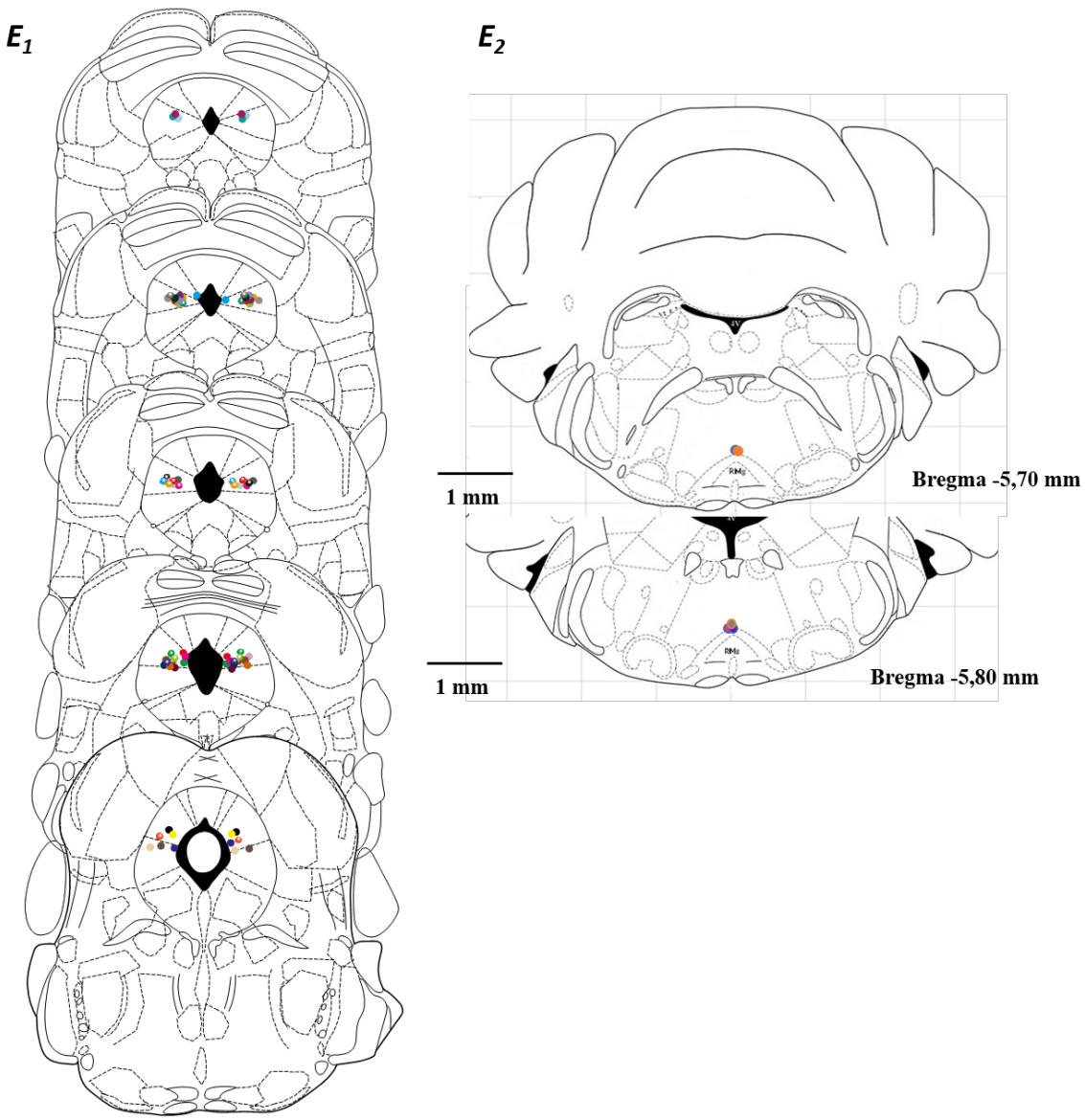

Figure 56 : Mechanical assessment of the different optical fibre implantation strategy. To determine if our implantation strategy induces any modification on the pain assessment, we compared the mechanical threshold from uncannulated animals to those with both cannula mono-implantation (RMg or spinal SC only) and cannula bi-implantation (RMg and SC) animals. Then, we observed no difference in the mechanical threshold between uncannulated animals and RMg implanted animal and SC implanted animal (Kruskal-Wallis test from 7 uncannulated animals, 12 RMg implanted animals and 13 SC implanted animals, p=0.4706, K=1.508, A) as well as no difference of the mechanical threshold between in both uncannulated animals and RMg-SC implanted animals (Mann-Whitney test from 7 uncannulated animals, 10 RMg-SC implanted animals, p=0.7468, U=31.5, B) as well as for bi-implanted animals compared to RMg implanted animals or SC implanted animals (Kruskal-Wallis test from 12 bi-implanted animals, 12 RMg implanted animals and 13 SC-implanted animals, p=0.5307, K=1.267, C). Bi, bi-implanted animal both RMg and SC, RMg only, RMg-implanted animals and SC only, spinal cord-implanted animals. (D) Schematic representation after verification of optical fibres location above the RMg or the spinal cord of 5-HT cre mice expressing ChR2 (D1-2) or ArchT (D3-4) or GFP (D5-6). (E) Schematic representation after verification of optical fibres location above the vlPAG (E1) or the RMg (E2) of SOM-IRES-cre mice expressing AAV inducible virus in the vlPAG.

III. RESULTS

A. MODULATION OF DESCENDING 5-HT NEURONS OF THE RMg ON SPINAL NOCICEPTIVE TRANSMISSION IN PHYSIOLOGICAL CONDITION

1. Consequences of optogenetic manipulation of 5-HT neurons in acute pain

a) *Inhibition of RMg 5-HT neurons induces mechanical hyperalgesia, mechanical allodynia and thermal hyperalgesia*

First, to establish the functional role of the 5-HT neurons of the RMg (RMg 5-HT) on the spinal nociceptive transmission, in freely moving 5-HT cre mice, optogenetic inhibition with ArchT opsin were performed using an optical cannula above the RMg or above the dorsal horn of the spinal cord (as described in the methods). We observed that optogenetic inhibition with green laser light (526.5nm, continuous green activated light for 2 min, 10mW) of RMg 5-HT neurons or RMg 5-HT descending fibres elicited a significant decrease in mechanical threshold and thermal latency that was suppressed after light switched off (*Figure* 56). Indeed, optogenetic inhibition with continuous green light of both 5-HT neurons or 5-HT descending fibres elicited a substantial decrease in mechanical threshold (Von Frey SUDO *Figure 56A1*, ArchT-5-HT, Friedman test $p<0.0001$, $F=19.86$; $n=12$ and ArchT-5-HT descending fibres, Friedman test $p<0.0001$, $F=21.41$; $n=10$) including a significant increase in the percentage of hind-paw responses to repeated normally innocuous stimuli (Repeated measure, *Figure 56*A2, ArchT-5-HT, Friedman test $p<0.0001$, $F=19.60$; $n=12$ and ArchT-5-HT descending fibres $p<0.0001$, $F=20.36$; $n=12$) revealing a mechanical allodynia and hyperalgesia that was suppressed after light switched off. By contrast, green light in both RMg 5-HT expressing GFP tag only (GFP-5-HT) or RMg 5-HT GFPpositive descending fibres did not change the mechanical threshold (Von Frey SUDO *Figure 56B1*, GFP-5HT, Friedman test $p>0.9999$, $F=0.6667$; $n=6$ and GFP-5-HT descending fibres, p=approximate close to 1; $n=10$; Repeated measure *Figure 61B2*, GFP-5-HT Friedman test $p=0.9095$, $F=0.4211$; $n=7$ and GFP-5-HT descending fibres $p>0.9999$, $F=1$; $n= 8$).

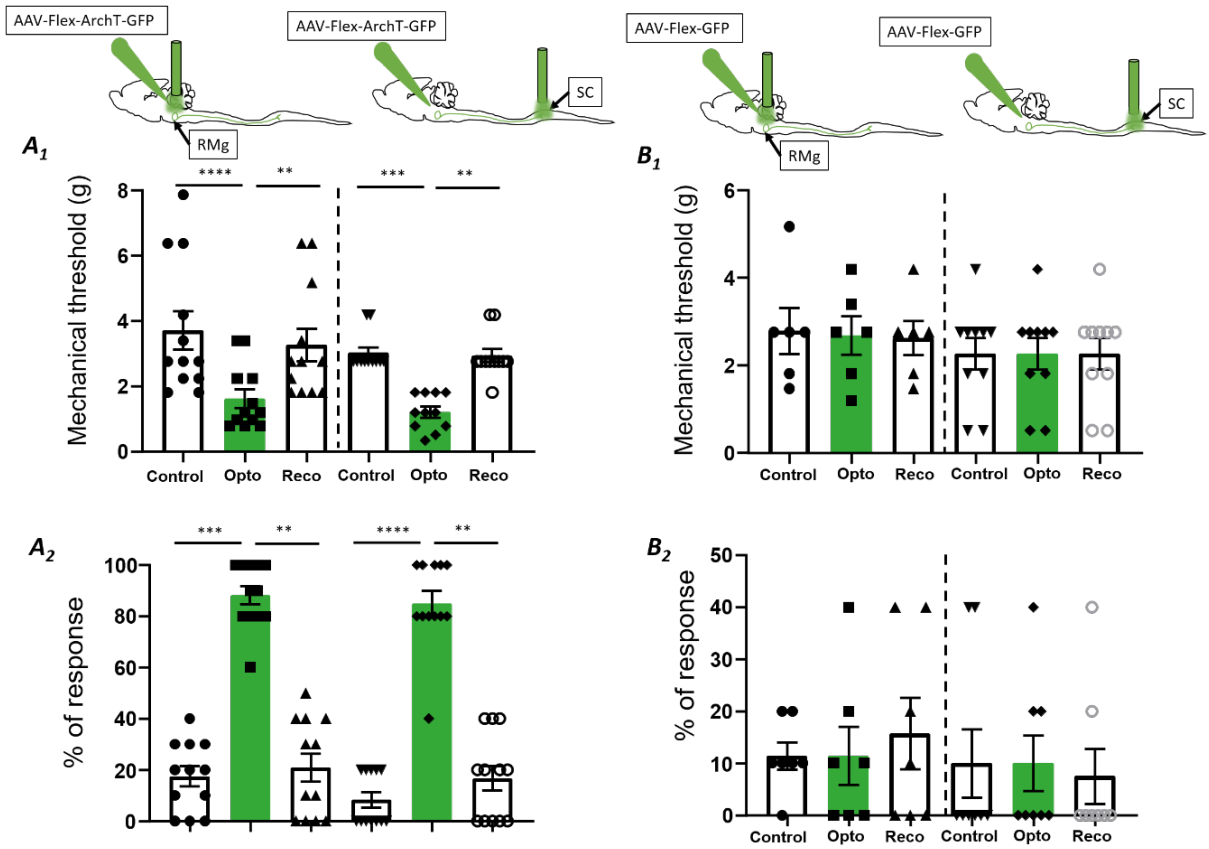

*Figure 57 : Mechanical assessment of 5-HT inhibition both at the level of RMg and spinal cord (SC): Optogenetic inhibition of ArchT-5-HT or ArchT-5-HT descending fibres in the spinal cord with continuous green light during 2 min induced a relevant decrease in mechanical threshold (A1, SUDO for ArchT-5-HT: 3.7 ± 0.6g before, 1.6±0.3g during and 3.3±0.5g post-stimulation; for ArchT-5-HT descending fibres: 3.0±0.2g before, 1.2±0.2g during and 2.9±0.2g post-stimulation) including an increase in the percentage of hind-paws response to repeated innocuous stimuli (A2, Repeated measure for ArchT-5HT: 17.5±3.9 % before, 88.3±3.7% during and 20.8±5.6% of response post-stimulation; for ArchT-5-HT descending fibres: 8.3±3% before, 85±5% during and 16.7±4.8% of response post-stimulation) resulting in to mechanical allodynia and hyperalgesia. On contrary, in control group expressing GFP alone optogenetic stimulation of GFP-5-HT neurons of the RMg (GFP-5-HT) or GFP-5-HT descending fibres in the spinal cord with continuous green light during 2 min induced no change in mechanical threshold (B1, SUDO, GFP-5-HT: 2.8±0.5g before, 2.7±0.4g during and 2.6±0.4g post-stimulation and for GFP-5-HT descending fibres: 2.3±0.4g before, 2.3±0.4g during and 2.3±0.4g post-stimulation; B2, Repeated measure with innocuous stimuli, GFP-5-HT: 11.4±2.6% before, 11.4±5.5% during and 15.7±6.9% of response post-stimulation and GFP-5-HT descending fibres: 10±6.5% before, 10±5.3% during and 7.5±5.3% of response post-stimulation). Measures are reported as mean ± SEM; A1, SUDO ArchT-5-HT of RMg **=p=0.0062, ****= p<0.0001 and ArchT-5-HT descending fibres SC **=p=0.0013, ***=p=0.0006; A2, Repeated Measure ArchT-5-HT of RMg **=p=0.0015, ***=p=0.0001 and ArchT-5-HT descending fibres SC **=p=0.0022 and ****=p<0.0001 from Dunn's post hoc test.*

We observed that optogenetic inhibition of both RMg 5-HT or RMg 5-HT descending fibres elicited a significant decrease in thermal latency resulting in thermal hyperalgesia (*Figure 58A*, Plantar test ArchT-5-HT, Friedman test p<0.0001, F=15.2; n=10 and ArchT-5-HT descending fibres, Friedman test p=0.0023, F=12.17; n=12) compare to optogenetic

manipulation fo RMg 5-HT neurons or descending fibres where no modification in thermal latency was observed (*Figure 58B*, Plantar test GFP-5-HT Friedman test p=0.4645, F=2; n= 5 and GFP-5-HT descending fibres, Friedman test p= 0.6539, F= 1.086; n=9).

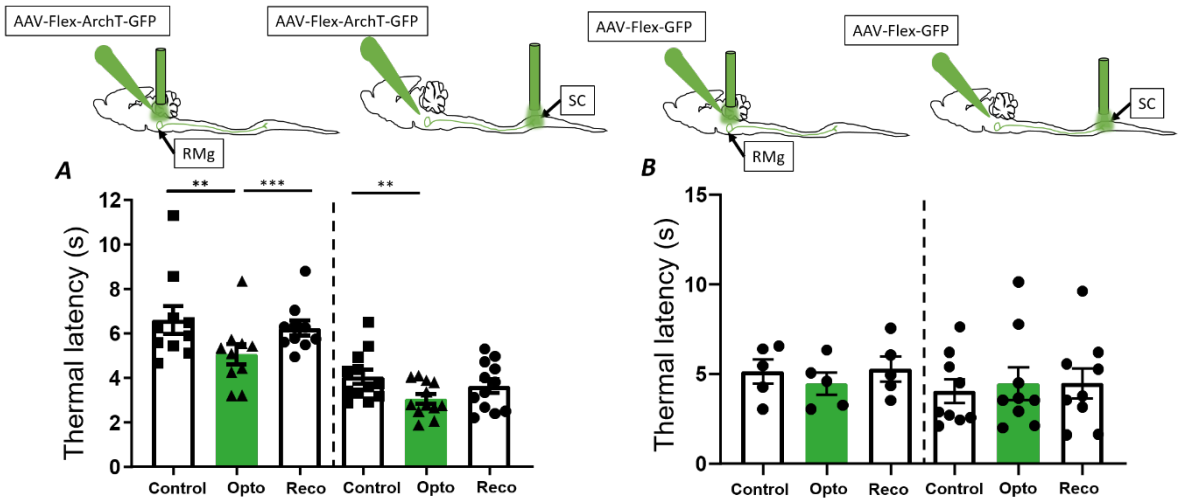

*Figure 58 : Thermal assessment of 5-HT inhibition both at the level of RMg and spinal cord (SC): Optogenetic inhibition of ArchT-5-HT or ArchT-5-HT descending fibres in the spinal cord with continuous green light during 2 min induced a relevant decrease in thermal latency (A, Plantar test, ArchT-5-HT: 6.6±0.6s before, 5.1±0.5s during and 6.2±0.3s post-stimulation and ArchT-5-HT descending fibres: 4.0±0.3s before, 3.1±0.2s during and 3.6±0.3s post-stimulation) resulting in thermal hyperalgesia. On contrary, in control group expressing GFP alone optogenetic stimulation of GFP-5-HT or GFP-5-HT descending fibres in the spinal cord induced no change in thermal latency (B, plantar test, GFP-5-HT: 5.1±0.7s before, 4.5±0.6s during and 5.3±0.7s post-stimulation and GFP-5-HT descending fibres: 4.1±0.7s before, 4.5±0.9s during and 4.5±0.8s post-stimulation). Measure are reported as mean ± SEM; A, ArchT-5-HT of RMg **=p=0.0035, ***=p=0.0007 and ArchT-5-HT descending fibres SC **=p=0.001 from Dunn's post hoc test.*

Consequently, inhibition of 5-HT neurons of the RMg leads to descending facilitation of pain transmission which let us hypothesise that within the RMg, 5-HT neurons are tonically active and may exert a tonic inhibition on the spinal transmission. Thus, to verify our hypothesis, we assessed whether 5-HT activation modulates spinal transmission.

b) *Activation of RMg 5-HT neurons induces mechanical and thermal analgesia*

As for 5-HT inhibition, in freely moving 5-HT cre mice micro-injected in the RMg with ChR2 opsin, optogenetic activation with 475nm blue activating light at 5Hz/5ms, 10mW of 5-HT neurons of the RMg (ChR2-5-HT) or their descending fibres above the spinal cord (ChR2-5-HT descending fibres) elicited a significant increase in both mechanical threshold and thermal latency and return to baseline after light switched off (*Figure 59*). For SUDO *Figure*

59A1, RMg 5-HT Friedman test p<0.0001, F=28.93; n=17, RMg 5-HT descending fibres, Friedman test p<0.0001, F=49.73; n=27 and for Repeated measure, *Figure 59A2*, ChR2-5-HT, Friedman test p<0.0001, F=30.18; n=18 and ChR2-5-HT descending fibres, p<0.0001, F=47.2; n=26.

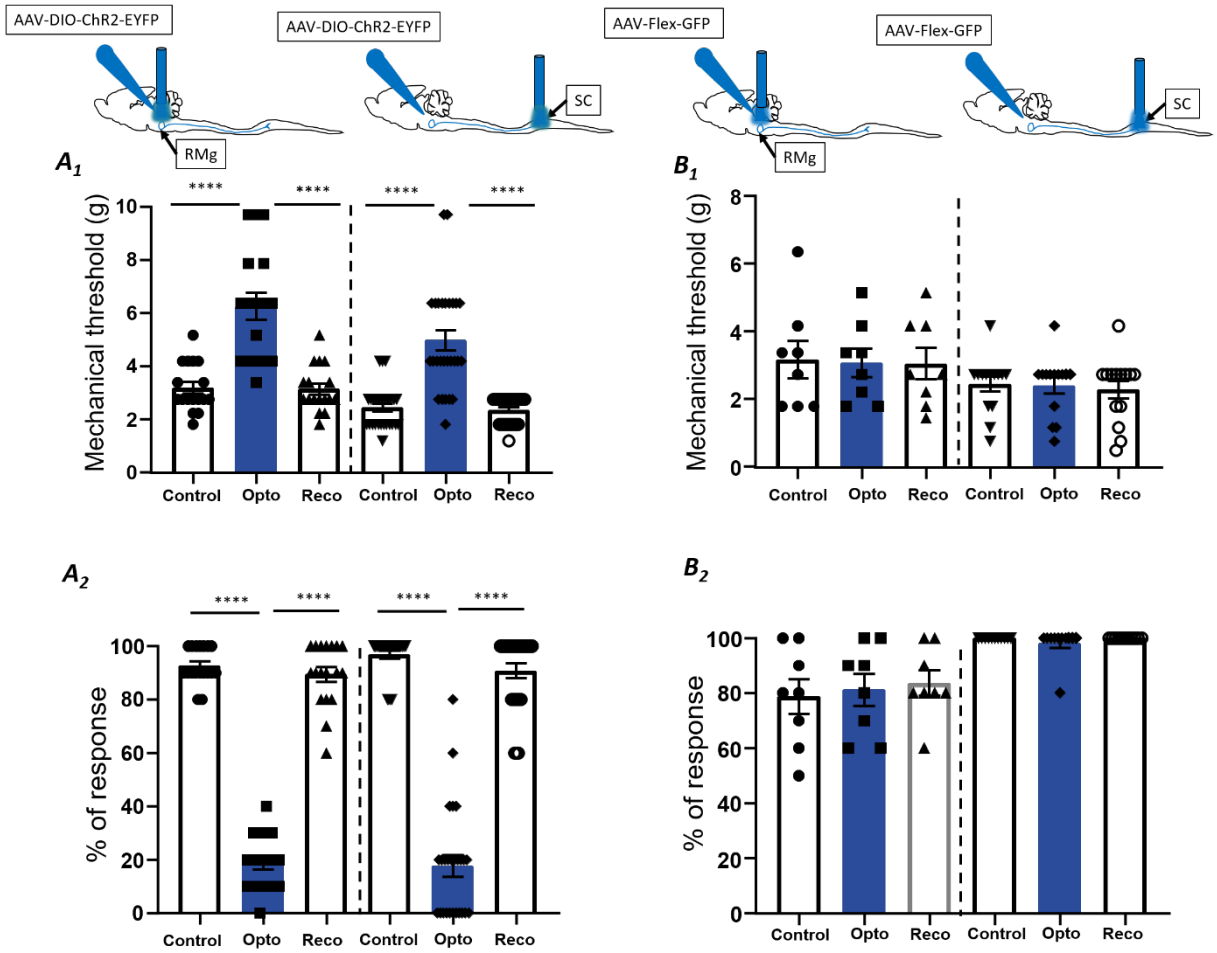

*Figure 59 : Mechanical assessment of 5-HT activation both in RMg and spinal cord (SC): Optogenetic activation of ChR2-5-HT neuron or ChR2-5-HT descending fibres (A1,B2) in the spinal cord with 475nm blue activating light at 5Hz5ms during 2 min induced a relevant increase in mechanical threshold (A1, SUDO, ChR2-5-HT: 3.2±0.2g before, 6.3±0.5g during and 3.2±0.2g post-stimulation; for ChR2-5-HT descending fibres: 2.4±0.2g before, 5±0.4g during and 2.4±0.1g post-stimulation; A2, Repeated measure with noxious stimuli in % of response, ChR2-5-HT: 92.8±1.6% before, 18.9±2.4% during and 89.4±2.7 post-stimulation and ChR2-5-HT descending fibres: 96.9±1.4% before, 17.7±4.1% during and 90.8±2.8% of response post-stimulation) resulting then in mechanical analgesia. On contrary, in control group expressing GFP alone optogenetic stimulation of GFP-5-HT or GFP-5-HT descending fibres in the spinal cord with blue activating light at 5Hz5ms during 2 min induced no change in mechanical threshold (B1, SUDO, GFP 5-HT: 3.2±0.6g before, 3.1±0.4g during and 3.1±0.5g post-stimulation and GFP-5-HT descending fibres: 2.5±0.2g before, 2.4±0.2g during and 2.3±0.3g post-stimulation; B2, Repeated measure with noxious stimuli in % of response, GFP-5-HT: 78.8±6.4% before, 81.3±5.8% during and 83.8±4.6 and GFP-RMg descending fibres: 100±0% before, 98.2±1.8% during and 100±0 post-stimulation). Measures are reported as mean ± SEM; A1, SUDO RMg ****=p<0.0001 and SC ****= p<0.0001; A2, Repeated Measure ChR2-5-HT of RMg ****=p<0.0001 and ChR2-5-HT descending fibres SC ****= p<0.0001 from Dunn's post hoc test.*

With regard to thermal latency (*Figure 60*), using plantar test, we observed that optogenetic activation of 5-HT neurons of the RMg (Plantar test *Figure 60A*, Friedman test p<0.0001, F=16.91; n=11 for ChR2-5-HT) or 5-HT descending fibres (Plantar test *Figure 60A*, Friedman test p<0.0001, F=39.93; n=28 for ChR2-5-HT descending fibres) induced a relevant increase in thermal latency resulting in a thermal analgesia.

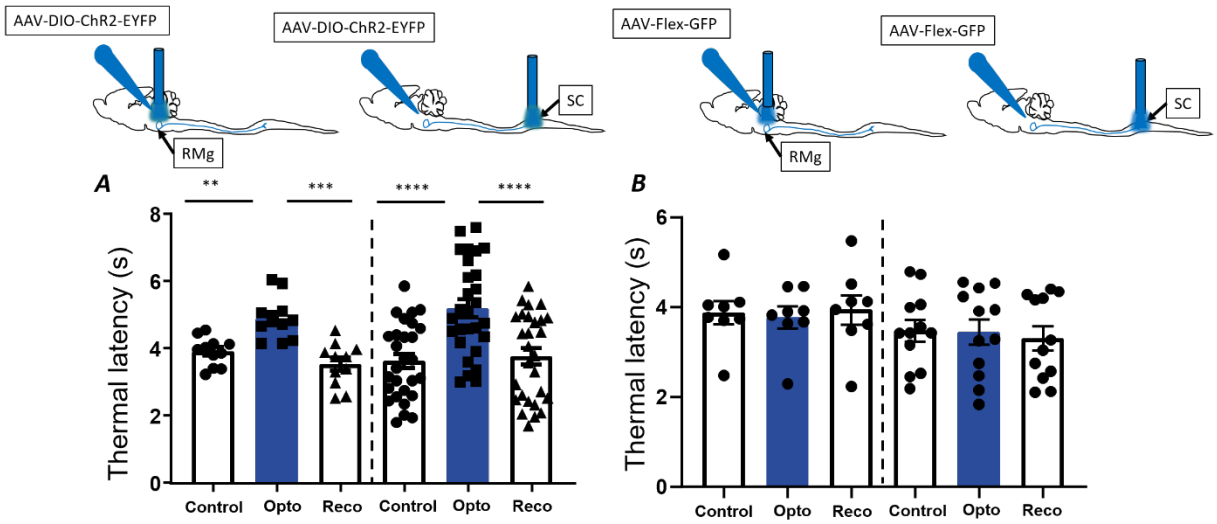

*Figure 60 : Thermal assessment of 5-HT activation above RMg or above dorsal horn spinal cord (SC): Optogenetic activation of ChR2-5-HT neurons or ChR2-5-HT descending fibres with 475nm blue activating light at 5Hz5ms during 2 min induced a relevant increase in thermal latency resulting in a thermal analgesia (A, Plantar test, ChR2-5-HT: 3.9±0.1s before, 4.9±0.2s during and 3.6±0.2s post-stimulation and ChR2-5-HT descending fibres: 3.6±0.2s before, 5.2±0.3s during and 3.8±0.2s post-stimulation). On contrary, in control group expressing GFP alone optogenetic stimulation of GFP-5-HT or GFP-5-HT descending fibres in the spinal cord induced no change in thermal latency (B, Plantar test, B, GFP-5-HT: 3.9±0.3s before, 3.8±0.2s during and 3.9±0.3s post-stimulation and GFP-5-HT descending fibres: 3.5±0.2s before, 3.4±0.3s during and 3.3±0.3s post-stimulation). Measure are reported as mean ± SEM; A, ChR2-5-HT of RMg **=p=0.0028, ***= p=0.0002 and ChR2-5-HT descending fibres SC ****=p<0.0001 from Dunn's post hoc test.*

Therefore, as we hypothesise, 5-HT neurons of the RMg exert a direct tonic descending inhibition on pain transmission resulting in an increase in both mechanical and thermal analgesia.

2. Consequences of optogenetic manipulation of 5-HT neurons on dorsal horn neurons.

To go further in our understanding of descending inhibitory effects mediated by RMg 5-HT, we sought to determine the spinal targets of RMg 5-HT. Taking into account on one hand, the fact that inhibition of descending 5-HT fibres leads to a mechanical allodynia and mechanical hyperalgesia (considered to be an expression of central sensitization phenomenon in which wide dynamic range neurons (WDRs) are supposed to be involved) and on the other

hand the presence of 5-HT fibres mostly in deep layer of the spinal dorsal horn where the density of WDR is more important, we therefore hypothesize that WDRs, which received inputs from low-velocity C fibres and are mainly second-order neurons of the spinal cord, are modulated by 5-HT descending neuron.

a) *RMg 5-HT neurons modulation modify WDRs integration property to noxious stimuli*

We first assessed the consequence of inhibition of RMg 5-HT descending fibres on pain transmission in the dorsal horn of the spinal cord (*Figure 61*). In anesthetised 5-HT cre mice expressing ArchT in RMg 5-HT, we performed single-unit electrophysiological recordings of spinal WDRs associated with optogenetic manipulation above the spinal cord with the same light pattern that we used for the behaviour (526.5nm continuous green inhibiting light with power set at 10mW). We observed that optogenetic inhibition of RMg 5-HT projecting to the dorsal horn elicited an increase in both WDR spontaneous activity (*Figure 61A*) and WDR response to nociceptive C fibre input (*Figure 61B*, Ordinary one-way ANOVA $p<0.0001$, $F=11.45$; $n=8$).

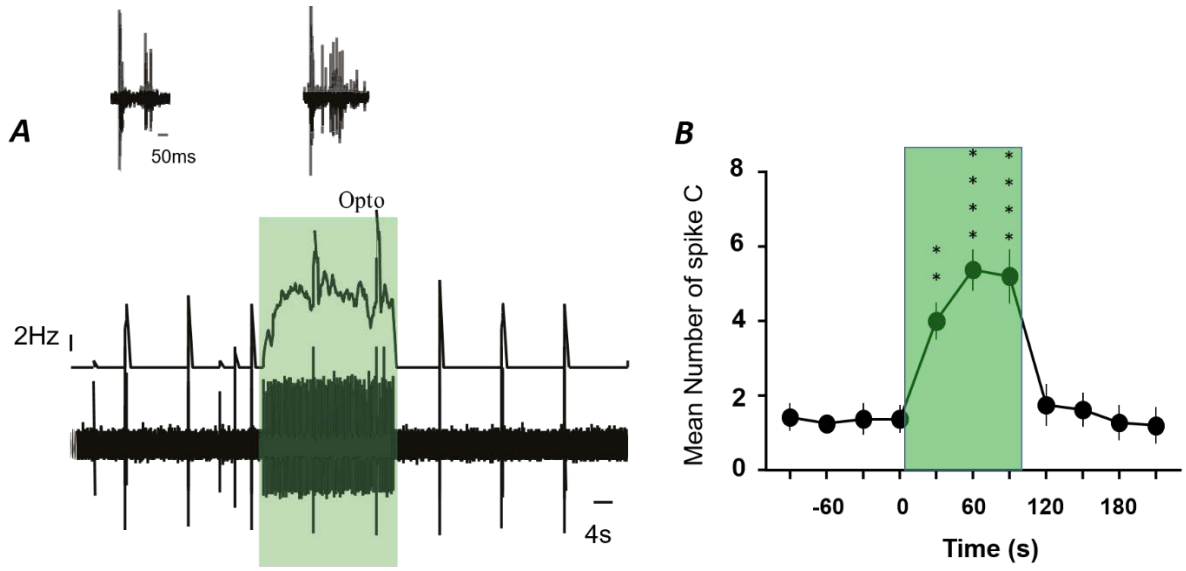

Figure 61 : In vivo single-unit recording of DHNs associated with optogenetic inhibition of 5-HT neuron of the RMg projecting to the dorsal horn of the spinal cord. A) one sample showing an increase of DHN response to noxious stimuli as well as an increase in DHN spontaneous discharge during optogenetic inhibition of Archt-5-HT descending fibres (above, representative WDR neuron response to noxious electrical stimuli recorded before and during optogenetic stimulation). B) Mean number DHNs responses to C-fibre input is increased during optogenetic stimulation of Archt-5-HT descending fibres (mean number of

*C-spike before 1.4±0.6, during 4.9±0.6 and after 1.5±0.5). Measure are reported as mean ± SEM; B, Mean number of C spike **= p=0.0021 and ****= p<0.0001 from Dunn's post hoc test.*

By contrast, optogenetic activation of RMg 5-HT descending fibres (475nm blue activating light at 5Hz5ms with power set at 10mW) in 5-HT cre mice expressing ChR2 in RMg 5-HT neurons induced a decrease in WDR response to nociceptive inputs (*Figure 62*, Friedman test p=0.0004, F=28.46; n=14).

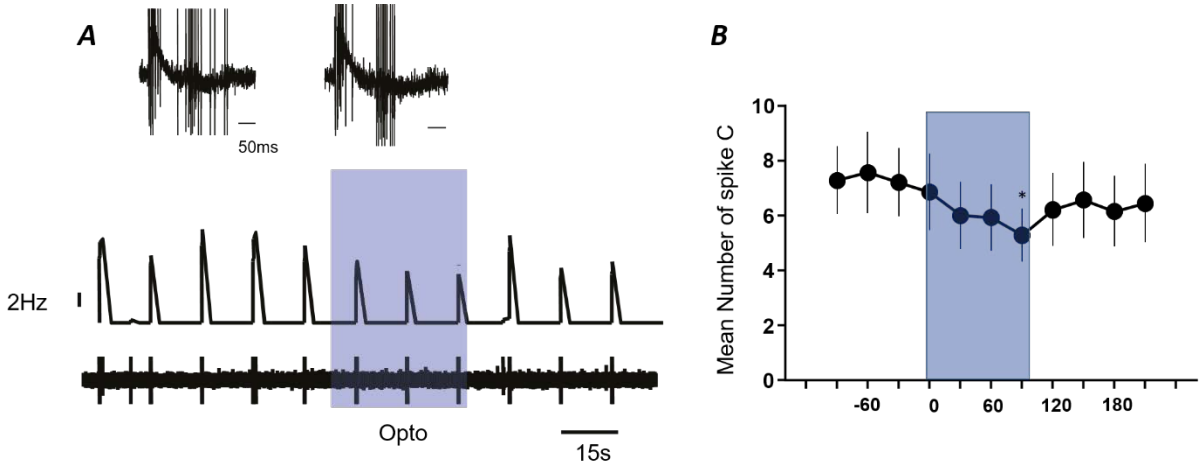

*Figure 62 : In vivo single-unit recording of DHNs associated with optogenetic activation of 5-HT descending fibres into the dorsal horn of the spinal cord. A) One sample showing a decrease of DHN response to noxious stimuli during optogenetic stimulation of ChR2-5-HT descending fibres (above, representative WDR neuron response to noxious electrical stimuli recorded before and during an optogenetic stimulation). B) Mean number DHNs responses to C-fibre input is decreased during optogenetic activation of ChR2-5-HT descending fibres (mean number of C-spike before 7.4±1.3, during 6.0±1.2 and after 6.3±1.3). Measure are reported as mean ± SEM; B, Mean number of C spike *= p=0.0373 from Dunn's post hoc test.*

Furthermore, we observed that optogenetic manipulation of RMg 5-HT descending fibres modified the sensitization properties of DHN (*Figure 63*). Indeed, by focusing on the WDR ability to express a Windup, which results in a progressive increase in WDR response to low frequency repetitive electrical stimulation of C-fibres with the same intensity, we observed that optogenetic inhibition of the RMg 5-HT descending fibres increased the windup coefficient (see methods; Two-tailed *t.test* p=0.0156, W=28; n=7 DHN), and optogenetic activation of the RMg 5-HT descending fibres decreased the windup coefficient (Two-tailed *t.test* p=0.0339; W=-60; n=13 DHN).

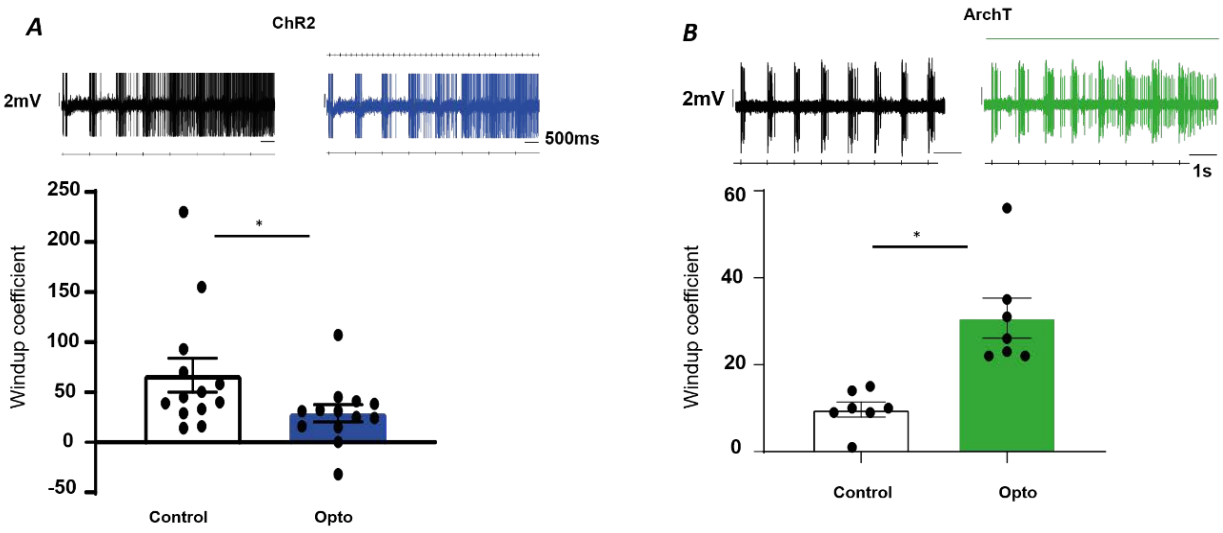

*Figure 63 : Consequence of optogenetic modulation of 5-HT descending fibres on the DHN windup. A-B) Above, one sample showing a decrease (A) or an increase (B) of DHN response resulting from repeated electrical C-fibres activation at 1Hz before and during optogenetic activation (in blue) or inhibition (in green). A) Optogenetic activation of 5-HT descending fibres resulted in a decrease of the windup coefficient (mean number of C-spike before 67.1±17.1 and during 28.7±8.6), (B) while optogenetic inhibition resulted in an increase of the windup coefficient (mean number of C-spike before 9.7±1.7 and during 30.7±4.6). Measure are reported as mean ± SEM; ChR2-5-HT, *=p= 0.0339 and ArchT-5-HT, *=p=0.0156 from Wilcoxon matched-pairs signed-rank test.*

Also, as a control of optogenetic stimulation (*Figure 64*), in anesthetised 5-HT cre mice expressing GFP only in RMg 5-HT, we performed single-unit electrophysiological recordings of spinal WDRs associated with light illumination above the spinal cord with the same light pattern that we used for optogenetic activation or inhibition (5Hz5ms at 475nm blue light or continuous green light for at 10mW respectively) and we observed no change in either DHN response to C-fibre activation or DHN windup coefficient.

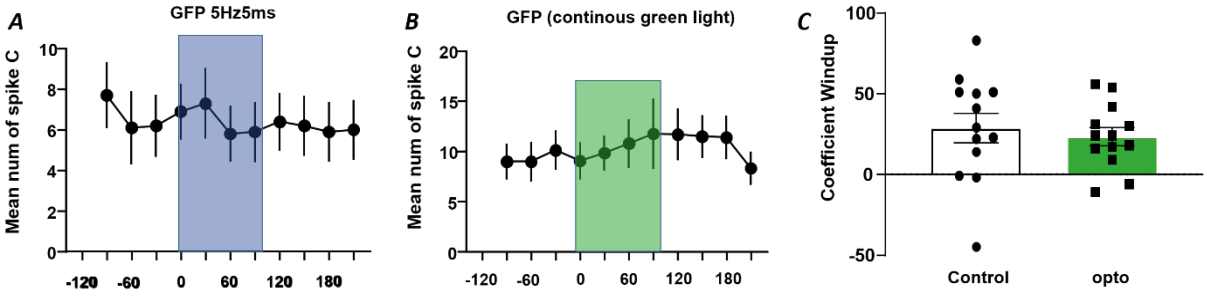

Figure 64 : In vivo single-unit recording of DHNs in 5-HT cre mice expressing GFP in the RMg 5-HT neuron associated with an optogenetic stimulation above the dorsal horn of the spinal cord. Whatever the optogenetic stimulation pattern, no change has been observed both in DHN C-evoked response (A, blue light, Friedman test p=0.3814, F=10.70; n=10 DHN and B, green light, Kruskal-Wallis test p= 0.9894, K=2.593; n=7 DHN) and DHN windup coefficient (C, Wilcoxon matched-pairs signed-rank test p=0.53, n=13 DHN).

Therefore, RMg 5-HT projecting to the dorsal horn, tonically inhibit nociceptive transmission by decreasing WDR excitability resulting from a decrease in WDR response to C-fibres inputs as well as a decrease in sensitization properties.

3. RMg 5-HT inhibitory influence is not gender dependent

Because it has previously been shown that pain integration may be under the influence of gender difference (Mogil and Bailey, 2010) we decided to find out if it was also the case for 5-HT descending pain modulation. Thus, we compared the effect of optogenetic stimulation of 5-HT descending fibres into the dorsal horn both in males and females (*Figure 65*). We observed no sex difference of 5-HT optogenetic stimulation-inducing inhibition on nociceptive transmission in both males and females whatever the modality measured. Indeed, optogenetic activation of 5-HT neurons induced on both male and female an increase in both mechanical threshold (*Figure 65A1*, SUDO, for male Friedman test $p<0.0001$, $F=28.44$ and for female $p<0.0001$, $F=21.41$; $n=16$ and 11 respectively) and thermal latency (*Figure 65A2*, Plantar test, male Friedman test $p<0.0001$, $F=24.47$ and female $p<0.0001$, $F=16.55$; $n=17$ and 11 respectively), resulting in both cases in a mechanical and thermal analgesia. Also WDR excitability was the same in anesthetised males and females. Indeed, optogenetic activation of 5-HT descending fibres induced in both males and females a decrease in DHNs response to noxious stimuli (*Figure 65B*, Friedman test $p=0.0164$, $F=18.73$; $n=11$ male WDR and $p=0.0018$, $F=24.61$; $n=6$ female WDR).

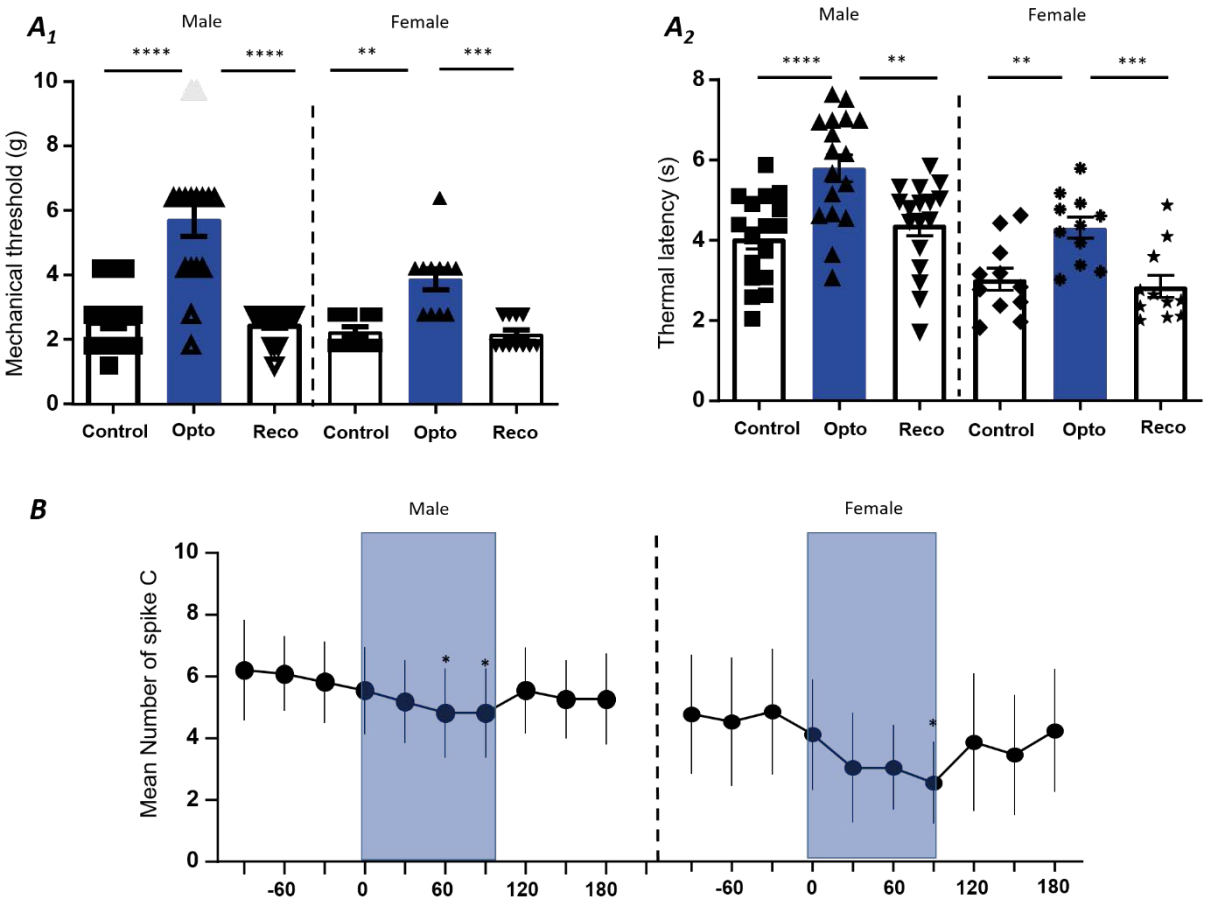

*Figure 65 : Gender do not influence tonic 5-HT-induced inhibition on pain transmission. Optogenetic activation of ChR2-5-HT descending fibres induced in both male and female, a relevant increase in mechanical threshold (A1 for male ChR2-5HT descending fibres: 2.6±0.2g before, 5.7±0.5g during and 2.5±0.1g post-stimulation; for female ChR2-5HT descending fibres: 2.2±0.1g before, 3.9±0.3g during and 2.2±0.1g post-stimulation) and thermal latency (A2 for male ChR2-5HT descending fibres: 4.0±0.3s before, 5.8±0.3s during and 0.3±0.3s post-stimulation; for female ChR2-5HT descending fibres: 3.0±0.3s before, 4.3±0.3s during and 2.9±0.3s post-stimulation). B) With regard to DHN excitability, DHNs C-fibre evoked response is decreased both in male and female during optogenetic stimulation of 5-HT descending fibres (male mean number of C-spike before 6.0±1.4, during 5.1±1.4 and after 5.7±1.5 optogenetic stimulation and female mean number of C-spike 4.8±2.0 before, 3.2±1.6 during and 4±2.1 after optogenetic stimulation; n=11 male DHN and 6 female DHN). Measure are reported as mean ± SEM; SUDO male, ****=p<0.0001 and female **=p<0.01, ***=p<0.001; Plantar test male **=p<0.01, ****=p<0.0001 and female **=p<0.01, ***= p<0.001; Mean number of C spike male *[1]=p=0.004, *[2]=p=0.0218 and female *p=0.0354 from Dunn's post hoc test.*

4. Target of RMg 5-HT neuron on the dorsal horn of the spinal cord

To go further in understanding this mechanism, we next wanted to determine the targets of 5-HT neurons on the dorsal horn microcircuits. We hypothesised that RMg 5-HT neuron inhibitory effect might be mediated through inhibitory neurons. To test this possibility, in Gad67-GFP mice (*Figure 66A1)*, we performed TPH2 immunostaining (*Figure 66A2*) and by

using microscopy image analysis, we observed potential synaptic button of 5-HT fibres onto GABA neurons in deep layer of the dorsal horn of the spinal cord (*Figure 66A3-4* represented in green).

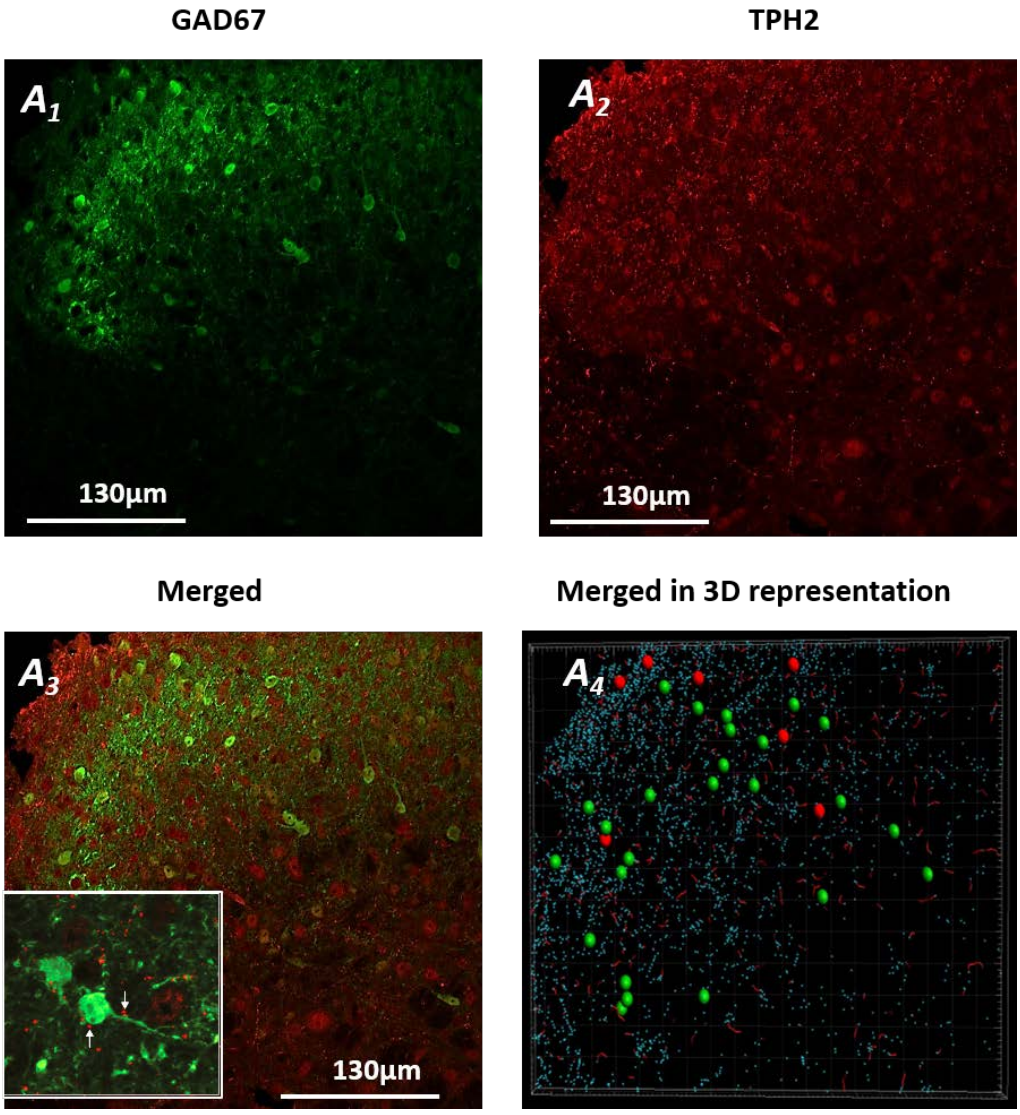

Figure 66 : Confocal image and 3D representation of immunostaining against TPH2 in thin slice of lumbar spinal cord of GAD67 mice. GFP positive neurons (in green) in deep layer of the spinal cord are contacted by TPH2 putative synaptic button (in red, arrow). 3D reconstruction of GAD 67/ TPH2 merged confocal image (A4), green sphere corresponding to TPH2 putative synaptic button close to GFP positive neuron and red sphere those far from GFP67 positive neuron.

To confirm these connections to the local inhibitory network, we compared, in 5-HT cre mice injected with AAV-CAG-FLEX-GFP, appositions between GFP staining and excitatory (TLX3) or inhibitory (PAX2) neurons and we found that 5-HT fibres are substantially more in apposition with inhibitory interneurons (*Figure 67*C, unpaired Two-tailed *t test* $p<0.0001$; n=10 for Pax2 and 9 for Tlx3).

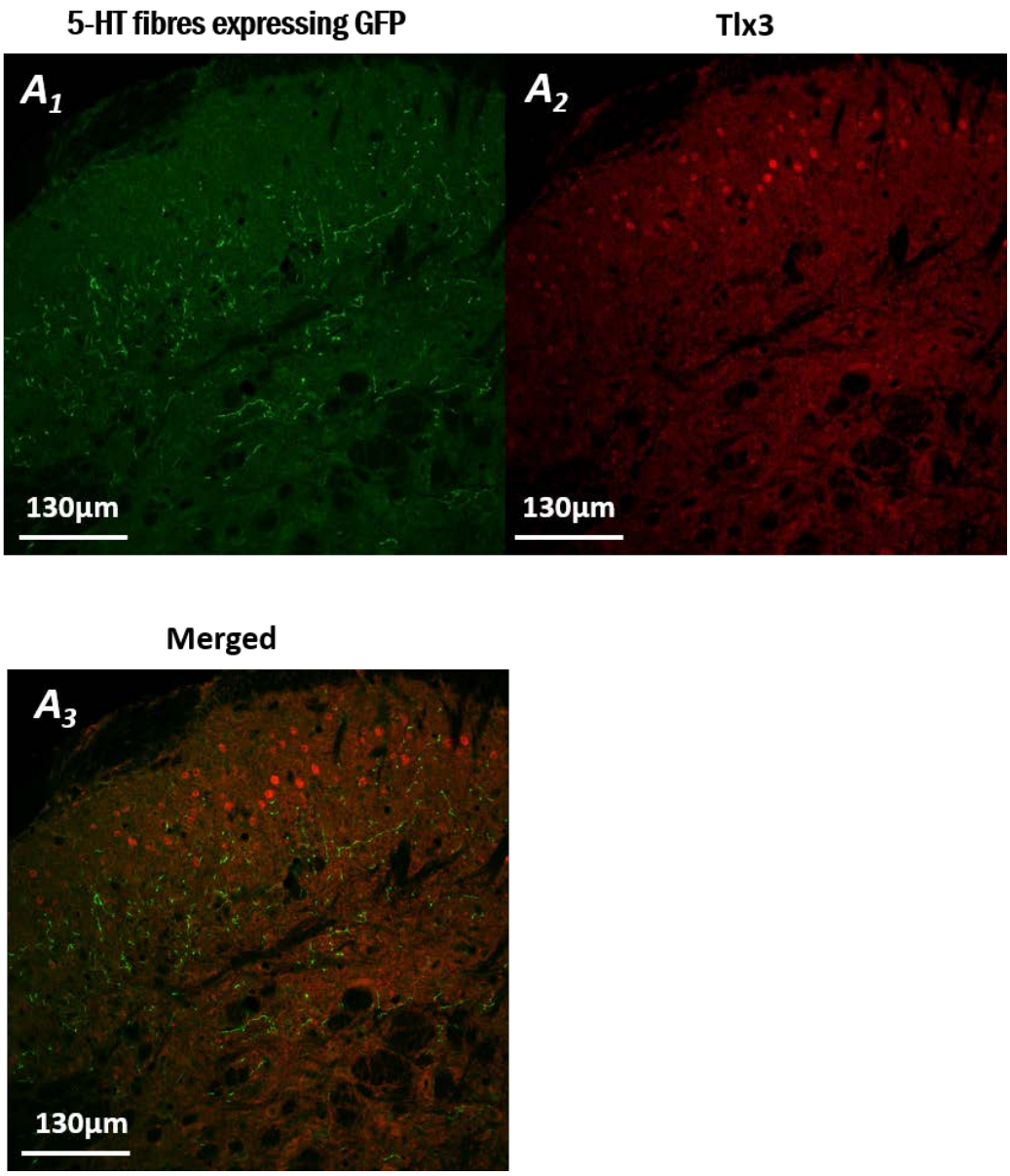
5-HT fibres expressing GFP
Tlx3
A1
A2
130µm
130µm
Merged
A3
130µm

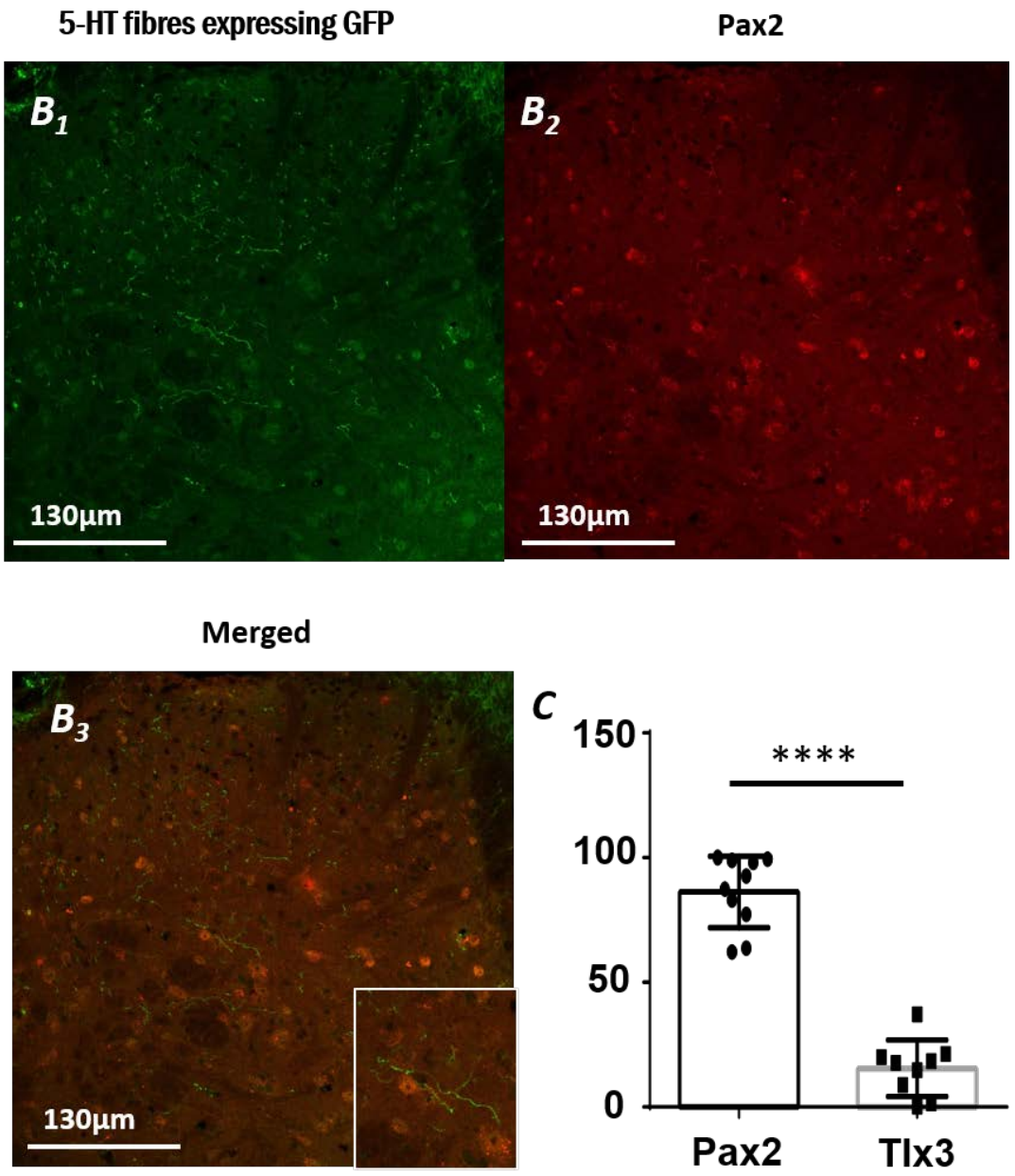

Figure 67 : Confocal image and 3D representation of AAV-flex-GFP expression in 5-HT descending fibres in combination with Tlx3 and Pax 2 staining in thin slice of the lumbar spinal cord of 5-HT cre mice. A1-3) Tlx3 excitatory marker immunostaining (red) showed superficial cell body that is not contacted by GFP fibres. B1-3) Pax2 inhibitory marker immunostaining (red) showed cell body in the dorsal horn of the spinal cord that is contacted with GFP fibre (green) from 5-HT neurons of the RMg. C) imaris 3D reconstruction allow quantification of contacts between cell bodies and fibres. Proportions of cell bodies contacted by GFP fibres on the total amount of cell bodies are plotted for Pax2 and Tlx 3 respectively. Proportions are substantially higher for Pax2 than for Tlx3 (82.23% for Pax2 and 15.49% for Tlx3, unpaired Two-tailed T.test p<0.0001.

Then, in order to determine if real synaptic contacts are present between RMg 5-HT and inhibitory neurons, we used Gad67-GFP*5-HTcre mice in which SynMYC-rev-WPRE was expressed 5-HT RMg 5-HT. into the RMg, we performed immunostaining in the dorsal horn of

the spinal cord of SynMyc together with GFP or parvalbumin *(Figure 68A and B)* and we found synaptic buttons of 5-HT fibres onto GABA and parvalbumin neurons.

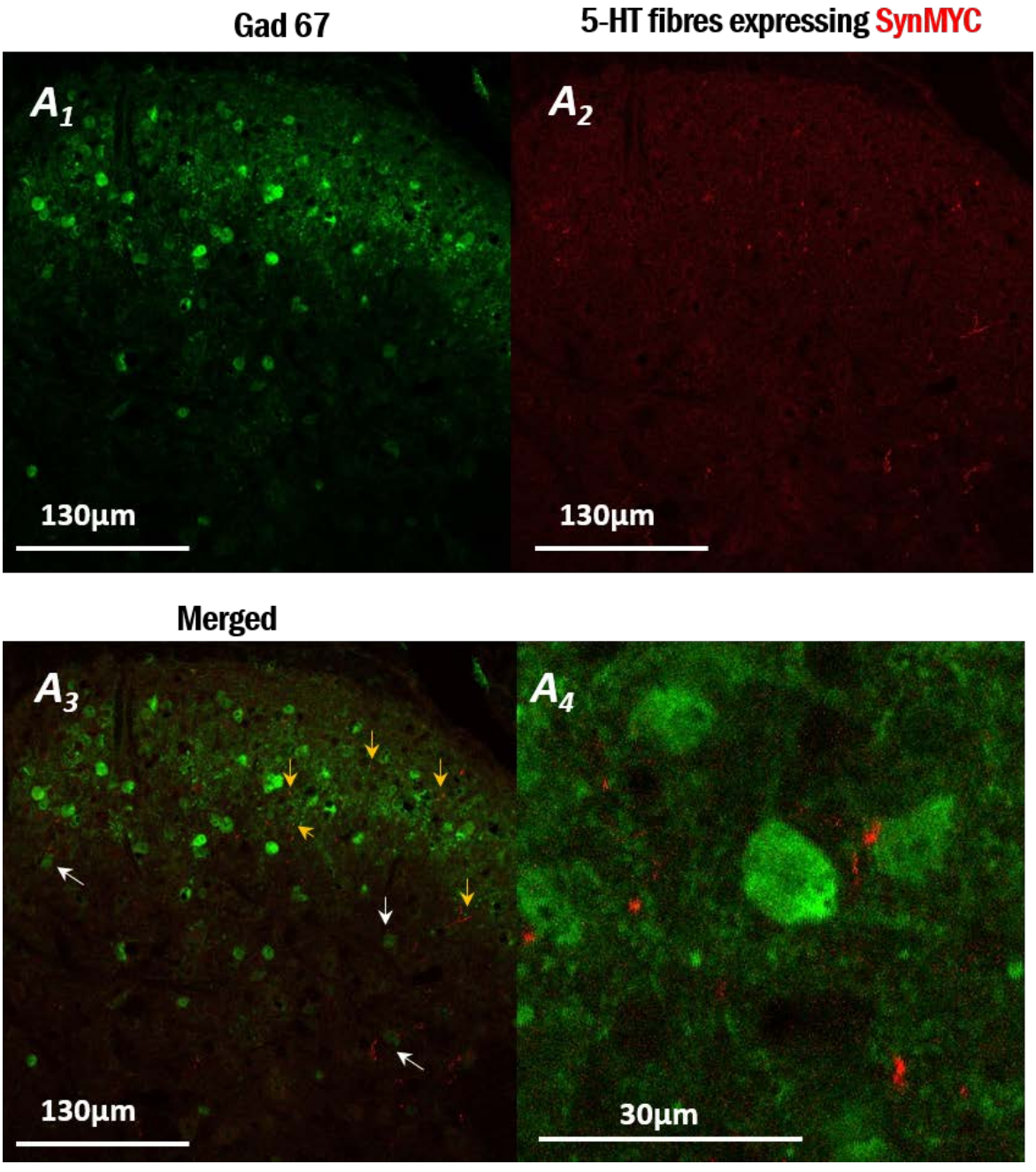

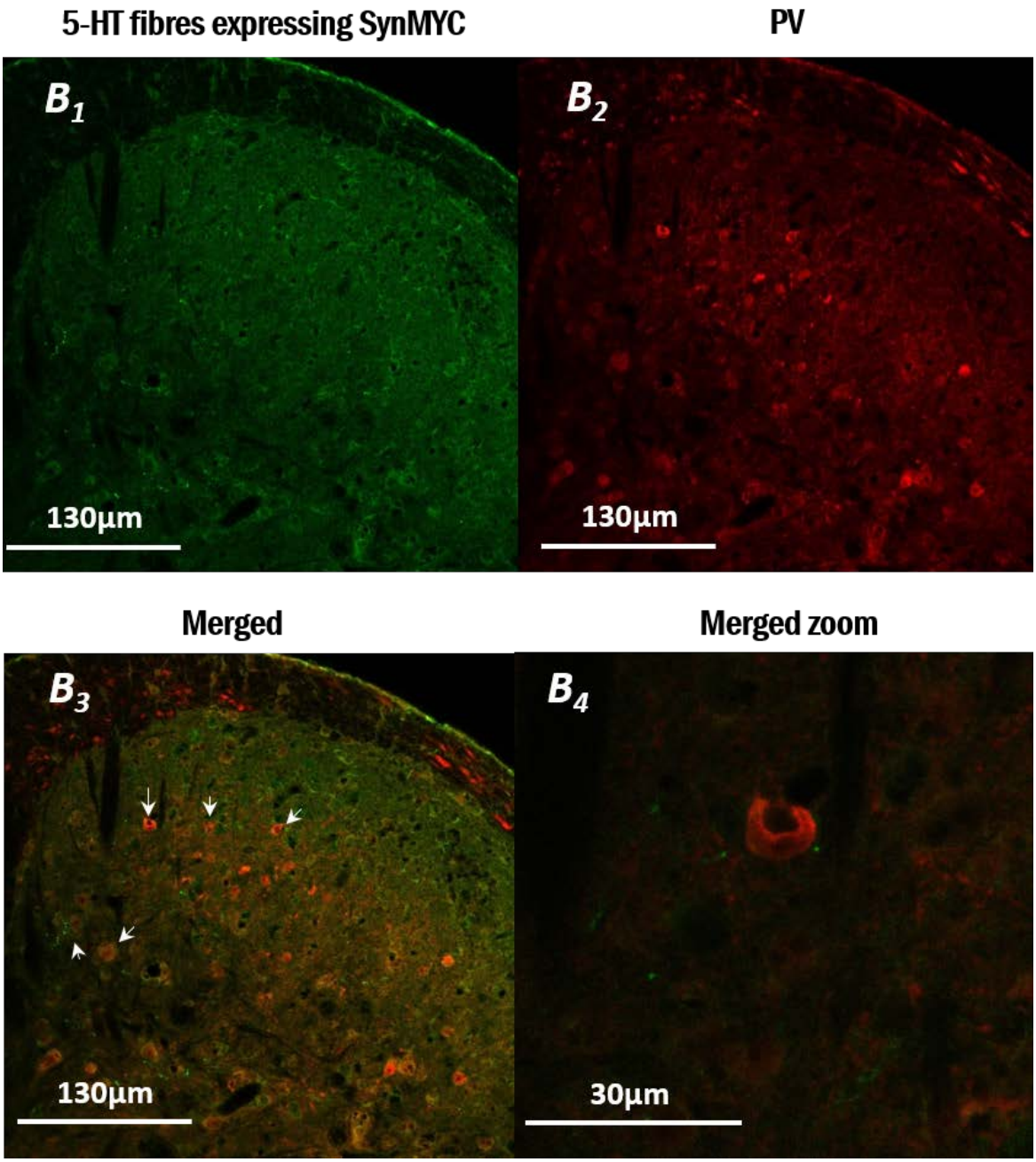

*Figure 68 : Confocal image of AAV-CAG-floxed-SynMYC-rev-WPRE expression (revealed in red for A1-3 and in green for B1-3) in 5-HT neurons of the RMg projecting to the dorsal horn in combination with Gad67 and Parvalbumin (PV) staining in thin slice of lumbar spinal cord of both Gad67-GFP*5-HTcre (A) and 5-HT cre mice (B). A1-4) Gad67-GFP positive staining (green) showed cell body (white arrow) and fibres (orange arrow) that are contacted by 5-HT synaptic buttons (in red). B1-4) PV immunostaining (red) showed mainly cells bodies in deep layer dorsal horn of the spinal cord that are contacted by 5-HT synaptic buttons (green).*

Thus, it can be concluded that the tonic descending inhibitory action of 5-HT neurons of the RMg on nociceptive pain transmission passes through the inhibitory interneuron of the spinal cord dorsal horn.

a) *RMg 5-HT descending inhibition on pain transmission is mediated by dorsal horn inhibitory interneurons.*

To verify this hypothesis, we performed optogenetic stimulation of RMg 5-HT in freely moving 5-HT cre mice expressing ChR2 opsin, with an intrathecal injection of picrotoxin (10µl of a competitive inhibitor of glycine receptors (GlyRs) and a non-competitive antagonist of γ-aminobutyric acid (GABAA) receptor) thus removing inhibition induced by GABAergic/glycinergic inhibitory neurons in the dorsal horn of the spinal cord (*Figure* 73). Optogenetic stimulation (475nm, 5Hz/5ms light activation for 2 min, 10mW) of 5-HT neurons, no longer elicited mechanical and thermal analgesia: mechanical threshold (*Figure 69A* SUDO picrotoxin, Friedman test p=approximate; n=5). Thermal latency (*Figure 69B* Plantar test picrotoxin, Friedman test p=0.9537, F=0.4; n=5) compare to the same optogenetic stimulation protocol in 5-HT cre mice with vehicle injection (*Figure 69A*, SUDO, Friedman test p=0.0123, F=10; n=5 and *Figure 69B*, Plantar test, Friedman test p=0.0239, F=7.6, n=5).

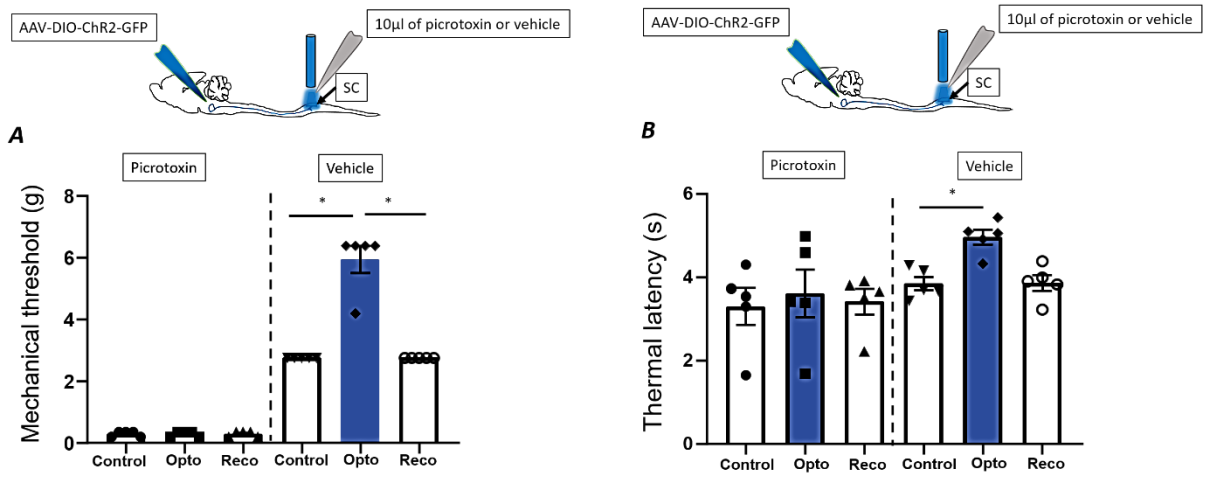

*Figure 69 : Mechanical (A) and Thermal (B) assessment in freely moving using an optogenetic activation of 5-HT descending fibres above the dorsal horn spinal cord(SC) associated with an intrathecal injection of picrotoxin or vehicle: A) Optogenetic activation of ChR2-5-HT descending fibres with 475nm blue activating light at 5Hz5ms during 2 min associated with intrathecal injection of picrotoxin induced no change in neither mechanical threshold (0.3±0.0g before, 0.3±0.0g during and 0.3±0.0g post-stimulation; n=5) nor in thermal latency (3.3±0.4s before, 3.6±0.6s during and 3.4±0.3s post-stimulation; n=5) compare to those with intrathecal vehicle injection where an increase in both mechanical threshold (2.8±0g before, 5.9±0.4g during and 2.8±0g post-stimulation; n=5) and thermal latency have been observed (3.8±0.2s before, 5±0.220s during and 3.9±0.2s post-stimulation; n=5). Measure are reported as mean ± SEM; A, SUDO vehicle *=p=0.0354 and B, plantar test *=p=0.0228 from Dunn's post hoc test.*

Blockade of the GABAa neurotransmission using an intrathecal picrotoxin injection suppressed the descending inhibitory effect elicited by the optogenetic activation of RMg 5-HT neurons expressing ChR2 opsin (*Figure 70*). Indeed, in these animals, optogenetic stimulation no longer induced a decrease of the C-evoked response to noxious stimuli (Friedman test p=0.1026, F15.90; n=11 DHN with picrotoxin DHN compare to p=0.0004, F=28.46; n=14 without picrotoxin).

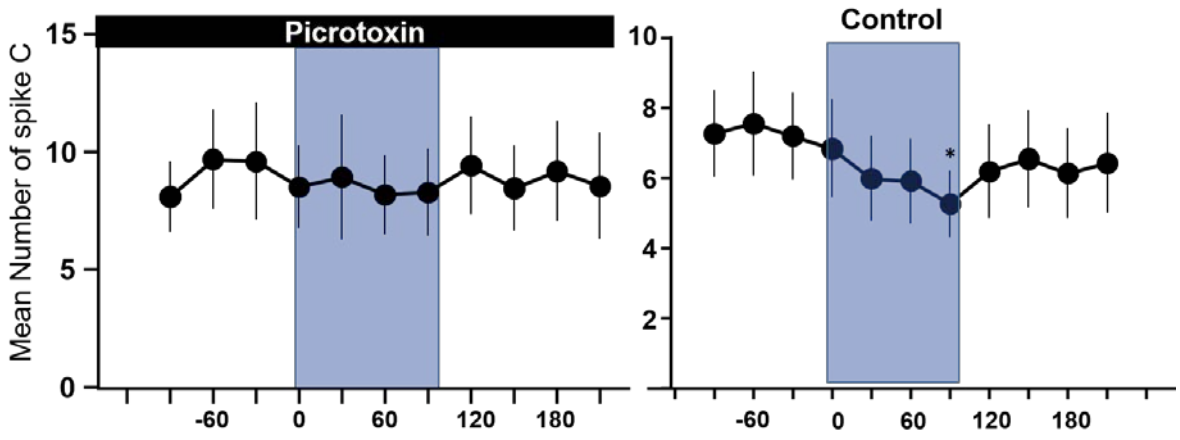

*Figure 70 : In vivo single-unit recording of DHNs in 5-HT cre mice expressing ChR2 in RMg 5-HT neuron associated with optogenetic stimulation. Intrathecal picrotoxin injection suppressed the descending inhibitory effect mediate by ChR2-5-HT neurons. Indeed, DHNs C-fibre evoked response is no longer modify during optogenetic stimulation of 5-HT neurons (mean number of C-spike before 9.2±2.0, during 8.6±2 and after 9±2.1 with intrathecal picrotoxin injection compared to mean number of C-spike before 7.4±1.3, during 6.0±1.2 and after 6.3±1.4 in control). Measure are reported as mean ± SEM. Mean number of C spike control, *= p=0.0373 from Dunn's post hoc test.*

Therefore, the descending 5-HT neurons projection to the dorsal horn, tonically inhibit nociceptive spinal transmission by acting on dorsal horn GABAergic/glycinergic inhibitory interneurons resulting in a decrease of DHN excitability. However, in previous studies, it has been shown that activation of 5-HT_3 receptors evoked GABA release in the spinal cord (Kawamata et al., 2003) and may enhanced inhibitory transmission in the spinal dorsal horn (Xie et al., 2012), therefore we hypothesised that RMg 5-HT descending action on Gabaergic/glycinergic inhibitory interneurons may pass through the activation of 5-HT_3 receptors activation.

To test that possibility, in 5-HT-cre mice (*Figure 71)*, we performed double immunostaining of 5-HT_3 receptor in combination with Pax2 and compared appositions between inhibitory (PAX2) neurons and 5-HT3 receptor and we found the presence of 5-HT_3 receptors on inhibitory interneurons.

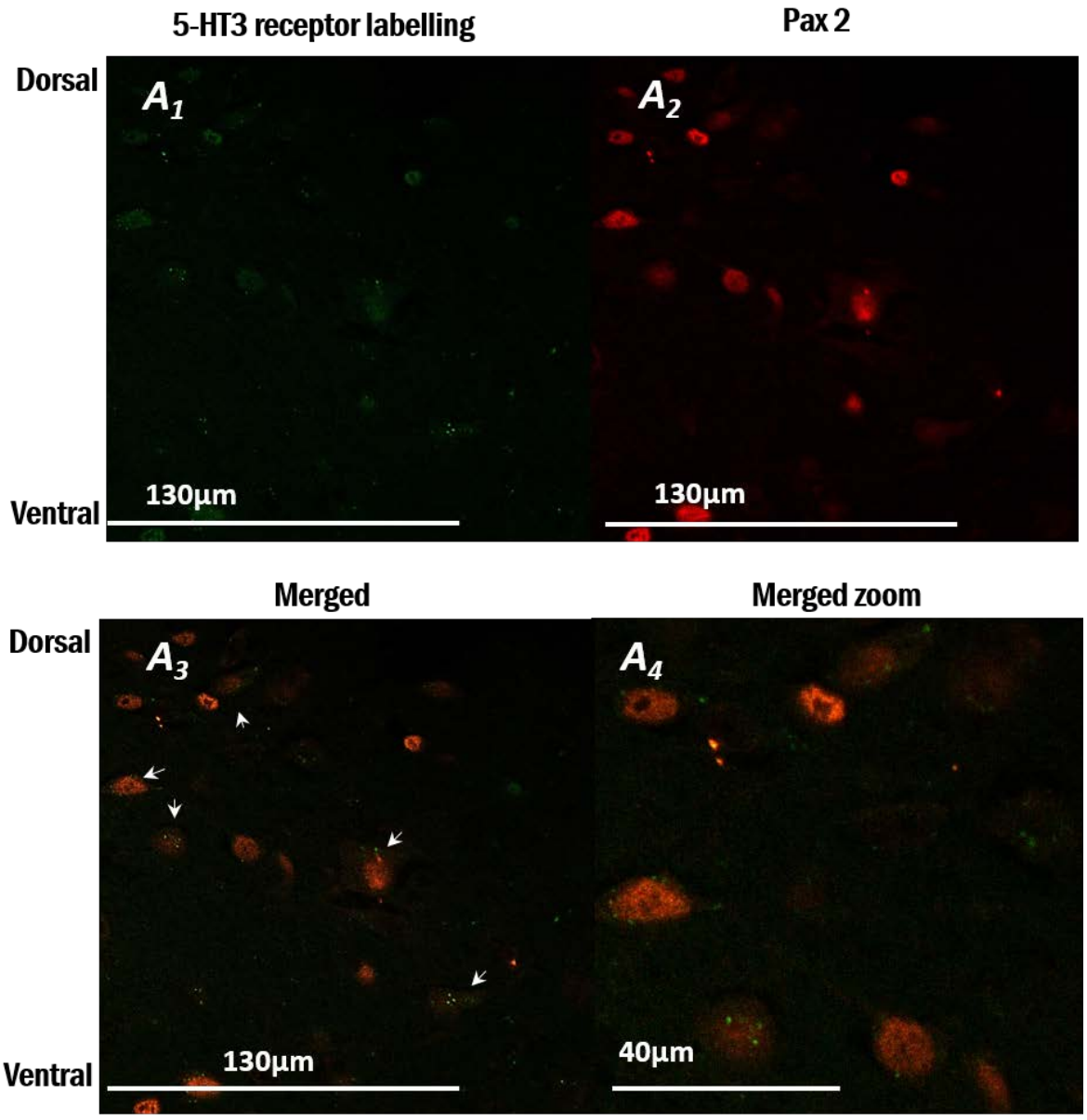

Figure 71 : Confocal image of immunostaning against 5-HT3 (A1) and Pax2 (A2) in thin slice of lumbar spinal cord of 5-HT cre mice. Pax 2 positive cells are colocalised with 5-HT3 staining confirming the presence of 5-HT3 receptors on spinal cord inhibitory interneurons (white arrows, A3-4).

b) *RMg 5-HT descending action on GABAergic/glycinergic inhibitory interneuron does not pass through 5-HT$_3$ receptors activation.*

To verify this hypothesis, we performed optogenetic stimulation of RMg 5-HT in freely moving 5-HT cre mice expressing ChR2 opsin, with an intrathecal injection of granisetron (10µl of a 5-HT$_3$ receptor antagonist) thus removing the ability to activate GABAergic/glycinergic inhibitory neurons in the dorsal horn of the spinal cord via this receptor

(*Figure 72)*. Optogenetic stimulation (475nm, 5Hz/5ms light activation for 2 min, 10mW) of 5-HT neurons, always elicited mechanical and thermal analgesia as for the vehicle: mechanical threshold, *Figure 72A1* SUDO granisetron, Friedman test p=0.0123, F=10; n=5; *Figure 72A2*, Repeated measure, granisetron, Friedman test p=0.0123, F=10; n=5 and *Figure 72B* Plantar test granisetron, Friedman test p=0.085, F=0.4; n=5 compare to the same optogenetic stimulation protocol in 5-HT cre mice with vehicle injection (*Figure 72A1*, SUDO, vehicle, Friedman test p=0.0123, F=10; n=5 and *Figure 72A2*, Repeated measure vehicle, Friedman test p=0.0123, F=10; n=5 *69B*, Plantar test, Friedman test p=0.0239, F=7.6, n=5).

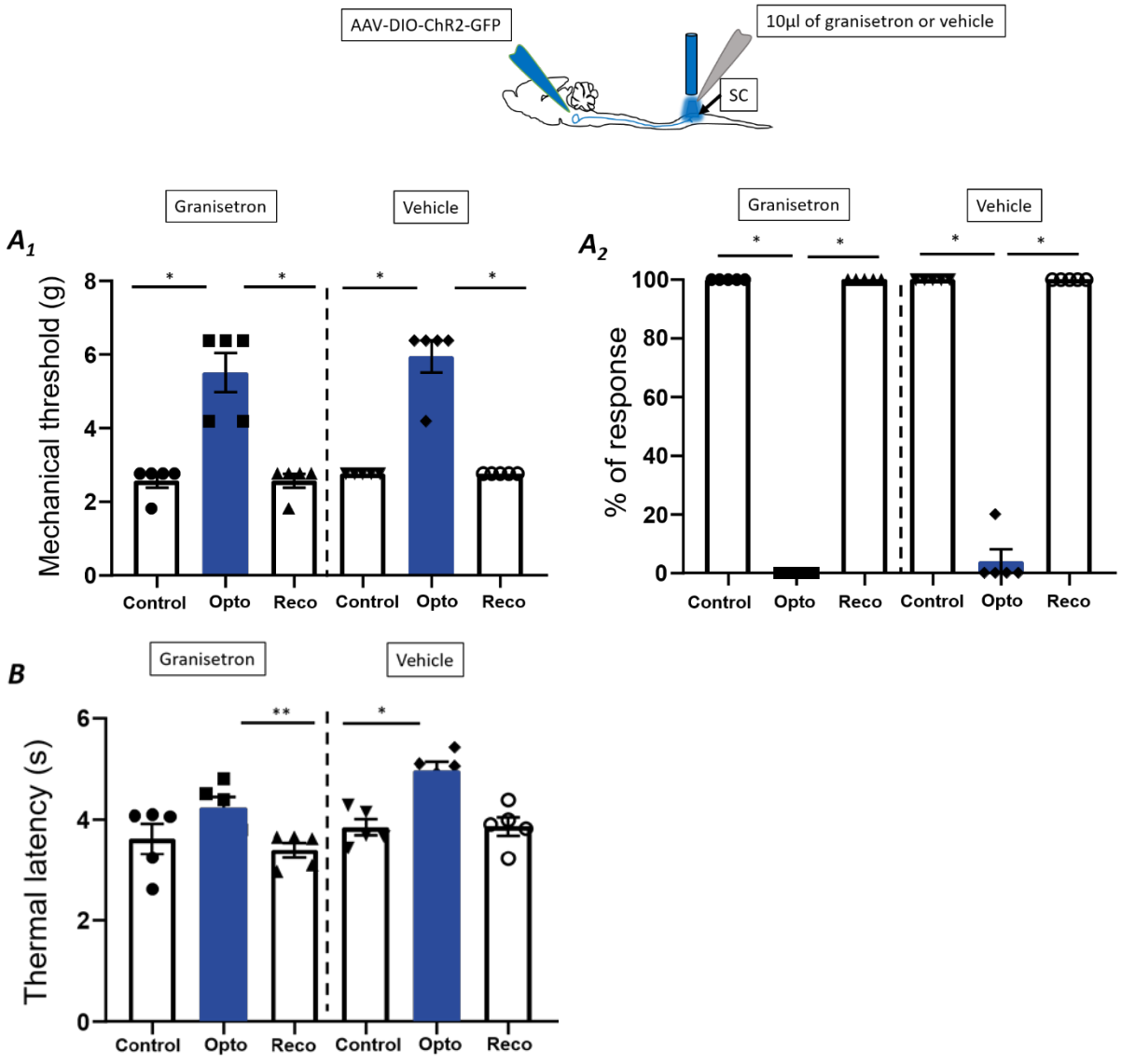

Figure 72 : Mechanical (A) and Thermal (B) assessment in freely moving using an optogenetic activation of 5-HT descending fibres above the dorsal horn spinal cord(SC) associated with an intrathecal injection of granisetron or vehicle: A) Optogenetic activation of ChR2-5-HT descending fibres with 475nm blue activating light at 5Hz5ms during 2 min associated with intrathecal injection of granisetron induced a significant increase of the mechanical threshold (SUDO, 2.6±0.2g before, 5.5±0.5g during and 2.6±0.19g post-stimulation; n=5 and Repeated measure, 100±0.0% before, 0±0.0% during and 100±0.0% post-stimulation;

*n=5) and the thermal latency (3.6±0.3s before, 4.2±0.2s during and 3.4±0.2s post-stimulation; n=5) as for those with intrathecal vehicle injection (SUDO 2.8±0g before, 5.9±0.4g during and 2.8±0g post-stimulation; n=5 and Repeated measure, 100±0.0% before, 4±4.00% during and 100±0.0% post-stimulation; n=5) and thermal threshold have been observed (3.8±0.2s before, 5±0.2s during and 3.9±0.2s post-stimulation; n=5). Measure are reported as mean ± SEM; A2, Repeated measure granisetron $*^1=*^2$=p=0.0354, vehicle $*^1=*^2$=p=0.0354; A2, SUDO granisetron $*^1=*^2$=p=0.0354, vehicle $*^1=*^2$=p=0.0354 and B, plantar test granisetron **=p=0.0089, vehicle *=p= 0.0228 from Dunn's post hoc test.*

Therefore, since no modification has been observed on the RMg 5-HT induced-descending pain inhibition following the blockade of 5-HT_3 receptors we can conclude that 5-HT_3 are not involved in the activation of GABAergic/glycinergic inhibitory interneurons resulting in the inhibition of the nociceptive transmission.

Next, we wanted to know how 5-HT neuron activity was modulated. Indeed, using an immunohistochemistry approach associating both confocal microscopy and 3D imaris images analysis (*Figure 73A 1-4* and *B1-4*, VGLUT1-3, GAD65-67 for glutamatergic and GABAergic inputs respectively), we observed that 5-HT neurons receive inputs from both glutamatergic and GABAergic neurons. In particular, these inputs include somatostatin neurons (SST, *Figure 73C1-4*). SST neurons derived from vlPAG and appear to have a sympathetic inhibitory effect on bulbospinal neurons (Bou Farah et al., 2016). vlPAG is also an important descending pain modulatory system through the rostral ventromedial medulla and is associated with spinal cord 5-HT release (Cui et al., 1999). vlPAG contains various subpopulations of neurons (GABAergic and glutamatergic neuron) that control pain transmission (Brenner et al., 2012). All this suggest that the 5-HT neural activity may be influenced by somatostatin neurons of vlPAG (vlPAG SST).

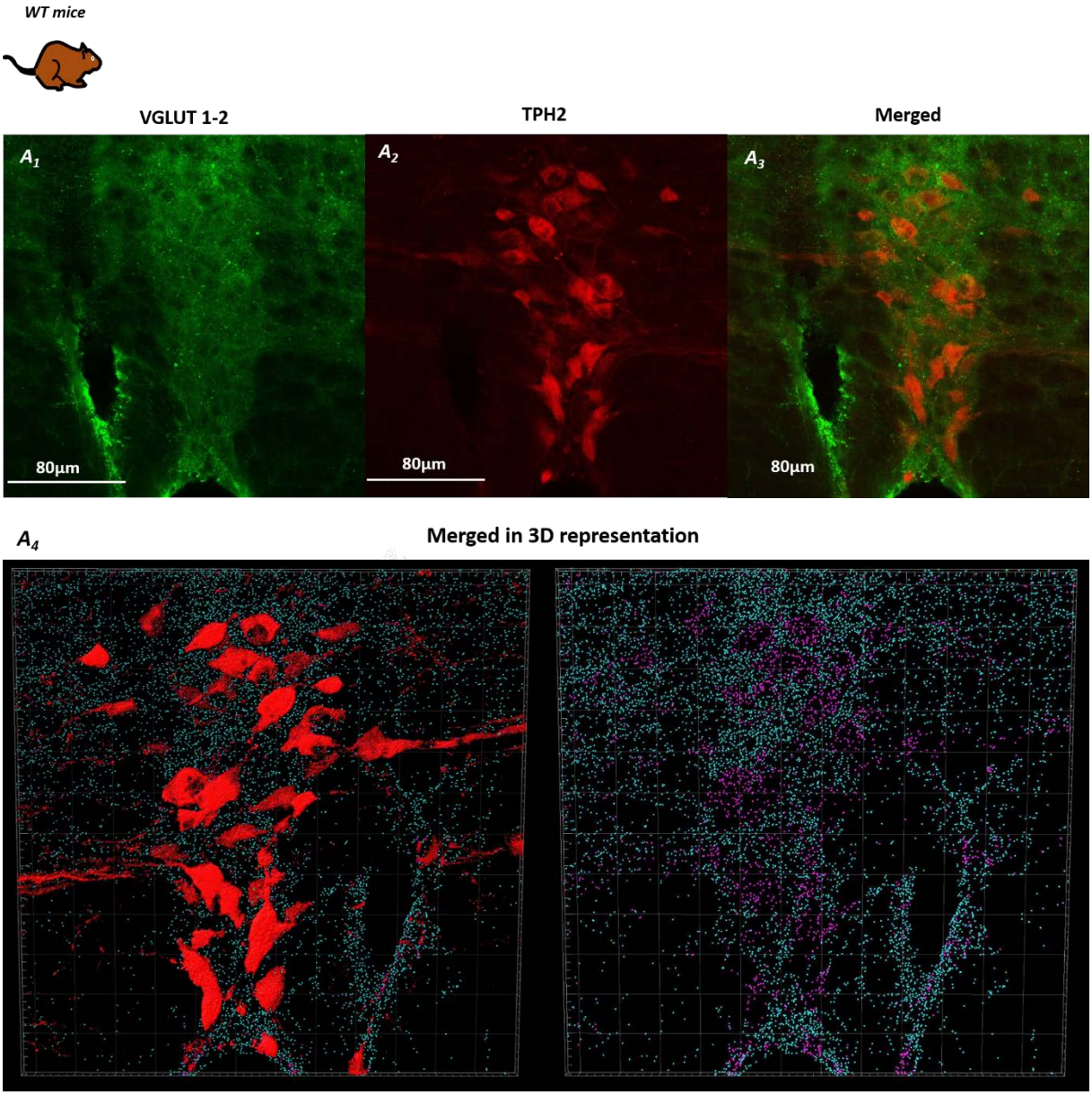
WT mice
VGLUT 1-2
TPH2
Merged
A1
A2
A3
80µm
80µm
80µm
A4
Merged in 3D representation

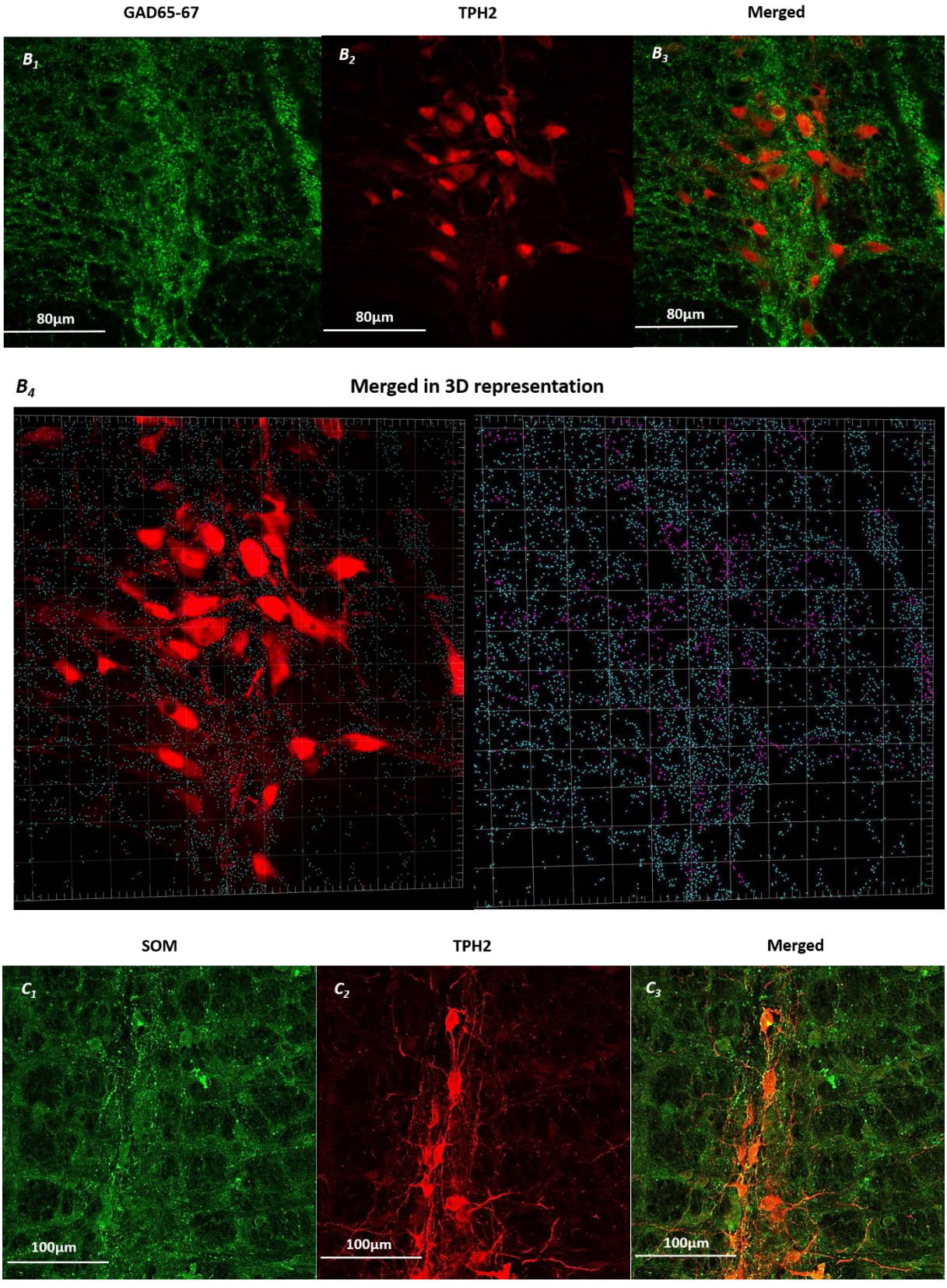
GAD65-67
TPH2
Merged
B1
B2
B3
80µm
80µm
80µm
B4
Merged in 3D representation
SOM
TPH2
Merged
C1
C2
C3
100µm
100µm
100µm

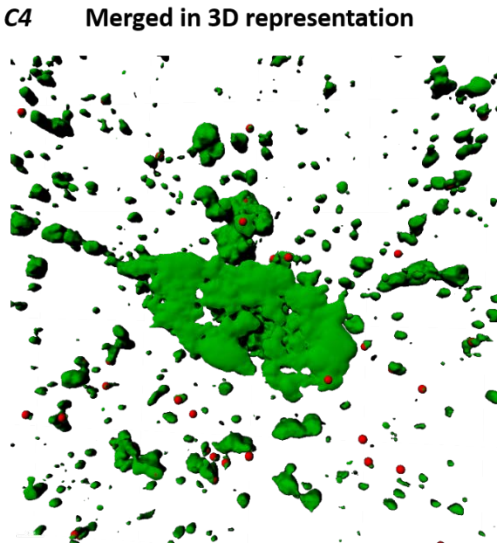

Figure 73 : Confocal image and 3D representation of GAD 65-67, VGLUT 1-3, TPH2 and SOM immunostaining in thin slice of RMg of WT mouse. Both GAD 65-67 and VGLUT 1-2 and TPH2 and SOM staining showed dense afferent inputs on 5-HT neurons. A1, B1 and C1 show glutamatergic, GABAergic and somatostatin staining respectively. A2, B2 and C2, TPH2 staining and A3, B3 and C3 a merge of both TPH2 and glutamatergic and GABAergic staining revealing that 5-HT neurons received dense inputs from both of them. A4, B4 and C4 represent a 3D reconstruction of VGLUT 1-2/TPH2, GAD 65-67/ TPH2 and SOM/TPH2 merged confocal image respectively (IMARIS microscopy image analysis software; Oxford instrument) revealing spots contact between VGLUT 1-2 spots (A4, in blue, 2199 VGLUT 1-2 spots are close to TPH2 neurons staining revealed in violet*) or GAD 65-67 spots (B4, in blue* on a total average of 5880 GAD 65-67 spots labelled in blue, 772 GAD 65-67 spots are close to TPH2 neurons staining revealed in violet*) or SOM spots (C4, in red) and 5-HT neurons (in red or green for the merge with somatostatin spots). WT for wild type mice.*

B. DESCENDING INFLUENCE OF SST NEURONS OF vlPAG ON PAIN TRANSMISSION.

1. Consequences of optogenetic manipulation of SST neurons in acute pain

a) *Inhibition of vlPAG SST neurons induces mechanical and thermal analgesia*

First of all, we established the functional role of SST neurons of the vlPAG (vlPAG SST) on the spinal nociceptive transmission. In freely moving SOM-IRES-CRE mice, optogenetic inhibition with ArchT opsin was performed using optical cannulas bilaterally implanted above the vlPAG (*Figure 74* and *75*). With regard to mechanical threshold, optogenetic inhibition (526.5nm continuous green inhibiting light for 2 min, power set at 10mw) of SST neurons of the vlPAG elicited a relevant increase in mechanical threshold and thermal latency with a return to baseline after light switched off (*Figure 74*) that was not observed in control

group expressing GFP alone. Indeed, using both Von Frey SUDO and repeated measure, we observed that optogenetic inhibition of SST neurons induced a significant increase in mechanical threshold (*Figure 74*A, SUDO, Friedman test p<0.0001, F=20.76; n=12) including a substantial decrease in the percentage of response of the hind-paws to repeated noxious stimuli (*Figure 74B*, Repeated measure, Friedman test p<0.0001, F=19.6; n=12) resulting in mechanical analgesia.

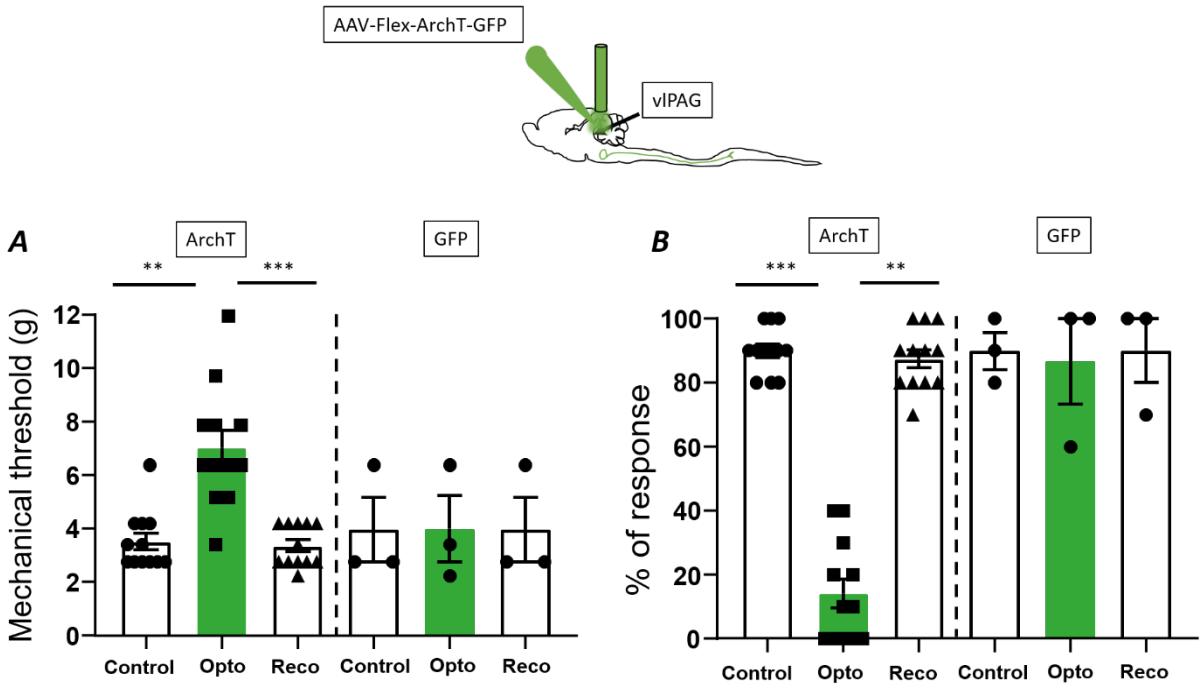

*Figure 74 : Mechanical assessment of SST inhibition in the vlPAG. Optogenetic inhibition with ArchT-SST neuron with 526.5nm continuous green inhibiting light during 2 min induced a relevant increase in mechanical threshold (A, SUDO, 3.5±0.3g before, 7.0±0.6g during and 3.4±0.2g post-stimulation) including a decrease in the percentage of hind-paws response to repeated noxious stimuli (B, Repeated measure in % of response: 90±2.1% before, 14.2±4.5% during and 87.5±2.8 post-stimulation) resulting in mechanical analgesia compared to control group expressing GFP alone where no modification has been observed (SUDO: 4±1.2g before, 4±1.2g during and 4±1.2g post-stimulation; n=3 and Repeated measure with noxious stimuli, 90±5.8% before, 86.67±13.3% during and 90±10% post-stimulation; n=3). Measures are reported as mean ± SEM; A, SUDO **=p=0.0010, ***=p=0.0002 and B, Repeated measure **=p=0.0015, ***=p=0.0001 from Dunn's post hoc test.*

With regard to thermal latency, using plantar test, we observed that optogenetic inhibition of SST neurons induced a significant increase in thermal latency resulting in thermal analgesia (*Figure 75*, Plantar test, Friedman test p<0.0001, F=20.67; n=12) compared to what we observed in GFP SST mice.

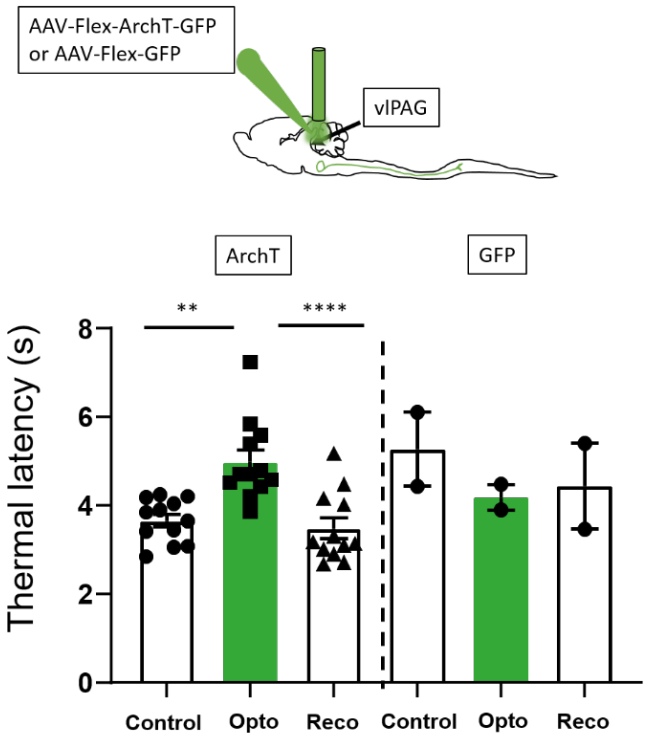

*Figure 75 : Thermal assessment of SST inhibition in the vlPAG. Optogenetic inhibition with ArchT-SST neuron with 526.5nm continuous green inhibiting light during 2 min induced a relevant increase in thermal latency (Plantar test: 3.5±0.3s before, 7.0±0.6s during and 3.4±0.2s post-stimulation) resulting in thermal hyperalgesia compared to the control group expressing GFP alone where no modification has been observed (Plantar test, 5.3±0.8s before, 4.2±0.3s during and 4.4±1s post-stimulation; n=2). Measures are reported as mean ± SEM; **=p=0.0085 and ****=p<0.0001 from Dunn's post hoc test.*

So unlike what we observed with 5-HT cre mice expressing ArchT in 5-HT neurons of the RMg, optogenetic inhibition of SST neurons of the vlPAG results in a downward inhibition of pain transmission that suggest that within the vlPAG, SST neurons are tonically active and may exert tonic facilitation on pain transmission.

b) *Activation of vlPAG SST neurons induces mechanical hyperalgesia and allodynia and thermal hyperalgesia*

As for the ArchT-SST mice, in freely moving SOM-IRES-CRE mice, optogenetic activation with ChR2 opsin was performed using optical cannulas bilaterally implanted above the vlPAG (*Figure 76* and *77*). With regard to mechanical threshold, optogenetic activation with blue laser light (475nm blue activated light at 2hz5ms for 2 min, power set at 10mW) of SST neurons of the vlPAG (ChR2-SST) elicited a significant decrease in mechanical threshold that was suppressed after light switched off (*Figure 76*). Indeed, using Von Frey SUDO and repeated measured, we observed that optogenetic activation of vlPAG SST neurons decreased substantially the mechanical threshold including a substantial increase in the percentage of

hind-paws response to repeated innocuous stimuli (*Figure 76A*, SUDO, Friedman test p<0.0001, F=20.24; n=17 and *Figure 76B*, Repeated measure p=0.0008, F=11.79; n=8) resulting in mechanical allodynia and hyperalgesia. Phenomenon that was not observed with SOM-IRES-CRE mice expressing GFP in SST neurons of the vlPAG using the same pattern of optogenetic activation (*Figure 76A*, SUDO, Friedman test p=0.1738, F=3.5, n=12; *Figure 76B*, Repeated measure, Friedman test p>0.9999, F=0.2; n=5).

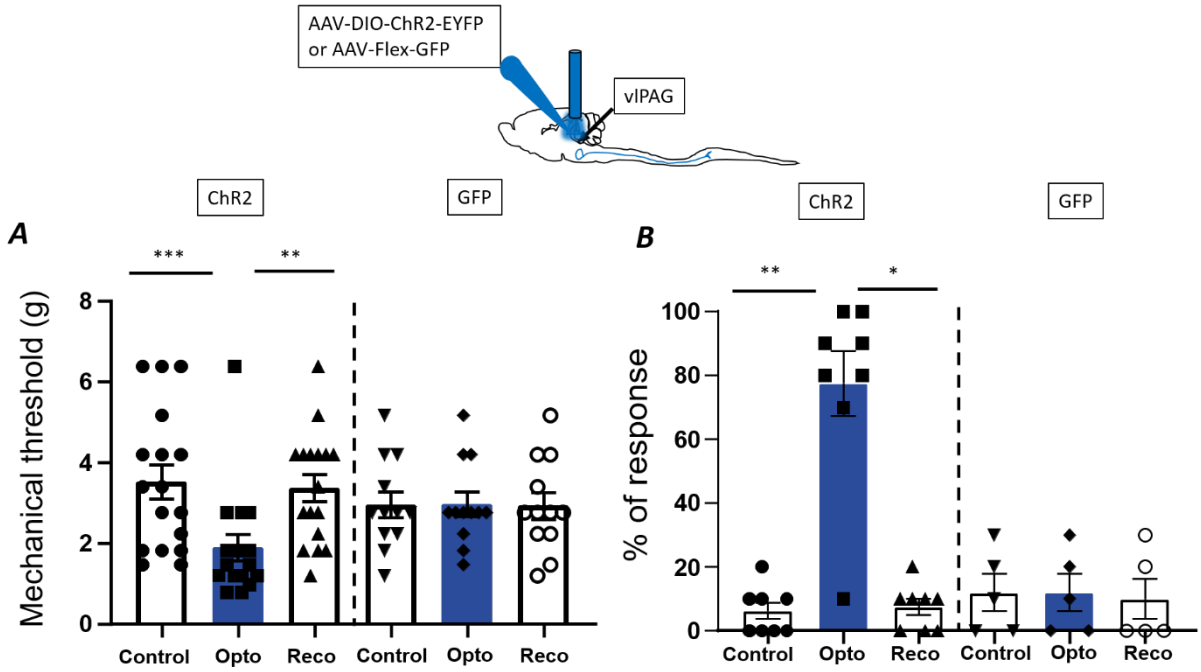

*Figure 76 : Mechanical assessment of SST activation in the vlPAG. Optogenetic activation with ChR2-SST neurons with 475nm blue activating light at 5Hz5ms during 2 min induced a relevant decrease in mechanical threshold (A, SUDO: 3.5±0.4g before, 1.9±0.3g during and 3.4±0.3g post-stimulation) including a substantial increase in the percentage of hind-paws response to repeated innocuous stimuli (B, Repeated measure in % of response: 6.3±2.6% before, 77.5±10.3% during and 7.5±2.5 post-stimulation) resulting in mechanical allodynia and mechanical hyperalgesia compared to control group expressing GFP alone where no modification has been observed (SUDO: 3±0.3g before, 3±0.3g during and 2.9±0.3g post-stimulation; Repeated measure with innocuous stimuli: 12±5.8% before, 12±5.8% during and 10±6.3% post-stimulation). Measures are reported as mean ± SEM; A, SUDO ChR2 **=p=0.0017, ***=p=0.0002; B, Repeated measure ChR2 *=p=0.0173 and **=p= 0.0054 from Dunn's post hoc test.*

With regard to thermal threshold, using plantar test, we observed that optogenetic activation of SST neurons induced a significant decrease in thermal threshold resulting in thermal hyperalgesia (*Figure 77*, Plantar test, Friedman test p=0.0006, F=14.92; n=13) compared to what we observed in GFP-SST mice where optogenetic stimulation of SST neuron of the vlPAG expressing GFP induced no modification of thermal latency (*Figure 77*, Plantar test, Friedman test p=0.6013, F=1.4; n=10).

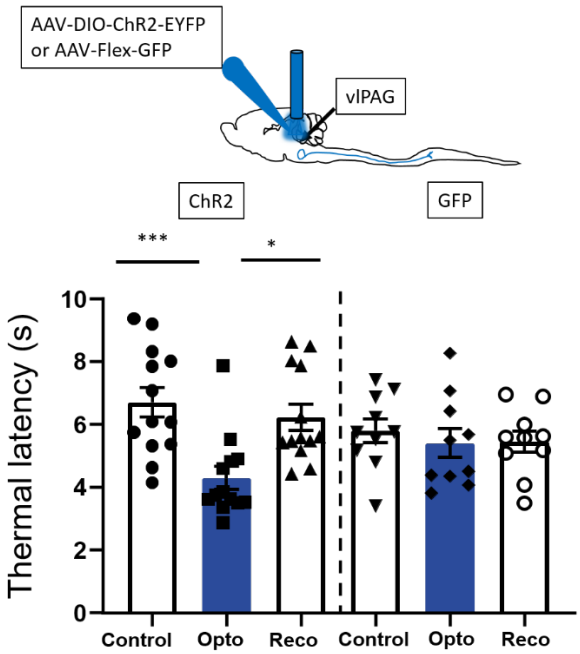

*Figure 77 : Thermal assessment of SST activation in the vlPAG. Optogenetic activation with ChR2-SST neuron with 475nm blue activating light at 5Hz5ms during 2 min induced a relevant decrease in thermal latency resulting in thermal hyperalgesia (Plantar test: 6.7±0.5s before, 4.3±0.4s during and 6.2±0.4s post-stimulation) compared to the control group expressing GFP in vlPAG of SST mice where no modification has been observed (Plantar test: 5.8±0.4s before, 5.4±0.5s during and 5.5±0.3s post-stimulation). Measures are reported as mean ± SEM; *=p=0.0121 and ***=p=0.0004 from Dunn's post hoc test*

Therefore, it can be concluded that SST neurons of the vlPAG exert a tonic descending facilitation on pain transmission. These results are the exact opposite to what we observed in 5-HT cre mice where optogenetic activation of 5-HT neurons of the RMg resulted in descending inhibition of the pain transmission.

2. Consequence of optogenetic manipulation of vlPAG SST neuron on dorsal horn neurons

We then assess the functional consequence of optogenetic modulation of SST neurons of the vlPAG on dorsal horn neurons. To do so, in anesthetised SOM-IRES-cre mice expressing ChR2 or ArchT opsin or GFP tag in vlPAG SST neuron, we performed single-unit electrophysiological recordings targeting WDRs associated with bilateral optogenetic stimulation above vlPAG with the same light pattern that we used for behavioural experiments.

a) *vlPAG SST neuron modulation modifies WDRs integration property to noxious stimuli*

In anesthetised SOM-IRES-cre mice expressing ArchT in the SST neurons of the vlPAG, bilateral optogenetic inhibition of SST neurons (526.5nm continuous green inhibiting light for with power set at 10mW) elicited a significant decreased both in WDR response to nociceptive C fibre transmission (*Figure 78A*, Friedman test p=0.0229, F=20.75; n=18) and of the windup coefficient (*Figure 78B*, Two-tailed *t test* p=0.0313, n=6 DHN), resulting in a decrease of DHN excitability.

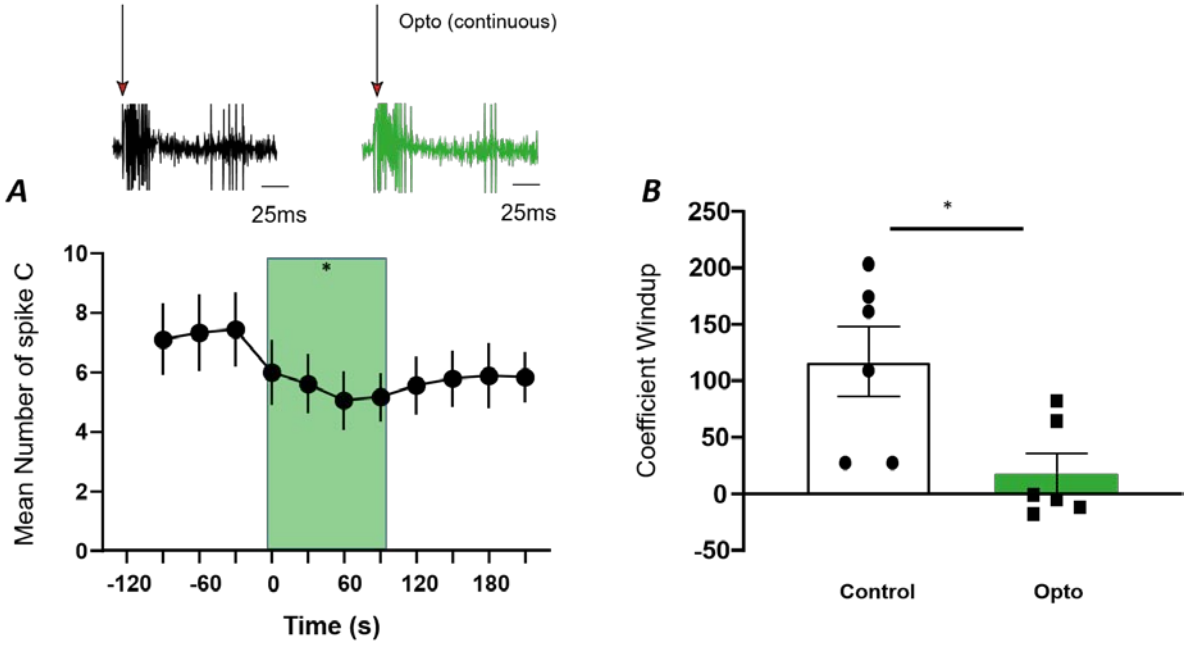

*Figure 78 : In vivo single-unit recording of DHNs associated with optogenetic inhibition of vlPAG SST neurons. A) Above, representative WDR neuron response to noxious electrical stimuli recorded before and during optogenetic stimulation. ArchT vlPAG SST optogenetic inhibition decreased DHN excitability resulting from both a decrease in the mean number of DHNs responses to C-fibre input (mean number of C-spike before 7.3±1.3, during 5.5±1 and after 5.8±1) and a decrease in the coefficient of windup (from 116.8±31.0 before to 18.3±17.6 during optogenetic stimulation). Measure are reported as mean ± SEM; Mean number of C spike *=p<0.0229 from Dunn's post hoc test and Coefficient Windup *= p=0.0313 from Wilcoxon matched-pairs signed-rank test.*

By contrast, bilateral optogenetic activation of SST neurons (475 nm blue activating light at 2hz5ms, power set at 10mW) with SOM-IRES-cre mice expressing ChR2 in SST neurons of the vlPAG elicited a significant increase of the WDR response to nociceptive C fibre transmission (*Figure 79A*, Friedman test p<0.0001, F=73.81; n=18 DHN) and a relevant

increase of windup coefficient (*Figure 79B*, Two-tailed *t test* p=0.0039; n=10 DHN) resulting in a hyper-excitability of DHN.

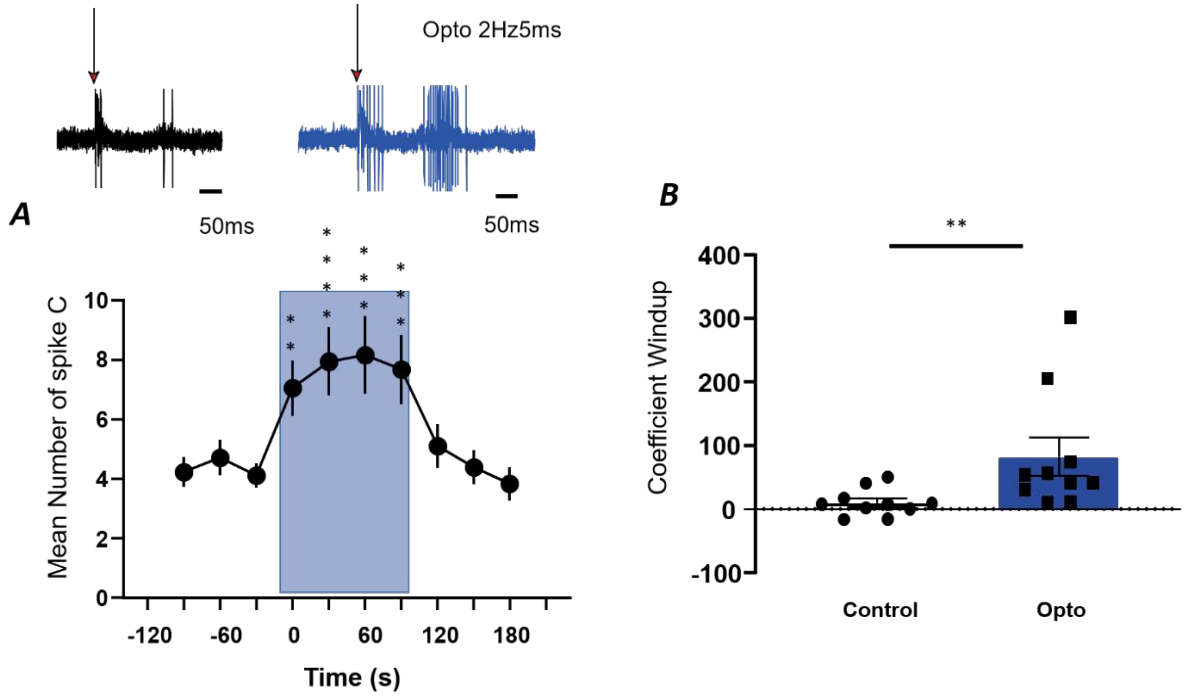

*Figure 79 : In vivo single-unit recording of DHNs associated with optogenetic activation of SST neurons of the vlPAG. A) Above, representative WDR neuron response to noxious electrical stimuli recorded before and during optogenetic stimulation. Optogenetic activation with ChR2-SST neurons increased DHN excitability resulting from both an increase in the mean number of DHNs responses to C-fibre input (mean number of C-spike before 4.4±0.5, during 7.7±1.1 and after 4.4±0.6) and an increase in the windup coefficient (from 10.1±6.8 before to 82.2±3 during optogenetic stimulation). Measure are reported as mean ± SEM; A, Mean number of C spike **= p=0.0010, ***[1]=p=0.0002, ***[2]=p=0.0003 and ****= p<0.0001 from Dunn's post hoc test and B, Coefficient Windup **= p=0.0039 from Wilcoxon matched-pairs signed-rank test.*

In addition to that, in anesthetised SOM-IRES-cre mice expressing GFP only in the vlPAG SST neurons, bilateral optogenetic stimulation in vlPAG SST neuron with both optical pattern (5Hz5ms at 475nm blue activating light or continuous green inhibiting light at 10mW respectively) induced no change in either DHN response to C-fibre activation (*Figure 80A*, Friedman test p=0.1743, F=3.650; n=10) or DHN windup coefficient (*Figure 80B*, Two-tailed *t test* p=0.6250, n=5 DHN).

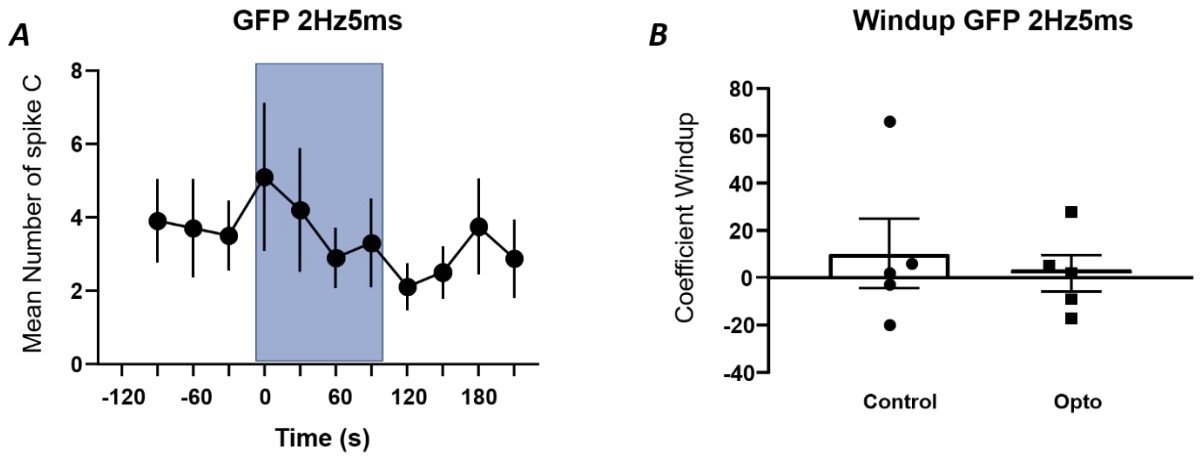

Figure 80 : In vivo single-unit recording of DHNs associated with optogenetic stimulation of vlPAG SST neuron. A) In SOM-IRES cre mice expressing GFP in the vlPAG associated with a bilateral optogenetic stimulation above the vlPAG, no change has been observed both in DHN C-evoked response (mean number of C-spike before 3.7±1.1, during 3.9±1.4 and after 2.8±0.9) and DHN windup coefficient (from 10.2±14.6 before to 1.8±7.6 during optogenetic stimulation).

Therefore, by contrast with RMg 5-HT neuron, vlPAG SST neurons facilitate the nociceptive transmission resulting in an increase in WDR excitability.

We then hypothesised that vlPAG SST facilitation on pain transmission may pass through RMg 5-HT neurons.

b) *vlPAG SST facilitation partly passes through RMg 5-HT neuron*

To verify our hypothesis, we developed a viral strategy, as described in the method, in which SOM-IRES cre mice were microinjected bilaterally in the vlPAG with AAV-CAG-FLEX-GFP (*Figure 81A*) associated with a bilateral injection of fluorogold 2% into the dorsal horn of the spinal cord (*Figure 81B*). Then, post-mortem, we performed immunostaining in cross-section of RMg against TPH2 (*Figure 81C*).

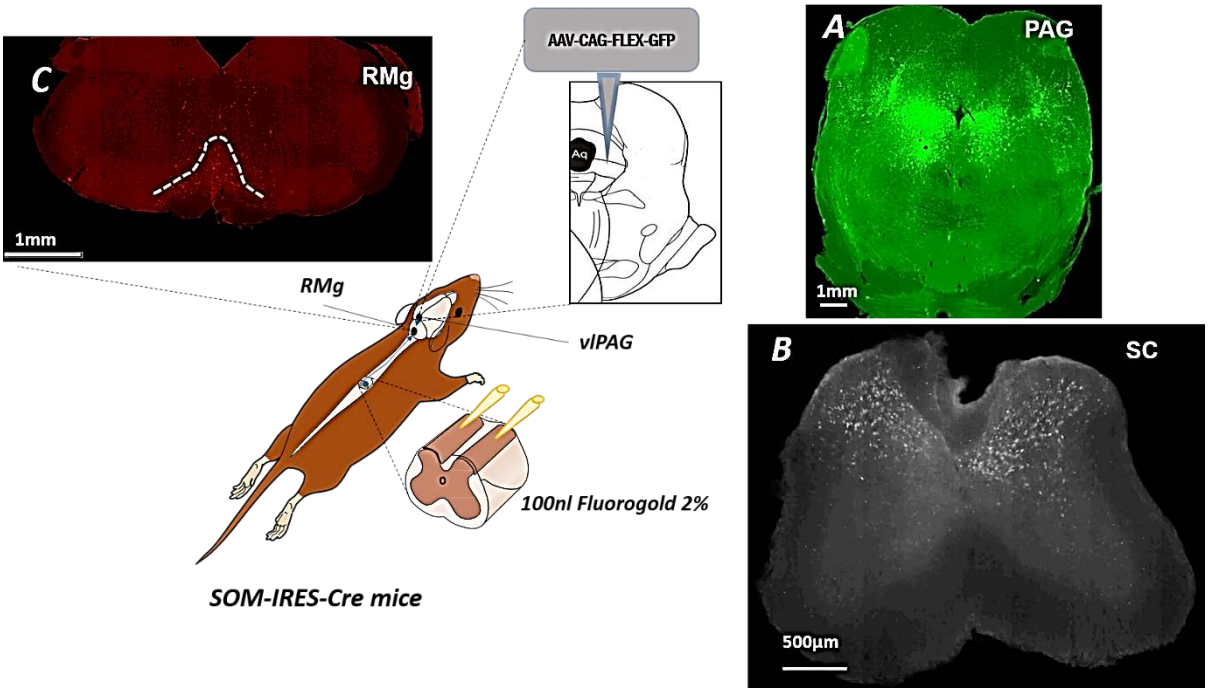

Figure 81 : Viral strategy where AAV-CAG-FLEX-GFP virus was microinjected bilaterally in the vlPAG (A) of SOM-IRES cre mice associated with a bilateral injection of fluorogold 2% into the dorsal horn of the spinal cord (B). Then in cross-section of the raphe Magnus we performed immunostaining against TPH2 (C). Images were obtained with an epifluorescence microscope.

We compared then, at the level of the RMg, apposition between TPH2 staining (*Figure* 82A1), GFP staining (*Figure 82A2*) and fluorogold (FG) autofluorescence (*Figure 82A3*) and we found colocalisation between GFP-SST fibres staining from the vlPAG, TPH2 immunostaining and FG staining from the spinal cord (*Figure 82A4*). Thus it can be concluded that vlPAG SST fibres project to the raphe Magnus and contact 5-HT neurons that project to the spinal cord.

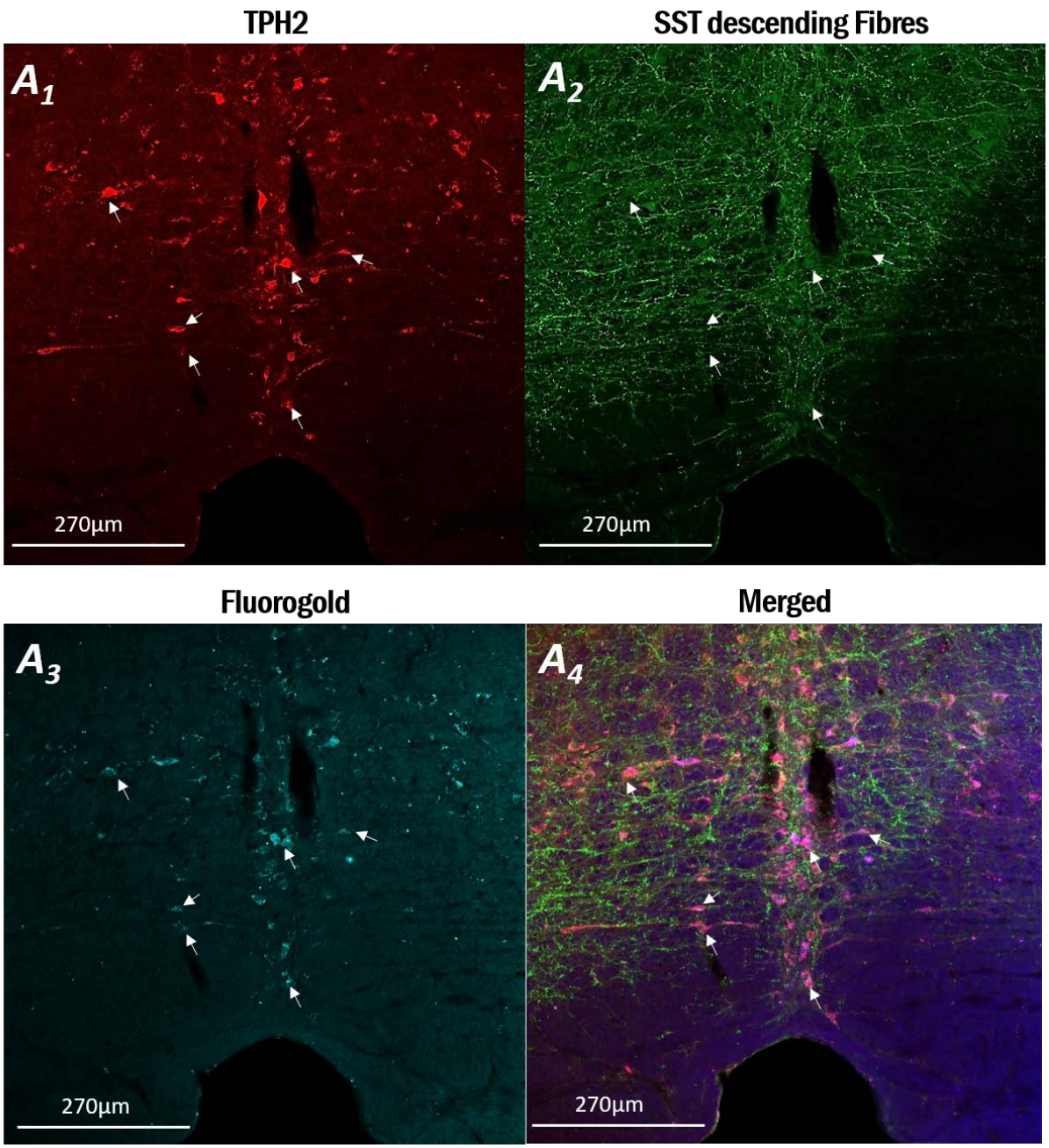
TPH2
SST descending Fibres
A1
A2
270µm
270µm
Fluorogold
Merged
A3
A4
270µm
270µm

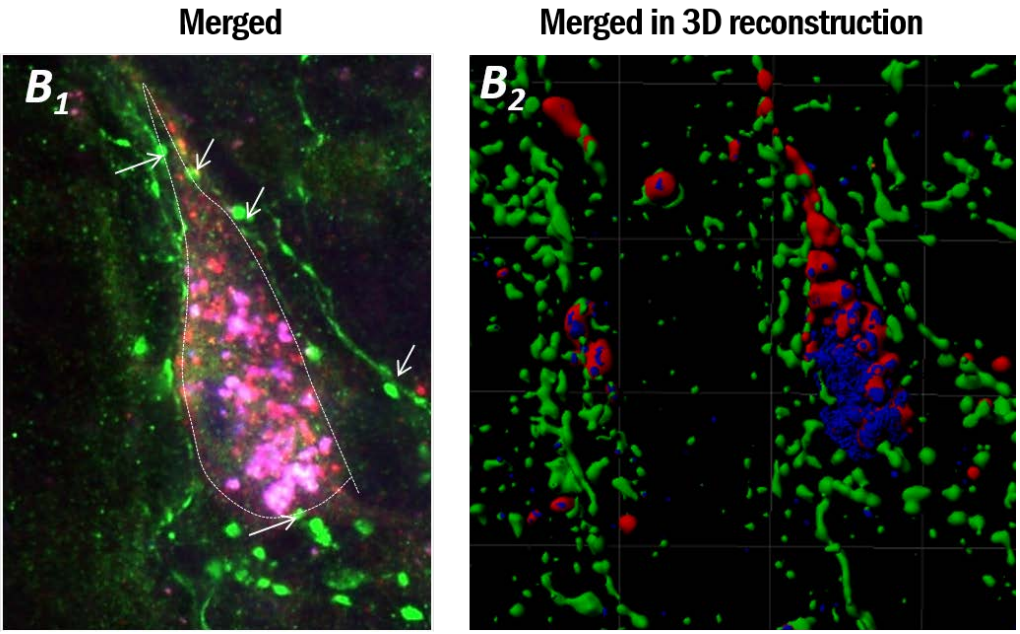

Figure 82 : Confocal image (A1-4 and B1) and 3D representation (B2) of vlPAG AAV-flex-GFP positive fibres (A2) with FG (A3) and TPH2 (A1) staining in thin cross-section of raphe Magnus of SOM-IRES cre mice. (A1) TPH2 immunostaining (in red) showing RMg 5-HT neurons positive neurons colocalised with FG staining (A3, in blue) from the spinal cord dorsal horn in contact with GFP- SST fibres form the vlPAG (A4, in green). (B2) Imaris 3D reconstruction of RMg TPH2 positive cell (in red) colocalises with FG staining (in blue) in contact with vlPAG SST positive fibre (in green) (B1).

To confirm the functional effect of these connections, in freely moving SOM-IRES-CRE mice expressing ChR2 opsin in SST neurons of the vlPAG, optogenetic activation was performed using an optical cannula implanted above the RMg. With regard to mechanical threshold, optogenetic activation with blue laser light (475nm blue activated light at 2hz5ms for 2 min, power set at 10mW) of SST descending fibres in RMg elicited a significant decrease in mechanical threshold (*Figure 83)* and thermal latency (*Figure 84)* that was suppressed after light switched off. *Figure 80A*, RMg SST Von Frey SUDO Friedman test p=0.0002, F=15.08; n=8 and *Figure 83B*, Repeated measure Friedman test p=0.0001, F=13.87; n=8 as well as what we had observed with an optogenetic stimulation of ChR2-SST neurons directly above the vlPAG (*Figure 83A*, Von Frey SUDO, Friedman test p<0.0001, F=20.24; n=17 and *Figure 80B*, Repeated measure Friedman test p=0.0008, F=11.79; n=8) and *Figure 84*, RMg SST Plantar test, *Figure 84*, Friedman test p=0.0080, F=9.250; n=8)

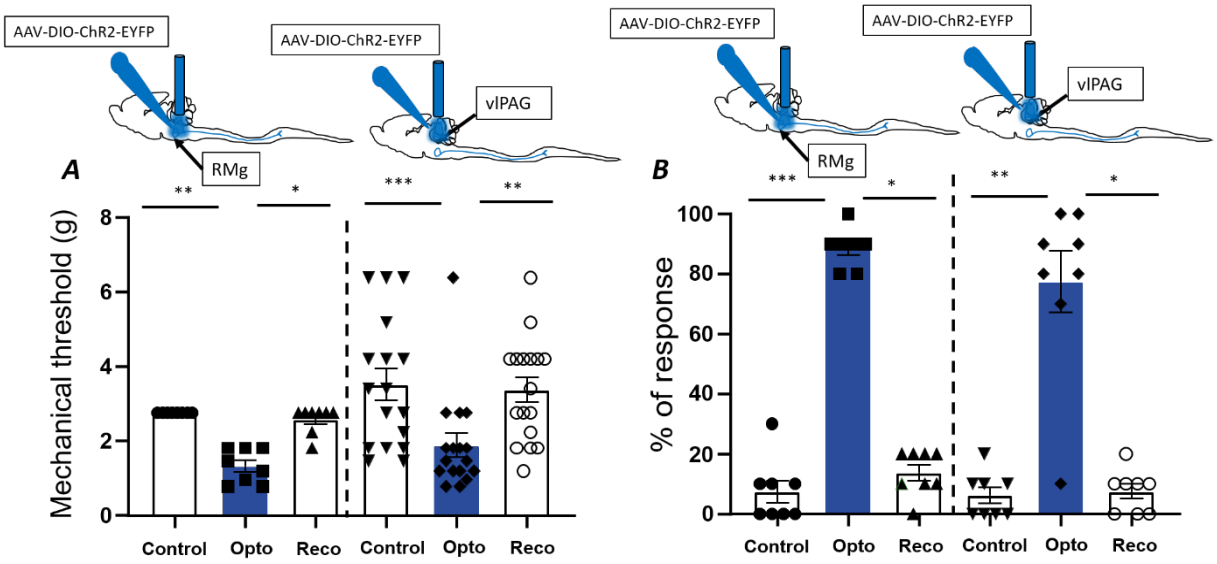

Figure 83 : *Mechanical assessment of SST descending fibres activation from the vlPAG above the RMg (ChR2-SST descending fibres) compare to SST neurons activation directly above the vlPAG (Chr2-vlPAG SST). Optogenetic activation of ChR2-SST neuron above the vlPAG or ChR2-SST descending fibre in the RMg with blue activating light at 2hz5ms during 2 min induced a relevant decrease in mechanical threshold (A, SUDO, ChR2-SST descending fibres: 2.8±0g before, 1.3±0.2g during and 2.6±0.1g post-stimulation compared to ChR2-vlPAG SST: 3.5±0.4g before, 1.9±0.3g during and 3.4±0.3g post-stimulation) including an increase in the percentage of hind-paws response to repeated innocuous stimuli (B, Repeated measure, for ChR2-SST descending fibres % of response: 7.5±3.6% before, 88.8±2.2% during and 13.8±2.6 post-stimulation compare to ChR2-vlPAG SST % of response: 6.3±2.6% before, 77.5±10.3% during and 7.5±2.5 post-stimulation) resulting in mechanical allodynia and hyperalgesia. Measures are reported as mean ± SEM; A, SUDO, ChR2-SST descending fibres RMg, *=p=0.0119, **=p=0.0023; ChR2-vlPAG SST of vlPAg, **=p=0.0017 and ***p=0.0002; B, Repeated measure, ChR2-SST descending fibres RMg, *=p=0.0248, ***=0.0009 and ChR2-vlPAG SST of vlPAG *=p=0.0173 and **=p=0.0054 from Dunn's post hoc test.*

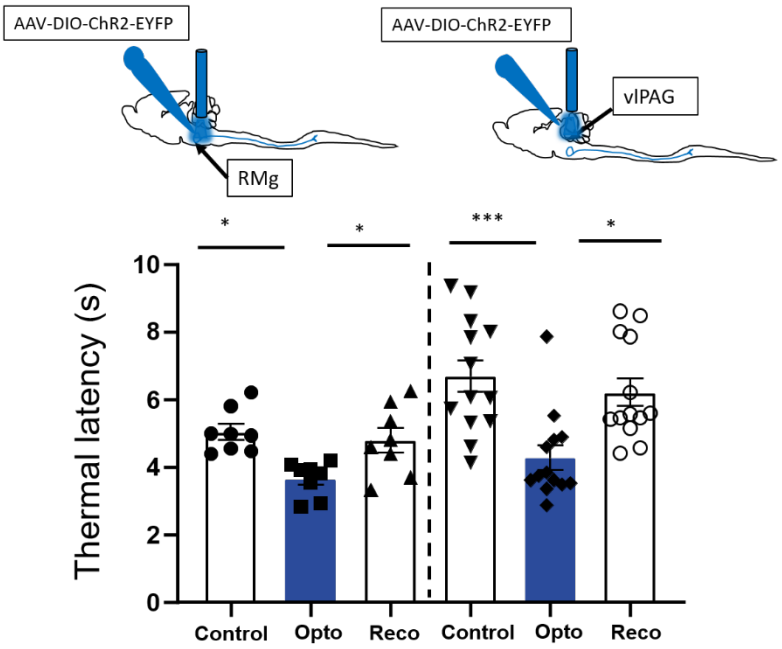

*Figure 84 : Thermal assessment of SST descending fibres activation from the vlPAG above the RMg (ChR2-SST descending fibres) compare to SST neurons activation directly above the vlPAG (Chr2-vlPAG SST).). Optogenetic activation of ChR2-SST neuron above the vlPAG or ChR2-SST descending fibre in the RMg with blue activating light at 2hz5ms during 2 min induced a relevant decrease in thermal latency resulting in thermal hyperalgesia (Plantar test, ChR2-SST descending fibres: 5.1±0.2s before,3.7±0.2s during and 4.8±0.4s post-stimulation compared to ChR2-vlPAG SST: 6.7±0.5s before, 4.3±0.4s during and 6.2±0.4s post-stimulation). Measures are reported as mean ± SEM; ChR2-SST descending fibres RMg *¹=p=0.0119, *²=p=0.0248 and ChR2-vlPAG SST of vlPAg *=p=0.0121 and ***=p=0.0004 from Dunn's post hoc test.*

In addition, in anesthetised SOM-IRES-cre mice expressing ChR2 opsin in vlPAG SST neurons, we observed that optogenetic stimulation (475 nm blue activating light at 2hz5ms, power set at 10mW) of vlPAG SST descending fibres in RMg also elicited a relevant increase of the WDR response to nociceptive C fibre transmission (*Figure 85*, $p<0.0001$, $F=34.33$; $n=9$ DHN) resulting in a hyper-excitability of WDR..

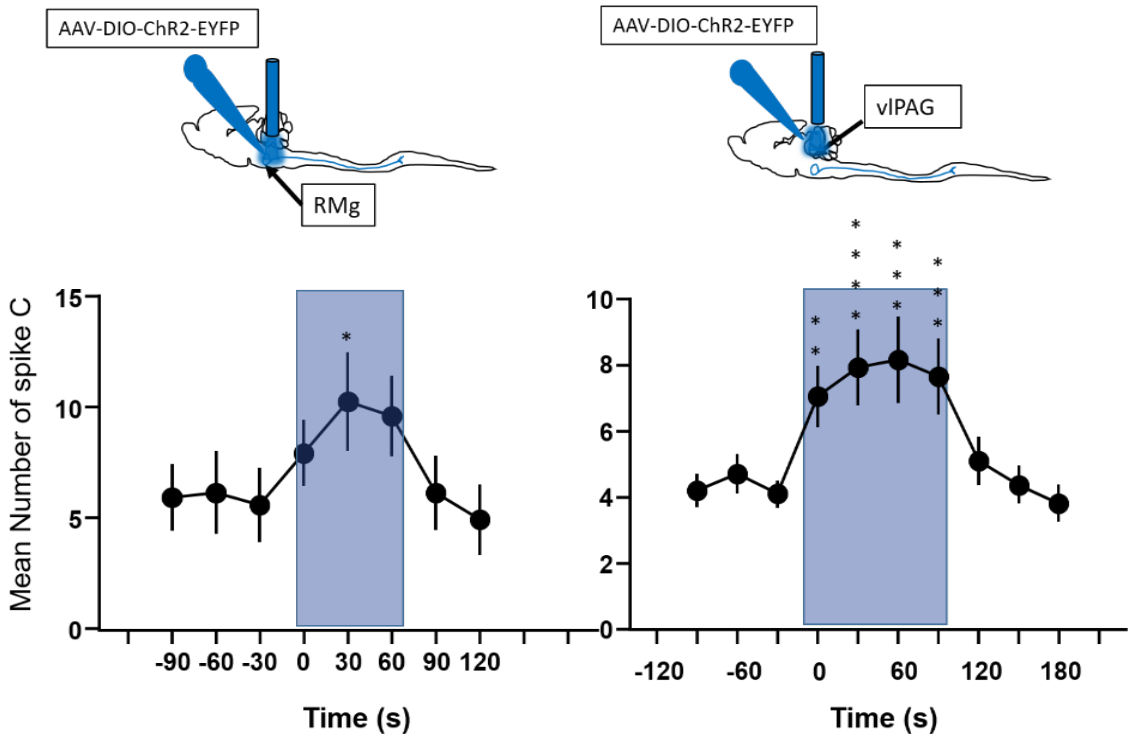

*Figure 85 : In vivo single unit recording of DHNs associated with an optogenetic activation of SST descending fibres above the RMg (ChR2-SST descending fibres) or SST neurons above the vlPAG (ChR2-SST). Optogenetic activation of ChR2-SST above the vlPAG or ChR2-SST descending fibres above the RMg with blue activating light at 2hz5ms during 2 min induced a relevant increase of DHN excitability resulting from an increase in the mean number DHNs responses to C-fibre input (ChR2-STT descending fibres mean number of C-spike before 5.5±1.6, during 10.5±1.7 and 5.7±1.4 after optical stimulation compare to ChR2 vlPAG SST mean number of C-spike before 4.4±0.5, during 7.7±1.1 and 4.4±0.6 after optical stimulation). Measure are reported as mean ± SEM; ChR2-STT descending fibres RMg *=p=0.0427 and ChR2-STT of vlPAG **= p=0.0010, ****= p<0.0001, ***[1]=p=0.0002 and ***[2]=p=0.0003 from Dunn's post hoc test.*

Therefore, as we hypothesize, vlPAG SSt neurons exert a tonic descending facilitation on pain transmission through probable inhibition of RMg 5-HT neurons.

Interestingly, with this viral approach (*Figure 86 and 87*), we also observed some vlPAG SST fibres in the dorsal horn of the spinal cord, especially in superficial layer (*Figure 87 A1-3*) as well as some FG staining colocalised with GFP-SST positive neurons in the vlPAG (*Figure 86A1-2*).

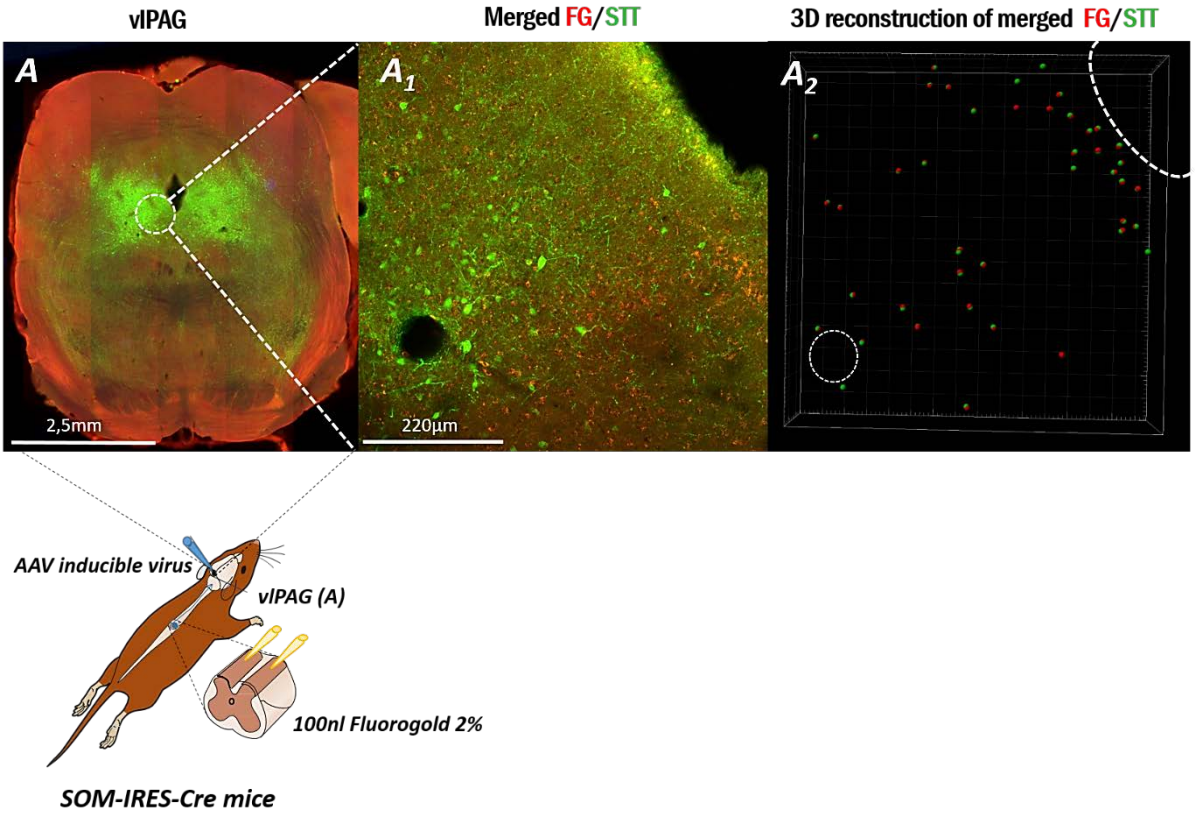

Figure 86 : Result of the viral strategy combined with the use of retrograde tracer (A). Confocal image (A1) and 3D reconstruction (A2) of cross-section of the vlPAG showing GFP positive cell in colacolise with FG staining from the spinal cord.

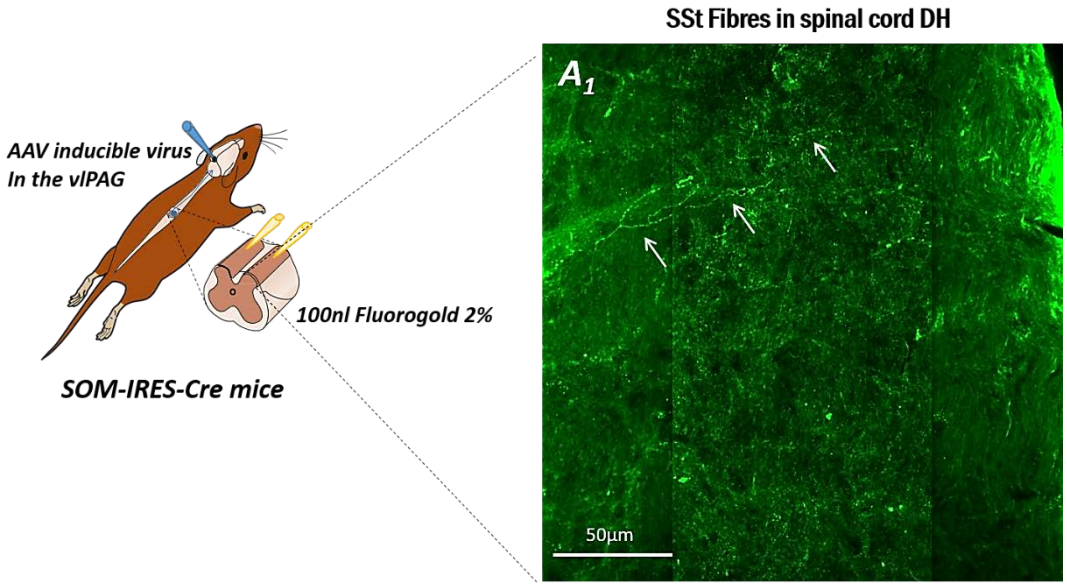

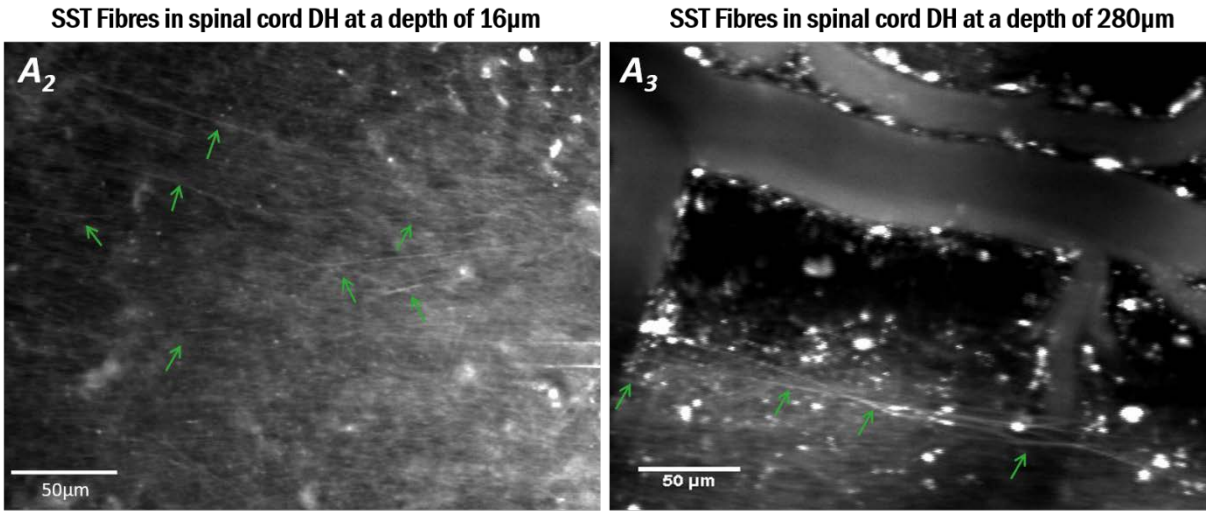

Figure 87 : Result of the viral strategy combined with the use of retrograde tracer. Confocal image (A1) of thin cross-section of the spinal cord showing vlPAG descending fibres (white arrows). In vivo biphoton microscope acquisition of vlPAG SST long-range fibres at a depth of 16 µm (A2, descending fibres) and 280µm (A3, superficial layer) into the dorsal horn of the spinal cord seen from above (green arrows).

Therefore, we hypothesise that vlPAG SST-induced descending facilitation may also pass through an inhibition directly in the dorsal horn neuron of the spinal cord.

c) *vlPAG SST-induce facilitation does not pass through dorsal horn spinal cord.*

To confirm the functional role of the spinal cord vlPAG SST descending fibres on nociceptive transmission, in anesthetised SOM-IRES-cre mice expressing ChR2 opsin in vlPAG SST neurons, we performed single-unit electrophysiological recording targeting WDRs associated with optogenetic stimulation above the spinal cord with the same light pattern that we used for the behaviour (2Hz5ms blue activating light at 475nm). Interestingly, we observed no change in either WDR response to C-fibre activation (*Figure* 88A, p=0.6987, F=0.7170; n=14 DHN) or WDR windup coefficient (*Figure* 88B, p>0.9999; n=7 DHN).

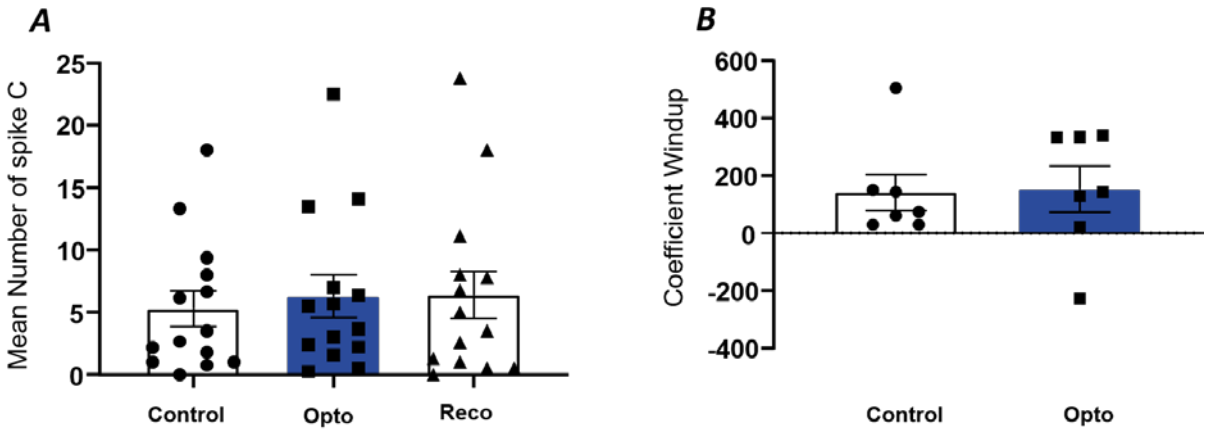

Figure 88: In vivo single-unit recording of DHNs associated with optogenetic activation of SST descending fibres above the dorsal horn of the spinal cord. Optogenetic activation of ChR2-SST descending fibres with blue activating light at 2hz5ms during 2 min above the spinal cord induced no change in DHN excitability neither in the mean number DHNs responses to C-fibre input nor in the windup coefficient (mean number of C-spike before 5.317±1.426, during 6.308±1.688 and after 6.412±1.894; n=14 DHN and for windup coefficient before 141.4±63.38 and during 153.1±79.21; n=7 DHN). Measure are reported as mean ± SEM.

Thus, although long-range SST neurons project to the spinal cord, they do not appear to influence nociceptive transmission.

We can, therefore, conclude that in conditions of acute pain, RMg 5-HT neurons exert a tonic inhibitory action on nociceptive transmission through direct action on Gabaergic/glycinergic inhibitory interneurons in the deep layer of the spinal dorsal horn and itself being under the influence of inhibitory somatostatin projection from the vlPAG.

However, RMg 5-HT, which exerts a tonic descending inhibition on pain transmission in acute pain, is known to facilitate pain transmission in pathological context (Gautier et al., 2017).

C. DESCENDING RMg 5-HT MODULATION ON SPINAL NOCICEPTIVE TRANSMISSION IN NEUROPATHIC PAIN.

Chronic pain in human is defined as a pain lasting for more than 3 to 6 months or persisting after a complete tissue healing or beyond the course of an acute disease. In the aim to mimic both the cardinal symptoms of clinically described neuropathic pain disorders and its duration in time, we used a spared nerve injury (SNI) model which resulted in consistent and reproducible pain hypersensitivity.

1. SNI leads as expect to mechanical and thermal hyperalgesia

First, we confirmed that SNI procedure resulted in a consistent neuropathic pain including a relevant decrease in the mechanical threshold and thermal latency observable 4 days later (*Figure* 89A, Ordinary one-way ANOVA SUDO, from j0 ipsi vs j0 contra, p=0.9977, n=20 and 20 respectively; j0 ipsi vs j4 ipsi, p<0.0001, n=20 and 19 respectively compared to j0 contra vs j4 contra, p=0.6103, n=20 and 19 respectively, to j0 ipsi vs j7 ipsi, p<0.0001, n=20 and 20 respectively compared to j0 contra vs j7 contra, p=0.9899; n=20 and 20 respectively and *Figure* 89B, Mann-Whithney test, plantar test j0 ipsi vs j0 contra, p=0.5294, n=24 and 24 respectively compared to j7 contra vs j7 ipsi, p=0.0007, n=18 and 18 respectively) that lasts over time and this in both females (*Figure* 89A1, Ordinary one-way ANOVA SUDO from j0 ipsi vs j0 contra, p>0.9999, n=12 and 12 respectively; j0 ipsi vs j4 ipsi, p<0.0001, n=12 and 8 respectively compared to j0 contra vs j4 contra, p=0.9967, n=12 and 8 respectively; to j0 ipsi vs j7 ipsi, p<0.0001, n=12 and 6 respectively compared to j0 contra vs j7 contra, p=0.9737, n=12 and 6 and *Figure* 89B1, Mann-Whithney test plantar test, j0 ipsi vs j0 contra, p=0.6139, n=13 and 13 respectively compared to j7 contra vs j7 ipsi, p=0.0157, n=7 and 7 respectively) and males (*Figure* 89A2, Ordinary one-way ANOVA SUDO from j0 ipsi vs j0 contra, p=0.9938, n=14 and 14 respectively; j0 ipsi vs j4 ipsi, p<0.0001, n=14 and 11 respectively compared to j0 contra vs j4 contra, p=0.1182, n=14 and 11 respectively; to j0 ipsi vs j7 ipsi, p<0.0001, n=14 and 14 respectively compared to j0 contra vs j7 contra, p=0.9477, n=14 and 14 and *Figure* 89B1, Mann-Whithney test plantar test, j0 ipsi vs j0 contra, p=0.2104, n=11 and 11 respectively compared to j7 contra vs j7 ipsi, p=0.0104, n=11 and 11 respectively).

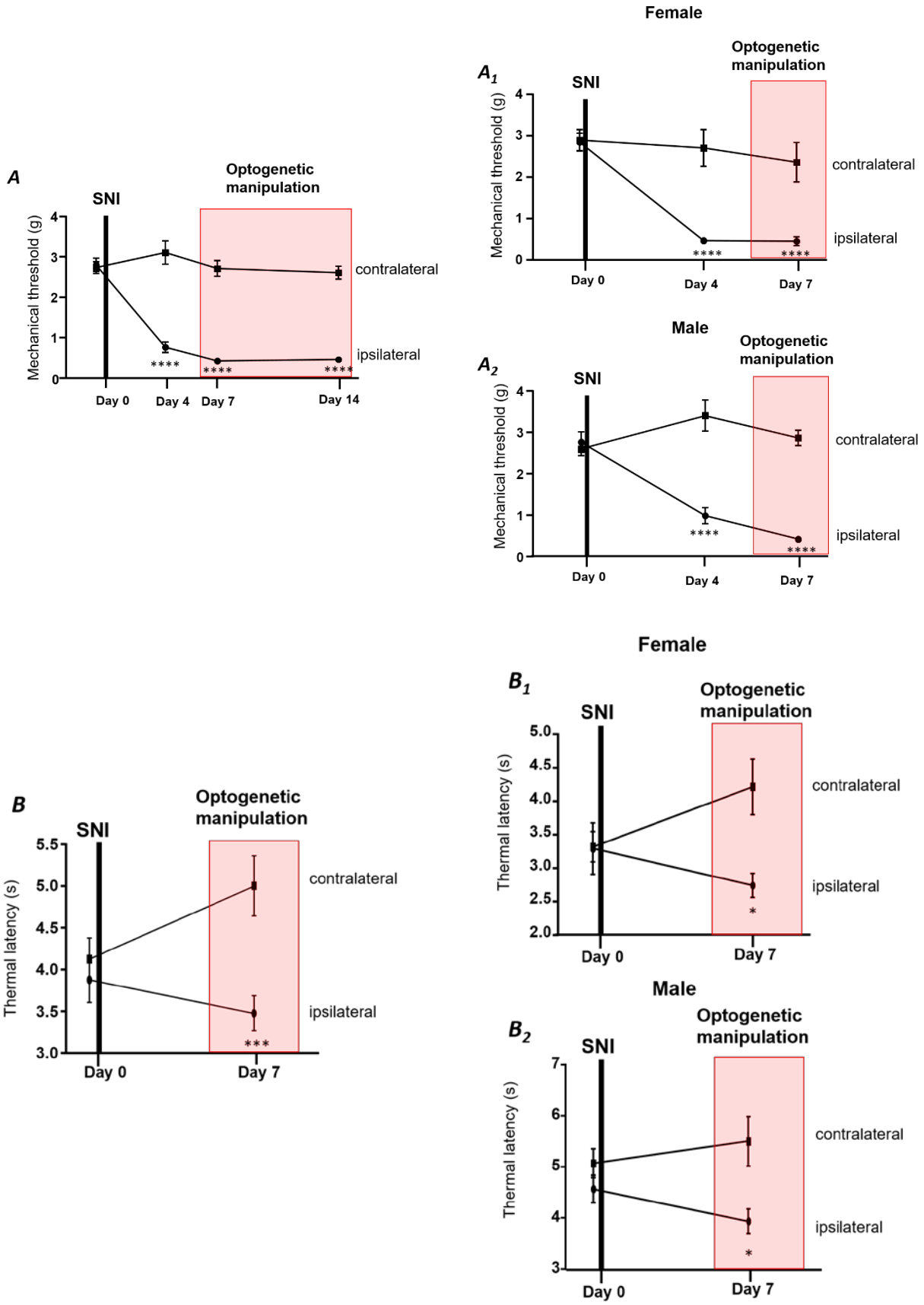

Figure 89 : Mechanical (A) and thermal (B) assessment of pain in SNI mice. Mechanical threshold and thermal latency after a sparse nerve injury substantially decrease in both females (A1-B1) and females (A2-B2). A) SUDO, ipsi from j0=2.7±0.2g,

*j4=0.8±0.1g, j7=0.4±0.0g to j14=0.5±0.0g; n=20, 19, 20, 6 respectively compared to contra from j0=2.5±0.1g, j4=3.102±0.291g, j7=2.7±0.2g to j14=2.6±0.2g; n=20, 19, 20,6 respectively. A1) SUDO female, ipsi j0=2.8±0.2g, j4=0.5±0.1g and j7=0.4±0.1g; n=12, 8 and 6 respectively compared to contra j0=2.9±0.3g, j4=2.7±0.4g and j7=2.4±0.5g, n=12, 8, 6 respectively. A2) SUDO male, ipsi j0=2.8±0.3g, j4=1±0.2g and j7=0.4±0.0g; n=14, 11 and 14 respectively compared to contra j0=2.6±0.2g, j4=3.4±0.4g and j7=2.9±0.2g, n=14, 11, 14 respectively. B) Plantar test, ipsi j0=3.9±0.3s and j7=3.5±0.2s; n=24 and 18 respectively compared to contra j0=4.1±0.3s and j7=5±0.4s; n=24 and 18 respectively. B1) Plantar test, female ipsi j0=3.3±0.4s and j7=2.7±0.2s; n=13 and 7 respectively compared to contra j0=3.3±0.2s and j7=4.2±0.4s; n=13 and 7 respectively. B2) Plantar test, male ipsi j0=4.6±0.3s and j7=3.9±0.2s; n=11 and 11 respectively compared to contra j0=5.1±0.3s and j7=5.5±0.5s; n=11 and 11 respectively. Measure are reported as mean ± SEM; SUDO, for all ****=p<0.0001, for female ****=p<0.0001 and male ****=p<0.0001 from Dunn's post hoc test; Plantar test for all ***=p=0.0007, for female *=p=0.0157 and male *=p=0.0104 from Mann-Whitney test. Pink rectangles show the period of optogenetic manipulations.*

2. Consequences of optogenetic manipulation of 5-HT neurons in neuropathic pain

a) *Inhibition of RMg 5-HT neurons does not influence the nociceptive transmission*

We performed optogenetic manipulation during the Second and third week after SNI surgical procedure (pink rectangle in *figure* 91). Interestingly, in freely moving 5-HT cre mice expressing ArchT opsin in 5-HT neurons of the RMg (the same group that we had used to perform mechanical and thermal assessment in acute pain condition), we observed that, after a sparse nerve injury, optogenetic inhibition with continuous green laser light (526.5nm continuous green inhibiting light for 2 min with power set at 10mW) of RMg 5-HT using an optical cannula above the RMg or above the dorsal horn of the spinal cord elicited no change in mechanical threshold and thermal latency (*Figure* 90 and 91). Mechanical threshold was not modified (*Figure* 90A1, SUDO, SNI-ArchT-5-HT, Friedman test p=0.7778, F=2; n=5 and SNI-ArchT-5-HT descending fibres, Friedman test p>0.9999, F=0.2857; n=5 and *Figure* 91B1 Repeated measure SNI-ArchT-5-HT, Friedman test p=0.3951, F=2.8; n=5 and SNI-ArchT-5-HT descending fibres, Friedman test p=0.1605, F=3.875; n=5) contrary to what we observed in the same animals before SNI procedure (*Figure* 90A2)).

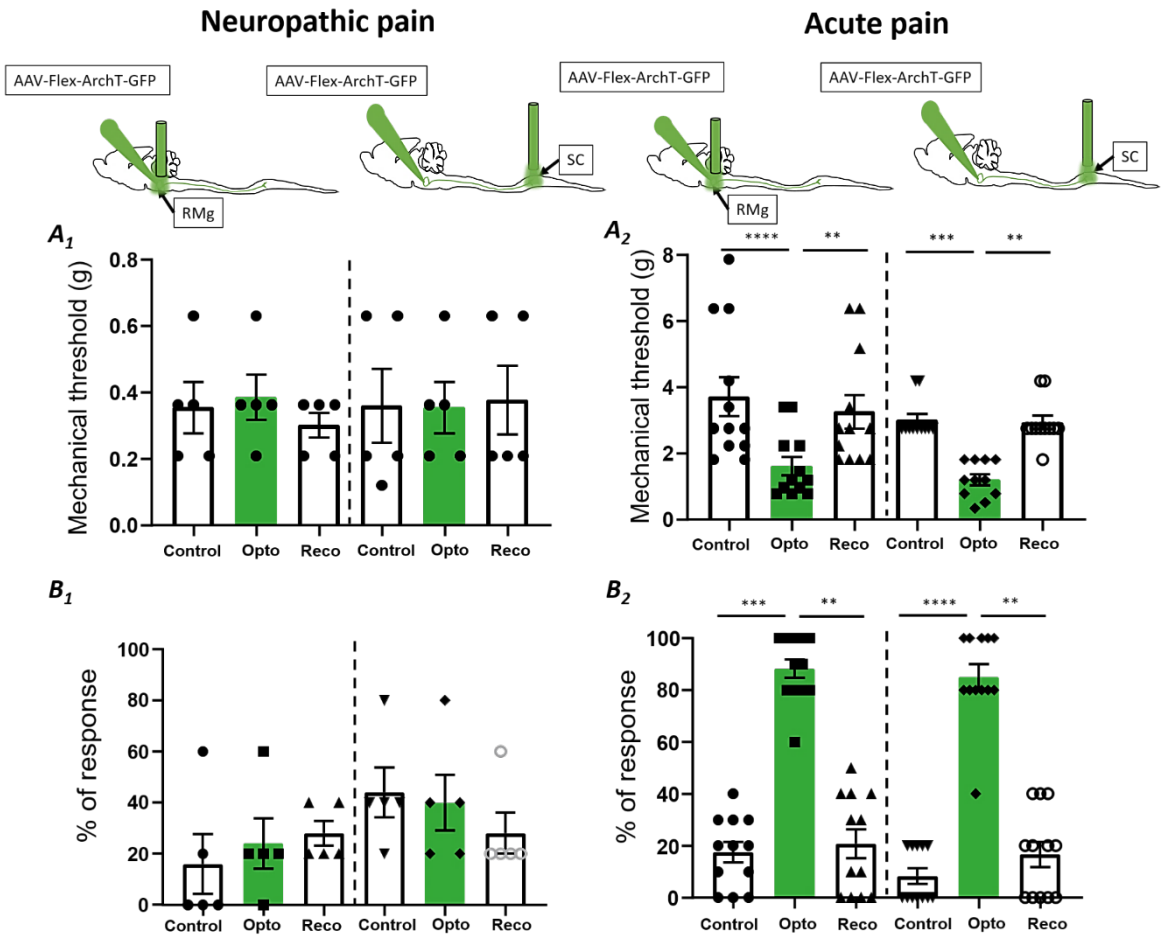

*Figure 90 : Mechanical assessment of 5-HT inhibition both at the level of RMg and spinal cord (SC) in neuropathic condition: Optogenetic inhibition of SNI-ArchT-5-HT or SNI-ArchT-5-HT descending fibres above the RMg or the spinal cord, respectively, with continuous green light during 2 min induced no change in mechanical threshold (A1, SUDO for SNI- ArchT-5-HT: 0.4±0.1g before, 0.4±0.1g during and 0.3±0.0g post-stimulation; for SNI-ArchT-5-HT descending fibres: 0.4±0.1g before, 0.4±0.1g during and 0.4±0.1g post-stimulation and B1, Repeated measure, with innocuous stimuli or to a lesser extent slightly noxious stimuli, for SNI-ArchT-5HT: 16±11.7% before, 24±10% during and 28±4.9% of response post-stimulation; for SNI-ArchT-5-HT descending fibres: 44±9.8% before, 40±11% during and 28±8% of response post-stimulation) contrary to what we had observed before the SNI where optogenetic inhibition of ArchT-5-HT above the RMg or ArchT-5-HT descending fibres above the spinal cord, had elicited a mechanical allodynia and hyperalgesia. Measures are reported as mean ± SEM; A2, SUDO, ArchT-5-HT of RMg **=p=0.0062, ****= p<0.0001 and ArchT-5-HT descending fibres SC **=p=0.0013, ***=p=0.0006; B2, Repeated Measure ArchT-5-HT of RMg **=p=0.0015, ***=p=0.0001 and ArchT-5-HT descending fibres SC **=p=0.0022 and ****=p<0.0001 from Dunn's post hoc test.*

Thermal latency was not changed (*Figure* 91A, Plantar test SNI-ArchT-5-HT, Friedman test p=0.3673, F=2.8; n=5 and SNI-ArchT-5-HT descending fibres, Friedman test p=0.6914, F=1.2; n=5) contrary to what we observed before the SNI where optogenetic inhibition of ArchT-5-HT or ArchT-5-HT descending fibres above both the RMg or the spinal cord respectively, had elicited a thermal hyperalgesia (*Figure 91B).*

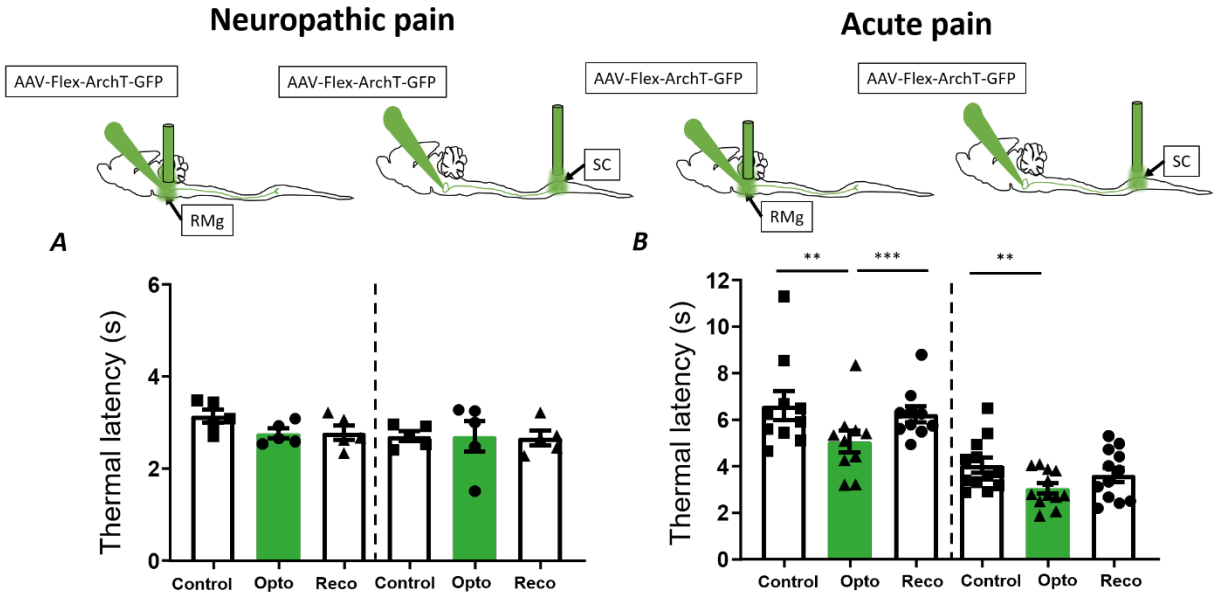

*Figure 91 : Thermal assessment of 5-HT inhibition both at the level of RMg and spinal cord (SC) in neuropathic condition: Optogenetic inhibition of SNI-ArchT-5-HT or SNI-ArchT-5-HT descending fibres above the RMg or the spinal cord, respectively, with continuous green light during 2 min induced no change in mechanical threshold (A, Plantar test for SNI- ArchT-5-HT: 3.135±0.149s before, 2.761±0.107s during and 2.779±0.160s post-stimulation and for SNI-ArchT-5-HT descending fibres: 2.707±0.107s before, 2.70±0.330s during and 2.665±0.159s post-stimulation) contrary to what we observed before the SNI where optogenetic inhibition of ArchT-5-HT above the RMg or ArchT-5-HT descending fibres above the spinal cord, had elicited a thermal hyperalgesia. Measure are reported as mean ± SEM; B, ArchT-5-HT of RMg **=p=0.0035, ***=p=0.0007 and ArchT-5-HT descending fibres SC **=p=0.001 from Dunn's post hoc test.*

Therefore, contrary to what we observed in acute pain conditions, in neuropathic pain conditions, the inhibition of 5-HT of the RMg does not modify the mechanical threshold or the thermal latency, suggesting that 5-HT, in neuropathic pain conditions, loses its tonic activity.

b) *Activation of RMg 5-HT neurons induces mechanical hyperalgesia and allodynia and thermal hyperalgesia.*

As for the inhibition, in freely moving 5-HT cre mice expressing ChR2 opsin in RMg 5-HT (the same group that we had used to perform mechanical and thermal assessment in acute pain condition), we observed that, after a spared nerve injury, optogenetic activation with a blue activating light (475nm, blue light at 5Hz/5ms, 10mW for 2 minutes) of RMg 5-HT using an optical cannula above the RMg or above the spinal cord dorsal horn elicited significant decrease in both mechanical threshold and thermal latency that was suppressed after light switched off (*Figure* 92 and 93. Mechanical threshold (*Figure* 92A1, SUDO, SNI-ChR2-5-HT, Friedman

test p=0.0041, F=11.47; n=6 and SNI-ChR2-5-HT descending fibres, Friedman test p<0.0001, F=34.86; n=18 and *Figure* 89A2, Repeated measure, SNI-ChR2-5-HT, Friedman test p=0.0054, F=9.478; n=6 and SNI-ChR2-5-HT descending fibres, Friedman p<0.0001, F=24.40; n=18). By Contrast, we confirmed before the SNI, that optogenetic manipulation elicited mechanical analgesia (*Figure* 92A2).

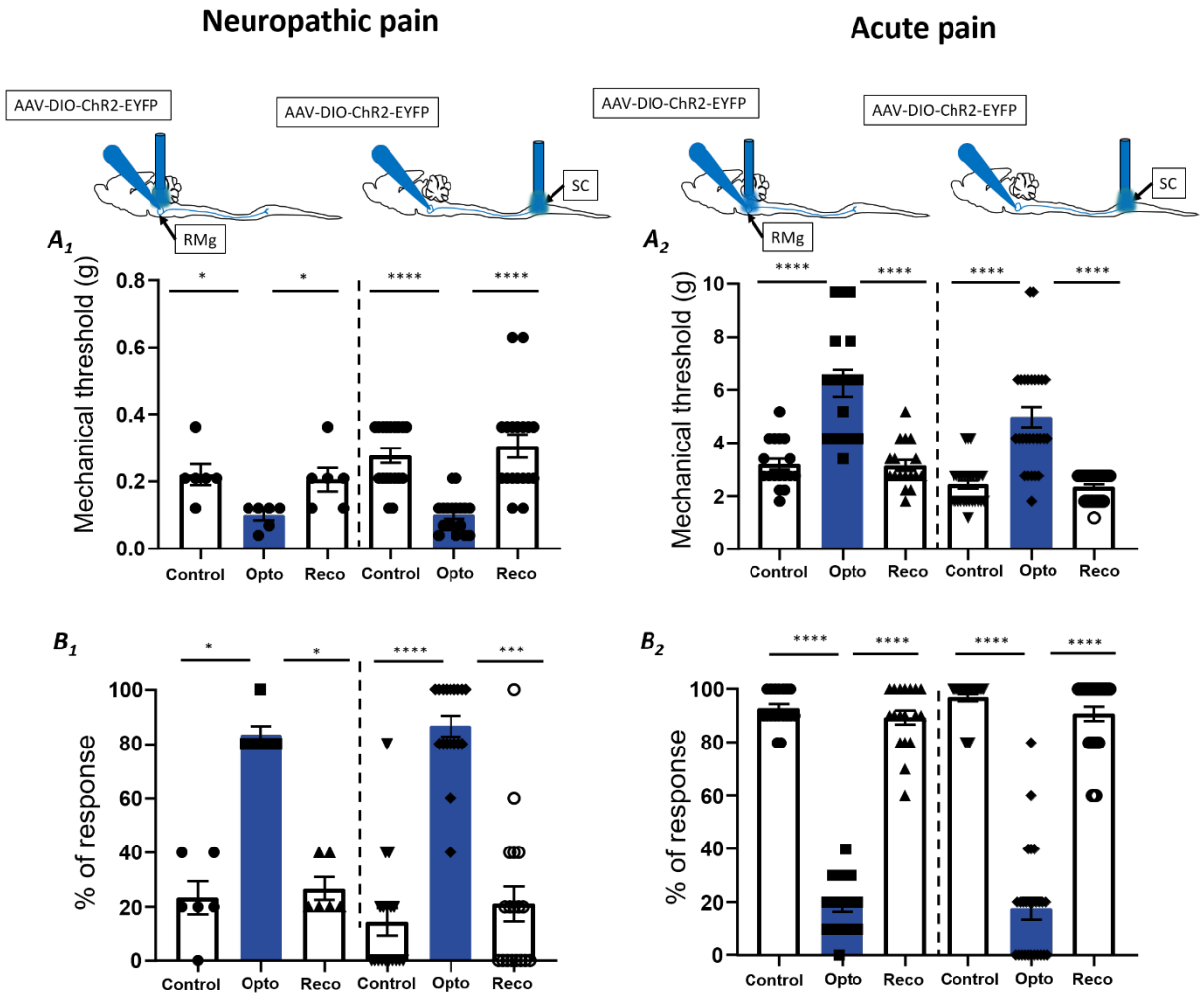

*Figure 92 : Mechanical assessment of 5-HT activation both at the level of the RMg and spinal cord (SC) in neuropathic pain condition: Optogenetic activation of SNI-ChR2-5-HT neurons or SNI-ChR2-5-HT descending fibres above the RMg or the spinal cord respectively, with 475nm blue activating light at 5Hz5ms during 2 min induced a relevant decrease in mechanical threshold (SUDO A1, SNI-ChR2-5-HT: 0.2±0.0g before, 0.1±0.0g during and 0.2±0.0g post-stimulation; for SNI-ChR2-5-HT descending fibres: 0.3±0.0g before, 0.1±0.0g during and 0.3±0.0g post-stimulation and B1, Repeated measure with innocuous stimuli: SNI-ChR2-5-HT: 23.3±6.1% before, 83.3±3.3% during and 26.7±4.2% post-stimulation; for SNI-ChR2-5-HT descending fibres: 14.4±5.0% before, 86.7±4% during and 21.1±6.3% post-stimulation) resulting then in mechanical allodynia and hyperalgesia as opposed to what has been observed in acute pain condition, where optogenetic activation of ChR2-5-HT above the RMg or ChR2-5-HT descending fibres above the spinal cord resulted in mechanical. Measures are reported as mean ± SEM; SUDO, A1, SNI-ChR2-5-HT of RMg: *[1]=p=0.0122, *[2]=p=0.0283 and SNI-ChR2-5-HT descending fibres SC, ****=p<0.0001; A2, ChR2-5-HT of RMg or ChR2-5HT-descending fibre SC, ****=p<0.0001 and Repeated measure, B1, SNI-ChR2-5-HT of RMg,*

*[*1]=p=0.0122, *[*2]=0.0283 and ChR2-5-HT descending fibres SC, ***=p=0.0007, ****=p<0.0001 and B2, ChR2-5-HT of RMg or ChR2-5HT-descending fibre SC, ****=p<0.0001 from Dunn's post hoc test.*

Thermal latency (*Figure* 93A Plantar test, Friedman test, SNI-ChR2-5-HT, p=0.0055, F=9.333; n=6 and SNI-ChR2-5-HT descending fibres, p<0.0001, F=21.33; n=18). Again, before SNI, optogenetic activation of RMg 5-HT elicited thermal analgesia (*Figure* 93B).

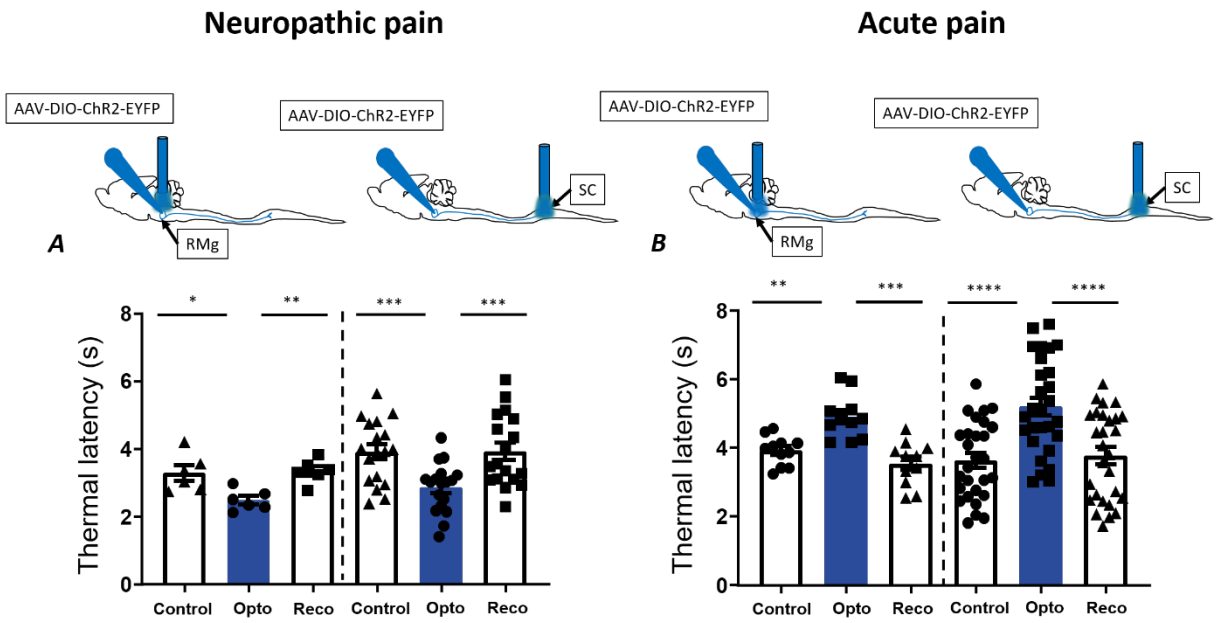

*Figure 93 : Thermal assessment of 5-HT activation both at the level of RMg and spinal cord (SC) in neuropathic condition: Optogenetic activation of SNI-ChR2-5-HT above the RMg or SNI-ChR2-5-HT descending fibres above the spinal cord with 475nm blue activating light at 5Hz5ms during 2 min induced a relevant decrease in thermal latency (A, Plantar test for SNI-ChR2-5-HT: 3.3±0.2s before, 2.5±0.1s during and 3.3±0.1s post-stimulation and SNI-ChR2-5-HT descending fibres: 3.9±0.2s before, 2.9±0.2s during and 3.9±0.3s post-stimulation) resulting then in thermal hyperalgesia as opposed to what we observed before the SNI where optogenetic activation of ChR2-5-HT above the RMg or ChR2-5-HT descending fibres above the spinal cord, had elicited a thermal analgesia. Measure are reported as mean ± SEM; A, SNI-ChR2-5-HT of RMg: *=p=0.0418, **=p=0.0078 and SNI-ChR2-5-HT descending fibres SC, ***=p=0.0001 and B, ChR2-5-HT of RMg, **=p=0.0028, ***=p=0.0002 and ChR2-5-HT descending fibres SC, ****=p<0.0001from Dunn's post hoc test.*

By contrast, in mice expressing only GFP tag, optogenetic manipulation had no effect. (*Figure* 94).

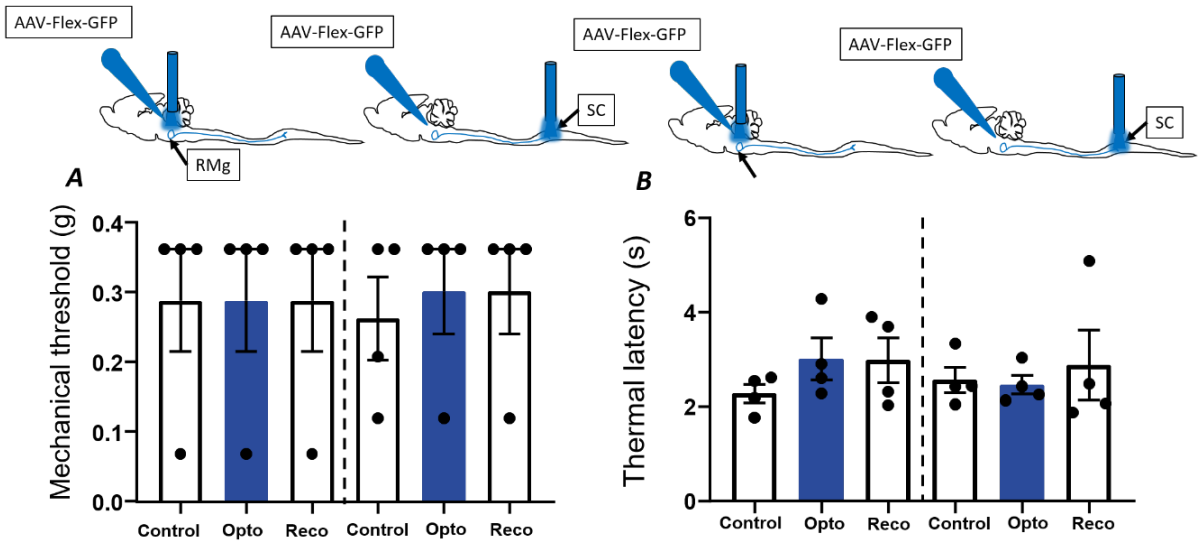

Figure 94 : Mechanical and thermal assessment of 5-HT activation both at the level of the RMg and spinal cord (SC) in neuropathic pain condition: Optogenetic stimulation of SNI-GFP-5-HT neurons or SNI-GFP-5-HT descending fibres above the RMg or the spinal cord respectively, with 475nm blue activating light at 5Hz5ms during 2 min induced no change in mechanical threshold (A, SUDO, SNI-GFP-5-HT: 0.3±0.0g before, 0.3±0.1g during and 0.3±0.1g post-stimulation, Friedman test p=approximate, n=4; for SNI-GFP-5-HT descending fibres: 0.3±0.1g before, 0.3±0.1g during and 0.3±0.1g post-stimulation, Friedman test p>0.9999, F=2; n=4) and thermal latency (B, Plantar test for SNI-GFP-5-HT: 2.3±0.2s before, 3.0±0.4s during and 3±0.5s post-stimulation, Friedman test p=0.4306, F=2; n=4 and SNI-GFP descending fibres: 2.6±0.3s before,2.5±0.2s during and 2.9±0.7s post-stimulation, Friedman test p=0.9306, F=0.5; n=4). Measures are reported as mean ± SEM.

Therefore, in neuropathic pain, 5-HT neurons of the RMg lose its analgesic effect and exert descending facilitation on pain transmission.

c) *RMg 5-HT descending facilitation is not influenced by gender*

However, in clinical practice, it has been shown that women are more likely to develop chronic neuropathic pain (Chenaf et al., 2018; IASP, 2019b) and we hypothesized that 5-HT of the RMg may contribute to this difference. We compared the effect of optogenetic activation of 5-HT descending fibres into the dorsal horn both in males and females expressing ChR2 opsin in RMg 5-HT with regard to the mechanical and thermal sensation and we observed no difference (*Figure* 95).Indeed, optogenetic activation of 5-HT neurons induced in male and female a significant decrease in both mechanical threshold (*Figure* 95A, SUDO, for male Friedman test $p<0.0001$, $F=18.73$ and for female $p<0.0001$, $F=14$; $n=11$ and 7 respectively) and thermal latency (*Figure* 95B, Plantar test, male Friedman test $p=0.0029$, $F=11.09$ and female $p=0.0027$, $F=10.57$; $n=11$ and 7 respectively), resulting in both cases in mechanical allodynia and mechanical and thermal hyperalgesia.

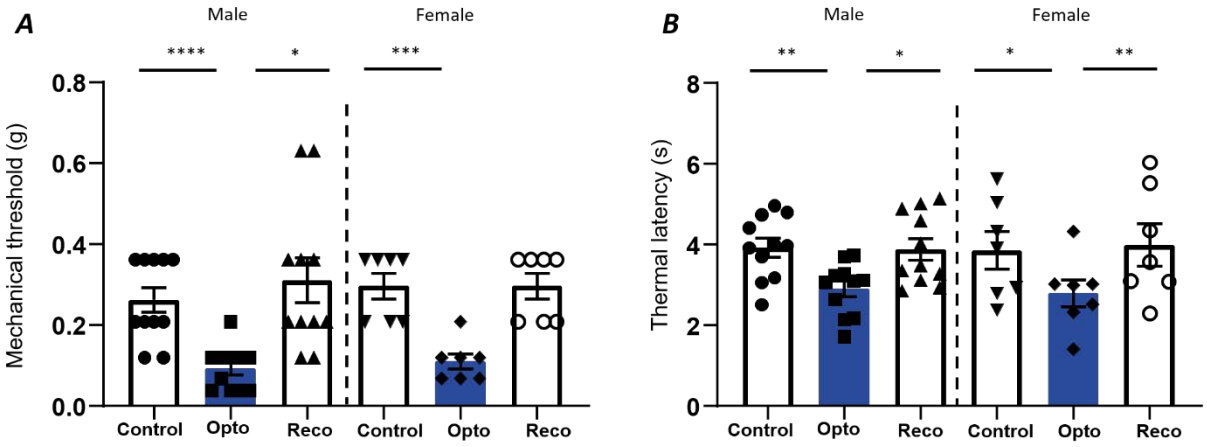

*Figure 95 : Gender do not influence 5-HT-induced facilitation on pain transmission in neuropathic pain. A) Optogenetic activation of SNI-ChR2-5-HT descending fibres induced in both male and female, a relevant decrease in mechanical threshold (A for male SNI-ChR2-5HT descending fibres: 0.3±0.0g before, 0.1±0.0g during and 0.3±0.1g post-stimulation; for female SNI-ChR2-5HT descending fibres: 0.3±0.0g before, 0.1±0.0g during and 0.2±0.0g post-stimulation) and thermal latency (B for male SNI-ChR2-5HT descending fibres: 3.9±0.2s before, 2.9±0.2s during and 3.9±0.3s post-stimulation; for female SNI-ChR2-5HT descending fibres: 3.9±0.5s before, 2.8±0.3s during and 4±0.5s post-stimulation) without any difference with regard to the intensity of 5-HT descending facilitation in both male and female (C, Net change induced by 5-HT optogenetic activation, SUDO for male -64.1±4.6% compare to female -60.4±6.7% and Plantar test for male -25.7±4% compare to female -26.6±5.1%). Measure are reported as mean ± SEM; SUDO male *=p=0.0112, ****=p<0.0001 and female ***=p=0.0004; Plantar test male *=p=0.0112, **=p=0.0057 and female *=p=0.0151, **=0.0066 from Dunn's post hoc test.*

3. Consequences of optogenetic manipulation of 5-HT neurons on dorsal horn neurons.

a) *In neuropathic pain condition, the modulation of 5-HT neurons of the RMg modify differently DHN excitability*

We next assessed the consequence of manipulation of RMg 5-HT on pain transmission within the dorsal horn (*Figure* 96 and 97). With regard to WDR excitability, in anesthetised 5-HT cre mice expressing ArchT in the 5-HT neurons of RMg, *in vivo* recording of the spinal WDRs associated with optogenetic stimulation above the spinal cord (526.5nm continuous green inhibiting light with power set at 10mW) showed no change in response to nociceptive C-fibre stimulation (*Figure* 96A)

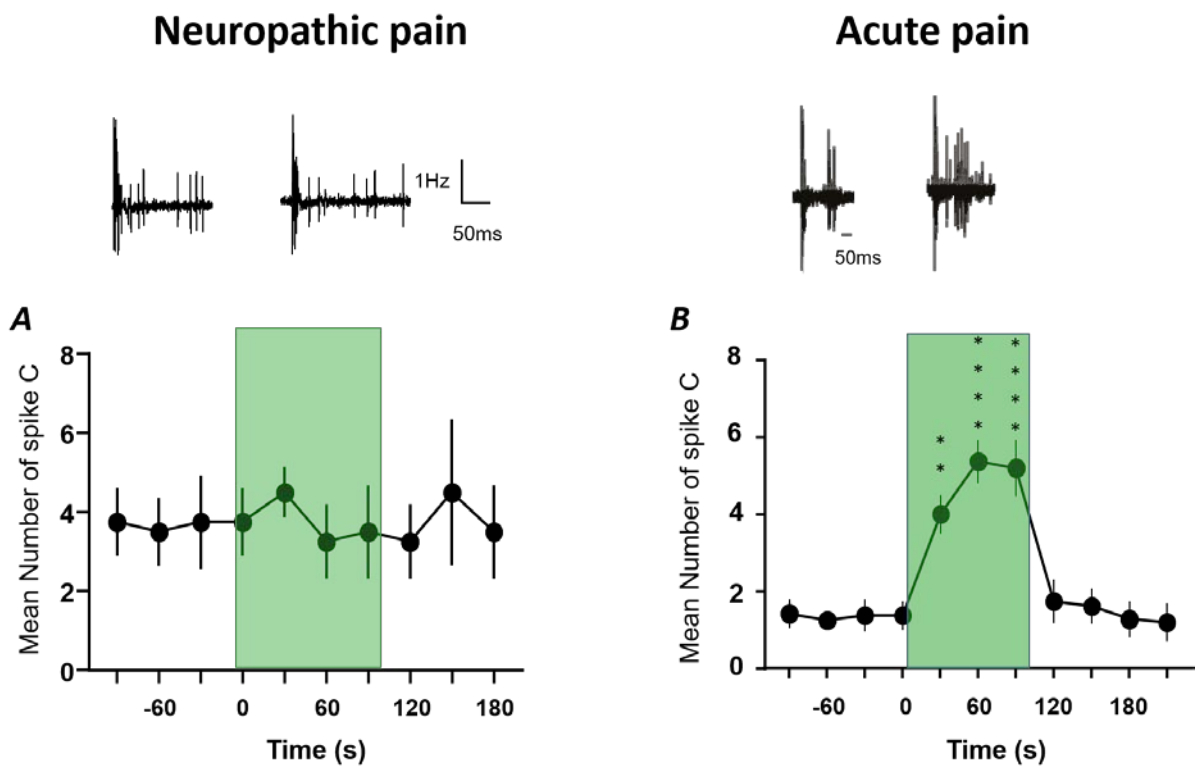

*Figure 96 : In vivo single-unit recording of DHNs associated with optogenetic inhibition of 5-HT neuron of the RMg projecting to the dorsal horn of the spinal cord in neuropathic pain condition. A-B above, representative WDR neuron response to noxious electrical stimuli recorded before and during optogenetic stimulation before (B) and after SNI procedure (A). In neuropathic pain condition (A), DHN excitability did not change during optogenetic stimulation of SNI-Archt-5-HT descending fibres (the mean number of C-spike before 3.7±1, during 3.8±1 and after 3.8±1.3; ordinary one-way ANOVA p=0.9961, F=0.1664; n=4) as opposed to what we observed before the SNI where optogenetic inhibition of SNI-Archt-5-HT descending fibres above the spinal cord, had resulted in DHN hyper-excitability. Measure are reported as mean ± SEM; B, Mean number of C spike **= p=0.0021 and ****= p<0.0001 from Dunn's post hoc test.*

By contrast, optogenetic activation of RMg 5-HT using 475nm blue activating light at 5Hz5ms induced a significant increase in WDR response to nociceptive inputs (*Figure* 97A2, Ordinary one-way ANOVA p=0.0013, F=5.187; n=7) resulting in DHN hyper-excitability which is the opposite to what we observed before the SNI.

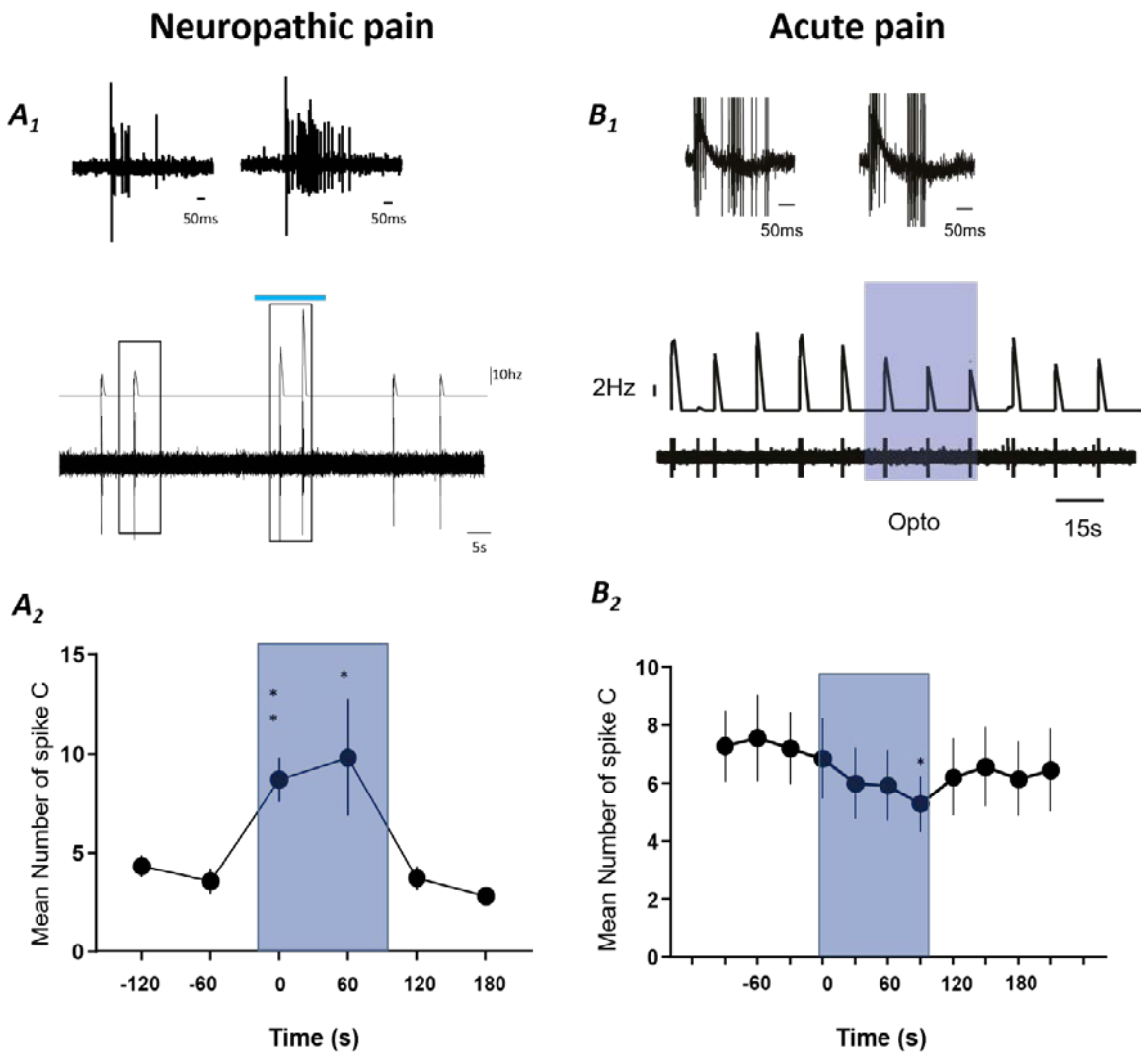

*Figure 97 : In vivo single unit recording of DHNs associated with optogenetic activation of 5-HT neurons of the RMg projecting to the dorsal horn of the spinal cord in neuropathic pain condition. One sample showing an increase (A1) or a decrease (B1) of DHN response to noxious stimuli during optogenetic stimulation of ChR2-5-HT descending fibres (above, representative WDR neuron response to a noxious electrical stimuli recorded before and during optogenetic stimulation before (B) and after SNI procedure (A)). In neuropathic pain condition (A2), the mean number DHNs responses to C-fibre input is increased during optogenetic activation of SNI-ChR2-5-HT descending fibres (mean number of C-spike before 4±0.6, during 9.3±2.0 and after 3.3±0.5) as opposed to what we observed before the SNI (B2) where optogenetic inhibition of SNI-Archt-5-HT descending fibres above the spinal cord, had resulted in a decrease of the DHN excitability (mean number of C-spike before 7.4±1.3, during 6.0±1.2 and after 6.3±1.4). Measure are reported as mean ± SEM; A, Mean number of C spike *= p=0.0274, **=0.0079 and B, Mean number of C spike *= p=0.0373 from Dunn's post hoc test.*

Therefore, in neuropathic pain condition, 5-HT neurons projecting to the dorsal horn, facilitate the nociceptive transmission by increasing WDR response to C-fibres inputs resulting in WDR hyper-excitability.

4. RMg 5-HT neurons target also inhibitory interneuron in the dorsal horn of the spinal cord in SNI condition

We then studied possible changes induce by neuropathic condition in RMg 5-HT targets onto the dorsal horn of the spinal cord (*Figure 98)*. To do so, as with the acute pain condition, we compared apposition between GFP staining and both excitatory (Tlx3, *Figure 98A2*) and inhibitory (Pax2 *Figure 98B2*) interneurons and we found that 5-HT fibres (*Figure 98A1-B1)* always mainly project onto inhibitory interneurons (*Figure 98A3-B3)*.

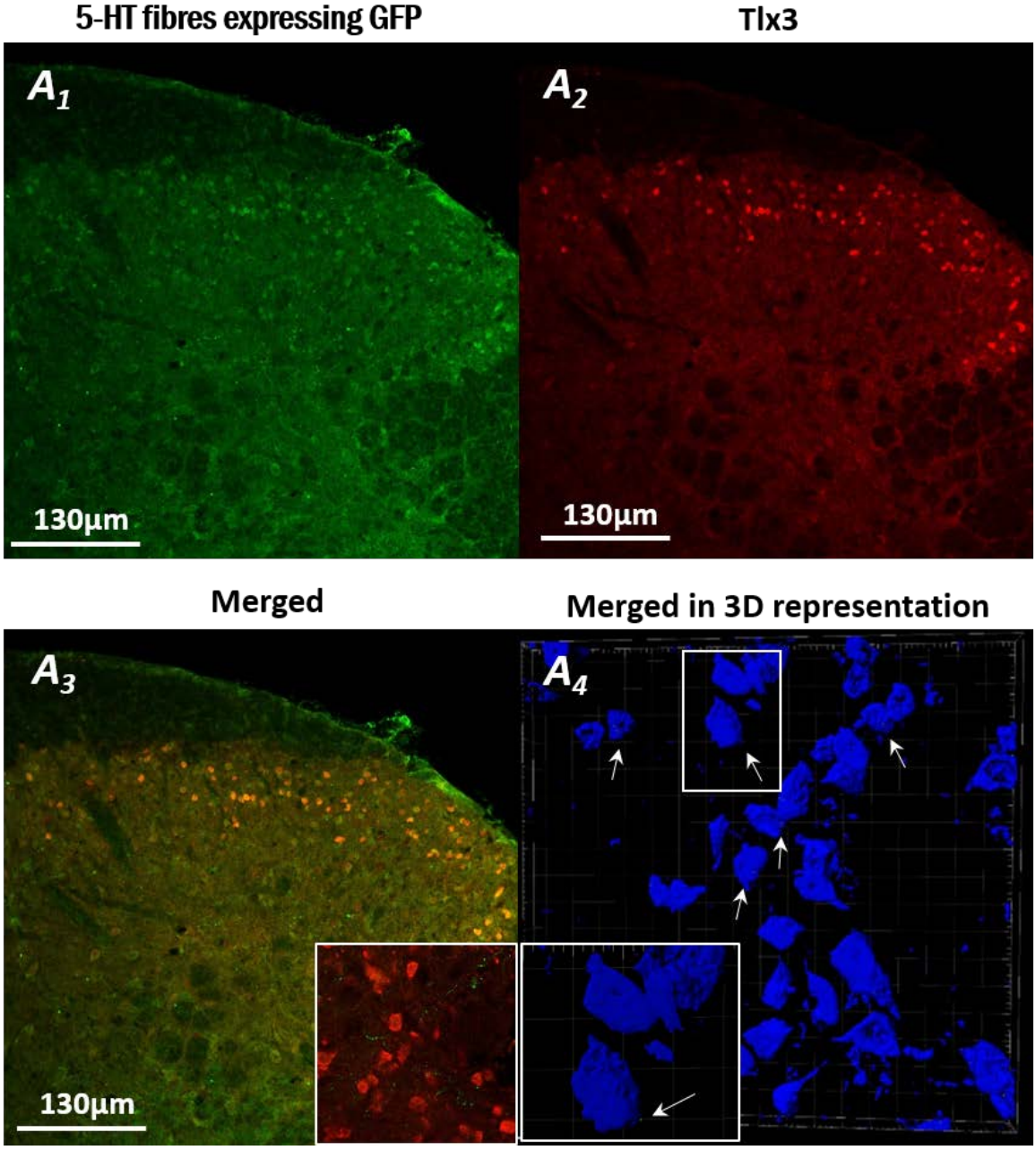

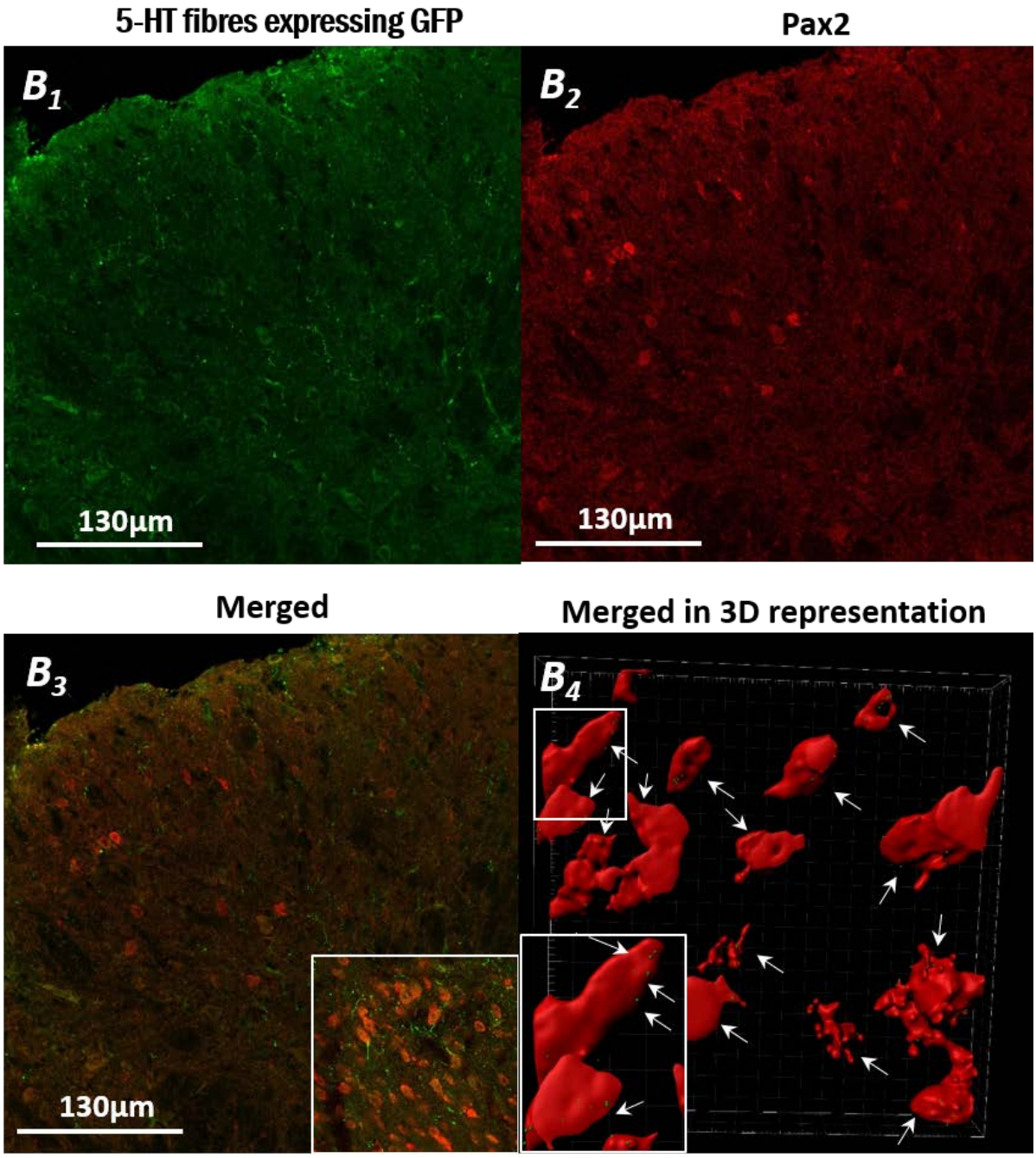

Figure 98 : Confocal image and 3D representation of AAV-flex-GFP expression in 5-HT neurons of the RMg projecting into the dorsal horn of the spinal cord in combination with Tlx3 (A) and Pax2 (B) staining in thin slice of lumbar spinal cord of 5-HT cre mice with a spared nerve injury. A1-4) Tlx3 excitatory marker immunostaining (red) showed superficial cell body that are very little contacted by GFP fibres (A4 white sparrow). B1-4) Pax2 inhibitory marker immunostaining (red) showed cell body in dorsal horn of the spinal cord that are mostly contacted with GFP fibre (B4 white sparrow) from 5HT neurons of the RMg.

Thus, it can be suggested that, in neuropathic pain conditions, the descending facilitation induced by RMg 5-HT neurons on nociceptive pain transmission passes also through the inhibitory interneuron of dorsal horn of the spinal cord, In neuropathic pain model including SNI, it has been shown that disinhibition mechanisms are responsible for a part of neuronal

hyper-excitability and pain hypersensitivity (Coull et al., 2005; Beggs et al., 2012), which suggest that the opposite serotonergic drive observed in control and SNI may be due to the change in chloride balance in afferent fibres or DHNs neurons that would switch inhibitory influences onto excitatory. (Lavertu et al., 2014).

D. INFLUENCE OF DHN CHLORIDE BALANCE ON RMg 5-HT MODULATION.

1. RMg 5-HT-induced pain facilitation is mediated by dorsal horn KCC2 cotransporter in SNI

a) *CLP 290 reverse the RMg 5-HT facilitation on pain transmission*

It has been shown that the chloride balance is mediated by the cationic chloride cotransporters KCC2 (Doyon, 2011; Kaila et al., 2014). A decrease in KCC2 activity or expression could lead to disinhibition mechanisms. We used a pharmacological approach to boost KCC2 in SNI 5-HT cre mice expressing ChR2 opsin in RMg 5-HT neurons. *Per os* treatment of SNI mice with CLP290 (Mapplebeck et al., 2019a), a specific enhancer of KCC2 transporters, induced a slight but significant increase in mechanical threshold and thermal latency (*Figure* 99). Indeed, in SNI mice where optogenetic activation of 5-HT descending fibres (SNI-ChR2-5-HT descending fibres) induced a mechanical allodynia and hyperalgesia (*Figure* 99A control, SUDO, SNI-ChR2-5-HT descending fibres, Friedman test $p<0.0001$, $F=23.41$; $n=12$ and *Figure* 99B control, Repeated measure SNI-ChR2-5-HT descending fibres, Friedman test $p<0.0001$, $F=20.57$; $n=12$) and thermal hyperalgesia (*Figure* 99C control Plantar test, SNI-ChR2-5-HT descending fibres, Friedman test $p=0.0018$, $F=12.67$; $n=12$) 1h30 after CLP290, the same optogenetic activation in the same animals induces a significant increase in mechanical threshold (*Figure* 99B CLP 290, SUDO, SNI-ChR2-5-HT descending fibres, Friedman test $p<0.0001$, $F=22.21$; $n=12$ and *Figure* 99B CLP290, Repeated measure SNI-ChR2-5-HT descending fibres, Friedman test $p<0.0001$, $F=21.51$; $n=12$) and thermal latency resulting in mechanical and thermal analgesia (*Figure* 99C CLP 290 Plantar test, SNI-ChR2-5-HT descending fibres, Friedman test $p<0.0001$, $F=20.67$; $n=12$) that was not present when the vehicle (i.e, HSPD 20%) alone was applied (*Figure* 99A vehicle, SUDO, SNI-ChR2-5-HT descending fibres, Friedman test $p<0.0001$, $F=22.74$; $n=12$ and *Figure* 99B vehicle, Repeated

measure SNI-ChR2-5-HT descending fibres, Friedman test p<0.0001, F=22.21; n=12 and *Figure* 99C vehicle Plantar test, SNI-ChR2-5-HT descending fibres, Friedman test p=0.0001, F=18.17; n=12).

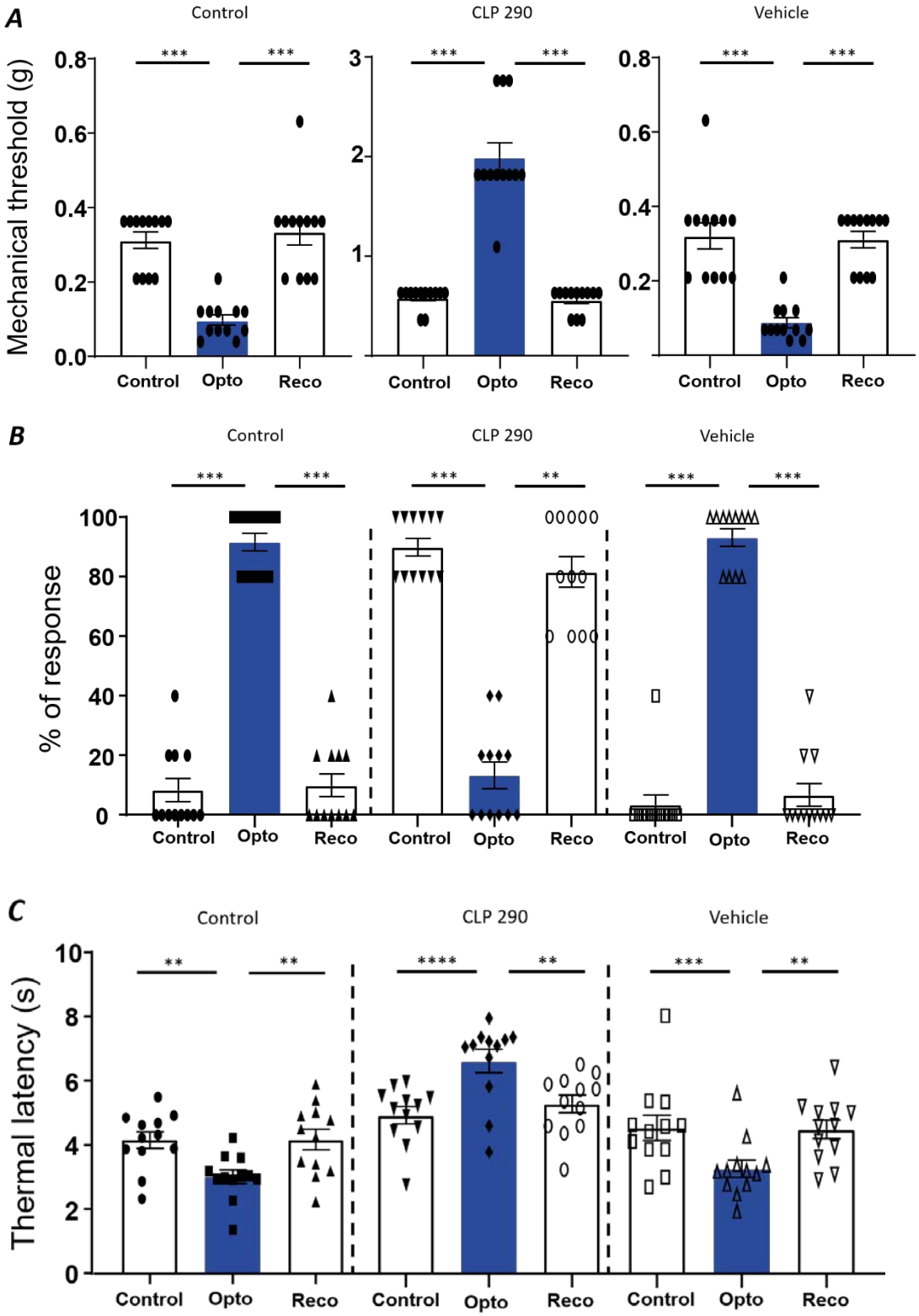

Figure 99 : CLP 290 treatment on 5-HT cre mice with a spared nerve injury expressing ChR2 opsin in 5-HT neurons of the RMg. CLP290 prevent mechanical and thermal hypersensitivity induced by optogenetic activation of 5-HT descending fibres. A, B and C control) In SNI mice, optogenetic stimulation induced a decrease in mechanical threshold (A control, SUDO for SNI-ChR2-

*5-HT descending fibres: 0.3±0.0g before, 0.1±0.0g during and 0.3±0.0g post stimulation) including an increase in the percentage of hind-paws response to repeated innocuous stimuli stimuli (B control, Repeated measure for SNI-ChR2-5-HT descending fibres: 8.3±3.9% before, 91.7±3.0% during and 10±3.9% of response post stimulation) and a decrease in thermal latency (C control, Plantar test, for SNI-ChR2-5-HT descending fibres: 4.3±0.3s before, 3.1±0.2s during and 4.3±0.3s post stimulation) resulting in mechanical allodynia and hyperalgesia and in thermal hyperalgesia. A, B and C clp290) In the same animals, 1h30min after CLP290 per os application, the same optogenetic stimulation induced an increase in mechanical threshold (A clp290, SUDO for SNI-ChR2-5-HT descending fibres: 0.6±0.0g before, 2±0.1g during and 0.6±0.0g post-stimulation) including an increase in the percentage of hind-paws response to repeated noxious stimuli (B clp 290, Repeated measure for SNI-ChR2-5-HT descending fibres: 90±3.0% before, 13.3±4.5% during and 81.7±5.2% of response post-stimulation) resulting in mechanical analgesia and an increase in thermal latency (C, clp 290, Plantar test, for SNI-ChR2-5-HT descending fibres: 5±0.3s before, 6.6±0.4s during and 5.3±0.3s post-stimulation) resulting in thermal analgesia. A, B and C vehicle) Whereas vehicle per os treatment has no effect on either the mechanical threshold (A vehicle, SUDO for SNI-ChR2-5-HT descending fibres: 0.3±0.0g before, 0.1±0.0g during and 0.3±0.0g post-stimulation; B vehicle, Repeated measure with innocuous stimuli for SNI-ChR2-5-HT descending fibres: 3.3±3.3% before, 93.3±2.8% during and 6.7±3.8% of response post-stimulation) and thermal latency (C vehicle, Plantar test, for SNI-ChR2-5-HT descending fibres: 4.6±0.4s before, 3.3±0.3s during and 4.5±0.3s post-stimulation). Measures are reported as mean ± SEM; A, SUDO, control ***[1]=p=0.0007, ***[2]=p=0.0003; CLP290 ***[1]=p=0.0007, ***[2]=p=0.0003 and vehicle ***=p=0.0005; B, Repeated measure, control ***=p=0.0005; CLP290 ***[1]=p=0.0001, **=p=0.0015 and vehicle ***[1]=p=0.0003, ***[2]=p=0.0007; C, Plantar test, control **[1]=p=0.0022, **[2]=p=0.0085; CLP290 **=p=0.0085, ****=p<0.0001 and vehicle **=p=0.0010, ***=p=0.0002 from Dunn's post hoc test.*

Therefore, in neuropathic conditions, RMg 5-HT-induced facilitation is due to chloride imbalance induced by a decrease in KCC2 activity. Boosting KCC2 can reverse the consequence of SNI.

b) *CLP 290 induced RMg 5-HT inhibition is not influenced by gender*

Then, we decided to find out if the restoration of RMg 5-HT inhibitory effect induced by the CLP290 treatment in SNI 5-HT cre mice was on the influence of gender. To do so, we compared in SNI 5-HT cre mice treated with CLP290, the effect of optogenetic activation on the mechanical and thermal sensation both in males and females (*Figure* 100) and we observed no difference(*Figure* 100A, SUDO, for male Friedman test p=0.0041, F=10.8 and for female p=0.0041, F=11.47; n=6 and 6 respectively) and thermal threshold (*Figure* 100B, Plantar test, male Friedman test p=0.0055, F=9.333 and female p=0.0001, F=12; n=6 and 6 respectively), resulting in both cases in mechanical and thermal analgesia.

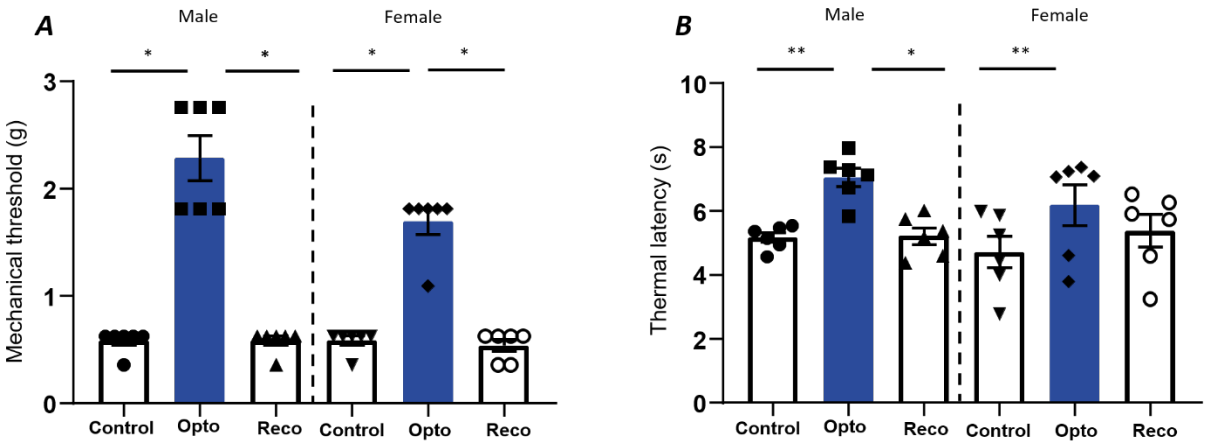

*Figure 100 : Gender do not influence CLP290 treatment-induced 5-HT descending inhibition on pain transmission in neuropathic pain. A) In SNI 5-HT mice treated with CLP290, optogenetic activation of SNI-ChR2-5-HT descending fibres induced in both male and female, a relevant increase in mechanical threshold (A for male clp290: 0.6±0.0g before, 2.3±0.2g during and 0.6±0.0g post-stimulation; for female clp290: 0.6±0.0g before, 1.7±0.1g during and 0.5±0.1g post-stimulation) and thermal latency (B for male clp290: 5.2±0.2s before, 7.1±0.3s during and 5.2±0.3s post-stimulation; for female clp290: 4.7±0.5s before, 6.2±0.6s during and 5.4±0.5s post-stimulation). Measure are reported as mean ± SEM; SUDO male *=p=0.0187 and female *[1]=0.0283, *[2]=p=0.0122; Plantar test male *=p=0.0418, **=p=0.0078 and female **=p=0.0011 from Dunn's post hoc test.*

c) *CLP 290 suppresses WDR hyperexcitability*

We next evaluated the effect of CLP290 in the control of WDR excitability by RMg 5-HT in anesthetised SNI mice (*Figure* 101). *In vivo* recordings of WDR show that CLP290 superfusion above the spinal cord dorsal horn suppressed the increase in WDR excitability induced by optogenetic activation of 5-HT descending fibres (*Figure* 101AB2, Ordinary one-way ANOVA p=0.0013, F=5.187; n=7).

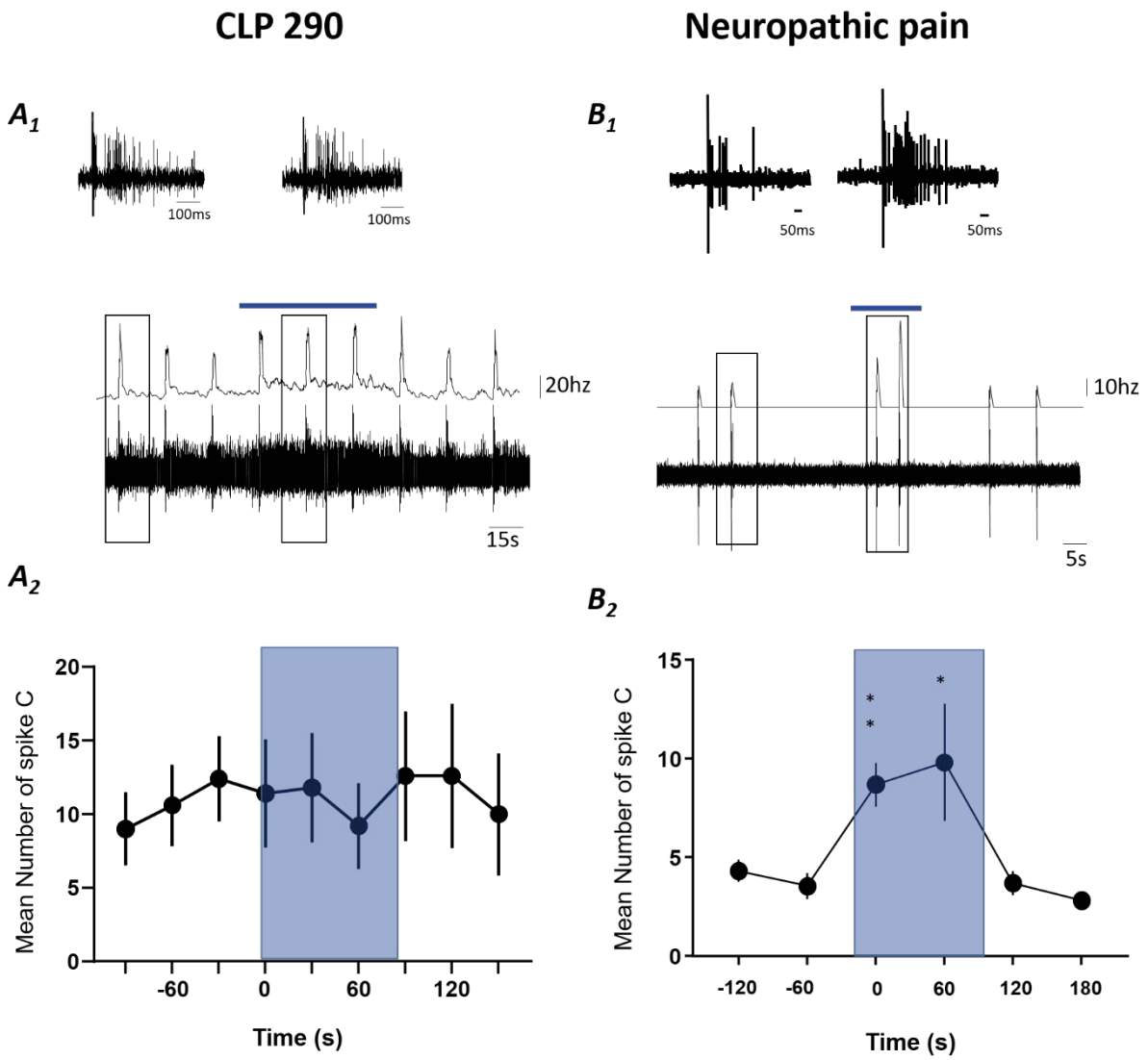

*Figure 101 : In vivo single unit recording of DHNs superfused with clp290 associated with optogenetic activation of 5-HT descending fibres above the dorsal horn of the spinal cord in neuropathic pain condition. One sample showing no change (A1) or an increase (B1) of DHN response to noxious stimuli during optogenetic stimulation of ChR2-5-HT descending fibres (above, representative WDR neuron response to a noxious electrical stimuli recorded before and during optogenetic stimulation with (A) or without clp290 superfusion (B)). In animals treated with CLP 290, the optogenetic activation of 5-HT descending fibres in SNI did not increase evoke response of DHNs to nociceptive stimulation (A2, mean number of C-spike before 10.7±2.7, during 10.8±3.4 and after 11.7±4.5) as opposed to what we observed in neuropathic animals *= p=0.0274, **=0.0079 from Dunn's post hoc test.*

Thus, in neuropathic pain conditions, WDR hyper-excitability induced by RMg 5-HT is a consequence of the decrease activity of the KCC2 cotransporter, suggesting that an impairment in KCC2 cotransporters activity alone may also induces a shift in the RMg 5-HT-induced inhibition on pain transmission in acute pain condition.

2. RMg 5-HT-induced inhibition on pain transmission is mediated by dorsal horn KCC2 cotransporter in acute pain

a) *Blockade of the spinal KCC2 reverse RMg 5-HT induced inhibition in acute pain*

To test for that hypothesis, we blocked the cationic-chloride cotransporter KCC2 with *ip* injections of furosemide (inhibitor of K-CL cotransporter including KCC2) in naïve 5-HT cre mice expressing ChR2 opsin in RMg 5-HT neurons.30 min after furosemide injection, we observed that optogenetic activation of RMg 5-HT descending fibres elicited a mechanical and thermal hypersensitivity (*Figure* 102). Indeed, in naive animals activation of RMg 5-HT descending fibres elicits an increase in mechanical threshold (*Figure* 102A control, SUDO, ChR2-5-HT descending fibres, Friedman test $p<0.0001$, $F=22.21$; $n=12$ and *Figure* 99B control, Repeated measure ChR2-5-HT descending fibres, Friedman test $p<0.0001$, $F=22.62$; $n=12$) and thermal latency (*Figure* 102C control Plantar test, ChR2-5-HT descending fibres, Friedman test $p=0.0001$, $F=18.17$; $n=12$), subsequent Furosemide injection induces a relevant decrease in mechanical threshold (*Figure* 102B Furosemide, SUDO, ChR2-5-HT descending fibres, Friedman test $p<0.0001$, $F=21.78$; $n=12$ and *Figure* 102B Furosemide, Repeated measure ChR2-5-HT descending fibres, Friedman test $p<0.0001$, $F=22.40$; $n=12$) and thermal latency (*Figure* 102C Furosemide Plantar test, ChR2-5-HT descending fibres, Friedman test $p=0.0001$, $F=18.77$; $n=12$) with the same optogenetic manipulation and that was not present when the vehicle alone was injected (*Figure* 102A vehicle, SUDO, ChR2-5-HT descending fibres, Friedman test $p<0.0001$, $F=22.74$; $n=12$ and *Figure* 102B vehicle, Repeated measure ChR2-5-HT descending fibres, Friedman test $p<0.0001$, $F=22.29$; $n=12$ and *Figure* 102C vehicle Plantar test, ChR2-5-HT descending fibres, Friedman test $p<0.0001$, $F=18.67$; $n=12$).

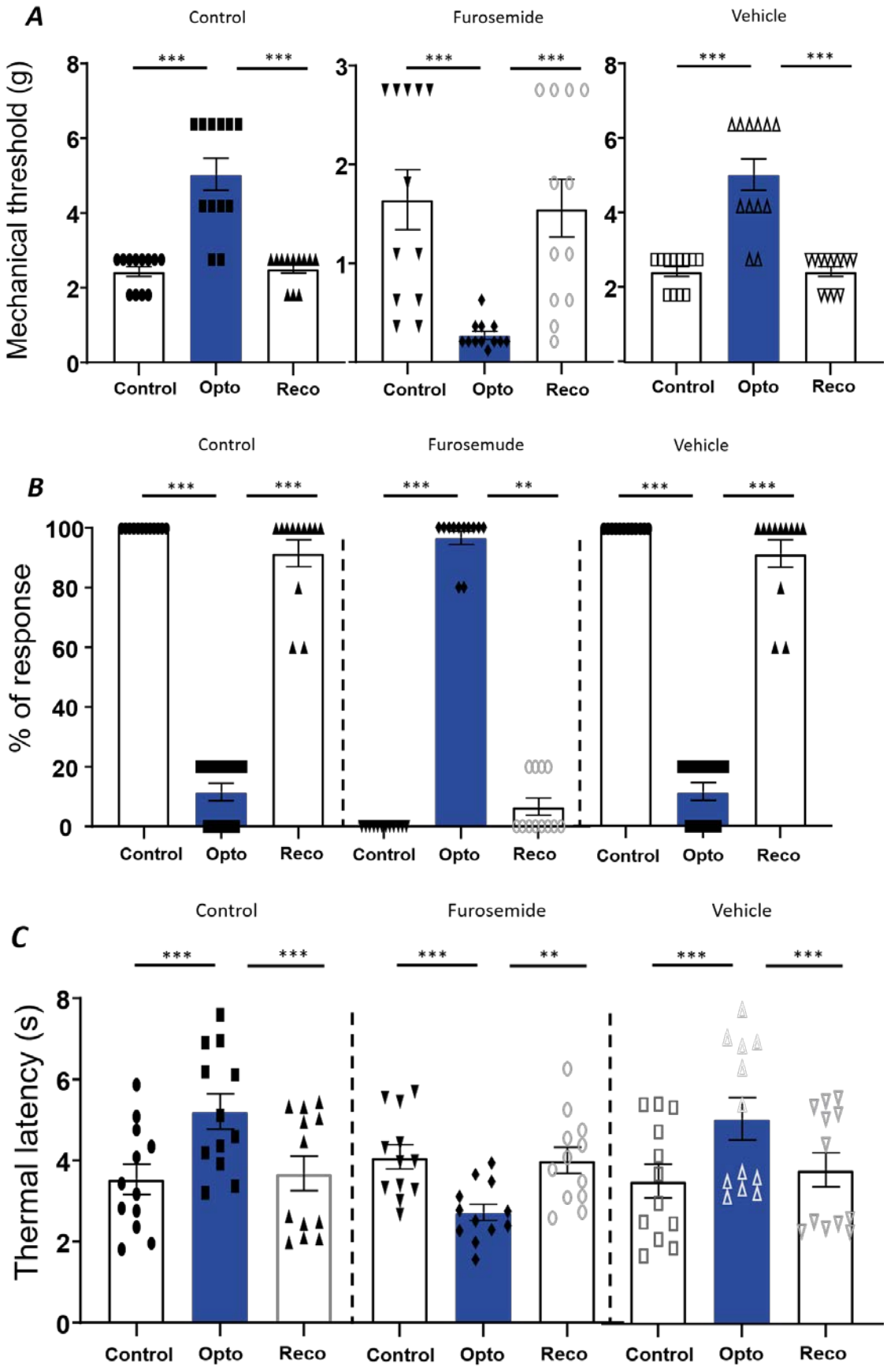

Figure 102 : In naive animals expressing ChR2 opsin in 5-HT neurons of the RMg, optogenetic activation of 5-HT descending fibres induced an increased in mechanical threshold (A control, SUDO for ChR2-5-HT descending fibres: 2.4±0.1g before,

*5.1±0.4g during and 2.5±0.1g post-stimulation) including a decrease in the percentage of hind-paws response to repeated noxious stimuli (B control, Repeated measure for ChR2-5-HT descending fibres: 100±0% before, 11.7±3% during and 91.7±4.6% of response post-stimulation) and an increase in thermal threshold (C control, Plantar test, for ChR2-5-HT descending fibres: 3.5±0.4s before, 5.2±0.4s during and 3.7±0.4s post-stimulation) resulting in mechanical and thermal analgesia. A, B and C furosemide) In the same animals, 30min after furosemide injection, the same optogenetic stimulation induced a decrease in mechanical threshold (A, SUDO furosemide for ChR2-5-HT descending fibres: 1.7±0.3g before, 0.3±0.0g during and 1.6±0.3g post-stimulation) including an increase in the percentage of hind-paws response to repeated innocuous stimuli (B, Repeated measure Furosemide for ChR2-5-HT descending fibres: 0±0% before, 96.7±2.2% during and 6.7±2.8% of response post-stimulation) and a decrease in thermal threshold (C, Plantar test furosemide, for ChR2-5-HT descending fibres: 4.1±0.3s before, 2.8±0.2s during and 4.0±0.3s post-stimulation) resulting in mechanical allodynia and hyperalgesia and in thermal hyperalgesia. A, B and C vehicle) Whereas vehicle injection has no effect on either the mechanical threshold (A vehicle, SUDO for ChR2-5-HT descending fibres: 2.4±0.1g before, 5.1±0.4g during and 2.4±0.1g post-stimulation; B vehicle, Repeated measure with noxious stimuli for ChR2-5-HT descending fibres: 98.3±1.7% before, 11.8±3.9% during and 88.3±3% of response post-stimulation) and thermal threshold (C vehicle, Plantar test, for ChR2-5-HT descending fibres: 3.6±0.4s before, 5.1±0.5s during and 3.8±0.4s post-stimulation). Measures are reported as mean ± SEM; A, SUDO, control ***[1]=p=0.0003, ***[2]=p=0.0007; furosemide **=p=0.0022, ***=p=0.0003 and vehicle ***=p=0.0005; B, Repeated measure, control **=p=0.0015, ***=p=0.0001; furosemides **=p=0.0022, ****=p<0.0001 and vehicle **=p=0.0044, ****=p<0.0001; C, Plantar test, control **=p=0.0010, ***=p=0.0002; furosemide **=p=0.0010, ***=p=0.0002 and vehicle **=p=0.0022, ****=p<0.0001 from Dunn's post hoc test.*

In conclusion, an alteration in KCC2 activity following peripheral nerve damage induces a switch in the RMg 5-HT control of nociceptive transmission from inhibition to facilitation cause by a KCC2-induced change in Chloride equilibrium. (Gagnon et al., 2013).

b) *KCC2 impairment induced facilitation is not influenced by gender*

Then, we decided to find out if the switch of RMg 5-HT effect induced by a blockade of KCC2 cotransporter in naïve 5-HT cre mice was under the influence of gender. To do so, we compared in naïve 5-HT cre mice treated with Furosemide, the effect of optogenetic activation of 5-HT descending fibres in males and females (*Figure* 103). We observed no difference in the descending facilitation induced by optogenetic activation of 5-HT descending fibres under furosemid (*Figure* 103A, Mechanical threshold, SUDO, for male Friedman test p=0.0041, F=11.47 and for female p=0.0082, F=10.33; n=6 and 6 respectively; *Figure* 103B, thermal latency Plantar test, male Friedman test p=0.0081, F=9 and female p=0.0055, F=9.333; n=6 and 6 respectively).

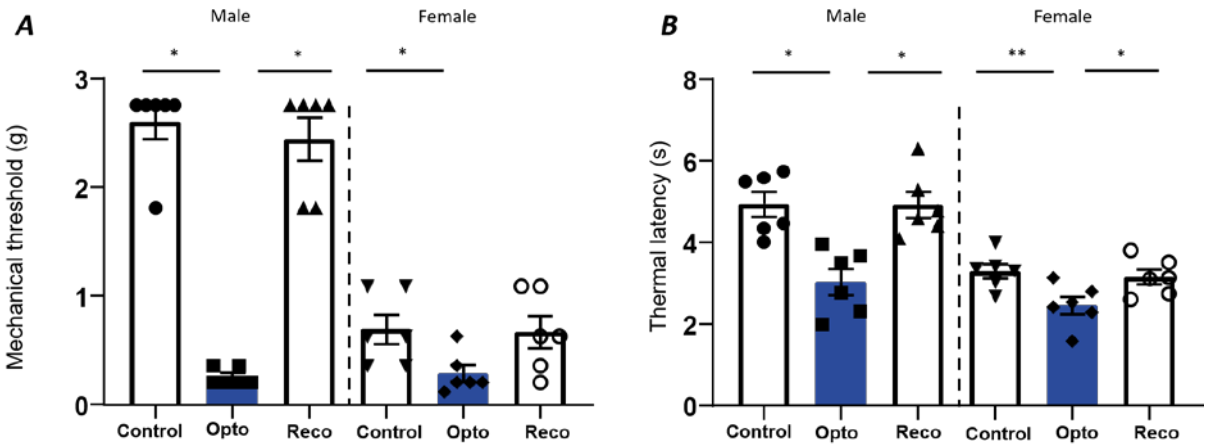

*Figure 103 : Gender do not influence furosemide-induced 5-HT descending facilitation on pain transmission in acute pain. A) In naïve 5-HT mice treated with furosemide, optogenetic activation of ChR2-5-HT descending fibres induced in both male and female, a relevant decrease in mechanical threshold (A for male furosemide: 2.6±0.2g before, 0.3±0.0g during and 2.4±0.2g post-stimulation; for female furosemide: 0.7±0.1g before, 0.3±0.1g during and 0.7±0.2g post-stimulation) and thermal latency (B for male furosemide: 5.0±0.3s before, 3.0±0.3s during and 4.9±0.3s post-stimulation; for female furosemide: 3.3±0.2s before, 2.5±0.2s during and 3.2±0.2s post-stimulation). Measure are reported as mean ± SEM; SUDO male $*^{1}$=p=0.0122, $*^{2}$=0.0283 and female *=p=0.0187; Plantar test male *=p=0.0187 and female *=p=0.0418, **=p=0.0078 from Dunn's post hoc test*

To conclude, pharmacological KCC2 manipulation oriented the sign of 5-HT descending influence on nociceptive transmission, that changes from pain inhibition to facilitation in pathological context.

IV. GENERAL DISCUSSION

Pain, defined as “an unpleasant sensory and emotional experience associated with actual or potential tissue damage, or described in terms of such damage” is a warning mechanism with a protective role to keep tissue damage to a minimum. Moreover, a descending endogenous mechanism controls pain sensation by filtering nociceptive inputs to some extent at the level of the dorsal horn of the spinal cord (Millan, 2002a). This descending control of pain, involving periaqueductal grey matter in the upper brainstem and the nucleus raphe Magnus in the rostral ventromedial medulla is one of the major system that control nociceptive transmission by exerting an efficient inhibitory tone to the dorsal horn of the spinal cord (Millan, 2002a; Fields, 2004; Lisovoski, 2006; Kim et al., 2018). It is now largely considered that a balance between both excitatory and inhibitory influence controls nociceptive transmission and that unbalanced influences are involved in pathological pain (Vanegas and Schaible, 2004; Ossipov et al., 2014). Among these excitatory and inhibitory influences are serotonin neurons, which have been shown to play a major role in pain control. However, it must be noted that many questions remained unanswered about the exact role of 5-HT of the raphe Magnus in pain control since 5HT exerts opposite modulations according to pathophysiological states (Bourgoin et al., 2017b).

By combining pharmacological, optogenetic, single-unit recordings and virus-based approaches associated with the used of transgenic mice expressing cre-recombinase in 5-HT and SST neurons respectively, we investigated the specifical role of serotoninergic projection from the raphe Magnus into the dorsal horn of the spinal cord in the descending pain modulation in acute and neuropathic pain condition.

A. CHARACTERIZATION OF THE ROLES OF RMg 5-HT NEURONS ON SPINAL NOCICEPTIVE TRANSMISSION IN PHYSIOLOGICAL CONDITION

First of all, by crossing ePet-cre mice (Scott et al., 2005a) to an Ai9 reporter mice (Madisen et al., 2010) generated in our animal facility, we first confirmed that cre-recombinase is restrained to 5-HT neurons in the raphe Magnus (RMg) as well as in the dorsal raphe (DR) and the median raphe (MR). Indeed co-localisation with tryptophan hydroxylase 2 (TPH2) a specific enzyme expressed exclusively in 5-HT neurons (Côté et al., 2003), show up to 83.8% co-localisation. We also observed an abundant population of 5-HT fibres in the spinal dorsal horn thus confirming 5-HT projections to the spinal cord. Using a Gad67-GFP mouse

(Tamamaki et al., 2003), we also observed that 5-HT neurons are not GABAergic neurons but have a high degree of interaction with them. Consequently, the ePet cre mice gave us a crucial tool to study the precise role of such neurons in nociceptive transmission. Then we assessed the validity of our viral approaches, using slices of RMg containing 5-HT neurons expressing ChR2 opsin 3 weeks after stereotaxic injection in the RMg of an AAV inducible virus including ChR2 opsin labelled with mCherry, we performed patch-clamp recordings in current-clamp mode and observed that optogenetic stimulation with blue activating light has induced a fast and reproducible neuronal depolarisation, and a train of 5Hz/5ms has also induced a train of action potentials that fair-fully followed light stimulation by contrast slices of RMg containing 5-HT neurons expressing ArchT-GFP, continuous optogenetic stimulation with green inhibiting light resulted in a strong hyperpolarisation which confirmed that our optogenetic approach allowed us to modulate the RMg 5-HT neurons activity. In addition, we noted that 5-HT neurons of the RMg specifically projected into the deep layer of the spinal cord since 5-HT fibres were visible at this level. Data which are in accordance with the literature (Benarroch, 2014; Gautier et al., 2017).

In a second time, in order to reliably alter the RMg 5-HT neurons activity, we performed optogenetic stimulation of those neurons using optical fibre placed above the RMg or the lumbar part of the spinal cord. In freely moving mice in absence of nerve injury, we observed that selective optogenetic inhibition RMg 5-HT elicited a significant mechanical and thermal hypersensitivity. This result shows that RMg 5-HT neurons are tonically active and inhibit the nociceptive transmission at the level of the spinal cord. Data which are in accordance with previous studies where it has been demonstrated a link between pain hypersensitivity and selective lesion of 5-HT neurons by a specific neurotoxin infused at the rostral ventral medulla, RVM (Wei et al., 1999). it is also in accordance with pain hypersensitivity associated with an important decrease in 5-HT expression due to 5HT neurons differentiation in mice lacking the transcription factor Lmx1b (Zhao et al., 2007). We also show that optogenetic activation of RMg 5-HT neurons elicited a significant mechanical and thermal analgesia. Therefore, we concluded that RMg 5-HT neurons exerted a tonic descending inhibition on pain transmission which is in accordance the literature (Schwaller et al., 2017). It has been shown in previous studies that a direct electrical stimulation of the RMg (Mayer and Liebeskind, 1974; Oliveras et al., 1975) generated a strong analgesic effect in response to noxious stimuli and this, due to the release of 5-HT at the level of the dorsal horn of the spinal cord (Bourgoin et al., 1980; Hentall et al., 2006) and therefore makes RMg 5-HT a key element of the inhibitory descending

endogenous pain control (Millan, 2002a; Suzuki et al., 2004; Zhao et al., 2014; Bourgoin et al., 2017c).

Then to decipher the spinal targets of RMg 5-HT neurons, we performed *in vivo* single-unit recordings of the dorsal horn neurons and focused on wide dynamic range (WDR) neurons that are mainly second-order neurons projecting to the upper brain structures and receive nociceptive inputs from low-velocity C fibres. We observed that optogenetic inhibition of RMg 5-HT resulted in an increase in WDR spontaneous activity and WDR response to nociceptive C fibre inputs as well as an increase in windup. Optogenetic activation of RMg 5-HT induced also both a significant decrease in WDR responses to nociceptive inputs and a significant decrease of windup *(Figure 104)*. We, therefore, revealed that 5-HT neurons of the RMg which projected to the deep layer of the dorsal horn, tonically inhibit nociceptive transmission by decreasing WDR excitability. Finally, these results strongly demonstrate the role of 5HT neurons in filtering nociceptive inputs and may explain their activation following nociceptive stimulation although RMg 5HT are not considered as on or off cells (Gau et al, 2013)field 2004).

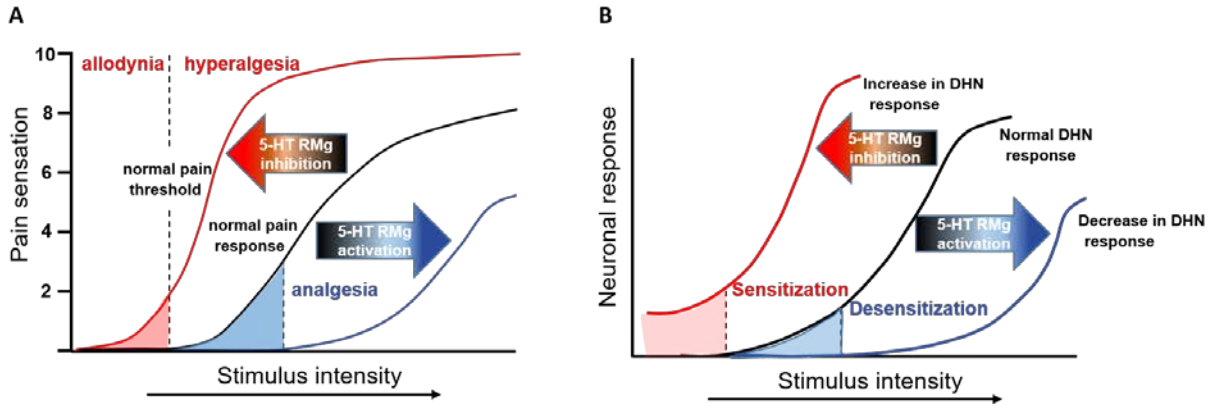

Figure 104 : Schematic representation of the consequence of RMg 5-HT optogenetic manipulation on pain transmission. A) In black, weak or innocuous stimuli do not evoke a pain sensation in normal condition partly due to a tonic inhibition exerts by 5-HT neurons of the RMg. In red, pain hypersensitivity in response to a stimulus after RMg 5-HT optogenetic inhibition, shifting the response function to the left. A moderate painful stimulus is now perceived as intense (i.e., pain hyperalgesia) and a previously innocuous stimulus can be perceived as painful (i.e., allodynia). In blue, pain inhibition in response to a stimulus after RMg 5-HT optogenetic activation, shifting the response function to the right. A moderate painful stimulus is less perceived as painful (i.e., pain analgesia). B) In black, weak or innocuous stimuli do not evoke WDR response in normal condition. In red, WDR hyper-excitability in response to a stimulus after RMg 5-HT optogenetic inhibition, shifting the response function to the left. A moderate painful stimulus elicited an increase in the dorsal horn neuron response and an increase in their ability to be sensitized. In blue, a decrease WDR excitability in response to a stimulus after RMg 5-HT optogenetic activation, shifting the response function to the right.

Furthermore, to go into more details, we next determined the targets of RMg 5-HT neurons on the dorsal horn microcircuits. Indeed, it has been shown in previous studies that 5-HT could enhance the release of GABA partly due to the activation of 5-HT_3R expressed on the surface of inhibitory interneurons and then inhibit sensory transmission (Xie et al., 2012). By using Gad67-GFP mice, we performed TPH2 immunostaining and observed potential 5-HT synaptic buttons onto GABA neurons in deep layers of the dorsal horn. To confirm these connections to the local inhibitory network, we compared, in 5-HT cre mice injected with a cre dependant AAV containing a GFP tag, appositions between GFP and excitatory (Tlx3) or inhibitory (PAX2) neurons and found that 5-HT fibres are substantially more in apposition with inhibitory interneurons. We next confirmed the presence of real contacts between RMg 5-HT fibres and inhibitory neurons, by using Gad 67-GFP*5-HT cre mice in which SynMYC-revWPRE was expressed in the RMg 5-HT neurons, we performed immunostaining on thin cross-section slice of lumbar spinal cord, of SynMyc in combination with GFP or parvalbumin and found synaptic buttons of 5-HT fibres onto GABA and parvalbumin neurons. We confirm the connections between RMg 5HT fibres and spinal inhibitory network by blocking GABAa and glycine receptors. This resulted in a blockade of optogenetic stimulation of RMg 5HT on pain behaviour and WDR hyperexcitability.

Therefore, we showed that RMg 5-HT tonic descending inhibition on pain transmission passed through direct excitation of GABAergic/glycinergic inhibitory interneurons in deep layer of the spinal cord which in turn inhibit spinal dorsal horn neuron. Data which is in line with the mode of action of 5-HT on spinal dorsal horn neuron as well as the modifications observed in the dorsal horn modulating the pain transmission, proposed in previous studies (Zhang et al., 2001; Kawamata et al., 2003; Lu and Perl, 2007; Sadlaoud et al., 2010; Thibault et al., 2014; Chalermkitpanit et al., 2017) *Figure 105*.

However, we observed no effect of a blockade of 5-HT_3 receptors using an intrathecal injection of granisetron (5-HT_3R antagonist) on RMg 5-HT-induced inhibition on pain transmission following optogenetic activation, thus demonstrating that RMg 5-HT induced inhibition does not pass through 5-HT_3R expressed on the surface of GABAergic/glycinergic inhibitory interneurons, data which is consistent with the fact that 5-HT_3R is not involved in acute pain control (Zeitz et al., 2002; Guo et al., 2014) and thus suggests the involvement of other receptors such as 5-HT_{2A} (Alba-Delgado et al., 2018)

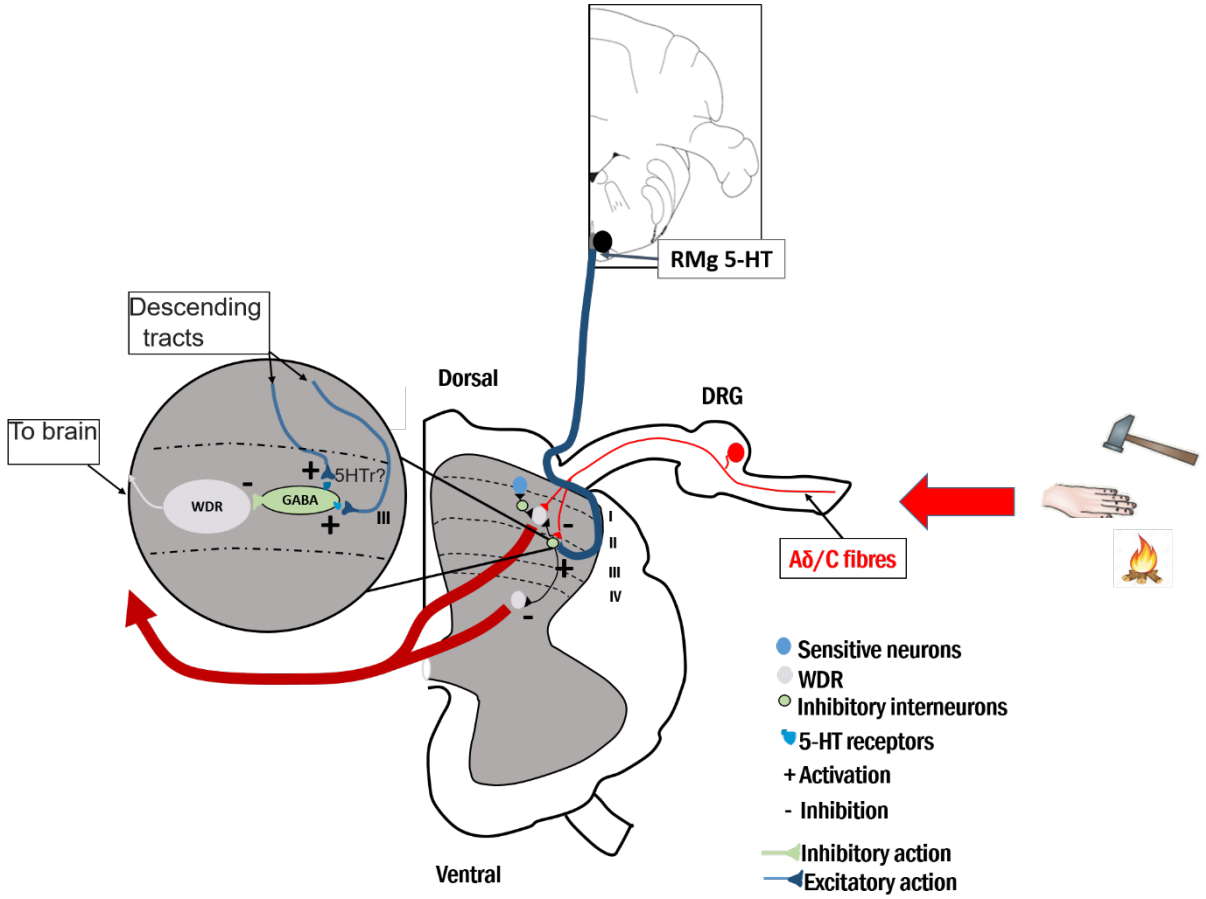

Figure 105 : Simplified schematic representation of tonic 5-HT descending inhibitory action into the spinal cord. Illustration of apposition between RMg 5-HT descending terminal and inhibitory interneuron which illustrate an inhibitory action of descending 5-HT on the spinal nociceptive transmission through activation of dorsal horn inhibitory interneurons resulting in a decrease in WDR response to C-fibres inputs as well as in a decrease in its ability to be sensitized. WDR, wide dynamic range projecting neuron.

B. 5-HT NEURONS OF THE RMg SEEMS TO BE CONNECTED TO THE STRESS INDUCED ANALGESIA NETWORK.

In a second step, through collaboration with the team of Cyril Herry, we tried to determine how RMg 5-HT neuron activity is modulated. To do so, we performed VGLUT1-3, GAD-65-67 and SST immunostaining for glutamatergic, GABAergic and SST inputs respectively in combination with TPH2 immunostaining in cross-section of thin RMg slice in naïve mice, and observed potential GABAergic, glutamatergic and SST inputs onto RMg 5-HT. Indeed, it has been shown that vlPAG contained various subpopulations of neurons that control pain transmission (Samineni et al., 2017) passing through rostral ventromedial medulla (Gebhart et al., 1983; Maione et al., 2006; Waters and Lumb, 2008) and associated with spinal cord 5-HT release (Cui et al., 1999). Moreover, SST neurons derived partly from vlPAG

appeared to have a sympathetic inhibitory effect on bulbospinal neurons (Bou Farah et al., 2016). We first established the functional role of SST neurons of the vlPAG on the spinal nociceptive transmission by using SOM-IRES-cre mice (Taniguchi et al., 2011). In freely moving mice, we performed optogenetic manipulations of those neurons using optical fibres bilaterally implanted above the vlPAG. Optogenetic inhibition of SST neurons elicited a significant mechanical and thermal analgesia. Consequently, SST neurons of the vlPAG exert a tonic downward facilitation of pain transmission maybe through disinhibitory mechanisms in the PAG (Connor et al., 2004). This facilitatory effect is confirmed with optogenetic activation of SST neurons that elicit a significant mechanical and thermal hypersensitivity. Therefore, we determine that SST neurons of the vlPAG exerted a tonic descending facilitation on pain transmission which is the exact opposite of the role of the RMg 5-HT on pain transmission. Data which is in accordance with the vlPAG facilitating role on pain transmission which is mediated by a subpopulation of the vlPAG (Connor et al., 2004; Samineni et al., 2017).

Next, to we performed *in vivo* single-unit recording of the WDR to determine if vlPAG SST control excitability in the dorsal horn of the spinal cord. We observed that bilateral optogenetic inhibition of vlPAG SST neurons expressing ArchT elicited both a significant decrease in WDR neurons response in response to nociceptive inputs and a significant decrease in windup. By contrast, bilateral optogenetic activation of SST neurons expressing ChR2 induced a significant increase in WDR response to nociceptive C fibre inputs as well as an increase in windup. Therefore, we showed that SST neurons of the vlPAG, tonically facilitate the nociceptive transmission by increasing WDR excitability. Results that can be linked to the phenomenon of tonic GABAergic interneurons inhibition observed on vlPAG glutamatergic neurons, which are thought to be the output projecting neurons controlling the descending inhibition of nociception (Tovote et al., 2016c; Samineni et al., 2017).

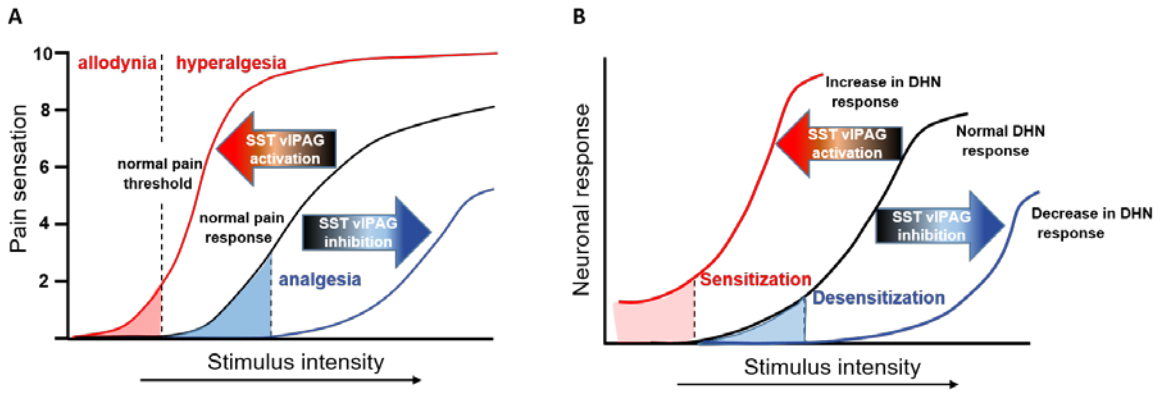

Figure 106 : Schematic representation of the consequence of vlPAG SST neuron optogenetic manipulation on pain transmission. A) In black, weak or innocuous stimuli do not evoke a pain sensation in normal condition. In red, pain

hypersensitivity in response to a stimulus after vlPAG SST neurons optogenetic activation, shifting the response function to the left. A moderate painful stimulus is now perceived as intense (i.e., pain hyperalgesia) and a previously innocuous stimulus can be perceived as painful (i.e., allodynia). In blue, pain inhibition in response to a stimulus after vlPAG SST neurons optogenetic inhibition, shifting the response function to the right. A moderate painful stimulus is less perceived as painful (i.e., pain analgesia). B) In black, weak or innocuous stimuli do not evoke WDR response in normal condition. In red, WDR hyper-excitability in response to a stimulus after vlPAG SST neurons optogenetic activation, shifting the response function to the left. A moderate painful stimulus elicited an increase in the dorsal horn neuron response and an increase in their ability to be sensitized. In blue, a decrease WDR excitability in response to a stimulus after vlPAG SST neurons optogenetic inhibition, shifting the response function to the right.

Furthermore, to go into more detail, we next assessed the targets of vlPAG SST neurons into the rostral ventral medulla (RVM) and in particular into the RMg. We use cre dependant AAV containing a GFP tag in SST cre mice associated with a bilateral injection of retrograde tracer (fluorogold 2%) into the dorsal horn of the spinal cord. We also performed TPH2 immunostaining on RMg cross-section. Comparing apposition between TPH2, GFP and fluorogold (FG) autofluorescence we found that vlPAG SST contacts RMG 5HT that project onto spinal cord. These results show for the first time the presence of long-range SST neurons in the vlPAG, in accordance with what is observed in other brain structures (réf). Second, it suggests a descending network controlling pain transmission involving vlPAG SST, 5HT neurons and dorsal horn of the spinal cord. We also found some vlPAG SST fibres projecting directly in the spinal cord.

Then, we studied the functional role of vlPAG SST- RMg5-HT circuit on pain transmission and we show that activation of SST fibres projecting in the RMg induces a significant mechanical and thermal hyperalgesia and increase in WDR excitability. By contrast, optogenetic activation of SST fibres projecting to the spinal cord had no effect. These results demonstrate the role of vlPAG SST-RMg 5HT circuit in controlling pain transmission at the level of the spinal cord. (Figure 107).

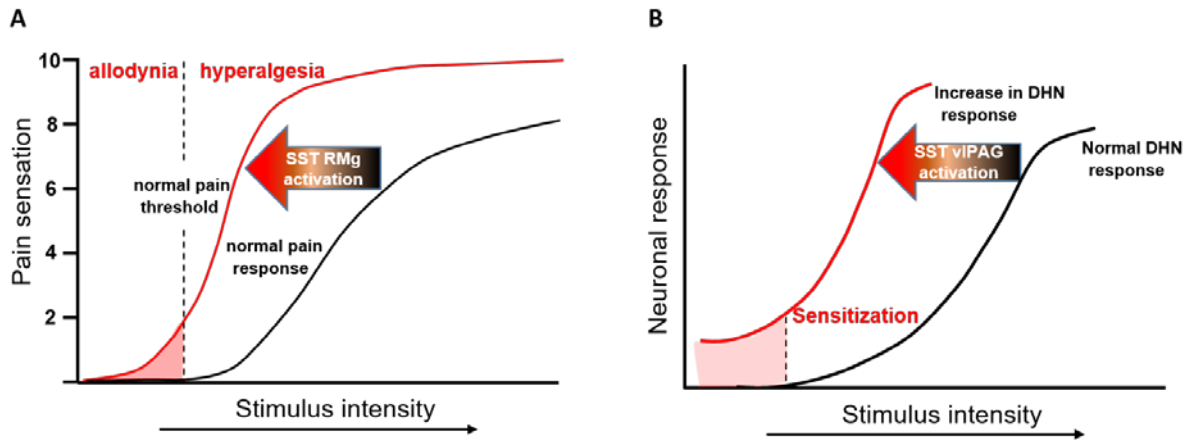

Figure 107 : Schematic representation of the consequence of vlPAG SST descending fibres optogenetic activation on pain transmission. A) In black, weak or innocuous stimuli do not evoke a pain sensation in normal condition. In red, pain hypersensitivity in response to a stimulus after vlPAG SST descending fibres optogenetic activation, shifting the response function to the left. A moderate painful stimulus is now perceived as intense (i.e., pain hyperalgesia) and a previously innocuous stimulus can be perceived as painful (i.e., allodynia). B) In black, weak or innocuous stimuli do not evoke WDR response in normal condition. In red, WDR hyper-excitability in response to a stimulus after vlPAG SST descending fibres optogenetic activation, shifting the response function to the left. A moderate painful stimulus elicited an increase in the dorsal horn neuron response and an increase in their ability to be sensitized.

Therefore, our results strongly suggest that SST neurons of the vlPAG exerted a tonic descending facilitation on pain transmission through probable inhibition of RMg 5-HT neurons. This is an interesting result because if we refer to the literature, PAG is considered as a key element of the PAG-RVM network participating in the inhibition of nociceptive transmission, especially in the context of fear. Therefore, our results suggest that the analgesia resulting from fear behaviour (Tovote et al., 2016c) mediate by vlPAG may pass through inhibition of vlPAG SST neurons that allow RMg 5-HT neurons disinhibition and activate a 5HT mediate descending inhibition of pain transmission.

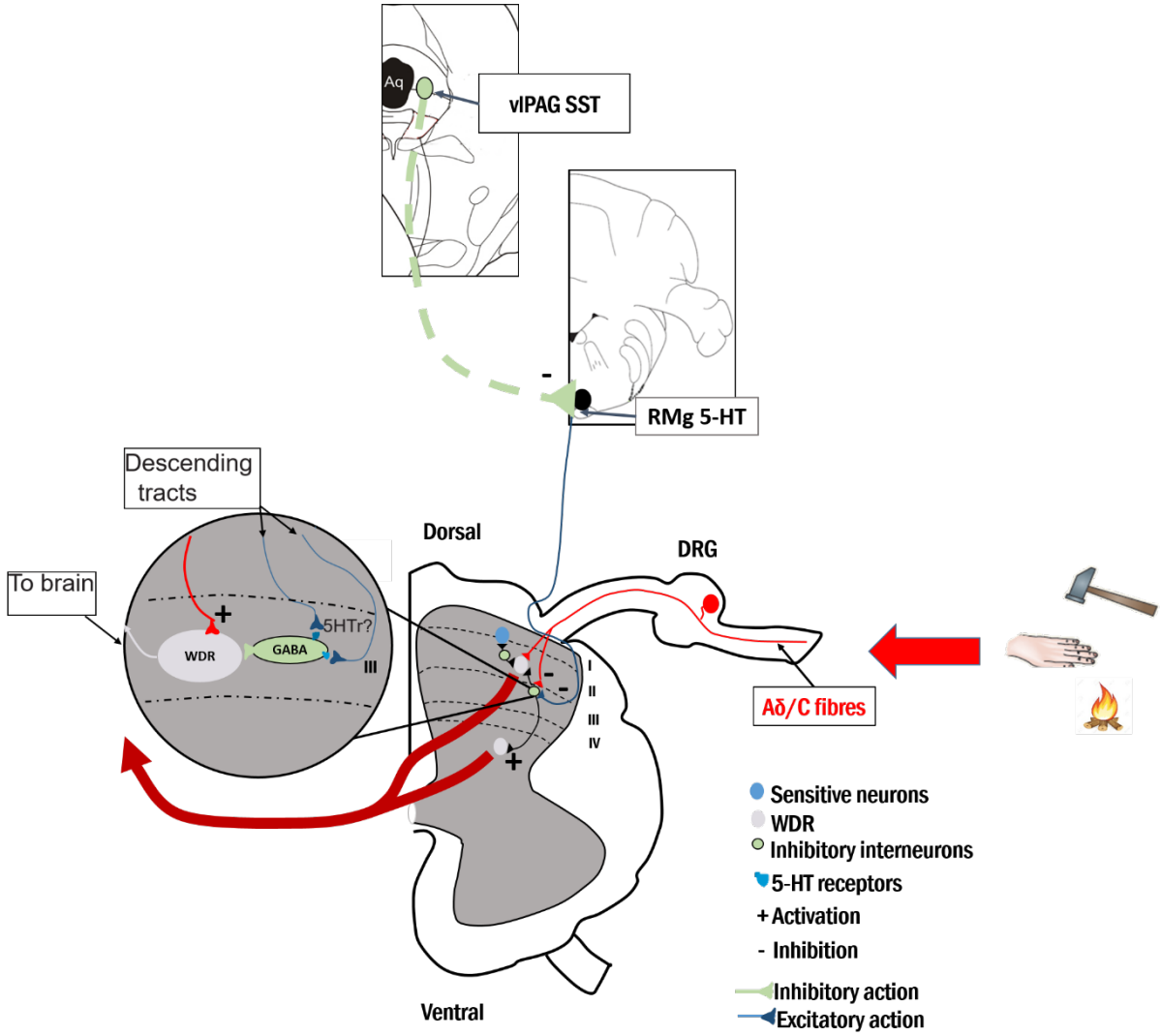

Figure 108 : Simplified schematic representation of vlPAG SST inhibitory action on pain transmission through RMg 5-HT. Illustration of descending facilitation mediates by vlPAG SST neurons on the spinal nociceptive transmission partly due to through inhibition of RMg 5-HT neuron resulting in an increase of WDR excitability as well as an increase in its ability to be sensitized. WDR, wide dynamic range projecting neuron.

C. CHARACTERIZATION OF THE ROLES OF RMg 5-HT NEURONS ON SPINAL NOCICEPTIVE TRANSMISSION IN NEUROPATHIC PAIN CONDITION

In neuropathic pain, 5HT is known to facilitate pain transmission (Rahman et al., 2006, 2011; Gautier et al., 2017). To study the consequences of optogenetic manipulation of RMg 5HT on nociceptive transmission in neuropathic pain, we used the spared nerve injury (SNI) model of peripheral neuropathy to mimic both the cardinal symptoms of clinically described neuropathic pain disorders and its duration in time. We first confirmed that SNI procedure elicits mechanical and thermal pain hypersensitivity. Interestingly, optogenetic inhibition RMg

5HT did not modify both mechanical and thermal sensitivity suggesting that in a pathological context, RMg 5-HT neurons lose its tonic activity, phenomenon that has not been observed in the past to my knowledge.

By contrast, optogenetic activation of RMg 5HT induced a significant decrease in mechanical pain threshold and thermal pain latency (Figure 94-95). Therefore, in neuropathic pain, 5-HT neurons of the RMg lose its analgesic effect and exert descending facilitation on pain transmission which is in accordance with the facilitation induced by 5-HT observed in the literature (Ossipov et al., 2014; Huang et al., 2019).

By performing, *in vivo* single-unit recoding targeting WDR, we showed that optogenetic inhibition of RMg 5-HT descending fibres showed no change in the WDR excitability, by contrast, optogenetic activation of 5HT RMg descending fibres resulted in WDR hyper-excitability. Therefore, in neuropathic pain condition, we showed that 5-HT neurons projecting to the dorsal horn, facilitate the nociceptive transmission by increasing WDR response to C-fibres inputs resulting in WDR hyper-excitability.

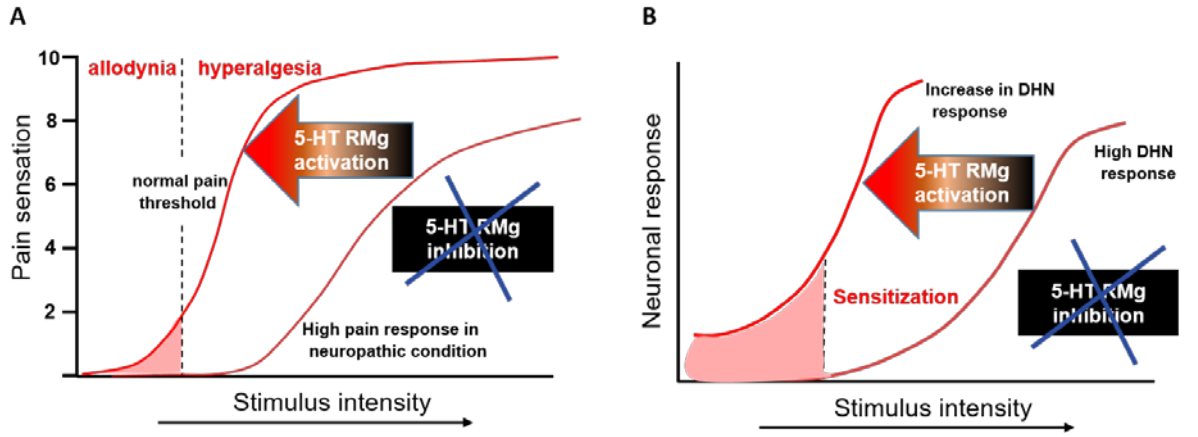

Figure 109 : Schematic representation of the consequence of RMg 5-HT optogenetic manipulation on pain transmission in neuropathic pain condition. A) In pink, weak or innocuous stimuli already evoke a pain sensation in neuropathic pain condition. In red, pain hypersensitivity in response to a stimulus after RMg 5-HT optogenetic activation, shifting the response function to the left. A moderate painful stimulus is now perceived as intense (i.e., pain hyperalgesia) and a previously innocuous stimulus can be perceived as painful (i.e., allodynia). RMg 5-HT optogenetic inhibition no longer induce pain modulation in response to a stimulus. B) In pink, weak or innocuous stimuli already evoke WDR response in neuropathic pain condition. In red, WDR hyper-excitability in response to a stimulus after RMg 5-HT optogenetic activation, shifting the response function to the left. A moderate painful stimulus elicited an increase in the dorsal horn neuron response and an increase in their ability to be sensitized. RMg 5-HT optogenetic inhibition no longer induce WDR modulation in response to a stimulus.

Next, we then assessed possible changes induce by neuropathy in RMg 5-HT targets onto the dorsal horn of the spinal cord. To do so, by comparing apposition between GFP staining and both excitatory (Tlx3) and inhibitory (Pax2) interneurons we found that 5-HT fibres still mainly project onto inhibitory interneurons which suggested the involvement of the dorsal horn

inhibitory interneuron in the descending facilitation mediate by the 5-HT of the RMg in neuropathic pain (Ciranna, 2006; Moon and Park, 2017).

D. IMPAIRMENT of CHLORIDE BALANCE RESULTS IN THE SHIFT OF RMg 5-HT MODULATION FROM INHIBITION TO EXCITATION ON PAIN TRANSMISSION.

In neuropathic pain model including SNI, it has been shown that disinhibition mechanisms mediated by an impairment in KCC2 (Doyon, 2011; Kaila et al., 2014) are responsible for a part of neuronal hyper-excitability and pain hypersensitivity (Coull et al., 2005; Beggs et al., 2012). Therefore, we assessed the consequence of the change in chloride equilibrium in afferent fibres or WDR neurons on the opposite serotonergic drive observed in control and SNI. by using a pharmacological approach to boost KCC2 in SNI mice. Indeed, 1h30 after *per os* treatment with CLP290 (a specific enhancer of KCC2 transporters (Lavertu et al., 2014; Chen et al., 2018; Mapplebeck et al., 2019b)) of SNI mice that express mechanical and thermal hypersensitivity, the same optogenetic stimulation of RMg 5-HT descending fibres in the same animals induces a significant mechanical and thermal analgesia that was not present after per os application of the vehicle alone. Therefore, in neuropathic conditions, we showed that RMg 5-HT-induced facilitation is due to chloride imbalance induced by a decrease in KCC2 activity consequently, boosting KCC2 can reverse the consequence of SNI (Bergeron et al., 2014; Chen et al., 2018; Mapplebeck et al., 2019b).

Furthermore, to go into more detail, we evaluated the effect of CLP 290 in the control of WDR excitability by RMg 5-HT neurons in SNI mice. We showed that CLP290 superfusion above the spinal cord suppressed the increase in WDR excitability induced by optogenetic activation of 5-HT descending fibres. Indeed, neither an increase in amplitude nor increase in evoked response of WDR upon 5-HT stimulation was observed (Figure 103). Thus, in neuropathic pain conditions, we showed that WDR hyper-excitability induced by RMg 5-HT is a consequence of the decreased activity of the KCC2 cotransporter.

Finally, we assessed the consequence of a blockade of KCC2 in naïve mice with ip injection of furosemide. We observed that optogenetic activation of RMg 5-HT descending fibres now elicited a mechanical and thermal hypersensitivity (Figure 104). Therefore, we showed that impairment in KCC2 cotransporters activity alone also induces a shift in the RMg 5-HT-induced inhibition on pain transmission in acute pain condition. Data which is in

accordance with the concept of GABA disinhibition leading to paradoxical post-synaptic excitation on nociceptive pain transmission (Doyon, 2011; Kaila et al., 2014; Lavertu et al., 2014). Indeed, it is considered that the inhibitory or excitatory effect mediated by both $GABA_A$ and glycine receptor are determined by level of the Cl^- concentration gradient across the cell membrane and alterations in the function of cation chloride cotransporters inducing changes in chloride ion driving force may reduce, eliminated or in this instance converted into paradoxical excitation. In physiological conditions in mature central neurons in the dorsal horn, cation chloride cotransporters KCC2 maintained the Cl^- reversal potential hyperpolarized (necessary for $GABA_A$ and glycine receptor to mediate inhibition) via Cl^- extrusion (Doyon, 2011; Kaila et al., 2014), thus the excitatory action of RMg 5-HT neurons on inhibitory interneurons results in an inhibition on pain transmission. However, an impairment both in KCC2 activity or expression following peripheral nerve injury induces a depolarizing shift in the Cl^- reversal potential weakening $GABA_A$/Gly-R-mediated inhibition. Consequently, an intracellular Cl^- accumulation occur in such an extent that intracellular chloride concentration exceeds the extracellular concentration and then $GABA_A$ receptors activation by GABA release of inhibitory interneurons following RMg 5-HT activation leads to an outflux of Cl^-, resulting in depolarization and excitation of second-order neurons (Price et al., 2005; Gagnon et al., 2013).

E. RMG 5-HT INFLUENCE ON PAIN TRANSMISSION IS NOT GENDER DEPENDENT

It has been observed in previous study that gender may influence the pain felt (Mogil and Bailey, 2010), Therefore we decided to assess its involvement on 5-HT descending pain modulation both in acute pain condition and in pathological pain condition. By comparing the effect of optogenetic stimulation of 5-HT descending fibres into the dorsal horn both in males and females in each situation interestingly, we observed no sex difference of 5-HT optogenetic stimulation-inducing inhibition or facilitation on nociceptive transmission in both males and females whatever the modality measured. Observations which can be explained by the fact that the influence of RMg 5-HT on pain transmission is modulated by the balance of KCC2 transporter and that KCC2 is uniquely responsible for regulating chloride and downregulation has been shown to contribute equally to pain hypersensitivity in males and females (Mapplebeck et al., 2019a).

In conclusion, in my thesis, we show that an alteration in KCC2 activity following peripheral nerve damage induces a switch in the RMg 5-HT control of nociceptive transmission from inhibition to facilitation caused by a KCC2-induced change in Chloride equilibrium which is not under the influence of the gender. (Gagnon et al., 2013; Lavertu et al., 2014; Alves and Lin, 2018; Mapplebeck et al., 2019b).

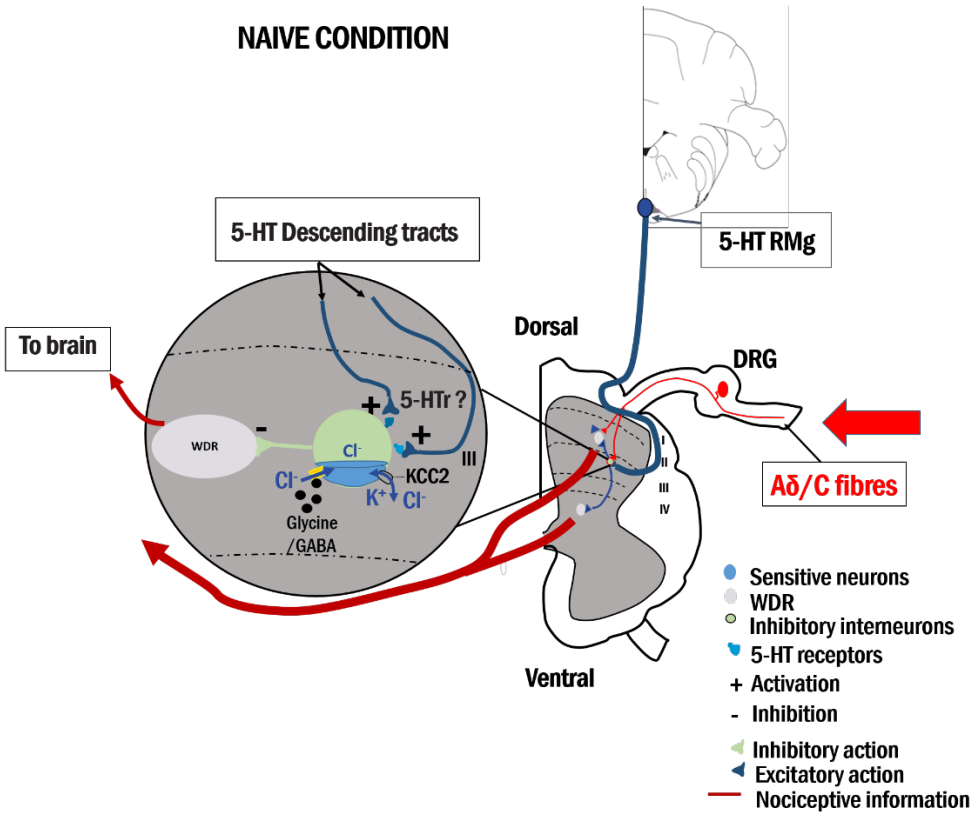

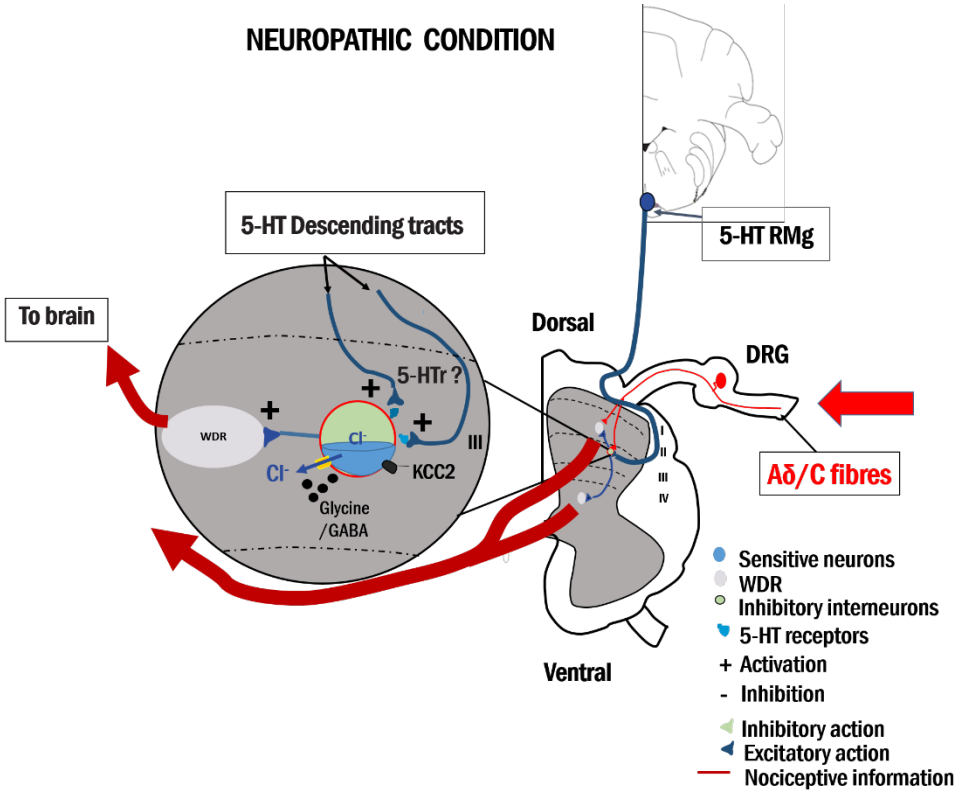

Figure 110 : In physiological condition, cation chloride cotransporters KCC2 maintained the Cl^- reversal potential hyperpolarized (necessary for $GABA_A$ and glycine receptor to mediate inhibition) via Cl^- extrusion, thus the excitatory action of RMg 5-HT neurons on inhibitory interneurons results in an inhibition on pain transmission. In neuropathic condition, an impairment both in KCC2 activity or expression following peripheral nerve injury induces a depolarizing shift in the Cl^- reversal potential weakening $GABA_A$/Gly-R-mediated inhibition. Therefore, an intracellular Cl^- accumulation occur in such an extent that intracellular chloride concentration exceeds the extracellular concentration and then $GABA_A$ receptors activation by GABA release of inhibitory interneurons following RMg 5-HT activation leads to an outflux of Cl^-, resulting in depolarization and excitation of second-order neurons.

REFERENCES

Aby, F., Whitestone, S., Landry, M., Ulmann, L., and Fossat, P. (2018). Inflammatory-induced spinal dorsal horn neurons hyperexcitability is mediated by P2X4 receptors: PAIN Rep. *3*, e660.

Adell, A., Carceller, A., and Artigas, F. (1993). In vivo brain dialysis study of the somatodendritic release of serotonin in the Raphe nuclei of the rat: effects of 8-hydroxy-2-(di-n-propylamino)tetralin. J. Neurochem. *60*, 1673–1681.

Aira, Z., Buesa, I., Gallego, M., García del Caño, G., Mendiable, N., Mingo, J., Rada, D., Bilbao, J., Zimmermann, M., and Azkue, J.J. (2012). Time-Dependent Cross Talk between Spinal Serotonin 5-HT2A Receptor and mGluR1 Subserves Spinal Hyperexcitability and Neuropathic Pain after Nerve Injury. J. Neurosci. *32*, 13568–13581.

Alba-Delgado, C., Mountadem, S., Mermet-Joret, N., Monconduit, L., Dallel, R., Artola, A., and Antri, M. (2018). 5-HT $_{2A}$ Receptor-Induced Morphological Reorganization of PKCγ-Expressing Interneurons Gates Inflammatory Mechanical Allodynia in Rat. J. Neurosci. *38*, 10489–10504.

Alenina, N., Bashammakh, S., and Bader, M. (2006). Specification and differentiation of serotonergic neurons. Stem Cell Rev. *2*, 6.

Al-Juboori, S.I., Dondzillo, A., Stubblefield, E.A., Felsen, G., Lei, T.C., and Klug, A. (2013). Light Scattering Properties Vary across Different Regions of the Adult Mouse Brain. PLoS ONE *8*, e67626.

Alves, J.M., and Lin, K. (2018). Neuropathic Pain: A Review of Interneuronal Disinhibition. Arch. Neurosci. *5*.

Antal, M., Petkó, M., Polgár, E., Heizmann, C.W., and Storm-Mathisen, J. (1996). Direct evidence of an extensive GABAergic innervation of the spinal dorsal horn by fibres descending from the rostral ventromedial medulla. Neuroscience *73*, 509–518.

Arita, H., Sakamoto, M., Hirokawa, Y., and Okado, N. (1993). Serotonin innervation patterns differ among the various medullary motoneuronal groups involved in upper airway control. Exp. Brain Res. *95*, 100–110.

Arita, H., Ichikawa, K., and Sakamoto, M. (1995). Serotonergic cells in nucleus raphe pallidus provide tonic drive to posterior cricoarytenoid motoneurons via 5-hydroxytryptamine2 receptors in cats. Neurosci. Lett. *197*, 113–116.

Arreola, R., Becerril-Villanueva, E., Cruz-Fuentes, C., Velasco-Velázquez, M.A., Garcés-Alvarez, M.E., Hurtado-Alvarado, G., Quintero-Fabian, S., and Pavón, L. (2015). Immunomodulatory effects mediated by serotonin. J. Immunol. Res. *2015*, 354957.

Azmitia, E.C., and Gannon, P.J. (1986). The primate serotonergic system: a review of human and animal studies and a report on Macaca fascicularis. Adv. Neurol. *43*, 407–468.

Backonja, M. "Misha," Dahl, J., Gordon, D., Rudin, N., Seghal, N., and Gravel-Sullivan, A. (2010). Classification of Pain - Pain Management.

Balkovetz, D.F., Tiruppathi, C., Leibach, F.H., Mahesh, V.B., and Ganapathy, V. (1989). Evidence for an imipramine-sensitive serotonin transporter in human placental brush-border membranes. J. Biol. Chem. *264*, 2195–2198.

Bardin, L. (2011). The complex role of serotonin and 5-HT receptors in chronic pain. Behav. Pharmacol. *22*, 390–404.

Barnes, N.M., and Sharp, T. (1999). A review of central 5-HT receptors and their function. Neuropharmacology *38*, 1083–1152.

Basbaum, A.I., and Fields, H.L. (1978). Endogenous pain control mechanisms: review and hypothesis. Ann. Neurol. *4*, 451–462.

Basbaum, A.I., and Fields, H.L. (1984). Endogenous pain control systems: brainstem spinal pathways and endorphin circuitry. Annu. Rev. Neurosci. *7*, 309–338.

Basbaum, A.I., Bautista, D.M., Scherrer, G., and Julius, D. (2009). Cellular and Molecular Mechanisms of Pain. Cell *139*, 267–284.

Beecher, H.K. (1946). Pain in Men Wounded in Battle. Ann. Surg. *123*, 96–105.

Beggs, S., Trang, T., and Salter, M.W. (2012). P2X4R+ microglia drive neuropathic pain. Nat. Neurosci. *15*, 1068–1073.

Behzadi, G., Kalén, P., Parvopassu, F., and Wiklund, L. (1990). Afferents to the median raphe nucleus of the rat: retrograde cholera toxin and wheat germ conjugated horseradish peroxidase tracing, and selective D-[3H]aspartate labelling of possible excitatory amino acid inputs. Neuroscience *37*, 77–100.

Beitz, A.J. (1982). The nuclei of origin of brainstem serotonergic projections to the rodent spinal trigeminal nucleus. Neurosci. Lett. *32*, 223–228.

Bel, N., Figueras, G., Vilaró, M.T., Suñol, C., and Artigas, F. (1997). Antidepressant Drugs Inhibit a Gial 5-Hydroxytryptamine Transporter in Rat Brain. Eur. J. Neurosci. *9*, 1728–1738.

Benarroch, E.E. (2014). Medullary serotonergic system: Organization, effects, and clinical correlations. Neurology *83*, 1104–1111.

Benzon, H.T., Raja, S., Liu, S.S., Fishman, S., and Cohen, S.P. (2018). Essentials of pain medicine (Philadelphia, PA: Elseiver).

Berger, M., Gray, J.A., and Roth, B.L. (2009). The Expanded Biology of Serotonin. Annu. Rev. Med. *60*, 355–366.

Bergeron, M.J., Castonguay, A., and De Koninck, Y. (2014). KCC2 : nouvelle cible thérapeutique pour le traitement de pathologies neurologiques. médecine/sciences *30*, 514–517.

Björklund, A., and Skagerberg, G. (1982). Descending monoaminergic projections to the spinal cord. Sjölund B Björklund Eds Brain Stem Control Spinal Mech. Elsevier Amst. 55–88.

Bockaert, J., Claeysen, S., Compan, V., and Dumuis, A. (2011). 5-HT(4) receptors, a place in the sun: act two. Curr. Opin. Pharmacol. *11*, 87–93.

Bonin, R.P., Bories, C., and De Koninck, Y. (2014). A Simplified Up-Down Method (SUDO) for Measuring Mechanical Nociception in Rodents Using von Frey Filaments. Mol. Pain *10*, 1744-8069-10–26.

Bou Farah, L., Bowman, B.R., Bokiniec, P., Karim, S., Le, S., Goodchild, A.K., and McMullan, S. (2016). Somatostatin in the rat rostral ventrolateral medulla: Origins and mechanism of action: Somatostatinergic projections to the RVLM. J. Comp. Neurol. *524*, 323–342.

Bouhassira, D., and Attal, N. (2012). Douleurs neuropathiques (Arnette).

Bouhassira, D., Attal, N., Alchaar, H., Boureau, F., Brochet, B., Bruxelle, J., Cunin, G., Fermanian, J., Ginies, P., Grun-Overdyking, A., et al. (2005). Comparison of pain syndromes associated with nervous or somatic lesions and development of a new neuropathic pain diagnostic questionnaire (DN4). Pain *114*, 29–36.

Bourgoin, S., Oliveras, J.L., Bruxelle, J., Hamon, M., and Besson, J.M. (1980). Electrical stimulation of the nucleus raphe magnus in the rat. Effects on 5-HT metabolism in the spinal cord. Brain Res. *194*, 377–389.

Bourgoin, S., Gautier, A., and Hamon, M. (2017a). Le yin et le yang de la sérotonine : un Janus dans les contrôles de la douleur. Douleur Analgésie *30*, 35–56.

Bourgoin, S., Gautier, A., and Hamon, M. (2017b). Le yin et le yang de la sérotonine : un Janus dans les contrôles de la douleur. Douleur Analgésie *30*, 35–56.

Bourgoin, S., Gautier, A., and Hamon, M. (2017c). Le yin et le yang de la sérotonine : un Janus dans les contrôles de la douleur. Douleur Analgésie *30*, 35–56.

Bourquin, A.-F., Süveges, M., Pertin, M., Gilliard, N., Sardy, S., Davison, A.C., Spahn, D.R., and Decosterd, I. (2006). Assessment and analysis of mechanical allodynia-like behavior induced by spared nerve injury (SNI) in the mouse. Pain *122*, 14.e1-14.

Bowker, R.M., and Abbott, L.C. (1990). Quantitative re-evaluation of descending serotonergic and non-serotonergic projections from the medulla of the rodent: evidence for extensive co-existence of serotonin and peptides in the same spinally projecting neurons, but not from the nucleus raphe magnus. Brain Res. *512*, 15–25.

Bowker, R.M., Westlund, K.N., Sullivan, M.C., Wilber, J.F., and Coulter, J.D. (1983). Descending serotonergic, peptidergic and cholinergic pathways from the raphe nuclei: a multiple transmitter complex. Brain Res. *288*, 33–48.

Brenchat, A., Rocasalbas, M., Zamanillo, D., Hamon, M., Vela, J.M., and Romero, L. (2012). Assessment of 5-HT7 Receptor Agonists Selectivity Using Nociceptive and Thermoregulation Tests in Knockout versus Wild-Type Mice. Adv. Pharmacol. Sci. *2012*.

Brenner, D.S., Golden, J.P., and Gereau, R.W. (2012). A Novel Behavioral Assay for Measuring Cold Sensation in Mice. PLoS ONE *7*.

Brown, A.G., and Fyffe, R.E. (1981). Form and function of dorsal horn neurones with axons ascending the dorsal columns in cat. J. Physiol. *321*, 31–47.

Burgess, C. (2019). Comment mieux comprendre la douleur ?

Camarata, P.J., and Yaksh, T.L. (1985). Characterization of the spinal adrenergic receptors mediating the spinal effects produced by the microinjection of morphine into the periaqueductal gray. Brain Res. *336*, 133–142.

Campero, M., Baumann, T.K., Bostock, H., and Ochoa, J.L. (2009). Human cutaneous C fibres activated by cooling, heating and menthol. J. Physiol. *587*, 5633–5652.

Carpenter, M.B. (1985). Core text of neuroanatomy (Baltimore: Williams & Wilkins).

Castro, M.E., Pascual, J., Romón, T., del Arco, C., del Olmo, E., and Pazos, A. (1997). Differential distribution of [3H]sumatriptan binding sites (5-HT1B, 5-HT1D and 5-HT1F receptors) in human brain: focus on brainstem and spinal cord. Neuropharmacology *36*, 535–542.

Cervero, F., and Laird, J.M.A. (1996). Mechanisms of touch-evoked pain (allodynia): a new model. Pain *68*, 13–23.

Chalermkitpanit, P., Thonnagith, A., Engsusophon, P., Charuluxananan, S., and Honsawek, S. (2017). Noradrenaline, Serotonin, GABA, and Glycine in Cerebrospinal Fluid during Labor Pain: A Cross-Sectional Prospective Study. Pain Res. Manag. *2017*.

Cheah, M., Fawcett, J., and Andrews, M. (2017). Assessment of Thermal Pain Sensation in Rats and Mice Using the Hargreaves Test. BIO-Protoc. *7*.

Chen, B., Li, Y., Yu, B., Zhang, Z., Brommer, B., Williams, P.R., Liu, Y., Hegarty, S.V., Zhou, S., Zhu, J., et al. (2018). Reactivation of Dormant Relay Pathways in Injured Spinal Cord by KCC2 Manipulations. Cell *174*, 521-535.e13.

Chenaf, C., Delorme, J., Delage, N., Ardid, D., Eschalier, A., and Authier, N. (2018). Prevalence of chronic pain with or without neuropathic characteristics in France using the capture–recapture method: a population-based study. PAIN *159*, 2394–2402.

Cheng, J. (2018). Overview of Pain States. In Fundamentals of Pain Medicine, J. Cheng, and R.W. Rosenquist, eds. (Cham: Springer International Publishing), pp. 3–6.

Chiu, I.M., von Hehn, C.A., and Woolf, C.J. (2012). Neurogenic Inflammation – The Peripheral Nervous System's Role in Host Defense and Immunopathology. Nat. Neurosci. *15*, 1063–1067.

Cho, H., Yang, Y.D., Lee, J., Lee, B., Kim, T., Jang, Y., Back, S.K., Na, H.S., Harfe, B.D., Wang, F., et al. (2012). The calcium-activated chloride channel anoctamin 1 acts as a heat sensor in nociceptive neurons. Nat. Neurosci. *15*, 1015–1021.

Christensen, A.J., Iyer, S.M., François, A., Vyas, S., Ramakrishnan, C., Vesuna, S., Deisseroth, K., Scherrer, G., and Delp, S.L. (2016). In Vivo Interrogation of Spinal Mechanosensory Circuits. Cell Rep. *17*, 1699–1710.

Cichon, J., Sun, L., and Yang, G. (2018). Spared Nerve Injury Model of Neuropathic Pain in Mice. BIO-Protoc. *8*.

Ciranna, L. (2006). Serotonin as a Modulator of Glutamate- and GABA-Mediated Neurotransmission: Implications in Physiological Functions and in Pathology. Curr. Neuropharmacol. *4*, 101–114.

Cleeland, C.S., Nakamura, Y., Mendoza, T.R., Edwards, K.R., Douglas, J., and Serlin, R.C. (1996). Dimensions of the impact of cancer pain in a four country sample: new information from multidimensional scaling. Pain *67*, 267–273.

Commons, K.G., and Valentino, R.J. (2002). Cellular basis for the effects of substance P in the periaqueductal gray and dorsal raphe nucleus. J. Comp. Neurol. *447*, 82–97.

Connor, M., Bagley, E.E., Mitchell, V.A., Ingram, S.L., Christie, M.J., Humphrey, P.P.A., and Vaughan, C.W. (2004). Cellular actions of somatostatin on rat periaqueductal grey neurons in vitro. Br. J. Pharmacol. *142*, 1273–1280.

Cortes-Altamirano, J.L., Olmos-Hernández, A., Jaime, H.B., Carrillo-Mora, P., Bandala, C., Reyes-Long, S., and Alfaro-Rodríguez, A. (2018). Review: 5-HT1, 5-HT2, 5-HT3 and 5-HT7 Receptors and their Role in the Modulation of Pain Response in the Central Nervous System. Curr. Neuropharmacol. *16*, 210–221.

Costigan, M., Scholz, J., and Woolf, C.J. (2009). Neuropathic Pain: A Maladaptive Response of the Nervous System to Damage. Annu. Rev. Neurosci. *32*, 1–32.

Côté, F., Thévenot, E., Fligny, C., Fromes, Y., Darmon, M., Ripoche, M.-A., Bayard, E., Hanoun, N., Saurini, F., Lechat, P., et al. (2003). Disruption of the nonneuronal tph1 gene demonstrates the importance of peripheral serotonin in cardiac function. Proc. Natl. Acad. Sci. U. S. A. *100*, 13525–13530.

Coull, J.A.M., Beggs, S., Boudreau, D., Boivin, D., Tsuda, M., Inoue, K., Gravel, C., Salter, M.W., and De Koninck, Y. (2005). BDNF from microglia causes the shift in neuronal anion gradient underlying neuropathic pain. Nature *438*, 1017–1021.

Craig, A.D. (1994). The thermal grill illusion: unmasking the burn of cold pain.

Cramer, G.D., Darby, S.A., and Cramer, G.D. (2014). Clinical anatomy of the spine, spinal cord, and ANS (St. Louis, Mo: Elsevier).

Cucchiaro, G., Chaijale, N., and Commons, K.G. (2005). The dorsal raphe nucleus as a site of action of the antinociceptive and behavioral effects of the alpha4 nicotinic receptor agonist epibatidine. J. Pharmacol. Exp. Ther. *313*, 389–394.

Cui, M., Feng, Y., McAdoo, D.J., and Willis, W.D. (1999). Periaqueductal gray stimulation-induced inhibition of nociceptive dorsal horn neurons in rats is associated with the release of norepinephrine, serotonin, and amino acids. J. Pharmacol. Exp. Ther. *289*, 868–876.

Dahlstroem, A., and Fuxe, K. (1964). Evidence for the existence of monoamine-containing neurons in the central nervous system. I. Demonstration of monoamines in the cell bodies of brain stem neurons. Acta Physiol. Scand. Suppl. SUPPL 232:1-55.

D'Amico, J.M., Murray, K.C., Li, Y., Chan, K.M., Finlay, M.G., Bennett, D.J., and Gorassini, M.A. (2013). Constitutively active 5-HT2/α1 receptors facilitate muscle spasms after human spinal cord injury. J. Neurophysiol. *109*, 1473–1484.

Davis, K.D., Meyer, R.A., and Campbell, J.N. (1993). Chemosensitivity and sensitization of nociceptive afferents that innervate the hairy skin of monkey. J. Neurophysiol. *69*, 1071–1081.

Decosterd, I., and Woolf, C.J. (2000). Spared nerve injury: an animal model of persistent peripheral neuropathic pain: Pain *87*, 149–158.

Descarries, L., and Mechawar, N. (2000). Ultrastructural evidence for diffuse transmission by monoamine and acetylcholine neurons of the central nervous system. Prog. Brain Res. *125*, 27–47.

Descarries, L., Riad, M., and Parent, M. (2010). Ultrastructure of the Serotonin Innervation in the Mammalian Central Nervous System. In Handbook of Behavioral Neuroscience, (Elsevier), pp. 65–101.

Descartes, R. (1648). Traité de l'homme (Chicoutimi: J.-M. Tremblay).

Dogrul, A., Ossipov, M.H., and Porreca, F. (2009). Differential mediation of descending pain facilitation and inhibition by spinal 5HT-3 and 5HT-7 receptors. Brain Res. *1280*, 52–59.

Dostrovsky, J.O., and Craig, A.D. (1996). Cooling-specific spinothalamic neurons in the monkey | Journal of Neurophysiology.

Doyon, N. (2011). Efficacy of Synaptic Inhibition Depends on Multiple, Dynamically Interacting Mechanisms Implicated in Chloride Homeostasis.

Duerschmied, D., Canault, M., Lievens, D., Brill, A., Cifuni, S.M., Bader, M., and Wagner, D.D. (2009). Serotonin stimulates platelet receptor shedding by tumor necrosis factor-alpha-converting enzyme (ADAM17). J. Thromb. Haemost. JTH *7*, 1163–1171.

Duraku, L.S., Hossaini, M., Hoendervangers, S., Falke, L.L., Kambiz, S., Mudera, V.C., Holstege, J.C., Walbeehm, E.T., and Ruigrok, T.J.H. (2012). Spatiotemporal Dynamics of Re-Innervation and Hyperinnervation Patterns by Uninjured CGRP Fibers in the Rat Foot Sole Epidermis after Nerve Injury. Mol. Pain *8*, 1744-8069-8–61.

Edmondson, E.A. (2017). Chapter 27 - Pain Processing and Modulation. In Neurology Secrets (Sixth Edition), J.S. Kass, and E.M. Mizrahi, eds. (Elsevier), pp. 375-388.e1.

Erb, W. (1874). Handbuch der Krankheiten des Nervensystems II (F.C.W. Vogel).

Faerber, L., Drechsler, S., Ladenburger, S., Gschaidmeier, H., and Fischer, W. (2007). The neuronal 5-HT3 receptor network after 20 years of research--evolving concepts in management of pain and inflammation. Eur. J. Pharmacol. *560*, 1–8.

Fanselow, M.S. (1986). Conditioned fear-induced opiate analgesia: a competing motivational state theory of stress analgesia. Ann. N. Y. Acad. Sci. *467*, 40–54.

Faraj, B.A., Olkowski, Z.L., and Jackson, R.T. (1997). Prevalence of high serotonin uptake in lymphocytes of abstinent alcoholics. Biochem. Pharmacol. *53*, 53–57.

Felten, D.L., and Sladek, J.R. (1983). Monoamine distribution in primate brain V. Monoaminergic nuclei: anatomy, pathways and local organization. Brain Res. Bull. *10*, 171–284.

Fields, H. (2004). State-dependent opioid control of pain. Nat. Rev. Neurosci. *5*, 565–575.

Fields, H.L. (1987). Pain.

Fields, H.L., and Basbaum, A.I. (2005). Central nervous system mechanisms of pain modulation. (Philadelphia, PA: Elsevier/Saunders).

Fields, H.L., Heinricher, M.M., and Mason, P. (1991). Neurotransmitters in nociceptive modulatory circuits. Annu. Rev. Neurosci. *14*, 219–245.

Fischman, S.M., Ballantyne, J.C., and Rathmell, J.P. (2010). Bonica's Management of Pain 4th Edition. 1698.

Fossat, P., Sibon, I., Le Masson, G., Landry, M., and Nagy, F. (2007). L-type calcium channels and NMDA receptors: a determinant duo for short-term nociceptive plasticity: L-calcium channel and NMDAr cooperation in windup. Eur. J. Neurosci. *25*, 127–135.

François, A., Low, S.A., Sypek, E.I., Christensen, A.J., Sotoudeh, C., Beier, K.T., Ramakrishnan, C., Ritola, K.D., Sharif-Naeini, R., Deisseroth, K., et al. (2017). A Brainstem-Spinal Cord Inhibitory Circuit for Mechanical Pain Modulation by GABA and Enkephalins. Neuron *93*, 822-839.e6.

Freynhagen, R., Parada, H.A., Calderon-Ospina, C.A., Chen, J., Rakhmawati Emril, D., Fernández-Villacorta, F.J., Franco, H., Ho, K.-Y., Lara-Solares, A., Li, C.C.-F., et al. (2019). Current understanding of the mixed pain concept: a brief narrative review. Curr. Med. Res. Opin. *35*, 1011–1018.

from School History (2018). An invocation to I em hetep, the Egyptian deity of medicine.

from TCM, Woodbridge (2019). Traditional Chinese Medicine (TCM).

Fulop-Miller, R. (1938). Triumph Over Pain (The Bobbs-Merrill company).

Gagnon, M., Bergeron, M.J., Lavertu, G., Castonguay, A., Tripathy, S., Bonin, R.P., Perez-Sanchez, J., Boudreau, D., Wang, B., Dumas, L., et al. (2013). Chloride extrusion enhancers as novel therapeutics for neurological diseases. Nat. Med. *19*, 1524–1528.

Gang, S., Nakazono, Y., Aoki, M., and Aoki N [corrected to Aoki, M. (1993). Differential projections to the raphe nuclei from the medial parabrachial-Kölliker-Fuse (NPBM-KF) nuclear complex and the retrofacial nucleus in cats: retrograde WGA-HRP tracing. J. Auton. Nerv. Syst. *45*, 241–244.

Gasser, H.S. (1941). The Classification of Nerve Fibers. 15.

Gautier, A., Geny, D., Bourgoin, S., Bernard, J.F., and Hamon, M. (2017). Differential innervation of superficial versus deep laminae of the dorsal horn by bulbo-spinal serotonergic pathways in the rat. IBRO Rep. *2*, 72–80.

Gebhart, G.F., Sandkühler, J., Thalhammer, J.G., and Zimmermann, M. (1983). Inhibition of spinal nociceptive information by stimulation in midbrain of the cat is blocked by lidocaine microinjected in nucleus raphe magnus and medullary reticular formation. J. Neurophysiol. *50*, 1446–1459.

Gobel, S., Falls, W.M., and Humphrey, E. (1981). Morphology and synaptic connections of ultrafine primary axons in lamina I of the spinal dorsal horn: candidates for the terminal axonal arbors of primary neurons with unmyelinated (C) axons. J. Neurosci. Off. J. Soc. Neurosci. *1*, 1163–1179.

Godínez-Chaparro, B., Barragán-Iglesias, P., Castañeda-Corral, G., Rocha-González, H.I., and Granados-Soto, V. (2011). Role of peripheral 5-HT4, 5-HT6, and 5-HT7 receptors in development and maintenance of secondary mechanical allodynia and hyperalgesia: Pain *152*, 687–697.

Goldscheider, . (1884). The specificity energy of the sensory nerves of the skin.

Green, G.M., Scarth, J., and Dickenson, A. (2000). An excitatory role for 5-HT in spinal inflammatory nociceptive transmission; state-dependent actions via dorsal horn 5-HT(3) receptors in the anaesthetized rat. Pain *89*, 81–88.

Guilbaud, G. (1997). Physiologie du circuit de la douleur (Philadelphia, PA: Elsevier/Saunders).

Guo, W. (2006). Supraspinal Brain-Derived Neurotrophic Factor Signaling: A Novel Mechanism for Descending Pain Facilitation. J. Neurosci. *26*, 126–137.

Guo, W., Miyoshi, K., Dubner, R., Gu, M., Li, M., Liu, J., Yang, J., Zou, S., Ren, K., Noguchi, K., et al. (2014). Spinal 5-HT3 receptors mediate descending facilitation and contribute to behavioral hypersensitivity via a reciprocal neuron-glial signaling cascade. Mol. Pain *10*, 35.

Hamon, M. (1995). Sérotonine — 5-hydroxytryptamine (5-HT). Epelbaum J 261–270.

Hamon, M., and Bourgoin, S. (1999). Serotonin and its receptors in pain controls. Nov. Asp. Pain Manag. Opioids Beyond 203–28.

Han, Z.S., Zhang, E.T., and Craig, A.D. (1998). Nociceptive and thermoreceptive lamina I neurons are anatomically distinct. Nat. Neurosci. *1*, 218–225.

Handwerker, H.O., Anton, F., and Reeh, P.W. (1987). Discharge patterns of afferent cutaneous nerve fibers from the rat's tail during prolonged noxious mechanical stimulation. Exp. Brain Res. *65*, 493–504.

Hannon, J., and Hoyer, D. (2008). Molecular biology of 5-HT receptors. Behav. Brain Res. *195*, 198–213.

Harriott, N.D., Williams, J.P., Smith, E.B., Bozigian, H.P., and Grigoriadis, D.E. (2018). Chapter Two - VMAT2 Inhibitors and the Path to Ingrezza (Valbenazine). In Progress in Medicinal Chemistry, D.R. Witty, and B. Cox, eds. (Elsevier), pp. 87–111.

Hendricks, T., Francis, N., Fyodorov, D., and Deneris, E.S. (1999). The ETS Domain Factor Pet-1 Is an Early and Precise Marker of Central Serotonin Neurons and Interacts with a Conserved Element in Serotonergic Genes. J. Neurosci. *19*, 10348–10356.

Hentall, I.D., Pinzon, A., and Noga, B.R. (2006). Spatial and temporal patterns of serotonin release in the rat's lumbar spinal cord following electrical stimulation of the nucleus raphe magnus. Neuroscience *142*, 893–903.

Hermann, D.M., Luppi, P.-H., Peyron, C., Hinckel, P., and Jouvet, M. (1997). Afferent projections to the rat nuclei raphe magnus, raphe pallidus and reticularis gigantocellularis pars h demonstrated by iontophoretic application of choleratoxin (subunit b). J. Chem. Neuroanat. 21.

Herr, N., Bode, C., and Duerschmied, D. (2017). The Effects of Serotonin in Immune Cells. Front. Cardiovasc. Med. *4*.

Hery, F., Faudon, M., and Ternaux, J.P. (1982). In vivo release of serotonin in two raphe nuclei (raphe dorsalis and magnus) of the cat. Brain Res. Bull. *8*, 123–129.

Hirst, W.D. (1998). Serotonin transporters in adult rat brain astrocytes revealed by [3H]5-HTuptake into glial plasmalemmal vesicles. Neurochem. Int. 11–22.

Hof, P.R., and Young, W.G. (2000). Comparative Cytoarchitectonic Atlas of the C57BL/6 and 129/Sv Mouse Brains (Elsevier).

Hökfelt, T., Arvidsson, U., Cullheim, S., Millhorn, D., Nicholas, A.P., Pieribone, V., Seroogy, K., and Ulfhake, B. (2000). Multiple messengers in descending serotonin neurons: localization and functional implications. J. Chem. Neuroanat. *18*, 75–86.

Hranilović, D., Lesch, K.P., Ugarković, D., Cicin-Sain, L., and Jernej, B. (1996). Identification of serotonin transporter mRNA in rat platelets. J. Neural Transm. Vienna Austria 1996 *103*, 957–965.

Huang, J., Gadotti, V.M., Chen, L., Souza, I.A., Huang, S., Wang, D., Ramakrishnan, C., Deisseroth, K., Zhang, Z., and Zamponi, G.W. (2019). A neuronal circuit for activating descending modulation of neuropathic pain. Nat. Neurosci. *22*, 1659–1668.

IASP (2019a). IASP Terminology - IASP.

IASP (2019b). - IASP.

Inazu, M., Takeda, H., Ikoshi, H., Sugisawa, M., Uchida, Y., and Matsumiya, T. (2001). Pharmacological characterization and visualization of the glial serotonin transporter. Neurochem. Int. *39*, 39–49.

Jeong, H.-J., Mitchell, V.A., and Vaughan, C.W. (2012). Role of 5-HT(1) receptor subtypes in the modulation of pain and synaptic transmission in rat spinal superficial dorsal horn. Br. J. Pharmacol. *165*, 1956–1965.

Kaila, K., Price, T.J., Payne, J.A., Puskarjov, M., and Voipio, J. (2014). Cation-chloride cotransporters in neuronal development, plasticity and disease. Nat. Rev. Neurosci. *15*, 637–654.

Kambrun, C., Roca-Lapirot, O., Salio, C., Landry, M., Moqrich, A., and Le Feuvre, Y. (2018). TAFA4 Reverses Mechanical Allodynia through Activation of GABAergic Transmission and Microglial Process Retraction. Cell Rep. *22*, 2886–2897.

Kawamata, T., Omote, K., Toriyabe, M., Yamamoto, H., and Namiki, A. (2003). The activation of 5-HT(3) receptors evokes GABA release in the spinal cord. Brain Res. *978*, 250–255.

Kayser, V., Elfassi, I.E., Aubel, B., Melfort, M., Julius, D., Gingrich, J.A., Hamon, M., and Bourgoin, S. (2007). Mechanical, thermal and formalin-induced nociception is differentially altered in 5-HT1A−/−, 5-HT1B−/−, 5-HT2A−/−, 5-HT3A−/− and 5-HTT−/− knock-out male mice. PAIN *130*, 235–248.

Keele, K.D. (1957). Anatomies of pain.

Keirsey, D. (1998). Please understand me II: temperament, character, intelligence (Del Mar, CA: Prometheus Nemesis).

Kim, J.-H., Gangadharan, G., Byun, J., Choi, E.-J., Lee, C.J., and Shin, H.-S. (2018). Yin-and-yang bifurcation of opioidergic circuits for descending analgesia at the midbrain of the mouse. Proc. Natl. Acad. Sci. U. S. A. *115*, 11078–11083.

Kirifides, M.L., Simpson, K.L., Lin, R.C., and Waterhouse, B.D. (2001). Topographic organization and neurochemical identity of dorsal raphe neurons that project to the trigeminal somatosensory pathway in the rat. J. Comp. Neurol. *435*, 325–340.

Kiyasova, V., and Gaspar, P. (2011). Development of raphe serotonin neurons from specification to guidance: Development of raphe serotonin neurons. Eur. J. Neurosci. *34*, 1553–1562.

Kwiat, G.C., and Basbaum, A.I. (1992). The origin of brainstem noradrenergic and serotonergic projections to the spinal cord dorsal horn in the rat. Somatosens. Mot. Res. *9*, 157–173.

LaMotte, C. (1977). Distribution of the tract of Lissauer and the dorsal root fibers in the primate spinal cord. J. Comp. Neurol. *172*, 529–561.

LaMotte, C.C., and de Lanerolle, N.C. (1983). Ultrastructure of chemically defined neuron systems in the dorsal horn of the monkey. III. Serotonin immunoreactivity. Brain Res. *274*, 65–77.

Lanfumey, L., and Hamon, M. (2004). 5-HT1 receptors. Curr. Drug Targets CNS Neurol. Disord. *3*, 1–10.

Lau, B.K., and Vaughan, C.W. (2014). Descending modulation of pain: the GABA disinhibition hypothesis of analgesia. Curr. Opin. Neurobiol. *29*, 159–164.

Lauder, J.M. (1990). Ontogeny of the Serotonergic System in the Rat: Serotonin as a Developmental Signal. Ann. N. Y. Acad. Sci. *600*, 297–313.

Lavertu, G., Côté, S.L., and De Koninck, Y. (2014). Enhancing K–Cl co-transport restores normal spinothalamic sensory coding in a neuropathic pain model. Brain *137*, 724–738.

Le Bars, D. (2002). The whole body receptive field of dorsal horn multireceptive neurones. Brain Res. Brain Res. Rev. *40*, 29–44.

Le Bars, D., and Chitour, D. (1983). Do convergent neurones in the spinal dorsal horn discriminate nociceptive from non-nociceptive information? Pain *17*, 1–19.

Le Bars, D., and Villanueva, L. (1988). Electrophysiological evidence for the activation of descending inhibitory controls by nociceptive afferent pathways. Prog. Brain Res. *77*, 275–299.

Lee, H.S., Kim, M.A., Valentino, R.J., and Waterhouse, B.D. (2003). Glutamatergic afferent projections to the dorsal raphe nucleus of the rat. Brain Res. *963*, 57–71.

Lee, H.S., Kim, M.-A., and Waterhouse, B.D. (2005a). Retrograde double-labeling study of common afferent projections to the dorsal raphe and the nuclear core of the locus coeruleus in the rat. J. Comp. Neurol. *481*, 179–193.

Lee, H.S., Lee, B.Y., and Waterhouse, B.D. (2005b). Retrograde study of projections from the tuberomammillary nucleus to the dorsal raphe and the locus coeruleus in the rat. Brain Res. *1043*, 65–75.

Leipzig (1875). Glossar und Text (Leipzig: Engelmann).

Lewis, T. (1935). Experiments relating to cutaneous hyperalgesia and its spread through somatic fibres.

Li, J.L., Kaneko, T., Nomura, S., Li, Y.Q., and Mizuno, N. (1997). Association of serotonin-like immunoreactive axons with nociceptive projection neurons in the caudal spinal trigeminal nucleus of the rat. J. Comp. Neurol. *384*, 127–141.

Li, Y.-Q., Takada, M., and Mizuno, N. (1993). The sites of origin of serotoninergic afferent fibers in the trigeminal motor, facial, and hypoglossal nuclei in the rat. Neurosci. Res. *17*, 307–313.

Light, A.R., Trevino, D.L., and Perl, E.R. (1979). Morphological features of functionally defined neurons in the marginal zone and substantia gelatinosa of the spinal dorsal horn. J. Comp. Neurol. *186*, 151–171.

Liljencrantz, J., and Olausson, H. (2014). Tactile C fibers and their contributions to pleasant sensations and to tactile allodynia. Front. Behav. Neurosci. *8*.

Lima, L.V., DeSantana, J.M., Rasmussen, L.A., and Sluka, K.A. (2017). Short-duration physical activity prevents the development of activity-induced hyperalgesia through opioid and serotoninergic mechanisms: PAIN *158*, 1697–1710.

Lisovoski, F. (2006). 2 ème partie : LES SYSTÈMES PHYSIOLOGIQUES DE CONTRÔLE DE LA TRANSMISSION. 2.

Liu, X.-G., and Sandkühler, J. (1997). Characterization of Long-Term Potentiation of C-Fiber–Evoked Potentials in Spinal Dorsal Horn of Adult Rat: Essential Role of NK1 and NK2 Receptors. J. Neurophysiol. *78*, 1973–1982.

Lloyd, D.P.C. (1962). THE CLASSIFICATION OF GALVANIC SKIN REFLEX AFFERENT FIBERS*. Proc. Natl. Acad. Sci. U. S. A. *48*, 814–817.

Lu, Y., and Perl, E.R. (2007). Selective action of noradrenaline and serotonin on neurones of the spinal superficial dorsal horn in the rat. J. Physiol. *582*, 127–136.

Lumb, B.M. (2002). Inescapable and Escapable Pain is Represented in Distinct Hypothalamic-Midbrain Circuits: Specific Roles for aδ- and C-Nociceptors. Exp. Physiol. *87*, 281–286.

Madisen, L., Zwingman, T.A., Sunkin, S.M., Oh, S.W., Zariwala, H.A., Gu, H., Ng, L.L., Palmiter, R.D., Hawrylycz, M.J., Jones, A.R., et al. (2010). A robust and high-throughput Cre reporting and characterization system for the whole mouse brain. Nat. Neurosci. *13*, 133–140.

Maione, S., Bisogno, T., de Novellis, V., Palazzo, E., Cristino, L., Valenti, M., Petrosino, S., Guglielmotti, V., Rossi, F., and Di Marzo, V. (2006). Elevation of endocannabinoid levels in the ventrolateral periaqueductal grey through inhibition of fatty acid amide hydrolase affects descending nociceptive pathways via both cannabinoid receptor type 1 and transient receptor potential vanilloid type-1 receptors. J. Pharmacol. Exp. Ther. *316*, 969–982.

Mapplebeck, J.C.S., Lorenzo, L.-E., Lee, K.Y., Gauthier, C., Muley, M.M., De Koninck, Y., Prescott, S.A., and Salter, M.W. (2019a). Chloride Dysregulation through Downregulation of KCC2 Mediates Neuropathic Pain in Both Sexes. Cell Rep. *28*, 590-596.e4.

Mapplebeck, J.C.S., Lorenzo, L.-E., Lee, K.Y., Gauthier, C., Muley, M.M., De Koninck, Y., Prescott, S.A., and Salter, M.W. (2019b). Chloride Dysregulation through Downregulation of KCC2 Mediates Neuropathic Pain in Both Sexes. Cell Rep. *28*, 590-596.e4.

Marinelli, S., Vaughan, C.W., Schnell, S.A., Wessendorf, M.W., and Christie, M.J. (2002). Rostral Ventromedial Medulla Neurons That Project to the Spinal Cord Express Multiple Opioid Receptor Phenotypes. J. Neurosci. *22*, 10847–10855.

Mason, P. (1999). Central mechanisms of pain modulation. Curr. Opin. Neurobiol. *9*, 436–441.

Mason, P. (2005). Ventromedial medulla: pain modulation and beyond. J. Comp. Neurol. *493*, 2–8.

Masson, J., Emerit, M.B., Hamon, M., and Darmon, M. (2012). Serotonergic signaling: multiple effectors and pleiotropic effects. Wiley Interdiscip. Rev. Membr. Transp. Signal. *1*, 685–713.

Maxwell, L., Maxwell, D.J., Neilson, M., and Kerr, R. (1996). A confocal microscopic survey of serotoninergic axons in the lumbar spinal cord of the rat: co-localization with glutamate decarboxylase and neuropeptides. Neuroscience *75*, 471–480.

McMahon, S.B., and Meyer, R.A. (2013). Wall and Melzack's textbook of pain (Philadelphia, PA: Elsevier/Saunders).

Melzack, R. (2001). Pain and the Neuromatrix in the Brain. J. Dent. Educ. *65*, 5.

Melzack, R., and Casey, K.L. (1968). SENSORY, MOTIVATIONAL, AND CENTRAL CONTROL DETERMINANTS OF PAIN. 19.

Melzack, R., and Wall, P.D. (1965). Pain Mechanisms: A New Theory. Science *150*, 971–978.

Mendell, L.M. (1966). Physiological properties of unmyelinated fiber projection to the spinal cord. Exp. Neurol. *16*, 316–332.

Mengod, G., Vilaró, M.T., Cortés, R., López-Giménez, J.F., Raurich, A., and Palacios, J.M. (2006). Chemical Neuroanatomy of 5-HT Receptor Subtypes in the Mammalian Brain. In The Serotonin Receptors, B.L. Roth, ed. (Totowa, NJ: Humana Press), pp. 319–364.

Merskey, H., and Bogduk, N. (1994). Classification of chronic pain: descriptions of chronic pain syndromes and definitions of pain terms (Seattle: IASP Press).

Meyer, R.A. (2006). Peripheral neural mechanisms of nociception In Wall and Melzack's textbook of pain (Philadelphia, PA: Elsevier/Saunders).

Meyer, R.A. (2013). Wall and Melzack's textbook of pain (Philadelphia, PA: Elsevier/Saunders).

Meyer, R.A., and Campbell, J.N. (1981). Myelinated nociceptive afferents account for the hyperalgesia that follows a burn to the hand. Science *213*, 1527–1529.

Meyer, R.A., Raja, S.N., and Campbell, J.N. (1985). Coupling of action potential activity between unmyelinated fibers in the peripheral nerve of monkey. Science *227*, 184–187.

Millan, M. (1997). The role of descending noradrenergic and serotoninergic pathways in the modulation of nociception: focus on receptor multiplicity. Handb. Exp. Pharmacol. Vol 130 Springer Berl. *130*, 385–446.

Millan, M.J. (2002a). Descending control of pain. Prog. Neurobiol. 120.

Millan, M.J. (2002b). Descending control of pain. Prog. Neurobiol. 120.

Mogil, J.S., and Bailey, A.L. (2010). Sex and gender differences in pain and analgesia. Prog. Brain Res. *186*, 141–157.

Mohammad-Zadeh, L.F., Moses, L., and Gwaltney-Brant, S.M. (2008). Serotonin: a review. J. Vet. Pharmacol. Ther. *31*, 187–199.

Moon, H.C., and Park, Y.S. (2017). Reduced GABAergic neuronal activity in zona incerta causes neuropathic pain in a rat sciatic nerve chronic constriction injury model.

Morgan, M.M., Whittier, K.L., Hegarty, D.M., and Aicher, S.A. (2008). Periaqueductal gray neurons project to spinally projecting GABAergic neurons in the rostral ventromedial medulla: Pain *140*, 376–386.

Mössner, R., and Lesch, K.P. (1998). Role of serotonin in the immune system and in neuroimmune interactions. Brain. Behav. Immun. *12*, 249–271.

Moyle, S. (2015). Pain Assessment and Management.

Müller, J. (1838). Elements of physiology (London Taylor & Walton).

Müller, C.P., and Jacobs, B.L. (2010). Handbook of the behavioral neurobiology of serotonin (Amsterdam: Elsevier/Academic Press).

Narboux-Nême, N., Sagné, C., Doly, S., Diaz, S.L., Martin, C.B.P., Angenard, G., Martres, M.-P., Giros, B., Hamon, M., Lanfumey, L., et al. (2011). Severe Serotonin Depletion after Conditional Deletion of the Vesicular Monoamine Transporter 2 Gene in Serotonin Neurons: Neural and Behavioral Consequences. Neuropsychopharmacology *36*, 2538–2550.

Neubert, M.J., Kincaid, W., and Heinricher, M.M. (2004). Nociceptive facilitating neurons in the rostral ventromedial medulla. Pain *110*, 158–165.

Ossipov, M.H., Dussor, G.O., and Porreca, F. (2010). Central modulation of pain. J. Clin. Invest. *120*, 3779–3787.

Ossipov, M.H., Morimura, K., and Porreca, F. (2014). Descending pain modulation and chronification of pain. Curr. Opin. Support. Palliat. Care *8*, 143–151.

Patetsos, E., and Horjales-Araujo, E. (2016). Treating Chronic Pain with SSRIs: What Do We Know? Pain Res. Manag. *2016*.

Peirs, C., Patil, S., Bouali-Benazzouz, R., Artola, A., Landry, M., and Dallel, R. (2014). Protein kinase C gamma interneurons in the rat medullary dorsal horn: distribution and synaptic inputs to these neurons, and subcellular localization of the enzyme. J. Comp. Neurol. *522*, 393–413.

Perl, E. (2007). Ideas about pain, a historical view.

Perrin, F.E., Gerber, Y.N., Teigell, M., Lonjon, N., Boniface, G., Bauchet, L., Rodriguez, J.J., Hugnot, J.P., and Privat, A.M. (2011). Anatomical study of serotonergic innervation and 5-HT1A receptor in the human spinal cord. Cell Death Dis. *2*, e218.

Pertovaara, A. (2006). Noradrenergic pain modulation. Prog. Neurobiol. *80*, 53–83.

Peyron, C., Petit, J.M., Rampon, C., Jouvet, M., and Luppi, P.H. (1998). Forebrain afferents to the rat dorsal raphe nucleus demonstrated by retrograde and anterograde tracing methods. Neuroscience *82*, 443–468.

Porreca, F., Burgess, S.E., Gardell, L.R., Vanderah, T.W., Malan, T.P., Ossipov, M.H., Lappi, D.A., and Lai, J. (2001). Inhibition of Neuropathic Pain by Selective Ablation of Brainstem Medullary Cells Expressing the μ-Opioid Receptor. J. Neurosci. *21*, 5281–5288.

Price, T.J., Cervero, F., and de Koninck, Y. (2005). Role of Cation-Chloride-Cotransporters (CCC) in Pain and Hyperalgesia. Curr. Top. Med. Chem. *5*, 547–555.

Puig, S., and Sorkin, L.S. (1996). Formalin-evoked activity in identified primary afferent fibers: systemic lidocaine suppresses phase-2 activity. Pain *64*, 345–355.

Rahman, W., Suzuki, R., Webber, M., Hunt, S.P., and Dickenson, A.H. (2006). Depletion of endogenous spinal 5-HT attenuates the behavioural hypersensitivity to mechanical and cooling stimuli induced by spinal nerve ligation. Pain *123*, 264–274.

Rahman, W., Bannister, K., Bee, L.A., and Dickenson, A.H. (2011). A pronociceptive role for the 5-HT2 receptor on spinal nociceptive transmission: an in vivo electrophysiological study in the rat. Brain Res. *1382*, 29–36.

Rampon, C., Peyron, C., Gervasoni, D., Pow, D.V., Luppi, P.H., and Fort, P. (1999). Origins of the glycinergic inputs to the rat locus coeruleus and dorsal raphe nuclei: a study combining retrograde tracing with glycine immunohistochemistry. Eur. J. Neurosci. *11*, 1058–1066.

Reali, C., Fossat, P., Landry, M., Russo, R.E., and Nagy, F. (2011). Intrinsic membrane properties of spinal dorsal horn neurones modulate nociceptive information processing in vivo. J. Physiol. *589*, 2733–2743.

de Resende, M.A., Silva, L.F.S., Sato, K., Arendt-Nielsen, L., and Sluka, K.A. (2011). Blockade of Opioid Receptors in the Medullary Reticularis Nucleus Dorsalis, but not the Rostral Ventromedial Medulla, Prevents Analgesia Produced by Diffuse Noxious Inhibitory Control in Rats With Muscle Inflammation. J. Pain Off. J. Am. Pain Soc. *12*, 687–697.

Reubi, J.C., Emson, P.C., Jessell, T.M., and Iversen, L.L. (1978). Effects of GABA, dopamine, and substance P on the release of newly synthesized 3H-5-hydroxytryptamine from rat substantia nigra in vitro. Naunyn. Schmiedebergs Arch. Pharmacol. *304*, 271–275.

Rexed, B. (1952). The cytoarchitectonic organization of the spinal cord in the cat. J. Comp. Neurol. *96*, 415–495.

Rexed, B. (1954). A cytoarchitectonic atlas of the spinal coed in the cat. J. Comp. Neurol. *100*, 297–379.

Ribeiro-do-Valle, L.E. (1997). Serotonergic neurons in the caudal raphe nuclei discharge in association with activity of masticatory muscles. Braz. J. Med. Biol. Res. Rev. Bras. Pesqui. Medicas E Biol. *30*, 79–83.

Ridet, J.L., Rajaofetra, N., Teilhac, J.R., Geffard, M., and Privat, A. (1993). Evidence for nonsynaptic serotonergic and noradrenergic innervation of the rat dorsal horn and possible involvement of neuron-glia interactions. Neuroscience *52*, 143–157.

Ringkamp, M., and Meyer, R.A. (2009). Science of pain (Amsterdam: Academic Press, Elsevier).

Rocha-González, H.I., Meneses, A., Carlton, S.M., and Granados-Soto, V. (2005). Pronociceptive role of peripheral and spinal 5-HT7 receptors in the formalin test. Pain *117*, 182–192.

Ruda, M.A. (1988). Spinal dorsal horn circuitry involved in the brain stem control of nociception. Prog. Brain Res. *77*, 129–140.

Ruda, M.A., and Gobel, S. (1980). Ultrastructural characterization of axonal endings in the substantia gelatinosa which take up [3H]serotonin. Brain Res. *184*, 57–83.

Ruda, M.A., Coffield, J., and Steinbusch, H.W.M. (1982). Immunocytochemical analysis of serotonergic axons in laminae I and II of the lumbar spinal cord of the cat. 12.

Rudnick, G. (1977). Active transport of 5-hydroxytryptamine by plasma membrane vesicles isolated from human blood platelets. J. Biol. Chem. *252*, 2170–2174.

Sadlaoud, K., Tazerart, S., Brocard, C., Jean-Xavier, C., Portalier, P., Brocard, F., Vinay, L., and Bras, H. (2010). Differential Plasticity of the GABAergic and Glycinergic Synaptic Transmission to Rat Lumbar Motoneurons after Spinal Cord Injury. J. Neurosci. *30*, 3358–3369.

Samineni, V.K., Grajales-Reyes, J.G., Copits, B.A., O'Brien, D.E., Trigg, S.L., Gomez, A.M., Bruchas, M.R., and Gereau, R.W. (2017). Divergent Modulation of Nociception by Glutamatergic and GABAergic Neuronal Subpopulations in the Periaqueductal Gray. Eneuro *4*, ENEURO.0129-16.2017.

Sandkühler, J. (2007). Understanding LTP in pain pathways. Mol. Pain *3*, 9.

Sasaki, M., Obata, H., Kawahara, K., Saito, S., and Goto, F. (2006). Peripheral 5-HT2A receptor antagonism attenuates primary thermal hyperalgesia and secondary mechanical allodynia after thermal injury in rats: Pain *122*, 130–136.

Saunders, J.B.DeC.M. (1967). HUANG TI NEI CHING SU WEN. Calif. Med. *107*, 125–126.

Schmidt, R.R., and Willis, W.D. (2007). Encyclopedia of Pain. 2803.

Scholz, J., and Woolf, C.J. (2002). Can we conquer pain? Nat. Neurosci. *5 Suppl*, 1062–1067.

Schwaller, F., Kanellopoulos, A.H., and Fitzgerald, M. (2017). The developmental emergence of differential brainstem serotonergic control of the sensory spinal cord. Sci. Rep. *7*, 2215.

Scott, M.M., Wylie, C.J., Lerch, J.K., Murphy, R., Lobur, K., Herlitze, S., Jiang, W., Conlon, R.A., Strowbridge, B.W., and Deneris, E.S. (2005a). A genetic approach to access serotonin neurons for in vivo and in vitro studies. Proc. Natl. Acad. Sci. *102*, 16472–16477.

Scott, M.M., Wylie, C.J., Lerch, J.K., Murphy, R., Lobur, K., Herlitze, S., Jiang, W., Conlon, R.A., Strowbridge, B.W., and Deneris, E.S. (2005b). A genetic approach to access serotonin neurons for in vivo and in vitro studies. Proc. Natl. Acad. Sci. *102*, 16472–16477.

Segu, L., and Calas, A. (1978). The topographical distribution of serotoninergic terminals in the spinal cord of the cat: Quantitative radioautographic studies. Brain Res. *153*, 449–464.

Sela, R.A., Bruera, E., Conner-spady, B., Cumming, C., and Walker, C. (2002). Sensory and affective dimensions of advanced cancer pain. Psychooncology. *11*, 23–34.

Sengupta, A., Bocchio, M., Bannerman, D.M., Sharp, T., and Capogna, M. (2017). Control of Amygdala Circuits by 5-HT Neurons via 5-HT and Glutamate Cotransmission. J. Neurosci. *37*, 1785–1796.

Serlin, R.C., Mendoza, T.R., Nakamura, Y., Edwards, K.R., and Cleeland, C.S. (1995). When is cancer pain mild, moderate or severe? Grading pain severity by its interference with function. Pain *61*, 277–284.

Snowball, R.K., Dampney, R.A., and Lumb, B.M. (1997). Responses of neurones in the medullary raphe nuclei to inputs from visceral nociceptors and the ventrolateral periaqueductal grey in the rat. Exp. Physiol. *82*, 485–500.

Sommer, C. (2004). Serotonin in Pain and Analgesia: Actions in the Periphery. Mol. Neurobiol. *30*, 117–126.

Stamp, J.A., and Semba, K. (1995). Extent of colocalization of serotonin and GABA in the neurons of the rat raphe nuclei. Brain Res. *677*, 39–49.

Ständer, S., Steinhoff, M., Schmelz, M., Weisshaar, E., Metze, D., and Luger, T. (2003). Neurophysiology of pruritus: cutaneous elicitation of itch. Arch. Dermatol. *139*, 1463–1470.

Stewart, W., and Maxwell, D.J. (2000). Morphological evidence for selective modulation by serotonin of a subpopulation of dorsal horn cells which possess the neurokinin-1 receptor: Serotoninergic axons in the dorsal horn. Eur. J. Neurosci. *12*, 4583–4588.

Sufka, K.J., and Price, D.D. (2002). Gate Control Theory Reconsidered. 14.

Suzuki, R., Rygh, L.J., and Dickenson, A.H. (2004). Bad news from the brain: descending 5-HT pathways that control spinal pain processing. Trends Pharmacol. Sci. *25*, 613–617.

Swieboda, P., Filip, R., Prystupa, A., and Drozd, M. (2013). Assessment of pain: types, mechanism and treatment. Ann. Agric. Environ. Med. AAEM *Spec no. 1*, 2–7.

Tainter, M.L. (1948). Pain. Ann. N. Y. Acad. Sci. *51*, 3–11.

Tamamaki, N., Yanagawa, Y., Tomioka, R., Miyazaki, J.-I., Obata, K., and Kaneko, T. (2003). Green fluorescent protein expression and colocalization with calretinin, parvalbumin, and somatostatin in the GAD67-GFP knock-in mouse. J. Comp. Neurol. *467*, 60–79.

Tan, L.L., Oswald, M.J., Heinl, C., Retana Romero, O.A., Kaushalya, S.K., Monyer, H., and Kuner, R. (2019). Gamma oscillations in somatosensory cortex recruit prefrontal and descending serotonergic pathways in aversion and nociception. Nat. Commun. *10*.

Taniguchi, H., He, M., Wu, P., Kim, S., Paik, R., Sugino, K., Kvitsani, D., Fu, Y., Lu, J., Lin, Y., et al. (2011). A Resource of Cre Driver Lines for Genetic Targeting of GABAergic Neurons in Cerebral Cortex. Neuron *71*, 995–1013.

Terman, G. (2001). Spinal mechanisms and their modulation. Manag. Pain 73–152.

Thibault, K., Van Steenwinckel, J., Brisorgueil, M.-J., Fischer, J., Hamon, M., Calvino, B., and Conrath, M. (2008). Serotonin 5-HT2A receptor involvement and Fos expression at the spinal level in vincristine-induced neuropathy in the rat. Pain *140*, 305–322.

Thibault, K., Calvino, B., Rivals, I., Marchand, F., Dubacq, S., McMahon, S.B., and Pezet, S. (2014). Molecular Mechanisms Underlying the Enhanced Analgesic Effect of Oxycodone Compared to Morphine in Chemotherapy-Induced Neuropathic Pain. PLoS ONE *9*.

Toda, K. (2007). The Terms Neurogenic Pain and Psychogenic Pain Complicate Clinical Practice: Clin. J. Pain *23*, 380–381.

Tovote, P., Esposito, M.S., Botta, P., Chaudun, F., Fadok, J.P., Markovic, M., Wolff, S.B.E., Ramakrishnan, C., Fenno, L., Deisseroth, K., et al. (2016a). Midbrain circuits for defensive behaviour. Nature *534*, 206–212.

Tovote, P., Esposito, M.S., Botta, P., Chaudun, F., Fadok, J.P., Markovic, M., Wolff, S.B.E., Ramakrishnan, C., Fenno, L., Deisseroth, K., et al. (2016b). Midbrain circuits for defensive behaviour. Nature *534*, 206–212.

Tovote, P., Esposito, M.S., Botta, P., Chaudun, F., Fadok, J.P., Markovic, M., Wolff, S.B.E., Ramakrishnan, C., Fenno, L., Deisseroth, K., et al. (2016c). Midbrain circuits for defensive behaviour. Nature *534*, 206–212.

Treede, R.D., Meyer, R.A., Raja, S.N., and Campbell, J.N. (1992). Peripheral and central mechanisms of cutaneous hyperalgesia. Prog. Neurobiol. *38*, 397–421.

Treede, R.D., Meyer, R.A., and Campbell, J.N. (1998). Myelinated mechanically insensitive afferents from monkey hairy skin: heat-response properties. J. Neurophysiol. *80*, 1082–1093.

Tschirdewahn, J., and Eyer, F. (2019). [Diagnostics and treatment of selected clinically relevant, acute drug intoxications]. Bundesgesundheitsblatt Gesundheitsforschung Gesundheitsschutz.

Tsuchiya, M., Yamazaki, H., and Hori, Y. (1999). Enkephalinergic neurons express 5-HT3 receptors in the spinal cord dorsal horn: single cell RT-PCR analysis. Neuroreport *10*, 2749–2753.

Turk, D.C., and Okifuji, A. Bonica's Management of Pain. Wolters Kluwer 49–50.

Vallbo, Å.B., Olausson, H., and Wessberg, J. (1999). Unmyelinated Afferents Constitute a Second System Coding Tactile Stimuli of the Human Hairy Skin. J. Neurophysiol. *81*, 2753–2763.

Van Steenwinckel, J., Brisorgueil, M.-J., Fischer, J., Vergé, D., Gingrich, J.A., Bourgoin, S., Hamon, M., Bernard, R., and Conrath, M. (2008). Role of spinal serotonin 5-HT2A receptor in 2',3'-dideoxycytidine-induced neuropathic pain in the rat and the mouse. Pain *137*, 66–80.

Vanderah, T.W., Ossipov, M.H., Lai, J., Malan, T.P., and Porreca, F. (2001). Mechanisms of opioid-induced pain and antinociceptive tolerance: descending facilitation and spinal dynorphin. Pain *92*, 5–9.

Vanegas, H., and Schaible, H.-G. (2004). Descending control of persistent pain: inhibitory or facilitatory? Brain Res. Brain Res. Rev. *46*, 295–309.

Vardeh, D., Mannion, R.J., and Woolf, C.J. (2016). Toward a Mechanism-Based Approach to Pain Diagnosis. J. Pain Off. J. Am. Pain Soc. *17*, T50-69.

Veenstra-VanderWeele, J., Anderson, G.M., and Cook, E.H. (2000). Pharmacogenetics and the serotonin system: initial studies and future directions. Eur. J. Pharmacol. *410*, 165–181.

Vertes, R.P., and Kocsis, B. (1994). Projections of the dorsal raphe nucleus to the brainstem: PHA-L analysis in the rat. J. Comp. Neurol. *340*, 11–26.

Vesalius, A., Oporinus, J., and Van Calcar, J.S. (1543). Andreae Vesalii Bruxellensis, ScholÃ¦ Medicorum PatauinÃ¦ Professoris : De humani corporis fabrica libri septem.

Viguier, F., Michot, B., Hamon, M., and Bourgoin, S. (2013). Multiple roles of serotonin in pain control mechanisms —Implications of 5-HT7 and other 5-HT receptor types. Eur. J. Pharmacol. *716*, 8–16.

Volpi-Abadie, J., Kaye, A.M., and Kaye, A.D. (2013). Serotonin Syndrome. Ochsner J. *13*, 533–540.

Vriens, J., Owsianik, G., Hofmann, T., Philipp, S.E., Stab, J., Chen, X., Benoit, M., Xue, F., Janssens, A., Kerselaers, S., et al. (2011). TRPM3 is a nociceptor channel involved in the detection of noxious heat. Neuron *70*, 482–494.

Walther, D.J., Peter, J.-U., Bashammakh, S., Hörtnagl, H., Voits, M., Fink, H., and Bader, M. (2003). Synthesis of serotonin by a second tryptophan hydroxylase isoform. Science *299*, 76.

Wang, Q.P., and Nakai, Y. (1994). The dorsal raphe: an important nucleus in pain modulation. Brain Res. Bull. *34*, 575–585.

Wang, F., Bélanger, E., Côté, S.L., Desrosiers, P., Prescott, S.A., Côté, D.C., and De Koninck, Y. (2018). Sensory Afferents Use Different Coding Strategies for Heat and Cold. Cell Rep. *23*, 2001–2013.

Wang, Q.P., Ochiai, H., and Nakai, Y. (1992). GABAergic innervation of serotonergic neurons in the dorsal raphe nucleus of the rat studied by electron microscopy double immunostaining. Brain Res. Bull. *29*, 943–948.

Waters, A.J., and Lumb, B.M. (2008). Descending control of spinal nociception from the periaqueductal grey distinguishes between neurons with and without C-fibre inputs. Pain *134*, 32–40.

Waxman, S.G. (2017). The Spinal Cord. In Clinical Neuroanatomy, (New York, NY: McGraw-Hill Education), p.

Wei, F., Dubner, R., and Ren, K. (1999). Nucleus reticularis gigantocellularis and nucleus raphe magnus in the brain stem exert opposite effects on behavioral hyperalgesia and spinal Fos protein expression after peripheral inflammation. Pain *80*, 127–141.

Wessberg, J., Olausson, H., Fernström, K.W., and Vallbo, A.B. (2003). Receptive field properties of unmyelinated tactile afferents in the human skin. J. Neurophysiol. *89*, 1567–1575.

Wheatcroft, J., Wakelin, D., Smith, A., Mahoney, C.R., Mawe, G., and Spiller, R. (2005). Enterochromaffin cell hyperplasia and decreased serotonin transporter in a mouse model of postinfectious bowel dysfunction. Neurogastroenterol. Motil. Off. J. Eur. Gastrointest. Motil. Soc. *17*, 863–870.

Willis, W.D., and Coggeshall, R.E. (1991). Structure of the Dorsal Horn. In Sensory Mechanisms of the Spinal Cord, W.D. Willis, and R.E. Coggeshall, eds. (Boston, MA: Springer US), pp. 79–151.

Willis, W.D.J., and Coggeshall, R.E. (2012). Sensory Mechanisms of the Spinal Cord: Volume 1 Primary Afferent Neurons and the Spinal Dorsal Horn (Springer Science & Business Media).

Woolf, C.J. (2011). Central sensitization: implications for the diagnosis and treatment of pain. Pain *152*, S2-15.

Woolf, C.J., and Costigan, M. (1999). Transcriptional and posttranslational plasticity and the generation of inflammatory pain. Proc. Natl. Acad. Sci. U. S. A. *96*, 7723–7730.

Woolf, C.J., Shortland, P., and Coggeshall, R.E. (1992). Peripheral nerve injury triggers central sprouting of myelinated afferents. Nature *355*, 75–78.

Wu, W., Elde, R., and Wessendorf, M.W. (1993). Organization of the serotonergic innervation of spinal neurons in rats—III. Differential serotonergic innervation of somatic and parasympathetic preganglionic motoneurons as determined by patterns of co-existing peptides. Neuroscience *55*, 223–233.

Xie, D.-J., Uta, D., Feng, P.-Y., Wakita, M., Shin, M.-C., Furue, H., and Yoshimura, M. (2012). Identification of 5-HT receptor subtypes enhancing inhibitory transmission in the rat spinal dorsal horn in vitro. Mol. Pain *8*, 58.

Yaksh, T.L., and Wilson, P.R. (1979). Spinal serotonin terminal system mediates antinociception. J. Pharmacol. Exp. Ther. *208*, 446–453.

Yam, M., Loh, Y., Tan, C., Khadijah Adam, S., Abdul Manan, N., and Basir, R. (2018). General Pathways of Pain Sensation and the Major Neurotransmitters Involved in Pain Regulation. Int. J. Mol. Sci. *19*, 2164.

Yang, G.B., Qiu, C.L., Aye, P., Shao, Y., and Lackner, A.A. (2007). Expression of serotonin transporters by peripheral blood mononuclear cells of rhesus monkeys (Macaca mulatta). Cell. Immunol. *248*, 69–76.

Yizhar, O., Fenno, L.E., Davidson, T.J., Mogri, M., and Deisseroth, K. (2011). Optogenetics in Neural Systems. Neuron *71*, 9–34.

Zagon, A. (1993). Innervation of serotonergic medullary raphe neurons from cells of the rostral ventrolateral medulla in rats. Neuroscience *55*, 849–867.

Zambreanu, L., Wise, R.G., Brooks, J.C.W., Iannetti, G.D., and Tracey, I. (2005). A role for the brainstem in central sensitisation in humans. Evidence from functional magnetic resonance imaging. Pain *114*, 397–407.

Zeitz, K.P., Guy, N., Malmberg, A.B., Dirajlal, S., Martin, W.J., Sun, L., Bonhaus, D.W., Stucky, C.L., Julius, D., and Basbaum, A.I. (2002). The 5-HT3 Subtype of Serotonin Receptor Contributes to Nociceptive Processing via a Novel Subset of Myelinated and Unmyelinated Nociceptors. J. Neurosci. *22*, 1010–1019.

Zemlan, F.P., and Schwab, E.F. (1991). Characterization of a novel serotonin receptor subtype (5-HT1S) in rat CNS: interaction with a GTP binding protein. J. Neurochem. *57*, 2092–2099.

Zhang, Z., Hefferan, M.P., and Loomis, C.W. (2001). Topical bicuculline to the rat spinal cord induces highly localized allodynia that is mediated by spinal prostaglandins. PAIN® *92*, 351–361.

Zhao, Z.-Q., Chiechio, S., Sun, Y.-G., Zhang, K.-H., Zhao, C.-S., Scott, M., Johnson, R.L., Deneris, E.S., Renner, K.J., Gereau, R.W., et al. (2007). Mice Lacking Central Serotonergic Neurons Show Enhanced

Inflammatory Pain and an Impaired Analgesic Response to Antidepressant Drugs. J. Neurosci. *27*, 6045–6053.

Zhao, Z.-Q., Liu, X.-Y., Jeffry, J., Karunarathne, W.K.A., Li, J.-L., Munanairi, A., Zhou, X.-Y., Li, H., Sun, Y.-G., Wan, L., et al. (2014). Descending Control of Itch Transmission by the Serotonergic System via 5-HT1A-Facilitated GRP-GRPR Signaling. Neuron *84*, 821–834.

Zhuo, M., and Gebhart, G.F. (1991). Spinal serotonin receptors mediate descending facilitation of a nociceptive reflex from the nuclei reticularis gigantocellularis and gigantocellularis pars alpha in the rat. Brain Res. *550*, 35–48.

Zufall, F. (1992). Neurotoxins as Tools in Characterization of γ-Aminobutyric Acid-Activated Chloride Channels. In Methods in Neurosciences, (Elsevier), pp. 323–331.